Calcium homeostasis and calciumactivated proteins in Alzheimer's disease

Kurbatskaya, Ksenia

Awarding institution:
King's College London

Calcium homeostasis and calcium-activated proteins in Alzheimer's disease

Ksenia Kurbatskaya

Thesis submitted in fulfilment of the degree of Doctor of Philosophy

Department of Basic and Clinical Neuroscience

Institute of Psychiatry, Psychology and Neuroscience

King's College London

August 2015

Declaration

I hereby declare that all of the work presented in this thesis is my own.

Ksenia Kurbatskaya

August 2015

Acknowledgements

I would like to thank my primary supervisor, Dr Wendy Noble, for her immense professional, moral and psychological support throughout the three years of my PhD placement at King's College London. With Wendy's encouragement, I was able to get behind the wheel of my own project early on, design my own research, and, hence, feel the gratification of leaving my own small footprint in the field of Alzheimer's. I would also like to thank my secondary supervisor, Dr Diane Hanger for continually providing guidance throughout my PhD, especially in Friday meetings. Finally I couldn't have done this project without the support of my family and friends.

Abstract

Ca^{2+} dyshomeostasis is considered to be an early pathogenic event in Alzheimer's disease (AD). Abnormal levels and activity of Ca^{2+}-regulated proteins are detected in post mortem AD brain, elevated neuronal Ca^{2+} is found in many cell and animal models of AD, and Ca^{2+}-dependent signalling pathways are recognized to contribute to neurodegeneration in these models. The aims of this project were 1) to further investigate changes in the levels or activity of Ca^{2+}-activated proteins in association with tau and Aβ accumulation during the progression of AD, and 2) elucidate novel mechanisms underlying Ca^{2+} dysregulation in AD. Post-mortem brain tissue was obtained from controls and AD cases at different stages of disease development (Braak II-VI). Biochemical analysis of these tissues revealed that calpain-1 activity is increased in Braak stage II to VI brain in comparison to controls, suggesting that changes in Ca^{2+}-sensitive signalling pathways occur very early during disease development. Elevated calpain-1 activity was associated with a transient upregulation of the endogenous calpain inhibitor, calpastatin, and preceded Aβ1-42 accumulation, activation of tau kinases, increased tau phosphorylation and synapse loss. These results corroborate findings from cell and animal models that Ca^{2+} dysregulation and calpain activation are upstream of tau phosphorylation and synapse loss in AD. In addition, end-stage (Braak stage VI) AD brains displayed elevated calpain-mediated cleavage of the sodium calcium exchanger 3 (NCX3), which normally extrudes excess cellular Ca^{2+},

suggesting that deficiencies in NCX3 function might contribute to the accumulation of excess intraneuronal Ca^{2+} in AD. In support of this, knockdown of NCX3 in primary neurons sensitized neurons to the toxic effects of Aβ1-42. In addition, treatment of neuronal cells with Aβ1-42 resulted in neurotoxicity which was associated with activation of poly(ADP-ribose) polymerase (PARP)-1, Ca^{2+} entry through transient receptor potential melastatin type 2 (TRPM2) channels, elevations in cytosolic Ca^{2+}, activation of calpain, calpain-regulated tau kinases and tau phosphorylation at epitopes of relevance to AD and synapse loss. Overall, this work lends further support to the hypothesis that altered Ca^{2+} homeostasis plays an important role in early AD pathogenesis, and has identified novel mechanisms in this process including abnormal regulation of PARP-1/TRPM2 signalling and NCX3 function.

Contents

List of Figures

List of Tables

Abbreviations

Aa	amino acid
ACh	acetylcholine
AChE	acetylcholinesterase
AD	Alzheimer's disease
ADAM10	a disintegrin and metalloprotease 10
ADPR	adenosine diphosphate ribose
AICD	amyloid precursor protein intracellular domain
AIF	apoptosis-inducing factor
AMPAR	α-amino-3-hydroxy-5-methyl-4-isoxazolepropionic acid receptor
ApoE	apolipoprotein E
APP	amyloid precursor protein
Aβ	amyloid-β
BACE	β-site amyloid precursor protein cleaving enzyme
CALHM1	calcium homeostasis modulator 1
CAMKK2	calcium/calmodulin-dependent protein kinase kinase 2
CAST	calpastatin
CBD	corticobasal degeneration
Cdk5	cyclin-dependent kinase 5
ChAT	choline acteyltransferase
CHO	Chinese hamster ovary
CICR	calcium-induced calcium release

CLA	clotrimazole
CREB	cAMP response element binding protein
CSF	cerebrospinal fluid
CTF	c-terminal fragment
DCD	delayed calcium deregulation
DS	Down's syndrome
ER	endoplasmic reticulum
FAD	familial Alzheimer's disease
FTD	frontotemporal dementia
GFAP	glial fibrillary acidic protein
GSK3	glycogen synthase kinase 3
GWAS	genome-wide association study
H_2O_2	hydrogen peroxide
HEK	human embryonic kidney
IL-1β	interleukin-1β
IP_3R	inositol triphosphate receptor
JNK	c-Jun N-terminal kinase
KCl	potassium chloride
LiCl	lithium chloride
LOAD	sporadic late onset Alzheimer's disease
LTP	long-term potentiation
MAP2	microtubule associated protein 2
MAPT	microtubule associated protein tau
MBD	microtubule binding domain

MCI	mild cognitive impairment
MEF	mouse embryonic fibroblast
NaCl	sodium chloride
NAD	nicotinamide adenine dinucleotide
NbM	nucleus basalis of Meynert
NCX	sodium calcium exchanger
NFT	neurofibrillary tangle
NMDAR	N-methyl-D-aspartate receptor
NSE	neuron specific enolase
PAR	poly(ADP-ribose) polymers
PARG	poly(ADP-ribose) glycohydrolase
PARP	ply(ADP-ribose) polymerase
PHF	paired helical filament
PMD	post mortem delay
PN	peroxynitrite
PRD	proline-rich domain
PS	presenilin
PSD95	postsynaptic density protein 95
PSP	progressive supranuclear palsy
R	microtubule binding repeat sequence
ROS	reactive oxygen species
RyR	ryanodine receptor
SERCA	sarcoendoplasmic reticulum calcium-ATPase
TNFα	tumor necrosis factor α

TREM2	triggering receptor expressed on myeloid cells 2
TRPM2	transient receptor potential melastatin type 2
VGCC	voltage-gated calcium channel
WHO	World Health Organization

CHAPTER 1

Introduction

1.1 The socioeconomic impact of AD

The recognition of Alzheimer's disease (AD) is attributed to the German psychiatrist Alois Alzheimer who, in 1906, first characterized the disorder in a 55 year old female patient (Stelzmann et al., 1995). Today, AD is widely known as one of the most common neuropsychiatric disorders that affects more than 40 million people worldwide - numbers estimated to double by 2030 (Alzheimer's Disease International, 2015). The rise in AD incidence is explained by demographic ageing due to improved health care; as age is the single biggest risk factor for developing AD, an increase in the population life-span also increases the likelihood of developing the disease. AD is the leading cause of dementia (60% of dementia cases) in people over 65, affecting approximately 6 % of that population age group and approximately 50 % of people over age 90. The World Health Organization (WHO) has identified AD as a public health priority due to its current catastrophic global cost of $605 billion (WHO, 2015). In the UK, two-thirds of the overall cost of dementia (£26 billion) are incurred by mostly low-income households, who are often driven into poverty and unemployment by having to resort to unpaid or private social care to support those affected by the disease.

The contribution of the NHS towards nursing care and costly treatment accounts for a significant proportion of the government health budget, and the rising demand for these services places great strain on NHS resources (Alzheimer's Society, 2015). In 2014, David Cameron addressed the UK's dementia crisis by pledging more funding towards AD research, with priorities of experimental drug development, advances in clinical infrastructure and improvement of patient access to new drugs. The initiative came in light of the market failure of numerous potential disease-modifying drugs, which despite showing marked benefit in pre-clinical studies, showed no efficacy in clinical trials (Schneider et al., 2014). This also led to some questions about our understanding of AD pathogenesis and conventional approaches to drug development (Mangialasche et al., 2010). The pharmaceutical industry has since been refocused to include the exploration of new drug targets and on developing symptomatic treatments to improve patient quality of life. However, these therapies remain some way from clinical use; therefore, there is still no treatment that can halt or reverse disease progression, and so AD remains an incurable, ultimately fatal condition. The latest research has shown that delaying AD onset by only three years would have significant benefit for disease sufferers by easing the severity of symptoms and reducing the number of families afflicted by the disease, as well as saving the country up to £5bn per year (Alzheimer's Research UK, 2015). Continued efforts from academic research institutions, the pharmaceutical industry and government bodies are therefore

required to enable the development of early diagnostic markers and new disease-targeting therapies with the potential to treat, delay or prevent AD.

1.2 AD clinical features and neurochemistry

1.2.1 Clinical features

AD is clinically characterized by progressive memory and cognitive deficits, neuropsychiatric changes and, in some cases, declining motor function (Alzheimer's Society, 2015). Although the progression of AD varies between individuals, it can generally be divided into three stages: the preclinical stage with no overt clinical symptoms, the middle stage which manifests as mild cognitive impairment (MCI) and the final stage of AD dementia (National Institute of Health, 2015). The first symptoms are typically observed during the MCI stage but are similar to the effects of normal ageing and, thus, do not always result in AD diagnosis. Individuals experience loss of short term memory, and may exhibit language impairment and poor judgment (Gagnon and Belleville, 2011; Parra et al., 2010). AD is typically diagnosed in patients exhibiting progressive memory loss (e.g. losing items and self-repetition), mild cognitive and intellectual impairment (e.g. problems handling money), difficulty performing normal daily tasks, as well as mood and personality changes (e.g. aggression, depression). In moderate AD, sensory processing and conscious thought are affected (Lyketsos et

al., 2011). Neuropsychiatric and behavioural symptoms include delusions, paranoia and hallucinations. Individuals lose the ability to distinguish familiar and unfamiliar faces, experience profound memory impairment and are unable to learn new things. In severe stages of AD, some individuals experience motor dysfunction (causing apraxia and incontinence), seizures, wasting from loss of appetite and they are prone to skin and other serious organ infections (Herrmann et al., 2007). This can be followed by longer periods of sleep in the terminal stages of disease, and finally death.

1.2.2 Neurochemistry

Most therapeutic agents currently used to treat AD act to counterbalance the neurochemical disturbances that have been long known to underlie AD symptoms (Keverne and Ray, 2008). Early post mortem examinations of AD patients revealed selective cholinergic denervation in the basal forebrain (Davies, 1976). This was later shown to be largely attributed to significant (up to 70%) reduction in choline acetyltransferase (ChAT) synthesis within the nucleus basalis of Meynert (nbM) and its cholinergic projections to the cortex, hippocampus and striatum (Perry et al., 1999). Reduced cholinergic activity in these areas is considered to be a major correlate of cognitive deficits in AD (Perry, Tomlinson et al. 1978). There are also observations of impaired choline transport, decreased acetylcholine (ACh) release, as well as reduced expression of muscarinic, nicotinic

and neuronal growth factor receptors within the nbM. The reason for transmitter system selectivity remains to be fully understood; however, there are reports of cholinergic denervation being linked to amyloid pathology (Kar et al., 2004; Teipel et al., 2014) (section 1.4.2). Currently used acetylcholinesterase (AChE) inhibitors, such as donepezil and galantamine, offer the most success in reducing behavioural and motor symptoms in AD by suppressing ACh metabolism, catalysed by AChE (Wilcock et al., 2003).

Another prominent neurochemical feature of AD is loss of glutamatergic transmission within the cortex and cortical projections to the hippocampus, striatum, substantia nigra and brain stem (Hardy et al., 1987). As glutamate is vital for long-term potentiation (LTP), the process that underpins memory and learning, glutamatergic denervation is thought to account for early short-term memory loss and dementia in AD (Francis, 2008). There are, thus, indications that pharmacologically promoting glutamatergic transmission may be of benefit to memory and cognition in AD. On the other hand, memantine, a N-methyl-D-aspartate receptor (NMDAR) antagonist, is one of the only agents shown to have a small effect in reducing the rate of cognitive decline in AD patients (Thomas and Grossberg, 2009), although this is usually transient. Memantine prevents excess stimulation of NMDARs by glutamate, thereby protecting neurons from excitotoxicity induced by intracellular Ca^{2+} overload (section 1.5) in response to NMDAR activation (Lipton, 2006). This explains why current therapeutics act to replenish cholinergic and not glutamate activity, as levels of the latter require

physiological fine-tuning, rather than simply increasing their overall levels, in order to maintain neuronal homeostasis (Parsons et al., 2007). Surprisingly, memantine has also shown to be effective in reducing memory and learning deficits in AD caused by glutamatergic deficiency in patients. Of relevance to the discussion of AD drugs above, memantine had the opposite effect on cognitive function in animal studies (Creeley et al., 2006).

1.3 AD genetics

The majority of AD cases are diagnosed in the elderly and these are classed as sporadic late-onset AD (LOAD). These cases lack a clear genetic component, but could result from a complex pattern of inheritance that is most likely caused by a combination of polygenic, environmental and lifestyle factors. In a small proportion of cases (between 0.1 and 2 %), AD presents before the age of 65 and is caused by monogenic mutations in three genes that are inherited in a Mendelian fashion. This type of disease is classed as familial early-onset AD (FAD), and is a more rapidly progressing dementia than LOAD. Genetic studies of both AD types have led to the establishment of the central hypothesis of AD pathogenesis, the amyloid cascade hypothesis (section 1.4), as well as identification of additional disease pathways and risk factors for AD.

1.3.1 FAD

In 1948, scientists described rare cases of Down's Syndrome (DS) individuals who, in their 4th and 5th decades of life, exhibited cognitive and behavioural changes and brain lesions characteristic of senile dementia (Jervis, 1948). These brain lesions were later determined to be virtually identical to those seen in the AD population (Lott, 1982); however, they developed much earlier in DS compared to AD. The reason for this was discovered to be an extra copy of the amyloid precursor protein (*APP*) gene mapped to chromosome 21, which is triplicated in DS (Tanzi et al., 1987; Robakis et al., 1987; Goldgaber et al., 1987). The extra *APP* copy results in increased production of APP protein and overproduction of the protein's cleavage product β-amyloid (Aβ), found in brain lesions in degenerating areas of both DS and AD brain (section 1.4.2). This was followed by the discovery that FAD is caused by autosomal dominant mutations in the APP gene (St George-Hyslop et al., 1987) that also affect APP processing to generate excess Aβ species. This signifies that APP biology is aberrant in both disorders and explains the early onset of dementia in DS.

FAD can be genetically subdivided into three subtypes (Bird, 1993) on the basis of mutations in *APP*, presenilins (*PS*) 1 and 2. APP is a type I transmembrane protein that is subject to differential proteolytic processing by cellular secretases (Sisodia, 1992). *PS1* and *PS2* encode presenilin 1 and 2 - large multi-pass transmembrane proteins that are found in numerous cellular compartments and

serve a variety of biological functions (reviewed by Vetrivel et al., 2006). Presenilins form the catalytic core of the proteolytic enzyme γ-secretase, which cleaves numerous type I membrane proteins, including APP (Steiner, 2008).

AD type 1 is caused by mutation of APP and accounts for up to 15 % of FAD cases; AD type 3 is caused by mutation of PS1 and occurs in the majority (30 to 70 %) of FAD cases, and AD type 4 is caused by mutation of PS2 and accounts for less than 5 % of FAD cases (Bird, 1993). FAD individuals with no identifiable mutations in the aforementioned genes have also been reported, signifying that other genetic factors may be causative to FAD (Cruts et al., 1998; Janssen et al., 2003). As FAD subtypes are clinically indistinguishable, differentiating between them requires sequence analysis of *PS1*, *PS2* and *APP* genes in carriers to identify the responsible mutations and confirm diagnosis. Over 170 *PS1*, 25 *APP* and 14 *PS2* gene mutations have been identified in families with FAD in different parts of the world (Cruts et al., 2012). Most of these mutations are base pair substitutions, with several insertions and deletions identified, as well as a rare APP duplication in cases of FAD with cerebral amyloid angiopathy (Cruts et al., 2012).

In FAD, PS1/2 mutations result in defective presenilins that interfere with γ-secretase proteolytic activity, one of the enzymes that cleaves APP to generate Aβ. In general, PS1/2 mutations alter APP processing to result in increased production of pathogenic 42 amino acid Aβ peptides (Aβ42) and cause accelerated amyloid deposition (section 1.4.2; Duff et al., 1996). It was later found

that presenilins also function as Ca^{2+}-conducting leak channels in lipid bilayers, and that PS1/2 mutations in FAD also cause deficient endoplasmic reticulum (ER) Ca^{2+} signaling (section 1.5.1; Tu et al., 2006).

APP mutations cluster around the secretase cleavage sites on exons 16 and 17 of the *APP* gene, and they also act to alter APP proteolysis. The first identified APP mutation at codon 717 in exon 17 (London V717I mutation), located near the γ-secretase cleavage site, was found to favour production of Aβ42 and alter APP subcellular localization (Goate et al., 1991). A double mutation at codons 670 and 671 in exon 16 (Swedish KM670/671NL mutation; APP_{SWE}), located near the β-secretase cleavage site at N-terminal βAPP, was shown to increase production of all Aβ peptides (Mullan et al., 1992). This mutation is commonly used in transgenic mouse models of AD (such as the widely used J20, Tg2576 and 3xTg models) as these mice go on to accumulate high levels of Aβ and develop amyloid plaques (Webster et al., 2014). A recently established Chinese hamster ovary (CHO) cell line stably expressing mutant APP provides a physiologically source of Aβ that has been shown to recapitulate AD phenotype in *vivo* (Walsh et al., 2002a).

Mutations in the *MAPT* gene encoding microtubule associated protein tau have not been linked to FAD, despite the well-documented importance of tau in AD pathogenesis (section 1.4.1). However, MAPT mutations are known to cause dementia in other neurodegenerative 'tauopathies', including frontotemporal dementia (FTD) and progressive supranuclear palsy (PSP) (Pickering-Brown et

al., 2004; Stanford et al., 2000). These mutations cause tau pathology and tau-associated neurodegeneration by altering the alternative splicing pattern of MAPT to change the normal ratio of tau isoform expression, altering tau protein function or increasing the propensity of tau to aggregate (section 1.4.2; Iovino et al., 2014; Spillantini and Goedert, 2013).

1.3.2 LOAD

Unlike in FAD, genetic inheritance is not observed in persons with LOAD. The single biggest risk factor for developing LOAD is age; however, genetic susceptibility is also thought to be a major contributing factor to LOAD prevalence and this appears to be more prominent in relatively early onset cases of sporadic AD (Mendez and Cummings, 2003). Other risk factors, including environmental and lifestyle factors, are thought to confer particular risk for the development of later onset LOAD cases (Alzheimer's Society, 2015). Early studies in identical and non-identical twins have revealed that there is some genetic component in more than 60 % of LOAD cases (Bergem et al., 1997); therefore, genetic abnormalities are considered to be an important primary cause of LOAD. Functional investigation of the effects of genetic risk factors are the subject of substantial research aimed at further understanding the biological basis of LOAD pathogenesis.

The development of relatively high throughput and inexpensive genetic screening technologies, such as genome-wide association studies (GWAS), involving large numbers of participants, has led to the identification of 20 new potential low risk loci for LOAD (Zou et al., 2014). The pathways in which the proteins encoded by these genes are active include calcium signaling, lipid and cholesterol metabolism, endocytosis, immunity, APP processing and synaptic function (Table 1). Moreover, recent GWAS of amyloid and tau transgenic animals shed insight into the genes responsible for the development of either pathology (section 1.4), as well as identifying genes that may influence early synaptic changes in AD and disease progression (Matarin et al., 2015). The introduction of whole exome sequencing technology has led to the identification of polymorphisms in the triggering receptor expressed on myeloid cells 2 (*TREM2*) gene, which increases LOAD risk by 5-fold (Guerreiro et al., 2013). Abnormal TREM2 function resulting from these polymorphisms is shown to disrupt microglial Aβ clearance, which increases cortical Aβ burden and is associated with downregulation of neuroprotective cytokine signalling (Rivest, 2015; Ito and Hamerman, 2012).

A recently identified variant of the *CALHM1* gene on chromosome 10 has also been shown to influence LOAD risk (Dreses-Werringloer et al., 2008). CALHM1 encodes a multipass membrane glycoprotein that is thought to form a component of an uncharacterized Ca^{2+} channel in the brain. According to Dreses-Werringloer and colleagues (2008), the 'channel' regulates cellular levels of Ca^{2+} and Aβ production, and dysfunctional polymorphic variants of CALHM1 result in

aberrant increases in intracellular Aβ and Ca^{2+}. CALHM1 also modulates Aβ levels in cerebrospinal fluid (CSF) in individuals at risk of AD (Koppel et al., 2011). These findings were the first genetic studies to suggest that changes in Ca^{2+} homeostasis are important for the development of AD, and are therefore of particular interest to this work.

By far the strongest genetic risk factor for LOAD is the *ε4* allele of apolipoprotein E (ApoE; Strittmatter et al., 1993). ApoE is a plasma protein involved in transportation and clearance of cholesterol and other cholesterol-like molecules, including Aβ (Mahley, 1988; Strittmatter et al., 1993). *ApoE ε4* is one of 3 *ApoE* alleles located on chromosome 19, the other being *ε2* and *ε3*. Most of the population carries the *ε3* allele which does not influence AD risk, while the rarer *ε2* allele has shown to reduce AD risk even in heterozygous individuals (Alzheimer's Drug Discovery Foundation, 2015). The *ε4* allele is present in approximately 20 % of the population, and dose-dependently increases LOAD susceptibility (Liu et al., 2013). A study in 42 families with LOAD has shown that *ε4* raises the risk of disease from 20% to 90%, and decreases the mean age of onset from 84 to 68 years (Corder et al., 1993). Moreover, homozygosity for *ε4* appears to be sufficient to cause AD by the age of 80. The presence of *ApoE ε4* has shown to exert damage through both loss and gain of function effects such as reducing Aβ clearance from the CNS or promoting Aβ deposition, respectively. (Castellano et al., 2011). There is some evidence of a link between *ApoE ε4* and tau pathology in AD (Glöckner et al., 2011), and ε4 carriers also expressing a *MAPT*

gene polymorphism are at a five-fold greater risk for developing LOAD (Raz and Miller, 2013). Table 1 lists the 23 genes that are currently known to confer LOAD risk.

Risk gene	***Chromosome***	***Protein***	***Implicated pathway***	***Primary reference***
CLU	8	Clusterin	Aβ pathway, lipid metabolism, inflammation, immunity and apoptosis	(Harold et al., 2009)
CR1	1	Complement Receptor 1	Aβ pathway, immunity	(Brouwers et al., 2012)
PICALM	11	Phosphatidyli-nositol Binding Clathrin Assembly Protein	Ca^{2+} regulation, Aβ toxicity, APP processing and synaptic function	(Harold et al., 2009)
BIN1	2	Bridging Integrator 1	Endocytosis, synaptic function and caspase-dependent apoptosis	(Seshadri et al., 2010)
EPHA1	7	Erythropoietin-Producing Hepatoma Receptor	Immunity	(Hollingworth et al., 2011)

ABCA7	19	ATP-Binding Cassette, Sub-Family A (ABC1), Member 7	APP processing, immunity and cholesterol metabolism	(Vardaraj an et al., 2015)
MS4A4A/ MS4A6E	11	Membrane-Spanning 4-Domains, Subfamily A, Member 4A/6E	Immunity (MS4A2) and cell surface signalling	(Hollingw orth et al., 2011)
CD33	19	Myeloid cell surface antigen CD33	Immunity and synaptic function	(Hollingw orth et al., 2011)
CD2AP	6	CD2-Associated Protein	Synaptic function and actin cytoskeleton	(Naj et al., 2011)
HLA-DRB5/DR B1	6	Major Histocompatib ility Complex, Class II, DR Beta 5/1	Immunity and inflammation	(Lambert et al., 2010)
SORL1	3	Sorting Protein-Related Receptor Containing LDLR Class A Repeats	Aβ pathway, lipid transport and endocytosis	(Dodson et al., 2006)

SLC24A4	14	$Na^+/K^+/Ca^{2+}$-Exchange Protein 4	Ca^{2+} homeostasis	(Lambert et al., 2013)
PTK2B	8	Protein tyrosine kinase 2 β	Signal transduction, synaptic function and stress response	(Lambert et al., 2013)
ZCWPW1	7	Zinc Finger, CW Type With PWWP Domain 1	Immunity, histone modification	(Lambert et al., 2013)
CELF1	11	CUGBP, Elav-Like Family Member 1	Gene regulation, cytoskeleton and axonal transport	(Lambert et al., 2013)
FERMT2	14	Fermitin Family Member 2	Tau and cell signalling	(Lambert et al., 2013)
CASS4	20	Cas Scaffolding Protein Family Member 4	Aβ pathway, cytoskeleton and axonal transport	(Lambert et al., 2013)
INPP5D	2	Inositol Polyphosphate-5-Phosphatase, 145kDa	Immunity and inflammation	(Lambert et al., 2013)
MEF2C	5	Myocyte Enhancer Factor 2C	Synaptic function, immunity and inflammation	(Lambert et al., 2013)

NME8	7	NME/NM23 Family Member 8	Cytoskeleton and axonal transport	(Lambert et al., 2013)
TREM2*	**6**	**Triggering Receptor Expressed On Myeloid Cells 2**	**Aβ clearance and immunity**	**(Guerreiro et al., 2013)**
ApoE ε4	**19**	**Apolipoprotein E *ε4***	**Aβ clearance and lipid transport**	(Strittmatter et al., 1993)
*CALHM1**	10	Calcium Homeostasis Modulator 1	Aβ pathway and calcium homeostasis	(Dreses-Werringloer et al., 2008)

Table 1.1 A list of the genetic factors currently known to increase risk of sporadic late-onset Alzheimer's disease (LOAD). The encoded proteins, chromosome loci, implicated pathways and primary references for each gene are given. Polymorphisms in the genes in bold confer high risk of developing LOAD. Asterisks denote genes also implicated in early-onset familial AD.

While 60 to 80 % of AD cases are heritable, the above loci identified by GWAS only account for a small proportion of heritability, even when combined with increased expression of the *ApoE ε4* allele (Manolio et al., 2009). Further studies are therefore required to identify potential genetic risk factors that may account for the missing heritability in AD.

1.4 AD neuropathology

The neuropathological hallmark of neurodegenerative diseases such as AD is the aggregation of insoluble, fibrous protein into brain lesions. Such protein aggregation is not limited to disease but does not normally occur until very late in life. In AD, these protein aggregates comprise neurofibrillary tangles (NFTs) and amyloid plaques. The spatial and temporal distribution of these lesions follows a characteristic pattern during disease development, enabling accurate post mortem diagnosis and disease staging (Braak and Braak, 1997), and also correlates with AD clinical phenotypes (Brosch and Matthews, 2014; Storandt et al., 2009).

1.4.1 NFTs

Early studies of NFT ultrastructure (Fig. 1.1) revealed that these lesions are primarily composed of microtubule-associated protein tau aggregated into β-sheet-rich paired helical filament (PHF) structures (Goedert et al., 1989; Iqbal et al., 1975; Wood et al., 1986; Yagishita et al., 1981). NFTs are intracellular protein accumulations, generally localized to somata of degenerating neurons and glia, but they can also occur in cell processes, where they are known as 'neuropil threads' (Braak et al., 1986). Following cell death, NFTs remain in the extracellular space as 'ghost tangles' which are associated with microglia or invading astrocytic processes (Ikeda, Haga, et al., 1992; Ikeda, Akiyama, et al., 1992).

NFTs have been found to correlate with neuronal loss and the severity of dementia in AD brain (Gómez-Isla et al., 1997; Bobinski et al., 1997; Arriagada et al., 1992; Lai et al., 2010), however, it is unclear whether NFTs themselves are cytotoxic or otherwise detrimental to their milieu. In fact, neuronal dysfunction and cognitive impairment correlate to 'prefibrillar' tau oligomers, suggesting that it is the pre-tangle tau modifications that mediate neurotoxic effects (Mufson et al., 2014; Patterson et al., 2011). Nevertheless, the importance of NFTs was highlighted by Eva and Heiko Braak in the late 1980s, who found that NFT spread follows a consistent hierarchical pattern throughout the brain as disease progresses and this permits neuropathological staging of AD and correlation of brain pathology to clinical phenotype (Braak and Braak, 1991). Since then, immunohistochemical analysis of NFTs has been the accepted method of post mortem 'Braak' staging of AD in research and clinical diagnosis (Fig 1.1). The mechanisms of NFT intra- and intercellular spread remain to be established, but are currently the topic of intensive research (Gendreau and Hall, 2013).

1.4.2 Tau

The presence of tau as the main component of NFTs prompted the hypothesis that tau changes are causally related to neurodegeneration. This was confirmed in documented cases of FTD with parkinsonism linked to chromosome 17 (FTD-17) caused by a common MAPT mutation (P30IL), where tau dysfunction led to

neuronal death (Poorkaj et al., 1998; Hutton et al., 1998). Since then, extensive research has aimed to elucidate how tau structure, function and post-translational modification can be disrupted to cause neuronal dysfunction and demise in these dementing diseases. Determining the significance of tau in AD aetiology has not been straight-forward due to the absence of a clear mutation-disease link (section 1.3.1); nevertheless, the modifications observed to occur to tau proteins prior to its aggregation into NFTs in AD models served as evidence that abnormal tau likely plays a role in AD pathogenesis and has also provided valuable insight into tau function (Martin et al. 2011; Johnson & Stoothoff 2004; Morris et al., 2015).

Tau is best known for its axonal expression in CNS neurons (Götz et al., 1995), although it is also recognised to localise to dendrites and cell soma (Hanger et al., 2009). A major function of tau is to stabilize microtubules for axonal transport, which it mediates by C-terminal binding to microtubule protein tubulin which promotes tubulin polymerisation and stabilisation. However, tau is also found localized to cell membranes and various intracellular domains, indicating that it has additional cellular functions (Brandt et al., 1995; Pooler and Hanger, 2010). Alternative splicing of tau around the N-terminus and microtubule-binding domain (MBD) generates six isoforms in adult human brain, which differ in their inclusion or exclusion of N-terminal inserts and microtubule binding repeat sequences ('R') - the latter of which differentially affects tau binding to

microtubules, microtubule stability and axonal dynamics (Goedert et al., 1989; Peck et al., 2011; Goedert and Jakes, 1990).

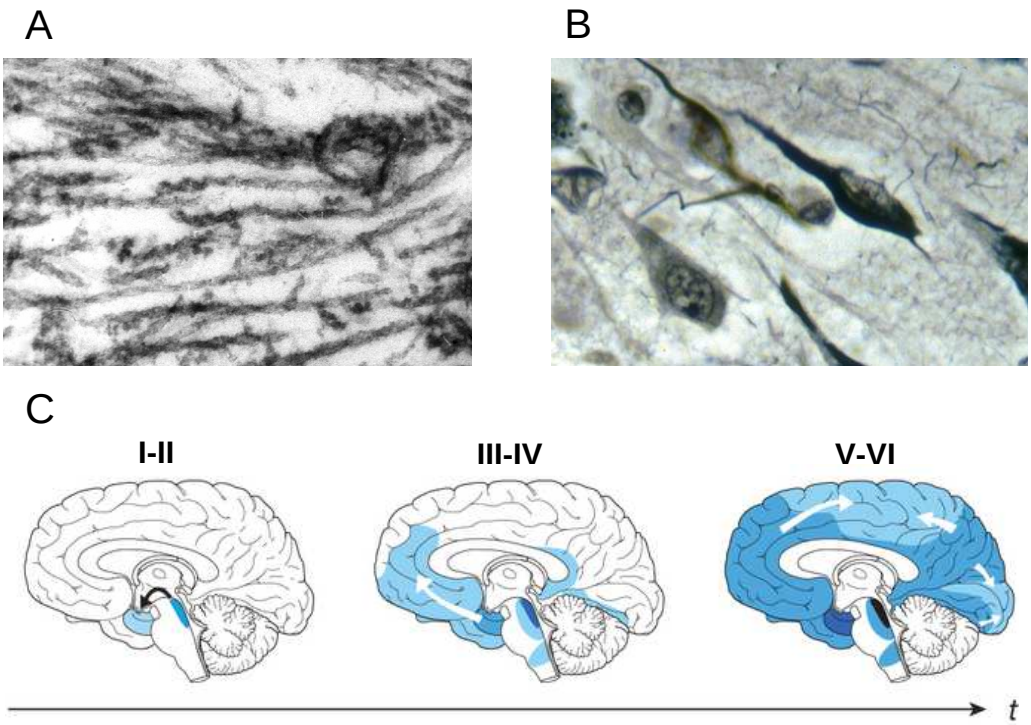

Fig. 1.1 AD brain is characterized by intraneuronal neurofibrillary tangles (NFTs) containing tau protein. NFT tau is abnormally modified which causes it to aggregate into (A) paired helical filaments (PHF), visualised here by electron microscopy, that are components of (B) NFTs, as shown here following silver staining of AD brain. (C) NFT load and distribution pattern are used in neuropathological staging (Braak I-VI) of AD. In early stages of AD (I-II), NFTs are localized to the transentorhinal region (CA1, subiculum and entorhinal cortex). They spread to the limbic system (hippocampus, amygdala) in later stages of disease (III-IV), as indicated by white arrows in panel C, and ultimately to the cortex and throughout most of the rest of the brain at end stage disease (V-VI). NFTs correlate with cognitive impairment in patients (adapted from Jucker and Walker, 2013).

The normal expression of 3R and 4R tau isoforms gives an approximately 1:1 ratio; however altered 3R to 4R tau ratios are seen in FTD-17 and other tauopathy brains, such as Pick's disease, and this is speculated to induce neurotoxic cascades in tau mutant animals (Fig. 1.2; Goode et al., 2000; Stoothoff et al., 2009; Bronner et al., 2005). AD brains show approximately equal expression of 3R and 4R tau; however, 4R tau has been implicated in NFT formation in models of AD (Goedert et al., 1989).

Tau processing is normally tightly regulated as it undergoes a number of post-translational modifications in both physiological and pathological conditions, including phosphorylation by protein and tyrosine kinases, as well as truncation, cross-linking, isomerization, glycation, nitration and ubiquitination (Morris et al. 2011; Morris et al., 2015). Tau docking to microtubules is regulated by phosphorylation of tau at numerous epitopes around the MBD, which alters MBD conformation and detaches tau from microtubules (Lindwall and Cole, 1984; Jho et al., 2010). Physiologically, this is important in enabling microtubule disassembly during developmental or post-injury neurite outgrowth; however, detached tau can accumulate in neurons and neurites, forming insoluble filaments and ultimately NFTs (Chuckowree and Vickers, 2003; Lee et al., 2001). Conversely, in the dephosphorylated state, tau is able to attach to and stabilize microtubules, enabling bidirectional axonal transport of proteins vital for neuronal function (Fig. 1.3) (Drubin and Kirschner, 1986; Hollenbeck and Saxton, 2005).

Tau was found to be hyperphosphorylated in NFTs in seminal studies of AD brain (Grundke-Iqbal et al., 1986), in primary neurons treated with fibrillar Aβ (Busciglio et al., 1995) and in tissue aggregates from tauopathy brain and tau mutant animals (Lee et al., 2001). While the link between tau phosphorylation and the propensity of tau to aggregate is unclear (Lippens et al., 2007), preventing tau phosphorylation at AD-relevant epitopes is shown to diminish tau aggregation and be neuroprotective (Perez et al., 2003; Hong et al., 1997; Noble et al., 2005). Tau inclusions in AD brain exhibit 45 phosphorylation sites (Fig. 1.2), in comparison to only 10 in control brain, indicating that abnormal tau phosphorylation is key to AD pathogenesis and that targeting tau kinases to reduce tau phosphorylation may be of therapeutic benefit (Hanger et al., 2009). Recent studies in transgenic animal models of AD have raised some doubts as to the pathogenic role of hyperphosphorylated tau (Morris et al., 2015), however, this may simply be an artefact of the model system used for study.

Considerable research has highlighted several prominent protein kinases that phosphorylate tau at serine/threonine residues and can affect its microtubule binding capacity in AD (Avila, 2006). These include the proline directed kinases glycogen synthase kinase-3 (GSK3), cyclin-dependent kinase 5 (cdk5), p38 and c-Jun N-terminal kinase (JNK). GSK3 is known to modify the majority of tau

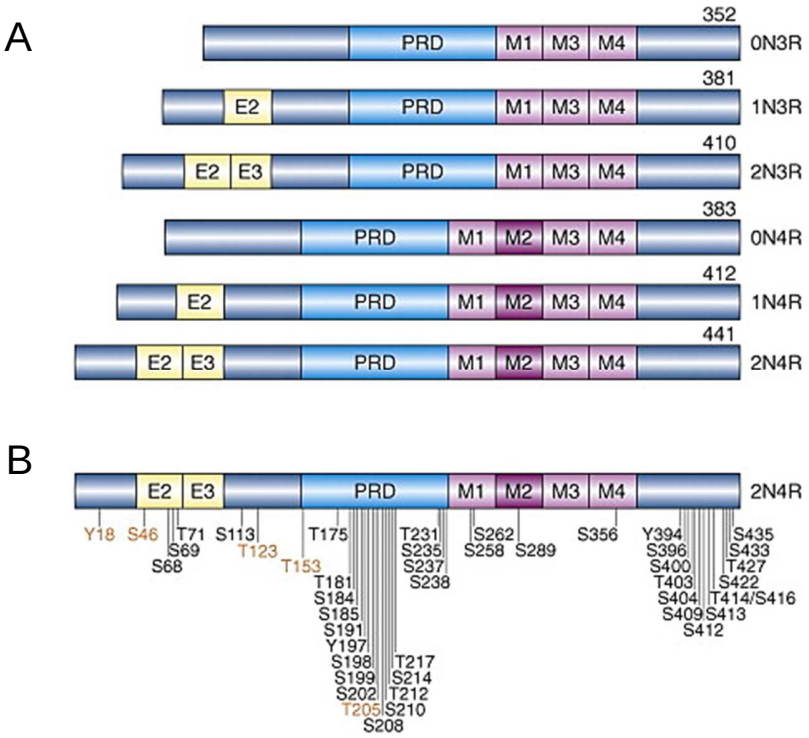

Fig. 1.2 AD brain contains six isoforms of CNS tau abnormally phosphorylated at multiple epitopes. (A) Alternative splicing, inclusion or absence of exons (E) 2, 3 and 10 give rise to the different tau isoforms, with varying numbers of N-terminal inserts (N) and microtubule binding repeats (R). Alzheimer's brain shows equal ratios of each isoform; however, other neurodegenerative diseases, such as FTD-17 and Pick's disease are associated with altered tau ratios. (B) Approximately 45 epitopes are shown to be abnormally phosphorylated in AD tau inclusions. These sites cluster in the proline rich domain (PRD) and in the C-terminal region, with a few sites contained within the microtubule-binding domain (MBD) of tau. Of these sites, 6 have been identified by phospho-specific antibody labelling (indicated in orange) while the remaining sites have been identified by mass spectrometry and/or Edman degradation (adapted from Hanger et al., 2009).

epitopes and has been linked to a variety of pathogenic cascades, including Aβ production, long term potentiation (LTP) impairment, inflammation and neuritic damage (DaRocha-Souto et al., 2012; Hooper et al., 2008). Cdk5 activity is also key to tau pathology as its overexpression in tau mutant mice is associated with

significant aggregation of tau and cortical NFTs (Noble et al., 2003), memory decline and neurodegeneration (Cruz et al., 2003). Inhibition of these tau kinases is neuroprotective in transgenic animals and brain slice cultures (Hinners et al., 2008; Selenica et al., 2007; Noble et al., 2005). However, growing evidence indicates reciprocal regulation between GSK3 and cdk5, which adds a level of complexity to targeting specific tau kinase inhibitors to treat AD (Engmann and Giese, 2009; Chow et al., 2014; Plattner et al., 2006). Moreover, it is unclear which phospho-epitopes are involved in the physiological regulation of microtubule stability, which are abnormally phosphorylated in pathological states and whether there is any overlap.

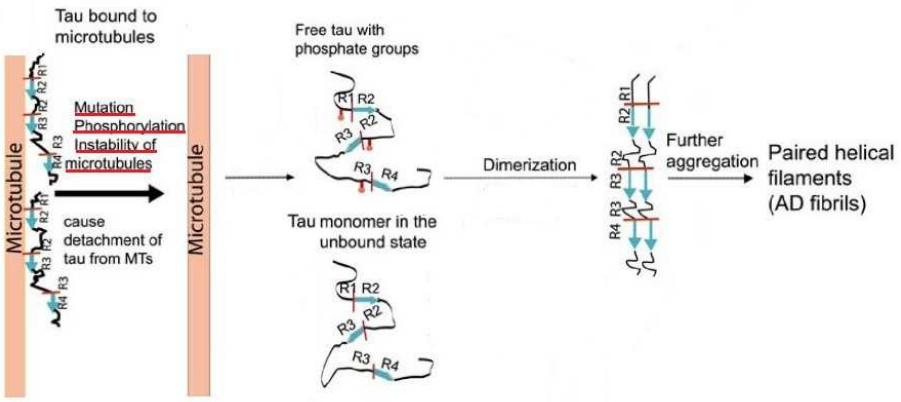

Fig. 1.3. Illustration of the mechanism by which tau aggregates and forms NFTs in AD. Tau is abnormally phosphorylated and aggregates into paired helical filaments (PHF) that eventually form neurofibrillary tangles (NFTs). Tau mutations, hyperphosphorylation of tau or instability of microtubules all cause tau to detach from microtubules. Both phosphorylated and dephosphorylated unbound tau monomers are prone to dimerization which leads to further aggregation into PHF (adapted from Mukrasch et al., 2005)

1.4.3 Amyloid plaques

Amyloid plaques were first observed in abundance in AD brain by Dr. Alzheimer, and have since been used to diagnose disease posthumously, together with NFTs (Wong et al., 1985). Also known as senile and neuritic plaques, amyloid plaques are extracellular deposits of primarily fibrillar and oligomeric Aβ, but are also found to sequester metal ions, proteoglycans and other cell components (reviewed by Atwood et al., 2002). Plaque-associated Aβ is generated by intraneuronal APP processing and the release of Aβ into the extracellular space as soluble peptides, which then aggregate into diffuse amorphous plaques (Ghiso and Frangione, 2002). Aβ is continuously deposited in the extracellular matrix throughout AD progression, and with increasing involvement of neurites, over time results in the formation of dense core neuritic plaques that are also tau-positive (Fig. 1.4). Unlike diffuse plaques, mature plaques stain with Congo red and Thioflavin S and have high β-sheet content, indicating the presence of misfolded fibrillar Aβ (Irvine et al., 2008).

Plaque formation is closely associated with the activation of microglia and astrocytes, which are seen to cluster around plaques in APP mutant mice and in post mortem AD brain (Rozemuller et al., 1986; Frautschy et al., 1998; Mrak et al., 1996). It is hypothesized by some that plaque-adjacent astrocytes exert a neuroprotective effect by forming a barrier that prevents pathological Aβ from damaging surrounding cells; however, activated astrocytes can also suppress

microglial phagocytosis of plaque material in *vitro*, thereby preventing efficient clearance of Aβ and allowing plaques to persist (DeWitt et al., 1998). Moreover, local secretion of soluble Aβ peptide induces astrocytic stress and Ca^{2+} dyshomeostasis, which are widely shown to differentially contribute to downstream neurodegenerative processes in AD (Verkhratsky et al., 2010, 2014; Alberdi et al., 2010; Kulijewicz-Nawrot et al., 2013; Garwood et al., 2011). Taken together, these findings point to a duality of the neuroinflammatory response in the early stages of AD, where glia mediate neuroprotective plaque homeostasis and Aβ clearance, while also perturbing neuronal function. In turn, the production of harmful oxidative and inflammatory molecules by activated glia argues that plaque formation may be a vital early neuroprotective response to AD mechanisms that is lost in the later stages of disease (Atwood et al., 2002).

Although the presence of plaques can predict onset of cognitive symptoms (Serrano-Pozo et al., 2011), it is widely debated whether or not plaques themselves underlie cognitive decline in AD. Clinicopathological studies have shown a weak direct correlation between plaque density and severity of cognitive impairment, and suggest that plaque pathogenesis is mediated by NFTs in late stage AD (Serrano-Pozo et al., 2011). Moreover, early synaptic changes relevant to cognitive deficits are shown to occur prior to plaque deposition in hippocampi of APP/PS1 mice (Cummings et al., 2015). However, the major genetic factors in AD (ApoE4, SORL1, APP and PS mutations; section 1.3.2) are all seen to directly potentiate plaque formation and strongly increase risk of dementia (Mayeux and

Hyslop, 2008). Similar to the situation with tau, recent research has focused on pre-fibrillar intermediates of Aβ which are likely to mediate synaptic dysfunction in AD (Castellani et al., 2008). This is paralleled by an emerging paradigm shift from brain lesions as neurodegenerative triggers to them being considered as neuroprotective 'host' responses to upstream pathogenic processes (Streit and Xue, 2012; Struble et al., 2010).

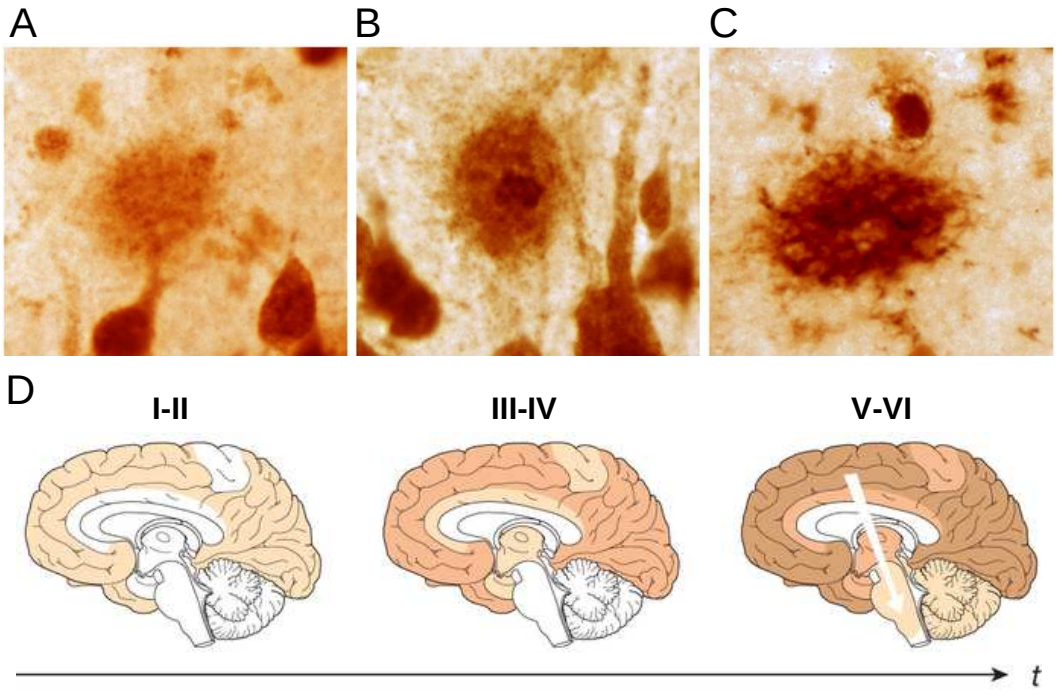

Fig. 1.4 AD brain is characterized by extracellular amyloid plaques containing β-amyloid (Aβ) protein. A-C show immunolabelled Aβ plaques from AD brain. Plaque morphology changes with continued deposition of Aβ from (A) diffuse, amorphous plaques to (B) dense core plaques with high fibrillar Aβ content and (C) tau-positive neuritic plaques. Amyloid deposition occurs in close proximity to neurofibrillary tangles (NFTs). (D) Plaques show the reverse distribution pattern to that of NFTs, with widespread cortical involvement early in disease and penetration to the transentorhinal region and subcortical brain areas (white arrow) in later disease stages. Plaque burden generally increases throughout disease progression. Unlike NFTs, amyloid plaques do not correlate with severity of cognitive phenotype and are not as consistent as NFTs to use for Braak (I-VI) staging (adapted from Jucker and Walker, 2013)

1.4.4 APP processing

The primary constituent of amyloid plaques, Aβ, is a peptide of varying length (38-43 aa) that is constitutively generated from proteolytic processing of APP (O'Brien and Wong, 2011; Zhang et al., 2011). APP is a large type 1 transmembrane protein comprising a long extracellular N-terminal domain, a single transmembrane region and a short cytoplasmic C-terminal tail. Alternative splicing of APP generates 8 isoforms that range from 365 to 770 amino acids (aa), the most common of which are 695, 751 and 770 aa in length, with 695 aa APP being highly expressed in the mammalian CNS (Reinhard et al., 2005). Although the function of APP remains poorly understood, its expression appears to be concentrated in areas of high synaptic activity, with studies suggesting roles for APP in synaptogenesis, synaptic plasticity, neurite growth and cell adhesion (Gralle and Ferreira, 2007). Nascent APP is intracellularly trafficked via the endoplasmic reticulum (ER) and trans-Golgi network, during which it undergoes several post-translational modifications, including O- and N-glycosylation and phosphorylation. APP then undergoes fast axonal transport in post-Golgi vesicles to dendritic and axonal surface membranes where it is expressed as mature protein and exerts its physiological functions (Haass et al., 2012).

APP is differentially metabolized by proteolytic secretases via two opposing pathways - the non-amyloidogenic and amyloidogenic secretory pathways (Zhang et al., 2011; Fig. 1.5). The non-amyloidogenic pathway precludes Aβ formation as

a result of cleavage of APP by α-secretase through the extracellular portion of the Aβ sequence, which generates a truncated C-terminal fragment (C83) lacking the N-terminal region of peptide. Subsequent cleavage of intramembranous APP by γ-secretase releases a truncated Aβ fragment (p3) and the APP intracellular domain (AICD). During amyloidogenesis, APP is extracellularly cleaved by β-secretase to yield a C-terminal fragment (C99), the direct precursor of Aβ, and a large ectodomain of APP (APPsβ). C99 is then cleaved by γ-secretase to release Aβ peptides of varying lengths. Amyloidogenic APP processing occurs on the plasma membrane and at the subcellular level, generating extracellular and intracellular pools of Aβ, both of which exert pathogenic effects in *vitro* (Vetrivel and Thinakaran, 2006; LaFerla et al., 2007).

The two major Aβ species produced from APP are the 40 and 42 aa peptides (Aβ-40 and Aβ-42). Aβ1-42 is able to rapidly aggregate in *vitro* as a result of secondary structural changes (higher β-sheet content and greater hydrophobicity) that enable oligomerization and protofibril formation (Ahmed et al., 2010). In AD patients, Aβ1-42 predominantly accumulates in neurons or is sequestered into neuritic plaques, while Aβ1-40 is found in high amounts in CSF (Portelius, Andreasson, et al., 2010; Gouras et al., 2000). Application of soluble Aβ1-42 oligomers to primary neurons causes neurotoxicity (Hartley et al., 1999; Atherton et al., 2014) and accumulation of Aβ1-42 in animals leads to synaptic loss and cognitive dysfunction (Stéphan et al., 2001; Walsh et al., 2002a). Moreover, Aβ1-42 has been extensively linked to tau phosphorylation and truncation, Ca^{2+}

abnormalities and oxidative stress, and is therefore considered an important upstream pathogenic trigger in AD (Zempel et al., 2010; De Felice et al., 2007; Ittner et al., 2010; Liang et al., 2010). Numerous studies, including this work, therefore use soluble oligomeric Aβ1-42 to model AD mechanisms in *vitro.*

In FAD, missense mutations in APP and PS1/2 shift homeostatic APP processing towards Aβ production, resulting in either 1) overproduction of all peptides, 2) increased Aβ1-42:40 ratio or 3) increased fibrillisation of Aβ (section 1.3.1; Morris et al., 2014; Weggen and Beher, 2012). While LOAD aetiology lacks mutations in *APP* or *PS1/PS2* genes, the majority of AD patients still show increased levels of brain and CSF Aβ, likely as a result of the presence of susceptibility genes and/or environmental factors (Lacor et al., 2004; Atherton et al., 2014). For example, high dietary cholesterol, associated with increased ApoE ε4 and LOAD risk (section 1.3.2), is known to affect Aβ production (Sing and Davignon, 1985). Cholesterol depletion promotes non-amyloidogenic APP processing in human embryonic kidney (HEK) cells overexpressing the α-secretase ADAM10 (Kojro et al., 2001), and reduces Aβ production in APP-transfected hippocampal neurons (Simons et al., 1998). Moreover, deficiency of proteases involved in physiological APP processing are thought to potentiate amyloidogenesis (Fig. 1.5; Selkoe, 2001).

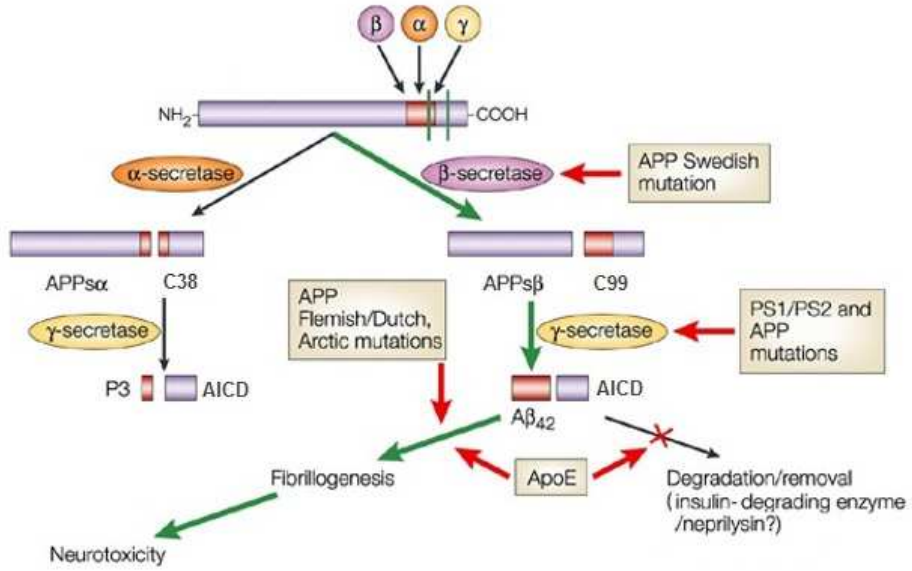

Fig 1.5 Amyloid precursor protein (APP) is proteolytically processed via two pathways: non-amyloidogenic (black arrows) and amyloidogenic (green arrows). Non-amyloidogenic APP processing precludes formation of pathogenic β-amyloid (Aβ) by α- and γ-secretase-mediated truncation of the Aβ sequence. Amyloidogenic APP processing results in Aβ formation through β- and γ-secretase-mediated cleavage around the Aβ sequence. Familial mutations favour amyloidogenesis, which may be also influenced by levels of apolipoprotein ε (ApoE) protein and physiological APP proteases (adapted from Sisodia and St George-Hyslop, 2002)

1.4.5 The amyloid cascade hypothesis of AD

The amyloid cascade hypothesis of AD proposes that brain Aβ protein, whether in soluble or fibrillar form, or contained within plaques, acts as the pathogenic trigger of cascades leading to formation of NFTs, perturbation of synaptic function

and ultimately neuronal demise (Reitz, 2012; Hardy and Higgins, 1992; Suzuki, 1997). Evidence from recent studies has shifted the focus from amyloid plaques, which are now argued by some to protect the brain from harmful chemicals generated during AD progression (Castellani et al., 2008; Atwood et al., 2002), to soluble Aβ oligomers, which are shown to directly perturb synaptic function and cause neurotoxicity in cell and animal models of AD (McLean et al., 1999; Haass and Selkoe, 2007; Sivanesan et al., 2013; Lue et al., 1999). However, decades of scientific research following the introduction of the amyloid hypothesis in the mid-1980s have led to evidence both for and against a primary role for Aβ in AD pathogenesis (reviewed by Morris et al., 2014).

The discovery that DS individuals with early dementia harbour a triple copy of APP, display increased Aβ production and AD-like brain lesions first linked AD phenotype to aberrant APP physiology and Aβ production (section 1.3.1). However, it is important to note that not all DS individuals develop AD (Zigman et al., 2008), suggesting that Aβ may not be the sole risk factor in DS and AD. While FAD cases are attributed to mutations in *APP* and *PS* genes, known to increase Aβ/Aβ1-42 production, these individuals comprise less than 1 % of all AD cases, while the rest suffer from LOAD that lacks mutations in the above genes (section 1.3). On the other hand, increased dosage of ApoE ε4 and polymorphisms in *TREM2* - the only known high risk LOAD loci to date - are both shown to modulate Aβ production and clearance (section 1.3.2). The notion that other pathogenic events, aside from increased Aβ production, cause AD is also supported by animal

models. APP and PS1 mutant rodents are shown to recapitulate several of the features of human AD, such as Ca^{2+} dyshomeostasis and synaptic dysfunction (Kuchibhotla et al., 2008; Webster et al., 2014; Cummings et al., 2015; Matarin et al., 2015); however, the recently established 3xTg-AD (triple transgenic AD) mouse expressing APP_{SWE}, $PS1_{M146V}$ and $MAPT_{PS01L}$ mutations was the first model to demonstrate a clear age-dependent onset of AD pathology (Oddo et al., 2003) that was consistent with human disease (Mastrangelo and Bowers, 2008; Volicer et al., 2001). In this model, early accumulation of soluble Aβ is followed by plaque deposition at 4 months and NFT formation at 6 months, and animals also exhibit synaptic deficits and circadian rhythm abnormalities (Oddo et al., 2003). These findings suggest that toxic Aβ oligomers may lie upstream of a pathogenic chain of events, including abnormal tau phosphorylation and synaptic dysfunction, which are shown to be critical to Aβ neurotoxicity (Zempel et al., 2010; Liang et al., 2010; Hung et al., 2005; Jin, Yin, Yu, et al., 2015).

Notably, perturbation of synaptic function is shown to be a central event in AD that underpins the progressive memory deficits and impaired learning abilities seen in patients (Selkoe, 2002). Early cortical biopsies revealed up to 35 % reduction in synaptic density within a few years of onset of clinical AD (Davies et al., 1987), with synapse loss correlating more robustly with early cognitive symptoms than plaques and tangles, gliosis or neuronal loss (Terry et al., 1991). The observations of increased levels of soluble Aβ in MCI patients (Lue et al., 1999) and, recently, decreased synaptic density in APP mutant mouse

hippocampus (Price et al., 2014) suggest a causal link between Aβ and synaptic dysfunction in AD. Indeed, APP transgenic mice display depletion of presynaptic terminals coupled with an increase in soluble Aβ at an early age, prior to plaques (Elder et al., 2010), and Aβ diminishes LTP, synapses and spine counts in neurons (Zempel et al., 2010). Furthermore, altered synaptic gene expression and function is seen to occur prior to plaque deposition in APP/PS1 mice (Cummings et al., 2015). Therefore, it is likely that the increasing soluble pool of Aβ is responsible for the synaptic and cognitive changes in AD. The mechanisms through which Aβ disrupts synaptic function are shown to include caspase-2 activation, (Pozueta et al., 2013; Bredesen et al., 2010), tau missorting (Hoover et al., 2010), oxidative stress (section 1.5.3; Forero et al., 2006) and Ca^{2+} dyshomeostasis (section 1.5.2 Sun et al., 2014).

Despite the above evidence that Aβ is, at least in part, responsible for the neuropathological features of AD, anti-Aβ therapies have so far failed to halt disease progression or alter cognitive phenotype in clinical trials (Conway et al., 2003). These therapies either directly targeted Aβ by active and passive immunization or prevented Aβ production through inhibition of γ- and β-secretases and PS (Morris et al., 2014). Recently, focus has been shifted to anti-tau therapies, which aim to prevent abnormal tau phosphorylation and aggregation by 1) inhibition of specific tau kinases, 2) directly immunizing against tau, and 3) disaggregating existing tau inclusions in the brain (Hanger et al., 2009). This group has previously shown that inhibition of GSK3 by lithium reduced tau

phosphorylation and rescued neurodegeneration and cognitive deficits in *vivo* (Noble et al., 2005), and other tau therapies have shown promise in multiple animal models of AD (reviewed by Brunden et al., 2009). Therefore, it is likely that combined therapies targeting multiple disease pathways, including Aβ and tau, may be required to effectively halt AD progression.

1.5 The Ca^{2+} hypothesis of AD

In the brain, Ca^{2+} functions as a ubiquitous intracellular messenger that orchestrates a host of glial and neuronal functions, including glial information exchange, neuronal excitability, synaptic transmission, plasticity and metabolism (Cheng et al., 2006; Deitmer et al., 1998). The functionality and viability of the different CNS cell types requires tight regulation of intracellular Ca^{2+} levels and signalling, as deviations from physiological concentrations can be cytotoxic and trigger pro-apoptotic and necrotic mechanisms of cell death (Berridge et al., 2000). The ways through which intracellular Ca^{2+} is fine-tuned include 1) regulated Ca^{2+} entry and exit via plasma membrane Ca^{2+}-permeable channels, receptors and protein pumps, 2) intracellular Ca^{2+} buffering, 3) sequestration of Ca^{2+} into intracellular stores and 4) extrusion of excess cellular Ca^{2+} (Fig. 1.6).

In AD, numerous components of the neuronal and glial Ca^{2+} toolkit are perturbed to result in intracellular Ca^{2+} overload and subsequent aberrant induction of Ca^{2+} signalling cascades (Grolla et al., 2013; Lim et al., 2014; Abramov et al., 2004;

Thibault et al., 2007). According to substantial evidence, including this work, these Ca^{2+} perturbations contribute to the early synaptic and cognitive changes seen in prodromal AD (Chakroborty and Stutzmann, 2011; Chakroborty et al., 2012; Rubio-Moscardo et al., 2013; Chakroborty et al., 2012; Supnet and Bezprozvanny, 2010), and mediate the subsequent neurodegenerative processes in later stages of AD (Buxbaum et al., 1994; Pierrot et al., 2006; Aarts and Tymianski, 2005).

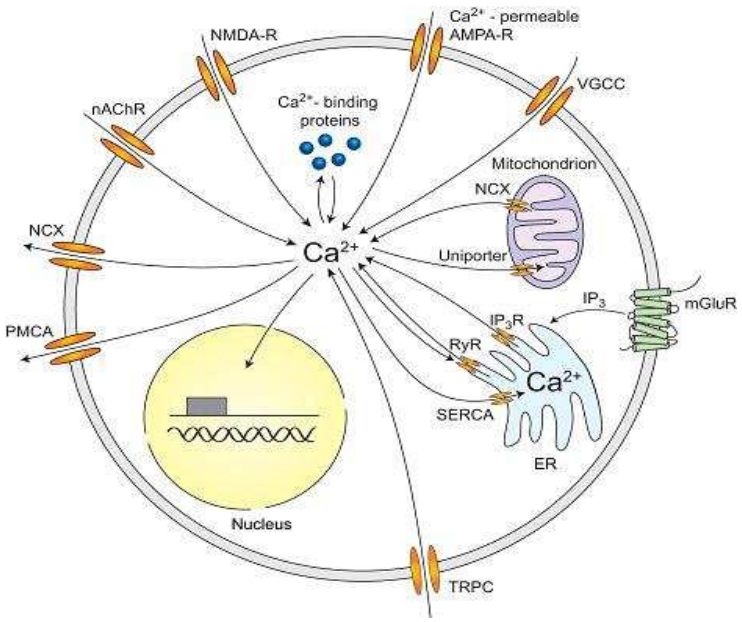

Fig 1.6 The fine-tuning of homeostatic intracellular Ca^{2+}concentrations is crucial for neuronal function. This is mediated by 1) regulated entry of Ca^{2+} through plasma membrane proteins, including voltage-gated calcium channels (VGCCs), N-Methyl-D-aspartate receptors (NMDA-R), non-NMDA glutamate receptors (AMPA-R), nicotinic acetylcholine receptors (nAChR), and transient receptor potential channels (TRPC), 2) intracellular Ca^{2+} buffering by Ca^{2+}-binding proteins, 3) sequestration of Ca^{2+} into endoplasmic reticulum (ER) and mitochondria via sarcoendoplasmic reticulum Ca^{2+} ATP-ase (SERCA) and sodium calcium exchanger (NCX) pumps, respectively, and 4) the extrusion of excess Ca^{2+} via protein pumps, including NCX and the plasma membrane Ca^{2+} ATP-ase (PMCA). In sporadic AD models, these mechanisms of Ca^{2+} regulation are differentially perturbed directly by Aβ or through Aβ-induced signalling cascades (Grienberger and Konnerth, 2012)

1.5.1 Ca^{2+} dysregulation in FAD

Disruptions of intracellular Ca^{2+} are thought to underlie the development of FAD (Etcheberrigaray et al., 1998) and this is replicated in several animal models of FAD (Honarnejad and Herms, 2012; Smith et al., 2005). In particular, PS1/2 mutations cause perturbations in ER Ca^{2+} homeostasis by altering the ER Ca^{2+} leak function of PS (Tu et al., 2006). In mouse embryonic fibroblasts, (MEF) ablation of *PS1* and *PS2* genes resulted in increased PS-mediated Ca^{2+} leak, which accounts for 80% of the total passive release from the ER (Tu et al., 2006). Expression of PS with FAD mutations in transgenic mice and cell lines also enhances Ca^{2+} release from ER via inositol 1,4,5-trisphosphate receptors (IP_3Rs), which contributes to cytosolic Ca^{2+} filling (Stutzmann et al., 2004, 2007). This is amplified by stimulation of ER Ca^{2+}-sensitive ryanodine receptors (RyR) by IP_3R-liberated Ca^{2+}, which mediates further RyR-mediated Ca^{2+} release from ER - a mechanism termed Ca^{2+}-induced Ca^{2+} release (CICR; Verkhratsky and Shmigol, 1996). In addition, increased activity of the sarcoendoplasmic reticulum calcium transport ATPase (SERCA) in PS1 mutant mice increases Ca^{2+} sequestration into the ER, which in turn leads to ER Ca^{2+} overload (Supnet and Bezprozvanny, 2010). Together, these fluctuations in intra-ER Ca^{2+} alter the activity of ER proteins to result in ER stress, which leads to impaired synaptic plasticity, excitotoxicity and apoptosis (Verkhratsky and Toescu, 2003; Rose and Konnerth, 2001; Sokka et al., 2007).

Post mortem cerebellar tissue from FAD patients carrying the PS1-E280A mutation display abnormal mitochondrial morphology, reduction of Ca^{2+}-dependent mitochondrial transport proteins adaptor protein mitochondrial Rho GTPase and protein kinesin heavy chain isoform 5C, and diminished cerebellar activity prior to plaque formation (Sepulveda-Falla et al., 2014). Moreover, respiratory stress associated with mitochondrial dysfunction occurs downstream of perturbed ER Ca^{2+} homeostasis and prior to brain lesions in AD brain (Celsi et al., 2009). It is therefore hypothesized that early disruption of intracellular Ca^{2+} stores and accelerated Aβ deposition, both induced by FAD mutations, act in concert to trigger downstream neurodegenerative processes, such as plaque formation, during the progression of AD.

1.5.2 Ca^{2+} dysregulation in LOAD

The initial finding that Aβ neurotoxicity is abolished in Ca^{2+} free solutions, or in the presence of L-type voltage gated Ca^{2+} channel (L-VGCC) antagonists, implicated the influx of extracellular Ca^{2+} in Aβ-mediated neurotoxicity (Brorson et al., 1995). Indeed, in cell culture, Aβ was found to upregulate the activity of Ca^{2+}-permeable membrane proteins, including VGCCs, NMDARs and Na^+/K^+-ATPases either by oxidative modification or direct binding to receptors (Mark et al., 1995; Kasparová et al., 2001; Ueda et al., 1997; Molnár et al., 2004), resulting in cytotoxic intracellular Ca^{2+} elevations. Notably, NMDAR expression was shown

to determine neuronal vulnerability to Aβ (Danysz and Parsons, 2012), and Aβ-induced excitotoxic Ca^{2+} elevations require excess stimulation of NMDAR receptors (Harkany et al., 2000a). Aβ was also shown to spontaneously insert voltage-sensitive Ca^{2+}-permeable pores in the lipid bilayer of plasma and mitochondrial membranes, which further promotes overload of cytosolic and mitochondrial Ca^{2+}, intramitochondrial accumulation of Aβ and mitochondrial dysfunction (Demuro et al., 2011; Chen and Yan, 2010). In individuals with high susceptibility to LOAD (section 1.3.2), single nucleotide polymorphisms of the CALHM1 channel increases neuronal Ca^{2+} permeability and Aβ production, and the ε4 ApoE allele dose-dependently increases cytosolic Ca^{2+} through activation of P- and Q-VGCCs (Dreses-Werringloer et al., 2008; Muller et al., 1998). Studies in primary cortical neurons have also revealed that Aβ-induced Ca^{2+} overload and neuronal death is mediated by depletion of ER Ca^{2+} stores (Suen et al., 2003; Ferreiro et al., 2006), which suggests that disrupted ER Ca^{2+} homeostasis is a shared feature of FAD and LOAD.

The excess accumulation of cytosolic Ca^{2+} in neural cells leads to the activation of Ca^{2+}-sensitive proteases, including calpains and caspases, which are known to contribute to a wide variety of neurodegenerative processes in AD (Chan and Mattson, 1999). Calpains are overactive in AD brain (Huh et al., 2001; Atherton et al., 2014; Nixon et al., 1994; Saito et al., 1993), and cause dysregulated proteolysis of key structural and signalling proteins, including cytoskeletal α-spectrin and tau (Atherton et al., 2014; Warren et al., 2007). Tau is pathologically truncated by

calpains to result in generation of toxic species that promote tau phosphorylation and aggregation, and are also directly toxic to neurons in cell models of AD (Flores-Rodríguez et al., 2015; Park and Ferreira, 2005; Liu et al., 2011), although the physiological significance of these fragments has been the subject of debate (Garg et al., 2011). Importantly, calpain-mediated N-terminal truncation and activation of key tau kinases, GSK3 and cdk5, causally links calpain activity to tau phosphorylation in multiple studies, including this work (Taniguchi et al., 2001; Jin, Yin, Yu, et al., 2015; Rao et al., 2014). The activation of caspases by calpains promotes further caspase-mediated tau cleavage and triggers caspase-dependent synaptic dysfunction and apoptotic signalling (Juin et al., 1998; Nakagawa and Yuan, 2000; Chan and Mattson, 1999), although the relevance of this for neurodegeneration in AD is also unclear (de Calignon et al., 2010). Early Ca^{2+} changes are also thought to alter APP function and metabolism through altered calpain activity, to promote further Aβ production, for instance through increased β-secretase activation (Kyratzi & Efthimiopoulos 2014; Buxbaum et al. 1994; Liang et al. 2010; Koppel et al. 2011; Pierrot et al. 2006; Mathews et al., 2002). In turn, accumulation of tau and Aβ in dendritic spines is shown to perturb the spine-specific Ca^{2+} transients that mediate memory formation, instead causing progressive global Ca^{2+} elevations that precede neuronal death (Michael Berridge, personal communicaton; Ittner et al., 2010; Zempel et al., 2010).

Recently, experiments in this laboratory, including this work, have shown that Aβ-induced calpain overactivation may also affect the extrusion of cytosolic Ca^{2+} in

AD (Chapter 3; Atherton et al., 2014). Primary neurons exposed to Aβ display increased calpain activity and generation of inactive and calpain-cleaved species of the sodium calcium exchanger (NCX) 3 (Atherton et al., 2014) - also observed here in end-stage AD brain. NCXs play a vital role in Ca^{2+} homeostasis as they provide the major route of Ca^{2+} efflux in conditions of excess intracellular Ca^{2+} (Verkhratsky et al., 2013). As shown in this work, perturbation of NCX3 function confers neuronal vulnerability to subtoxic doses of Aβ, which suggests that impaired Ca^{2+} extrusion may also contribute to excitotoxicity and neuronal death in AD (Atherton et al., 2014).

1.5.3 Oxidative stress and Ca^{2+} regulation in AD

Oxidative stress, the build-up of reactive oxygen species (ROS) to an extent that exceeds the antioxidant capacity of a cell, increases neuronal vulnerability to excitotoxicity by inducing aberrant Ca^{2+} signalling (Naziroğlu, 2011). Multiple studies have shown that Aβ induces oxidative stress in neurons, which leads to DNA damage and activation of DNA-dependent nuclear poly(ADP-ribose) polymerase-1 (PARP-1; De Felice et al., 2007; Canevari et al., 2004; Fonfria et al., 2005; Abeti et al., 2011). Depending on the 'repairability' of the DNA damage, PARP-1 determines cell fate either by initiating DNA repair or signalling apoptosis (Andrabi et al., 2006; Fonfria et al., 2005). Active PARP-1 catalyzes the synthesis of ADP-ribose (ADPR) polymers (PAR), which are attached to nuclear acceptor

proteins for genomic stability, or translocate to the cytoplasm for signal transduction to different cellular compartments (Scovassi and Poirier, 1999). PARP signalling and 'PARylation' are in turn regulated by nuclear poly(ADP-ribose) glycohydrolase (PARG), which hydrolyses PAR into free ADPR. In the cytoplasm, ADPR acts as a potent activator of transient receptor potential melastatin type 2 (TRPM2) - a non-selective Ca^{2+}-conducting channel that is highly expressed in the brain (Xie et al., 2010). ADPR binds and activates TRPM2, leading to channel pore opening and entry of Ca^{2+} down an electrochemical gradient.

PARP activity and PAR formation are increased in AD brain (Love et al., 1999), suggesting that downstream aberrant TRPM2 stimulation and disrupted Ca^{2+} homeostasis could contribute to neuronal death in AD. Indeed, PARP-induced activation of TRPM2 channels was required for Aβ neurotoxicity in primary striatal neurons, as inhibition of TRPM2 activity either by pharmacological blockade, co-expression of the endogenous short isoform TRPM2-S which lacks functional activity, or small interference RNA targeting TRPM2 rescued excitotoxicity and neurodegeneration caused by H_2O_2 or Aβ (Fonfria et al., 2005). However, it is uncertain at which stage TRPM2 is activated during the time course of neuronal Ca^{2+} changes induced by Aβ. For example, PARP-1 is activated rapidly following stereotactic injection of NMDA into mouse striatum, and is required for NMDAR-dependent excitotoxicity in these animals (Mandir et al., 2000). On the other hand, TRPM2 channels were found to modulate NMDAR subunit expression,

thereby conferring neuronal vulnerability to ischaemic neuronal death (Alim et al., 2013). Moreover, it remains to be determined whether changes in TRPM2 expression and function underlie neurodegenerative or neuroprotective processes in AD. Figure 1.7 illustrates the differential effects of Aβ on neuronal regulation and signalling, as shown in cell models of AD.

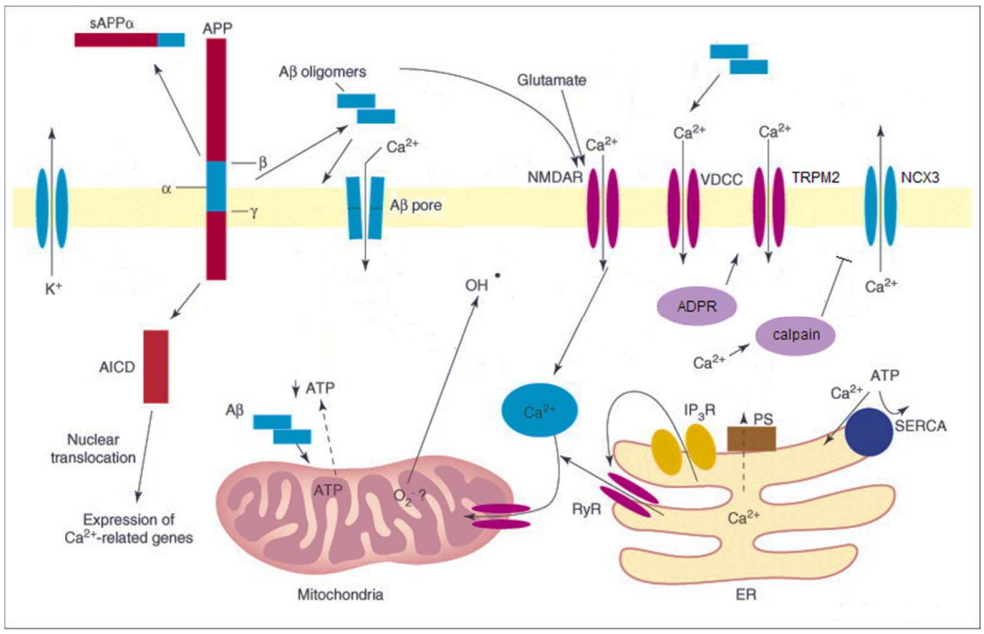

Fig 1.7 In cell models of AD, Aβ proteolytically cleaved from APP disrupts intracellular Ca^{2+} homeostasis. This occurs through 1) stimulation of excess influx of extracellular Ca^{2+} through plasma membrane VGCCs, NMDARs and TRPM2 channels, 2) increased release of Ca^{2+} from the ER and 3) impaired extrusion of excess cytosolic Ca^{2+} through NCX3. Aβ directly modifies VGCC and NMDAR activity and indirectly activates TRPM2 channels through increased PARP activity and ADPR synthesis. The Aβ-induced increases in Ca^{2+} cause aberrant activation of calpains, which proteolytically cleave NCX3, and increased Ca^{2+} influx into mitochondria, followed by mitochondrial stress (adapted from Park et al., 2014)

1.6 Aims and objectives of this thesis

The aim of this study was to further investigate the mechanisms underlying Ca^{2+} dyshomeostasis in AD, as well as to gain insights into the role of Ca^{2+} in downstream neurodegenerative processes that occur during the progression of disease.

The specific objectives of this work were to investigate:

1. Changes in Ca^{2+}-activated proteins in post mortem brain from different stages of AD, with comparison to brains from other neurodegenerative diseases and control tissue
2. The mechanisms through which Aβ induces neural Ca^{2+} dyshomeostasis
3. The contribution of Ca^{2+}-activated proteins to Aβ-induced pathogenic mechanisms and neurotoxicity

CHAPTER 2

Materials and Methods

2.1 Materials

All reagents used for the experiments described in this thesis were obtained from Sigma-Aldrich Company, Ltd., Dorset, UK, detailed below, unless otherwise stated. All plasticware used for tissue culture was purchased from Fischer Scientific Ltd., UK. Ultrapure water was used in preparation of all solutions and was dispensed from an Elgar® Maxima water purification system (Veolia Water Ltd., UK). All reagents and materials used for tissue culture were sterilised by autoclaving at 15lb/inch^2 for 90 min.

2.1.1 General molecular biology reagents

Oligonucleotides

Table 2.1 lists the synthetic phosphorothioated sense and antisense oligonucleotides used to suppress NCX3 expression.

Oligonucleotide	Sequence (5' → 3')	Source	Primary Reference
NCX3-as1	GCCATACACAAGAG	Eurofins MWG Operon LLC, Germany	(Iwamoto and Kita, 2006)
NCX3-s1	CTCTGTGTATGGC	Eurofins MWG Operon LLC, Germany	(Iwamoto and Kita, 2006)

Table 2.1. Phosphorothioated sense and antisense oligonucleotides used for molecular experiments. The oligonucleotide name, sequence, manufacturer and primary references are given.

Transfection Reagents

Lipofectamine 2000® (Invitrogen Ltd., UK)

OptiMEM I (Invitrogen Ltd., UK)

2.1.2 Cell culture materials

Primary cortical cultures

Poly-D-lysine 10 µg/ml poly-D-lysine

Complete Neurobasal™ medium	Neurobasal™ medium without phenol red (Life technologies Ltd., UK) 1 % (v/v) B27 supplement 2 M L-glutamine (PAA Laboratories) 60 units/ml penicillin (PAA Laboratories) 100 units/ml streptomycin (PAA Laboratories)
Trypsin/ ethylenediaminetetraacetic acid (EDTA)	Trypsin(EDTA) 1x in Hank's Balanced Salt Solution (HBSS; Life Technologies Ltd., UK), without Ca^{2+} and Mg^{2+}
DNase I	Components supplied with Papain dissociation system

	(Worthington Biochemical Corporation, New Jersey, USA) 2000 U/ml deoxyribonuclease in Earl's Balanced Salt Solution (EBSS; Life Technologies, Ltd., UK)
Albumin-ovomucoid protease solution	Components supplied with Papain dissociation system (Worthington Biochemical Corporation, New Jersey, USA) 10 mg/ml ovomucoid 10 mg/ml albumin in EBSS
HBSS	Without Ca^{2+} and Mg^{2+} (Life Technologies, Ltd. UK)

Trypan blue	0.4 % trypan blue solution (Thermo Fischer Scientific Inc., MA, USA)

SH-SY5Y cultures

Supplemented DMEM: F-12	Dulbecco's modified eagle medium (DMEM; Lonza Ltd., UK) with Ham's F-12 (1:1) with 15 mM 4-2(2-hydroxyethyl)-1-piperazineethanesulfonic acid (HEPES) with phenol red 10 % (v/v) foetal bovine serum (FBS) (Sera Laboratories International) 2 M L-glutamine (PAA Laboratories)

60 units/ml penicillin (PAA Laboratories)

100 units/ml streptomycin (PAA Laboratories)

2.1.3 General cell biology solutions

Chemical and biological agents for cell culture

Chemical and biological agents used to treat primary neuronal cultures are summarised in Table 2.2.

Chemical/biological agent	Primary target/function	Source
SB750139	Poly(ADP-ribose) polymerase (PARP) inhibitor	Obtained under a Material Transfer Agreement (MTA) from Glaxo-Smith Kline Plc., UK

Calpeptin	Calpain inhibitor (Tsujinaka et al., 1988)	Merck Chemicals Ltd., UK
(+)-MK 801 Maleate	Irreversible N-methyl-D-aspartate receptor antagonist, prevents Ca^{2+} influx	Merck Millipore Ltd., UK
Caspase inhibitor IV	Irreversible pan-caspase inhibitor	Merck Millipore Ltd., UK
Lithium Chloride (LiCl)	Salt, glycogen synthase kinase inhibitor	Sigma-Aldrich Ltd., UK
Sodium Chloride (NaCl)	Salt, used as vehicle in LiCl experiments	Sigma-Aldrich Ltd., UK
Potassium Chloride (KCl)	Neuronal depolarization agent	Sigma-Aldrich Ltd., UK
Hydrogen peroxide (H_2O_2)	Reactive oxygen species, induces oxidative stress	Sigma-Aldrich Ltd., UK

β-amyloid (Aβ) 1-42, human	Synthetic Aβ1-42 peptide, models amyloid cascade in *vitro*	California Peptide Research Inc., CA, USA
β-amyloid (Aβ) 1-42, human	Secreted from 7PA2 Chinese Hamster Ovary (CHO) cells stably expressing mutant (V717F) human amyloid precursor protein (APP)	Professor D. Walsh (Harvard Medical School)

Table 2.2. Chemical and biological agents used to treat primary neuronal cultures. Agent name, primary target and manufacturer are given.

Protein buffering and tissue lysis solutions

Phosphate-buffered saline (PBS)	1 PBS tablet dissolved in 200ml ultra-pure H_2O to give a final concentration of: 10 mM phosphate 137 mM NaCl 2.7 mM KCl, pH 7.4 In ultra-pure H_2O

PBS-T	PBS containing 50 mM Tween-20 In ultra-pure H_2O
Tris-buffered saline (TBS)	50 mM Tris, pH 7.6 150 mM NaCl In ultra-pure H_2O
TBS homogenization buffer	50 M TBS, pH 7.4 2 mM ethylene glycol tetraacetic acid (EGTA) Mini protease inhibitor cocktail tablet, 1 tablet in 10 ml (Roche Diagnostics Ltd., UK) In ultra-pure H_2O
Extra strong lysis buffer (ESLB)	10 mM Tris-HCl, pH 7.5

	75 mM NaCl 0.5 % (w/v) sodium dodecyl sulfate (SDS) 20 mM sodium deoxycholate 1 % (v/v) Triton X-100 2 mM Na_3VO_4 1.25 mM NaF 10 mM EDTA Mini protease inhibitor cocktail tablet, 1 tablet in 10 ml (Roche Diagnostics Ltd., UK) In ultra-pure H_2O
2 x protein loading buffer (National Diagnostics Ltd., UK)	0.5 M Tris-HCl, pH 6.8 4.4 % (w/v) SDS 20 % (v/v) glycerol

	2 % (v/v) 2-mercaptoethanol (β-ME)
	0.01 % (w/v) bromophenol blue

2.1.4 Enzyme-linked immuno-sorbent assay (ELISA)

Standard diluent buffer	ESLB
	TBS
	Mini protease inhibitor cocktail tablet, 1 tablet in 10ml (Roche Diagnostics Ltd., UK)
Sample diluent buffer	TBS
	Mini protease inhibitor cocktail tablet, 1 tablet in 10ml (Roche Diagnostics Ltd., UK)
Standard Reconstitution Buffer	55 mM $NaHCO_3$, pH 9.0

in ultrapure H_2O

Remaining components and solutions were provided with:

Human Aβ1-40 ELISA kit, Invitrogen Ltd., UK

Human Aβ1-42 ELISA kit, Invitrogen Ltd., UK

2.1.5 SDS polyacrylamide gel electrophoresis (SDS-PAGE)

Acrylamide gels for SDS-PAGE were prepared by diluting stocking solutions from National Diagnostics Ltd. (UK) in ultra-pure H_2O.

Final gel compositions were:

7.5 % resolving gel, pH 8.8	7.5 % (v/v) acrylamide
	25 % (v/v) resolving buffer
	0.01 % (w/v) ammonium persulphate (APS)

	0.1 % (v/v) N, N, N', N' tetramethylethylenediemine (TEMED) In ultra-pure H_2O
10 % resolving gel, pH 8.8	10 % (v/v) acrylamide 25 % (v/v) resolving buffer 0.01 % (w/v) APS 0.1 % (v/v) TEMED In ultra-pure H_2O
12 % resolving gel, pH 8.8	12 % (v/v) acrylamide 25 % (v/v) resolving buffer 0.01 % (w/v) APS 0.1 % (v/v) TEMED In ultra-pure H_2O

16 % resolving gel, pH 8.8	16 % (v/v) acrylamide 25 % (v/v) resolving buffer 0.01 % (w/v) APS 0.1 % (v/v) TEMED In ultra-pure H_2O
4 % stacking gel, pH 8.8	4 % (w/v) acrylamide 25 % (v/v) stacking buffer 0.075 % (w/v) APS 0.1 % (v/v) TEMED In ultra-pure H_2O
Gel running buffers	10x Tris-Glycine-SDS-PAGE Buffer (Scientific Laboratory Supplies, Ltd., UK) Diluted to 1x in ultrapure H_2O

	10x Tris-Tricine-SDS-PAGE Buffer (Scientific Laboratory Supplies, Ltd., UK) Diluted to 1x in ultrapure H_2O

Western blotting

Immunoblotting transfer buffer (Scientific Laboratory Supplies, Ltd., UK)	10x Tris-Glycine-Buffer 20 % (v/v) methanol in ultrapure H_2O
Ponceau S red solution	7 % (v/v) glacial acetic acid 0.2 % (w/v) Ponceau S red in ultrapure H_2O

5 % milk blocking solution	5 % (w/v) non-fat skimmed milk powder in PBS
Odyssey blocking solution	Odyssey blocking solution (LiCor Biosciences, NE, USA) diluted 1:1 with PBS
5% BSA blocking solution	5 % bovine serum albumin (BSA) (w/v) in PBS

Protein molecular weight markers

Precision Plus® Protein All Blue Standard (Bio-Rad Laboratories Inc., CA, USA) with 10 pre-stained bands ranging from 250kDa to 10kDa

2.1.6 Live microscopy

Extracellular (EC) buffer (pH 7.4)	121 mM NaCl 6 mM $NaHCO_3$ 5.4 mM KCl

	5.5 mM D-Glucose
	0.8 mM $MgCl_2$
	25 mM HEPES
	1.8 mM $CaCl_2$
	in ultrapure H_2O
Ca^{2+}-free EC buffer (pH 7.4)	121 mM NaCl
	6 mM $NaHCO_3$
	5.4 mM KCl
	5.5 mM D-Glucose
	0.8 mM $MgCl_2$
	25 mM HEPES
	in ultrapure H_2O
High K^+ EC buffer (pH 7.4)	5 mM NaCl
	129 mM KCl

	30 mM D-Glucose 1 mM $MgCl_2$ 25 mM HEPES 2 mM $CaCl_2$ in ultrapure H_2O
Fluo-4-AM	1 mM fluo-4-AM (Life Technologies, UK) in anhydrous DMSO
Pluronic® F-127	20% (Life Technologies, UK) in anhydrous DMSO

2.1.7 Immunocytochemistry (ICC)

4 % paraformaldehyde (PFA)	4 % (w/v) PFA in PBS, or diluted in PBS from 16 % liquid

	PFA stock solution (Alfa Aesar, Johnson Matthey Co., MA, USA)
Permeabilisation solution	5 % (w/v) BSA 0.05 % (v/v) Triton X-100 In PBS
Blocking solution	5 % (w/v) BSA 0.05 % (v/v) Triton X-100 In PBS
Hoechst 33342	10 mg/ml bisbenzimide H33342 trihydrochloride (Hoescht 33342) In PBS

2.1.8 Antibodies

Table 2.3 lists details of the primary antibodies used for western blotting (WB).

Antibody	Epitope and Specificity	Species	Dilution	Source	Blocking reagent
DAKO	Total tau, phosphorylation-independent	Rabbit IgG	1:20,000	Dako Ltd., UK	5 % milk blocking solution
PHF-1	Tau phosphorylated at Ser396/404	Mouse IgG	1:2000	Kind gift from Prof Peter Davis (Albert Einstein College of Medicine, New York)	5 % milk blocking solution

CP13	Tau phosphorylated at Ser202	Mouse IgG	1:200	Kind gift from Prof Peter Davis (Albert Einstein College of Medicine, New York)	5 % milk blocking solution
Tau-1	Tau dephosphorylated at Ser 195/198/199/202	Mouse IgG	1:5000	Merck Millipore Ltd., UK	5 % milk blocking solution
6E10	Amino acids 1-17 of human Aβ sequence	Mouse IgG	1:500	Cambridge Biosciences Ltd., UK	5 % bovine serum albumin blocking solution

22c11	Amino acids 66-88 of A4 portion of amyloid precursor protein	Mouse IgG	1:1000	Merck Millipore Ltd., UK	5% bovine serum albumin blocking solution or 5% milk blocking solution
Cdk5 (J-3)	Amino acids 1-291 of cyclin dependent kinase 5, total	Mouse IgG	1:25	Santa-Cruz Biotechnologies Inc., CA, USA	5% bovine serum albumin blocking solution
P35 (C-19)	C-terminal P35	Rabbit IgG	1:25	Santa-Cruz Biotechnologies Inc., CA, USA	5% bovine serum albumin

					blocking solution
GSK3 (1H8)	Total glycogen synthase kinase 3 α and β (GSK-3α/β)	Mouse IgG	1:1000	Enzo Life Sciences Ltd., Exeter, UK	5 % milk blocking solution
pGSK3	GSK-3α/β phosphorylated at Ser21 (α) and Ser9 (β)	Rabbit IgG	1:500	Cell Signalling Inc., MA, USA	5 % milk blocking solution
Calpain-1	Calpain-1 large subunit	Rabbit IgG	1:500	Cell Signalling Inc., MA, USA	5 % milk blocking solution

Calpain-1	Calpain-1 large subunit	Mouse IgG	1:500	Kind gift from Prof. R. A. Nixon (Nathan S. Kline Institute, NY, USA)	5 % milk blocking solution
Calpastatin (CAST)	Calpastatin, total	Rabbit IgG	1:500	Cell Signalling Inc., MA, USA	Odyssey blocking solution
BACE (D10E5)	Total β-secretase (BACE)	Rabbit IgG	1:500	Cell Signalling Inc., MA, USA	5 % bovine serum albumin blocking solution

Active caspase-3	Caspase-3 cleaved at Asp175	Rabbit IgG	1:1000	Cell Signalling Inc., MA, USA	Odyssey blocking solution
α-spectrin (AA6)	α-spectrin (non-erythroid)	Mouse IgG	1:1000	Merck Millipore Ltd., UK	5 % milk blocking solution or Odyssey blocking buffer
NCX3	NCX3	Rabbit IgG	1:1000	Kind gift from Prof Kenneth Phillipson (UCLA, California)	Odyssey blocking solution

Transient receptor potential channel melastatin 2 (TRPM2)	Amino acids 650-700 of human TRPM2	Rabbit IgG	1:300	Bethyl Laboratories Inc., Texas, USA	Odyssey blocking buffer
PARP (C-2-10)	C-terminal portion of DNA binding domain of PARP	Mouse IgG	1:500	Enzo Life Sciences Ltd., Exeter, UK	Odyssey blocking buffer
Synapsin	Synapsin Ia and Ib isoforms	Rabbit IgG	1:400	Merck Millipore Ltd., UK	5 % milk blocking solution

NR2B	Amino acids 1437-1482 of NR2B subunit of NMDA receptor	Rabbit IgG	1:500	Merck Millipore Ltd., UK	Odyssey blocking buffer
Post-synaptic density protein 95 (PSD95)	Total PSD-95	Rabbit IgG	1:500	Cell Signalling Inc., MA, USA	5% bovine serum albumin blocking solution
β-actin	N-terminal end of the β-isoform of actin	Rabbit IgG	1:5000	Abcam Plc., UK	5 % milk blocking solution
β-actin (AC-74)	N-terminal end of the β-isoform of actin	Mouse IgG	1:5000	Sigma-Aldrich Company Ltd., UK	5 % milk blocking solution

NSE (BBS/NC/ VI-H14)	Human neuron specific enolase	Mouse IgG	1:2000	Dako, Ltd., UK	5 % milk blocking solution

Table 2.3. Primary antibodies used for western blotting (WB). Information on epitope and antigen, species, working dilution, manufacturer and blocking solution are given.

Table 2.4 lists the primary antibodies used for immunocytochemistry (ICC).

Antibody	Specificity	Species	Dilution	Source
Microtubule-associated protein 2 (MAP2; AP20)	MAP2	Mouse IgG	1:100	Merck Millipore Ltd., UK
MAP2	MAP2	Rabbit IgG	1:100	Merck Millipore Ltd., UK

Glial fibrillary acid protein (GFAP) (2A5)	GFAP	Rabbit IgG	1:500	Dako Ltd., UK
6E10	Amino acids 1-17 of human Aβ	Mouse IgG	1:500	Cambridge Biosciences Ltd., UK
Poly(ADP-ribose) (PAR) (10H)	PAR polymers	Mouse IgG	1:400	Merck Millipore Ltd., UK

TRPM2	Amino acids 650-700 of TRPM2	Rabbit IgG	1:300	Bethyl Laboratories Inc., Texas, USA

Table 2.4. Primary antibodies used for immunocytochemistry (ICC). Information on epitope and antigen, species, working dilution and manufacturer are given. All antibodies were diluted in 5 % bovine serum albumin solution with 0.01% Tween in PBS.

Table 2.5 lists the secondary antibodies used for WB.

Antibody	Dilution	Source
Alexa Fluor® 700 goat anti-mouse IgG	1:10,000	Molecular Probes, Invitrogen Ltd., UK
Alexa Fluor® 800 goat anti-rabbit IgG	1:5000	Molecular Probes, Invitrogen Ltd., UK
Goat anti-rabbit IgG HRP-linked	1:2000	GE Healthcare Life Sciences, Buckinghamshire, UK.

Goat anti-mouse IgG HRP-linked	1:2000	GE Healthcare Life Sciences, Buckinghamshire, UK.

Table 2.5. Secondary antibodies used for western blotting (WB). Information on species, working dilution and manufacturer are given. All antibodies were diluted in 5 % milk blocking solution in PBS

Table 2.6 lists the secondary antibodies used for ICC.

Antibody	Dilution	Source
Alexa Fluor®567 goat anti-mouse IgG	1:250	Molecular Probes, Invitrogen Ltd., UK
Alexa Fluor® 567 goat anti-rabbit IgG	1:250	Molecular Probes, Invitrogen Ltd., UK
Alexa Fluor® 488 goat anti-mouse IgG	1:250	Molecular Probes, Invitrogen Ltd., UK

Alexa Fluor® 488 goat anti-rabbit IgG	1:250	Molecular Probes, Invitrogen Ltd., UK

Table 2.6. Secondary antibodies used for immunocytochemistry (ICC). Information on species, working dilution and manufacturer are given. All antibodies were diluted in 5 % bovine serum albumin solution with 0.01 % Tween in PBS

2.1.9 Cell death assays

LIVE/DEAD® Cell Viability Assay

LIVE/DEAD® Fixable far red Dead Cell Stain Kit (Invitrogen Ltd., UK)

Reagents supplied by the manufacturer.

2.1.0 Post mortem human brain

Post-mortem human frontotemporal cortex was obtained from the Medical Research Council Neurodegenerative Disease Brain Bank. Case details are summarized in Table 2.7.

Braak stage	Case No.	Sex	Age (years)	PMD (h)	Case notes
CTRL*	A047/02	F	87	22	Normal adult brain
CTRL	A239/03	M	78	47	Early tau pathology, no neuritic plaques
CTRL	A040/07	F	82	13	Argyrophilic grains low to moderate density
CTRL	A124/04	M	59	50	Normal adult brain
CTRL	A150/01	M	40	40	Normal adult brain
CTRL	A134/00	M	86	6	Normal adult brain

II	A153/06	F	92	17	Some tau deposition
II*	A063/10	F	90	50	Mild Alzheimer's-type changes and mild amyloid angiopathy
II	A073/05	M	93	~33	Mild Alzheimer's-type changes
II	A310/09	F	84	35	Alzheimer's changes, consistent with patient's age
III	A276/05	M	92	11	Mild Alzheimer's-type changes

III	A209/08	F	70	38	Possible Alzheimer's disease (CERAD) BNE stage III
III*	A045/12	M	86	52	Ageing changes
IV	A097/13	M	82	28	Alzheimer's disease with limbic TDP-43 pathology
IV	A078/13	M	86	53	Alzheimer's disease with extensive severe amyloid angiopathy
IV	A223/12	F	83	22	Alzheimer's disease (limbic stage) and moderate to

					severe amyloid angiopathy
IV*	A175/12	F	89	56	Alzheimer's disease HP tau stage VI severely affecting limbic system and moderately extending to neocortex
V	A331/07	F	80	13	Alzheimer's disease with mild amyloid angiopathy
V	A187/07	F	82	69	Alzheimer's disease with mild amyloid angiopathy

V*	A122/04	M	86	26	Alzheimer's disease with moderate amyloid angiopathy
VI	A168/05	F	84	36	Braak VI
VI*	A094/04	M	88	46	Definite Braak VI
VI	A059/07	F	92	42	Braak VI
VI	A191/07	F	69	16	Braak VI

Table 2.7. Post mortem cases from which control and AD frontotemporal cortex were obtained. Information is given on sex, age, post mortem delay (PMD) and case diagnostic notes. Asterisks (*) refer to cases from which frozen tissue sections were used for immunohistochemical studies.

2.2 Methods

2.2.1 Cell Culture

SH-SY5Y cells

SH-SY5Y cells were maintained in supplemented DMEM: F-12 medium (section 2.1.2) in 175 cm^3 culture flasks at 37 ˚C in a humidified atmosphere of 5 % CO_2. Cells were passaged every 5 days, upon reaching approximately 80 % confluency in culture. To passage cells, DMEM: F-12 was aspirated from flasks and cells were washed twice with sterile PBS. Cells were then incubated with 1 ml of 0.05 % Trypsin/0.02 % EDTA for 5 min at 37 ˚C. Flasks were shaken to aid cell detachment, which was checked under a light microscope. To stop the Trypsin reaction, 4 ml supplemented DMEM: F-12 medium was added to flasks. Cells were mechanically dissociated using a 10 ml Stripette® serological pipette (Sigma-Aldrich Co., Ltd., UK) and the presence of single cells was confirmed under a light microscope. The cell suspension was then diluted 5-fold in supplemented DMEM: F-12 and re-seeded in fresh 175 cm^3 culture flasks.

Primary cortical cultures

Sterile culture plastic was coated with 10 µg/ml PDL overnight at 37 ˚C and washed once with sterile ultrapure H_2O prior to cell plating. Cortical neurons

were isolated from embryonic day 18 (E18) Sprague-Dawley rats (Charles River) as previously described (Ackerley et al., 2000). Briefly, pregnant rats were sacrificed by Schedule 1 methods, according to the (Scientific Procedures) Act 1986. Embryos and embryonic brains were removed under aseptic conditions. Cortices were dissected from embryonic brains in ice cold HBSS (section 2.1.2).

Cortices were dissociated under sterile conditions using reagents from the Papain Dissociation kit (Worthington Biochemical Corp., NJ, USA). Cortical tissue was minced in a petri dish containing HBSS and the cell solution transferred into a 50 ml falcon tube. Excess HBSS was removed and 2.5 % trypsin solution was added to cortices. The cell suspension was then incubated at 37 ˚C for 30 minutes with occasional agitation to enable dissociation. DNase was then added to cortices to minimize 'sticky' DNA fragments and tissue clumping, and the falcon tube was inverted twice. The solution was then removed and replaced with supplemented phenol red-free Neurobasal™ media without allowing cortices to dry. The cortices were then placed into 1 ml trituration solution and mechanically dissociated by vigorous trituration with a sterile 5 ml pipette until all cortices were fully dissociated. The tissue solution was next strained through a sterile 70 μM nylon strainer (BD Biosciences Corp., MA, USA) into a 50 ml falcon tube to yield a homogenous single cell suspension. Cells were then centrifuged for 5 minutes at 1000 x g (av) using a Sorvall® Legend T Plus bench-top centrifuge (DJB Labcare Ltd., UK). The supernatant was discarded and the cell pellet re-suspended into 1ml Neurobasal™ per embryonic brain. A sample of the cell suspension was

stained with trypan blue and cell density was calculated using a haemocytometer. Cells were then plated at the required density on PDL-coated plates. Cultures were maintained in supplemented Neurobasal™ medium at 37 ˚C in a humidified atmosphere of 5 % CO_2 for 4-14 days *in vitro* (DIV).

Treatment of primary cortical cultures with oligonucleotides

Rat E18 cortical cultures were plated on 18 mm coverslips (Marienfeld Superior, Germany) at a density of 250,000 cells per well. Cultures were treated at 4 DIV with antisense and sense phosphorothioated oligodeoxynucleotides, specific for rat NCX3 (Iwamoto & Kita, 2006). The 5'-3' sequence of NCX3 antisense: GCCATACACAAGAG; the 5'-3' sequence of NCX3 sense: CTCTTGTGTATGGC (section 2.1.1). Cultures were incubated with 5μM oligodeoxynucleotides and Lipofectamine 2000® (Life Technologies, UK), a lipid-based transfection reagent for eukaryotic cells, according to the manufacturer's protocol. For each well, 16μl oligodeoxynucleotides were mixed with 1μl Lipofectamine 2000® and 70μl Opti-MEM® I (Life Technologies, UK) and incubated for 20 min at room temperature to allow formation of liposome-DNA complexes. During this time, the conditioned media was removed from cultures and replaced with 1 ml per well of Opti-MEM® pre-warmed to 37 ˚C. Conditioned media was kept for later use. Transfection mix was topped up with Opti-MEM® and mixed gently. Opti-MEM® was removed from cultures and 1 ml of transfection mix was added drop-wise to cells, following

which cells were incubated for 4 hours at 37 ˚C. Afterwards, the transfection mix was removed and replaced with conditioned media. After 24 hours of incubation with oligodeoxynucleotides to allow adequate suppression of endogenous protein transcription, cultures were treated with vehicle or a subtoxic (1μM) concentration of oligomeric Aβ1-42 for a further 16 hours.

Pharmacological treatment of primary cortical cultures and SH-SYFY cells

For treatment with chemical agents, primary cortical cultures were plated in six well plates at a density of 1 million cells per well, while SH-SY5Y cells were plated in 12 well plates on 18 mm glass coverslips at a density of 100,000 cells per coverslip. The agents used, as well as the vehicle used to prepare stock solutions and the final concentrations used are detailed in Table 2.8. Control cultures were treated with corresponding appropriate vehicles

Chemical/biological agent	Vehicle/diluent	Stock concentration	Working concentration
SB750139	Dimethyl sulfoxide (DMSO)	100 mM	1 μM

Calpeptin	Ultrapure H_2O	20 mM	10 µM
MK-801	Ultrapure H_2O	10 mM	1 µM
Caspase inhibitor IV	DMSO	5 mM	100 µM
LiCl	Ultrapure H_2O	1 M	5 – 20 mM
NaCl	Ultrapure H_2O	1 M	5 – 20 mM
KCl	Ultrapure H_2O	129 mM	50 mM
H_2O_2	Ultrapure H_2O	30 %	1 mM
Aβ 1-42, human (synthetic)	Ultrapure H_2O	500 µM	1 µM, 10 µM
Aβ 1-42, human (secreted)	DMEM	>500 pg/ml	>500 pg/ml

Table 2.8. Details of agents used to treat cell cultures. The diluent, stock and working concentrations for each agent are shown.

Preparation of soluble oligomeric Aβ

Human Aβ1-42 purchased from California Peptide Inc. (CA, USA) was dissolved in sterile ultrapure H_2O to a stock concentration of 500 μM, as described by Town et al., (2002). This preparation yields predominantly soluble Aβ oligomers. Aβ oligomers were added either directly to cultures, to the centre of each well, or were diluted in culture medium before adding to cultures to give a final concentration of 1-10 μM. Cultures were gently agitated to ensure uniform distribution of Aβ to cells. Control cultures were treated with an equal volume of ultrapure H_2O.

2.2.2 Protein extraction

Preparation of tissue homogenates from human brain

Frozen post-mortem human frontotemporal cortex was prepared in two different ways, depending on the protein of interest. Tissue was dissected and homogenized at 50 mg/ml in TBS homogenization buffer using an electric homogeniser (Ultra Turrax® T8, Werke GmbH & Co., Germany) for analysis of α-spectrin, calpain I, caspase-3, NCX3, TRPM2 and PARP. Tissue was homogenized at 100 mg/ml in extra strong lysis buffer and then sonicated for 10 seconds at output setting 4 with a VibraCells™ sonicator (Sonics & Materials INC, USA) for analysis of total and cleaved tau and tau phosphorylation epitopes (DAKO, tau1,

PHF1 and CP13). During this, tissue and homogenates were constantly kept on ice to minimize protein degradation. Samples were then centrifuged at 25,000 x g (av) for 20 minutes at 4 ˚C on a 5415R desktop centrifuge (Eppendorf Ltd., UK). Supernatants were collected, mixed with 2 x protein loading buffer at a 1:1 ratio and stored at -80 ˚C until required.

Preparation of cell lysates from cell cultures

Rat E18 cortical cultures were prepared as described in section 2.2.1. Culture medium was aspirated and cultures were washed twice in PBS pre-warmed to 37˚C. Cells were scraped into 250 µl PBS and centrifuged for 10 seconds at 13,000 g. Supernatants were then discarded and pellets were re-suspended in 75-100 µl ESLB with 1 protease inhibitor cocktail tablet per 10ml buffer (section 2.1.3). Cortical lysates were sonicated for 10 s and then centrifuged at 4˚C for 20 min. Supernatants were discarded and pellets were resuspended with 75 µl ESLB. Lysates were then mixed with equal volumes (75 µl) of 2 x sample buffer (section 2.1.3) prior to western blotting.

2.2.3 Quantitative Aβ ELISA

Aβ1-40 and Aβ1-42 ELISA

Human Aβ1-40 and Aβ1-42 ELISA kits were purchased from Invitrogen Ltd., and ELISA experiments performed according to the manufacturer's instructions. All reagents provided in the kits were equilibrated at room temperature for 10 min prior to experiments. Human post-mortem brain homogenates previously homogenized in extra-strong lysis buffer (ESLB; section 2.1.3) were used. 4 µl of each sample was added to 296 µl TBS buffer containing Mini protease inhibitor cocktail tablet (1 tablet in 10 ml, Roche Diagnostics Ltd., UK) to provide a 1:75 dilution of all samples. ELISA Aβ standards of known concentrations (10,000, 500, 250, 125, 62.5, 31.35, 15.63, 7.81 and 0 pg/ml for Aβ1-40 and 100,000, 10,000, 1000, 500, 250, 125, 62.5, 31.25, 15.63 and 0 pg/ml for Aβ1-42) were prepared from recombinant human Aβ1-40 and Aβ1-42 peptides provided in the kits. Standards were reconstituted in filtered sodium bicarbonate buffer (section 2.1.4) as instructed, and were then serially diluted in TBS buffer containing protease inhibitor cocktail (section 2.1.3) to achieve an equivalent 1:75 dilution of all standards. 50 µl of each standard and sample were added in duplicate to the 96 well plate provided in the kit. 50 µl of primary detection antibody was then added to all wells and the plates incubated at room temperature for 3 hours with agitation. All material was discarded from wells to remove any unbound protein and plates were washed with diluted wash buffer (section 2.1.4) four times. 100

µl goat anti-rabbit-HRP linked detection antibody was then added to each well and plates were incubated at room temperature for a further 30 min with agitation. All material was discarded from wells and plates were washed a further four times with wash buffer. Following this, 100 µl of stop solution (stabilised chromogen) was added to each well. Plates were incubated at 37 ˚ C for 1 h 30 min in the dark until a colour change (indicative of HRP reaction) was observed in wells. Absorbances were read at 450 nm using a Wallac 1420 Victor3™ plate reader (Perkin Elmer Ltd., UK). A standard curve was generated using absorbance values of protein standards using Excel (Microsoft Corp., USA) and this was used to calculate Aβ concentrations in pg/mg tissue.

2.2.4 SDS-Polyacrylamide Gel Electrophoresis (SDS-PAGE) and Western Blotting

SDS-PAGE

Prior to SDS-PAGE, samples were prepared in two different ways, depending on the protein of interest. For analysis of C-terminal APP fragments (including Aβ) protein samples were diluted 1:1 in 2 x Novex® Tricine SDS Sample Buffer (Life Technologies, UK) and boiled at 85 ˚C for 2 minutes to denature and reduce proteins. For analysis of all other proteins, samples were diluted 1:1 in 2 x protein loading buffer (National Diagnostics Ltd., UK) and boiled at 100 ˚C for 5 minutes.

All samples were then centrifuged at 10, 000 x g (av) for 30 seconds on a 5414R desktop centrifuge (Eppendorf Ltd., UK) to remove cell debris and insoluble material.

Polyacrylamide gels were cast in 1.0 mm plastic cassettes purchased from Life Technologies (UK). Resolving gel solutions ranged from 7.5-16 % polyacrylamide and were prepared as described in section 2.1.5. Liquid gel solutions were poured into cassettes and left to fully polymerize for at least 15 minutes. Isopropanol was added to the top of the resolving gel immediately after pouring to eliminate bubbles and ensure a uniform interface between the resolving and stacking gels. After polymerization of the resolving gel, isopropanol was thoroughly washed off using ultrapure H_2O. Stacking gels of 4 % polyacrylamide were prepared as described in section 2.1.5 and poured immediately after preparation, with 1mm plastic combs (Life Technologies, UK) inserted to form wells prior to gel polymerisation. Alternatively, pre-cast 1.0mm, 15 well Novex® 16 % Tricine Protein Gels were purchased from Life Technologies (UK).

Gels were inserted into the XCell SureLock™ Mini-Cell electrophoresis system (Life Technologies, UK), which were then filled with 1 x running buffer (glycine- or tricine-based, depending on the preparation and gel type used) until the wells were fully submerged. Proteins were separated by electrophoresis at 150 V for 90 minutes. PrA mixture of protein molecular weight markers (section 2.1.5) was loaded in the first lane of gels to allow for determination of protein size.

Western blotting

Following SDS-PAGE, proteins were transferred onto Protran® nitrocellulose membranes (BA85, 0.45 μm pore size, Whatman Ltd., UK) in XCell II™ Blot Modules (Life Technologies, UK) using XCell SureLock™ Mini-Cell Electrophoresis Systems (Life Technologies, UK) filled with 1 x transfer buffer (section 2.1.5). Prior to transfer, membranes were soaked in transfer buffer for at least 2 min to ensure buffer permeation into membrane pores. Protein was transferred at 30 V for 2 h on ice. For some proteins, successful transfer was determined by brief incubation of membranes in Ponceau S red stain (section 2.1.5) at room temperature, followed thorough PBS washing to remove the solution. The negatively-charged Ponceau S red stain reversibly binds to positively charged protein amino groups and non-covalently to non-polar groups, which allows all protein to be detected without interfering with subsequent immuno-labelling.

Membranes were incubated in 5 % milk blocking solution, 5 % BSA blocking solution or Odyssey® Blocking Buffer (Li-cor Biosciences Ltd., UK), depending on primary antibody, to prevent non-specific binding. Membranes were gently rocked for 1 hour at room temperature in blocking solution on a Stuart® SSL4 see-saw rocker (Bibby Scientific Ltd., UK). Primary antibodies were prepared in appropriate blocking solution and were added to membranes, which were then incubated overnight at 4 ˚C with gentle agitation on a MaxQ™ 4000 benchtop refrigerated digital shaker, Thermo Fisher Scientific Inc. (USA). The next day,

primary antibodies were removed and membranes were washed 3 times in PBS for 5 minutes. The appropriate secondary antibodies were diluted in 5 % milk blocking solution and then added to membranes to incubate in for 1 hour at room temperature, with gentle agitation on a Stuart® SSL4 see-saw rocker (Bibby Scientific Ltd., UK). The secondary antibodies were then removed and membranes were washed a further 3 times in PBS.

Proteins were detected by two methods, depending on compatibility with primary antibody. Membranes incubated in fluorophore-tagged secondary antibodies (section 2.1.8) were scanned for infra-red fluorescence emission at 700 nm (red) and 800 nm (green) wavelength on an Odyssey® infrared scanning system (Li-cor Biosciences Ltd., UK) which allows simultaneous detection of two target antigens, and thus two proteins. Scanning intensity of membranes was optimized according to the strength of the background and antigen signals in order to allow for quantification of integrated signal intensity within a linear range. Only protein bands showing the expected molecular weight were quantified using Odyssey® analysis software V3.0 (Li-cor Biosciences Ltd., UK), and background signal was subtracted automatically. Measured signal intensities were exported to Excel (Microsoft Corp., USA), and calculations were performed to standardise amounts of protein of interest against those of housekeeping proteins (β-actin for rat protein and NSE for human protein) within the same sample. Data was then exported to Graphpad Prism (Ver 6, Graphpad software Inc., CA, USA) for statistical analysis.

For proteins that could not be detected using the Odyssey® system, signals were visualized using an enhanced version of the chemiluminescence reaction (ECL). Membranes were incubated in secondary antibodies conjugated to horse radish peroxidase (HRP) (section 2.1.8) for 1 hour at room temperature with rocking, followed by 3 PBS washes of 10 minutes each. Membranes were then incubated in Pierce® ECL Western Blotting Substrate (Thermo Scientific, IL, USA) at room temperature for 2 minutes. The blotting substrate was mixed to comprise equal volumes of enhanced luminol reagent and oxidizing reagent (1 ml each per membrane). During incubation of membranes in substrate, HRP catalyzes the oxidation of luminol into a light-emitting reagent that allows visualization of the protein of interest complexed with the HRP-tagged antibody. The amount of light emitted from the oxidation reaction directly correlated with the amount of protein and its location on the membrane. Compared to conventional chemiluminescence, ECL enhances light emission more than 1000-fold, which allows for detection of protein at 1 to 10 pg. Membranes were then placed between two sheets of acetate film in an 18 x 24 cm CAWO X-ray screen (Scientific Laboratory Supplies Ltd., UK), and the sheets smoothed out to eliminate air pockets between membrane and acetate. Images were developed in a dark room, by placing high performance chemiluminescence film (Amersham, UK) on top of the membrane. Films were exposed for varying times to optimize detection (30 seconds to 1 hour, depending on the primary antibody affinity) and developed using a SRX-101A Medical Film Processor (Konica Minolta Medical Imaging, USA).

Films were then digitalized and protein amounts were quantified using open-source ImageJ software (v 1.41o, National Institute of Health, USA).

To ensure equal protein content in post mortem samples prior to analysis, preliminary western blots to determine housekeeping protein amounts (e.g NSE) were run for all samples and these were quantified as previously above. Samples were then normalised to the lowest protein concentration by dilution in appropriate buffer.

2.2.5 Cell Death Assays

LIVE/DEAD® Fixable Dead Cell Assay

The viability of rat primary cortical cultures before and after treatment was assessed using a LIVE/DEAD® Fixable Far Red Dead Cell Stain Kit (L10120, Life Technologies, UK) according to the manufacturer's protocol. The amine-reactive stain provided reacts with amines on the cell plasma membrane and with free amines in the cytosol of cells with compromised membranes to yield a fluorescent signal, allowing quantification of the proportion of dead cells in a cell population. One vial of stain was dissolved in 50 µl anhydrous DMSO prior to use. Conditioned media was removed from culture wells and the cells were briefly washed once in PBS pre-warmed to 37 ˚C. The stain was diluted 500-fold in pre-warmed PBS to give a final working concentration and mixed thoroughly to ensure a uniform

distribution. The stain was then added to cultures and left to incubate for 30 minutes at 37 ˚C with 5 % atmospheric CO_2 in a dark humidified incubator to allow time for binding and permeation into cells. The stain was then removed and the cells briefly washed twice with pre-warmed PBS. The fluorescent signal was detected at a fluorescence emission wavelength of 700 nm using the Odyssey® infrared scanning system (Li-cor Biosciences Ltd., UK). To determine the effects of treatment on cell death, the difference in fluorescent intensities in treated cells was then calculated as a proportion of fluorescent intensities in control cells.

2.2.6 Immunocytochemistry

Cultures grown on glass coverslips were washed once with PBS pre-warmed to 37 ˚C to remove media and then fixed in 4 % (v/v) paraformaldehyde (PFA) in PBS for 5 minutes at 37 ˚C with 5 % atmospheric CO_2 in a humidified incubator. Cells were then washed 3 times with PBS, 5 minutes for each wash, to remove all traces of PFA, and permeabilised in permeabilisation solution (section 2.1.7) for 2 minutes at room temperature. Cells were then washed a further 3 times in PBS-T and, to prevent non-specific binding of primary antibodies, BSA blocking solution was added for 1 hour at room temperature on a Stuart® SSL4 see-saw rocker (Bibby Scientific Ltd., UK). Primary antibodies diluted in BSA blocking solution were then added to cells immediately after blocking and incubated for a further hour at room temperature. Primary antibodies were then removed and

the cells washed 3 times in PBS-T. The appropriate species of fluorophore-conjugated secondary antibodies diluted in BSA blocking solution were then added to cells to incubate for 1 hour at room temperature. This was followed by a further 3 PBS-T washes. The nuclear stain Hoescht 33342 was diluted at 1:1000 and added to cultures to incubate for 2 minutes at room temperature. Cultures were then thoroughly washed 3 times with PBS-T to remove all traces of the stain. Cells were mounted on glass microscope slides using fluorescence mounting media (Dako Ltd., UK) and kept at 4 ˚C, in darkness until used for imaging.

Cells were imaged using a Leica Microsystems (LLC., Germany) DM5000B fluorescence microscope using the appropriate filter sets (Leica Microsystems LLC., Germany) and images were captured on a CTR5000 camera using Leica Microsystems (LLC., Germany) AIF lite software. All settings (exposure, gain and intensity) were kept constant between treatments and images. Images of 3 random regions per coverslip, and 3 coverslips per treatment condition, were captured. Quantification of immuno-positive cells, relative fluorescence intensities and co-localization analysis, when required, were performed using open-source ImageJ software (v 1.41o, National Institute of Health, USA).

2.2.7 Live microscopy

Fluo-4 Ca^{2+} imaging

Ca^{2+} imaging experiments were conducted in primary cortical neurons and SH-SY5Y cells plated onto 18mm glass coverslips (Marienfeld, Germany). Neurons were imaged at 7 to 10 DIV. SH-SY5Y cells were imaged at passage 18 to 20 and were allowed to reach approximately 80% confluency before plating on coverslips. On the day of experimentation, 1 mM stock of fluo-4 AM Ca^{2+} indicator (cell permeable) was diluted in 10 ml extracellular solution (section 2.1.6) to give a final working concentration of 2.5 μM. The solution was supplemented with Pluronic® F-127 (section 2.1.6) diluted from 20% stock to achieve a 1:1 concentration with fluo-4 AM. This facilitated solubilisation and cellular dispersal of acetoxymethyl ester, important for effective binding of cytosolic Ca^{2+}. Following removal of Neurobasal™ or DMEM/F-12 medium (section 2.1.2) from neurons or SH-SY5Y cells, respectively, coverslips were incubated in fluo-4 AM solution (0.5 ml per coverslip) for 30 min at 37 ºC in a humidified incubator. The fluorescent indicator solution was then aspirated and coverslips were incubated in extracellular solution for a further 30 min at 37 ºC in a humidified incubator. This allowed de-esterification of the indicator and binding of it to Ca^{2+}.

Coverslips were placed in an open Ludin imaging chamber (Life Imaging Services, Switzerland) and sealed using high-vacuum silicone grease (Sigma-Aldrich Co, Ltd., UK.). 0.5ml of extracellular solution was added to the chamber, which was

then positioned on the stage of a Zeiss Axiovert 200M inverted live imaging microscope (Carl Zeiss Ltd., UK) and maintained in a 5 % CO_2 environment and 37 ºC (respectively controlled by 'The Brick' gas mixer and 'The Box' temperature control system, Life Imaging Services, Switzerland) throughout experimentation. Recordings were conducted using a Lambda LS illuminator (Sutter Instrument Co., CA, USA) to provide excitation at 485 nm, with fluorescence emission detected at 520 nm with a Lambda 10-3 filter wheel (Sutter Instrument Col, CA, USA). Cells were visualized under brightfield through a 40X oil lens (Leica Microsystems LLC., Germany) and fluorescent images were captured using a Cascade II: 512 camera (Photometrics LLC., AZ, USA) and MetaMorph® imaging software (Molecular Devices LLC., CA, USA). For each experiment, images were captured using 100 ms exposure and 1 s interval (1 image acquired per second) for a duration of 10 min. Excitation intensities and exposure times were kept to the minimum required for signal detection in order to reduce photobleaching and phototoxicity. Cells that were not successfully loaded with Fluo-4 or did not depolarize with 50 mM KCl were excluded from analysis.

Where appropriate, cells were pre-treated with compounds (section 2.2.1) for 3 hours prior to imaging. These compounds were added simultaneously to fluo-4 incubations, washes and Aβ mixtures. Before Aβ treatments, extracellular solution was removed from the closed chamber and replaced with a pre-prepared mixture of compound in extracellular solution, immediately before recording. Images were analysed using ImageJ software (v.1.41o, NIH, USA) and a 'Ca^{2+}

analyser' plugin (designed by K. J de Vos, University of Sheffield, Sheffield, UK). Signal values were acquired and measured by defining 'regions of interest' in selected cells using the 'Ca^{2+} analyser plugin'. Excel (Microscoft Corp., USA) for analysis. Changes in Ca^{2+} fluorescence were calculated as change in fluorescence/resting Ca^{2+} fluorescence ($\Delta f/f$).

2.2.8 Statistical Analyses

The normality of data was assessed using the D'Agostino-Pearson omnibus test using GraphPad Prism v6.0 (La Jolla, CA, USA) software. Unpaired t-tests were used to compare and determine the statistical difference between two sample sets. Comparison of two or more groups of data was made using one way analysis of variance (ANOVA) with Tukey's post-hoc analysis. Two-tailed Spearman's rank correlation tests with linear regression were used for correlation analyses. Differences were considered as statistically significant when $p < 0.05$ (*).

CHAPTER 3

Elevated calpain activity causes cleavage of NCX3 and precedes tau phosphorylation and loss of synaptic proteins in Alzheimer's disease brain

3.1 Introduction

Characteristic deposition of Aβ in extracellular senile plaques and aggregation of hyperphosphorylated tau in intraneuronal neurofibrillary tangles (NFTs) are associated with synaptic and neuronal dysfunction in Alzheimer's disease (AD; Noble et al., 2013). Substantial research points to neuronal Ca^{2+} dyshomeostasis as a key mediator of neurodegeneration in AD (Berridge, 2014; Lim et al., 2014). Increased production of Aβ has been shown to elevate cytosolic Ca^{2+} (Kuchibhotla et al., 2008) by increasing its influx through native ion channels, receptors (Supnet and Bezprozvanny, 2010; Wang and Mattson, 2014) and the formation of Ca^{2+}-permeable amyloid pores (Demuro et al., 2011), enhanced release of Ca^{2+} from intracellular stores (Nelson et al., 2010; Supnet and Bezprozvanny, 2010) and inactivation of Ca^{2+}-extruding protein pumps (Atherton et al., 2014). Prolonged elevation of intracellular Ca^{2+} initiates excitotoxic cascades that involve activation of Ca^{2+}-sensitive proteins such as calcium/calmodulin-

dependent protein kinase (CAMKK2; Mairet-Coello et al., 2013), calcineurin (Wu et al., 2010; Mohmmad Abdul et al., 2011) and calpain (Town et al., 2002; Atherton et al., 2014).

Calpains are a family of Ca^{2+}-activated cysteine proteases that are strongly implicated in AD because of their roles in altering key disease proteins, including APP to regulate Aβ levels (Morales-Corraliza et al., 2012), tau (Ferreira and Bigio, 2011), dynamin-1 to affect memory, and synaptic proteins such as the NMDAR subunit NR2B to impair synaptic health (Simpkins et al., 2003; Kelly et al., 2005). Calpain is also involved in the activation of key tau kinases, such as glycogen synthase kinase 3 (GSK3; Goñi-Oliver et al., 2007) and cyclin-dependent kinase 5 (cdk5; Lee et al., 2000) that phosphorylate tau and enable tau-mediated neurodegenerative processes in *vivo* (Noble et al., 2003; Cruz et al., 2003; Gómez-Sintes et al., 2007).

Multiple studies have demonstrated elevated calpain activity in late stage AD brain (Saito et al., 1993), particularly in neurons containing NFTs (Grynspan et al., 1997). Elevated calpain activity in AD brain is associated with increased cleavage of numerous calpain substrates in these tissues (Jin et al., 2015; Liu et al., 2005; Wu et al., 2007; Atherton et al., 2014). Recently, a strong link between calpain activation, calpain-mediated cleavage of GSK3, GSK3 activation and tau phosphorylation at key disease epitopes has been demonstrated in late stage AD (Jin et al., 2015). Calpain has also shown to cleave the sodium calcium exchanger

3 (NCX3; Bano et al., 2005). NCX3 is one member of a family of three ion exchangers that extrude Ca^{2+} in exchange for Na^{+} in conditions of high cytosolic Ca^{2+} (Lytton, 2007). In a cell-based model of ischaemia, inactivation of NCX3 upon its cleavage by calpain led to retention of intracellular Ca^{2+}, further calpain activation and resultant glutamate-induced neurotoxicity (Bano et al., 2005) - results confirmed in additional models (Brustovetsky et al., 2010a). Calpain activity is known to be increased in AD brain (Saito et al., 1993), thereby suggesting that NCX3 activity and function may also be altered by calpain in AD, where it may contribute to the excitotoxic elevations of Ca^{2+} that are believed to occur early during the development of AD.

To investigate these events in more detail, the aims of this chapter were to 1) determine whether or not calpain activation is increased and is associated with NCX3 cleavage in AD brain relative to brain from controls and other neurodegenerative tauopathies, and 2) to investigate the stage of AD development at which calpain activity is first increased and 3) to determine any temporal associations between elevated calpain activity, alterations in tau kinases, tau and synaptic markers during the progression of AD. To achieve this, postmortem brain from Braak stage II to VI AD tissue was compared with that from age-matched controls.

3.2 Results

It was first important to determine if calpain activity is altered in association with NCX3 cleavage in AD brain relative to control brain. In addition, to determine if these changes are specific to AD or are a feature of other neurodegenerative diseases, brain from patients diagnosed with frontotemporal dementia with tau mutations (FTD-Tau), progressive supranuclear palsy (PSP), and corticobasal degeneration (CBD) was also analyzed. FTD-tau, PSP and CBD are characterized by accumulation of tau pathology in the absence of increased Aβ production. Comparison of biochemical changes in these "pure" tauopathies with those in AD brain therefore allows comment on events particularly relevant for tau-associated neurodegeneration. Lysates from postmortem brain were prepared as described in section 2.1.10 and were assessed by western blotting using antibodies directed towards key proteins of interest.

3.2.1 Calpain-1 activity is increased in AD brain and brains from other tauopathies

Calpain-1 is a Ca^{2+}-activated cysteine protease that exists as an 80 kDa pro-enzyme and undergoes autolytic activation to yield 76 and 58 kDa active fragments (Baki et al., 1996; Veeranna et al., 2004). To determine if calpain activity is altered in neurodegenerative tauopathy brain, lysates from post

mortem control and end stage tauopathy brains were immunoblotted with an antibody specifically against active (76 kDa) calpain-1. These blots revealed a single prominent band of 76kDa (Fig. 3.1), as previously described (Atherton et al., 2014). To control for gliosis and/or neuronal protein loss resulting from neurodegeneration or post mortem delay, blots were also probed with an antibody against neuronal specific enolase (NSE) as a loading control. Standardization of bands to NSE allowed normalization of protein amounts in each sample. Quantitation of normalized band intensities revealed that active calpain-1 is significantly increased in AD tissue ($p < 0.001$), as well as in PSP, CBD and FTD tissue ($p < 0.05$) compared to controls (Fig. 3.1B). These findings are in accordance with previous reports of elevated calpain-1 activity in AD brain (Saito et al., 1993), and in addition this study reveals that increased calpain-1 autolysis to its active subunit occurs in other neurodegenerative tauopathies that are not characterized by Aβ accumulation.

3.2.2 CAST activity is reduced in AD and tauopathy brain

The endogenous calpain inhibitor, calpastatin (CAST), is a key intracellular regulator of calpain-1 activity that helps to prevents calpain over-activation induced by prolonged elevations of intracellular Ca^{2+} (Murachi, 1990). Reduced amounts or activity of CAST has previously been linked with the increased calpain activity observed in AD brain (Saito et al., 1993; Rao et al., 2008). Here, CAST

activity was examined in AD and tauopathy cortical lysates by immunoblotting with an antibody detecting CAST holoprotein (110-120 kDa), active calpain-cleaved CAST species (37-75 kDa) - that together with CAST holoprotein have inhibitory activity - and inactive CAST fragments (< 25 kDa; Fig. 3.1). Amounts of active CAST were quantified as a proportion of total CAST and revealed a significant reduction in CAST activity in AD ($p < 0.001$), CBD ($p < 0.01$), PSP and FTD brains ($p < 0.05$), compared to control (Fig. 3.1C). Corresponding increased amounts of inactive CAST were found in these diseased brain lysates compared to controls (Fig. 3.1D). This data supports previous evidence demonstrating decreased CAST activity in AD brain (Saito et al., 1993; Rao et al., 2008), and also shows similar changes in other tauopathy brains.

3.2.3 Calpain cleavage of NCX3 is increased in AD brain

The NCX3 belongs to a family of 3 plasmalemmal pumps that extrude excess Ca^{2+} to maintain homeostatic intracellular levels (Lytton, 2007). NCXs are subject to cleavage by proteases, including calpain, which inactivates the exchanger by preventing its binding to Ca^{2+} (Bano et al., 2005, 2007).

Amounts of full-length and cleaved NCX3 were measured by immunoblotting lysates prepared from post mortem brain with an antibody previously shown to detect NCX3 holoprotein (110 kDa), calpain-cleaved (~60kDa) and caspase-cleaved (~66 kDa) NCX3 species, in primary neurons (Bano et al., 2005). Bands

of these expected sizes were apparent in the postmortem brain lysates assessed here (Fig. 3.1A). The density of protein bands were quantified and following normalization to NSE amounts in each sample, it was found that there was significantly less full-length NCX3 in AD tissue compared to controls ($p < 0.01$; Fig. 3.1E) in line with previous findings (Sokolow et al., 2011). This was paralleled by a significant increase in the amounts of calpain-cleaved NCX3, quantified as a proportion of total NCX3 ($p < 0.01$; Fig. 3.1F). This latter finding is consistent with observations of elevated calpain-1 activity in these samples. Amounts of full-length and calpain-cleaved NCX3 were not altered in any other disease group (Fig. 3.1 E, F), suggesting that calpain cleavage of NCX3 is specific to AD. In addition, there were no changes in the amounts of caspase-cleaved NCX3 in any neurodegenerative disease brain when compared to control (Fig. 3.1G), supporting previous findings that there are no increases in caspase-3 activity in cortical tissues from these diseased brains (Atherton et al., 2014). Since exchanger activity is disrupted upon calpain cleavage of NCX3 (Bano et al., 2007), these findings indicate that normal NCX3 function is lost in AD, which might suggest that impaired NCX3 function could contribute to dysregulation of intracellular Ca^{2+} in AD.

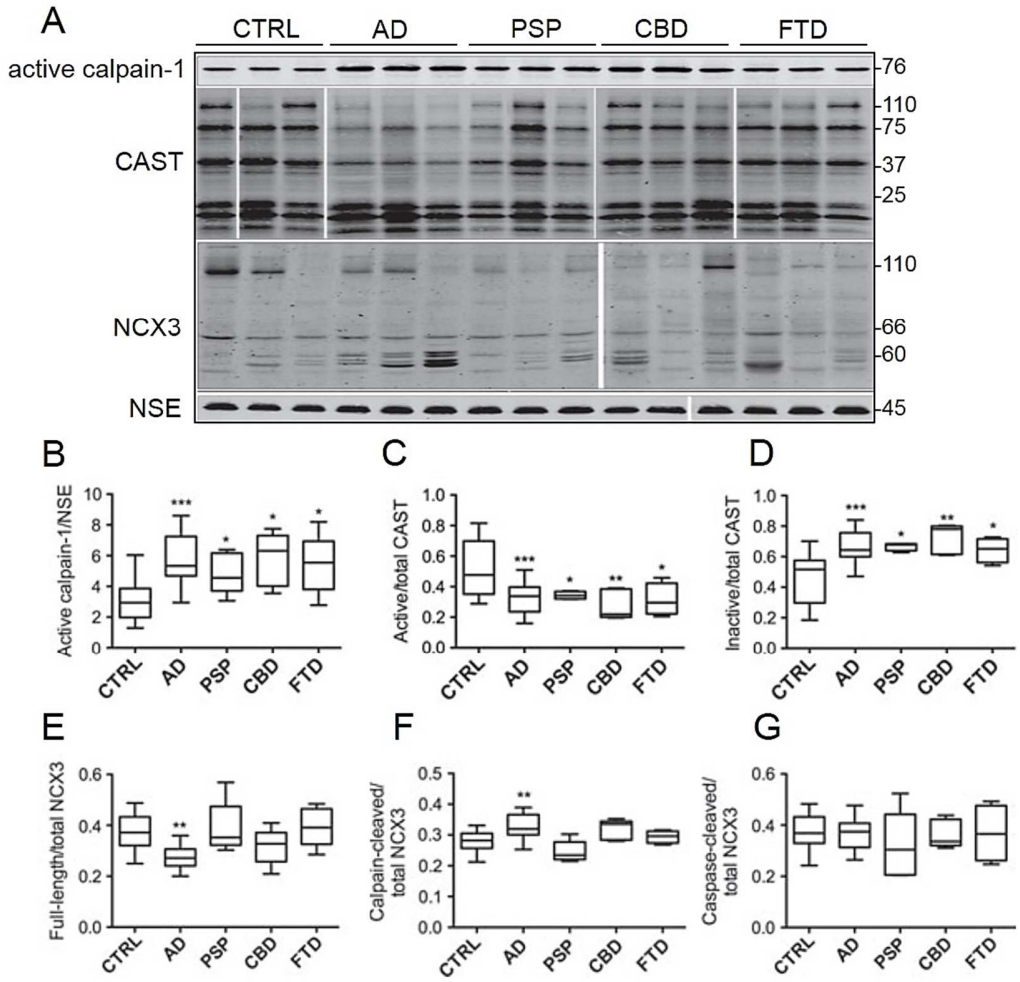

Fig. 3.1 Calpain-1 activity and calpain-mediated NCX3 cleavage are elevated in AD brain. (A) Representative immunoblots of post mortem cortical lysates. Blots were probed with antibodies against active calpain-1 at 76 kDa, NCX3 holoprotein at 110 kDa, caspase-3 cleaved NCX3 at 66 kDa and calpain-cleaved NCX3 at approximately 60 kDa. An antibody against calpastatin (CAST) detects 110 kDa holoprotein , active CAST fragments of > 25 kDa and inactive fragments of < 25 kDa. Blots were also probed with an antibody against neuron-specific enolase (NSE), a 46 kDa protein. Box plots show protein amounts of (B) active calpain-1 relative to NSE, (C) active CAST and (D) inactive CAST, both as a proportion of total CAST, (E) NCX3 holoprotein, (F) calpain-cleaved NCX3 and (G) caspase-cleaved NCX3, all as a proportion of total NCX3. CTRL: control (n = 20), AD: Alzheimer's disease (n = 20), PSP: progressive supranuclear palsy (n = 5), CBD: corticobasal degeneration (n = 5), FTD: frontotemporal dementia with tau mutations (n = 4). *p < 0.05, **p < 0.01, ***p < 0.001.

3.2.4 NCX3 expression sensitizes neurons to Aβ-induced neurotoxicity

Elevated calpain-mediated NCX3 cleavage was only detected in AD brain, and not in neurodegenerative diseases characterized by only tau pathology, suggesting that the inactivation of NCX3 by calpain might be related to increased Aβ concentrations, and therefore could mediate Aβ-induced neurotoxicity. This group, and many others, have previously shown that treatment of primary cortical neurons with Aβ leads to calpain-1 activation, and subsequent neurotoxicity (Town et al., 2002; Atherton et al. 2014;), and this group showed that these events were associated with calpain-mediated NCX3 cleavage (Atherton et al., 2014).

To further investigate the connection between Aβ-induced neuronal death and NCX3, primary cortical neurons were transfected for 24 h with phosphorothioated sense or antisense oligonucleotides specific for rat NCX3, as previously described (Iwamoto and Kita, 2006). Western blotting of neuronal lysates confirmed knockdown of NCX3 protein by antisense NCX3 oligonucleotides (Fig. 3.2A). Quantification of protein bands, following normalisation to β-actin amounts, showed that there was a significant ($p < 0.05$) reduction (38.5 ± 12.6 %) in full-length NCX3 protein amounts when compared to control treated cells, in line with previously published data (Ranciat-McComb et al., 2000). There were no changes in the amounts of cleaved NCX3 species following treatment of cells with antisense oligonucleotides, possibly reflecting a

slower turnover rate of these fragments than that of full-length NCX3 (Fig. 3.2A). As expected, sense oligonucleotides to NCX3 did not alter NCX3 protein levels (Fig. 3.2B).

Following oligonucleotide treatment, cultures were also treated with a subtoxic dose of oligomeric Aβ (1μM) for a further 16 h. This treatment alone did not significantly alter cell death in cultures (Fig. 3.2C). In contrast, application of 1μM Aβ to cultures pre-treated with antisense NCX3 oligonucleotides caused a significant increase in cell death when compared to vehicle-treated or sense NCX3 oligonucleotide transfected cells ($p < 0.01$; Fig. 3.2C). These findings highlight a close association between NCX3 amounts and Aβ neurotoxicity. It is likely that cellular mechanisms exist to compensate for the loss of NCX3 function, and these may explain the relatively modest effect of NCX3 suppression on Aβ-induced neuronal loss observed in these experiments. Indeed, compensation by other NCX family members was previously shown to compensate for NCX3 suppression in cultured rat cerebellar granule cells treated with glutamate (Bano et al., 2007). Nonetheless, these findings suggest that reduced expression of functional NCX3 sensitizes primary neurons to the neurotoxic effects of Aβ.

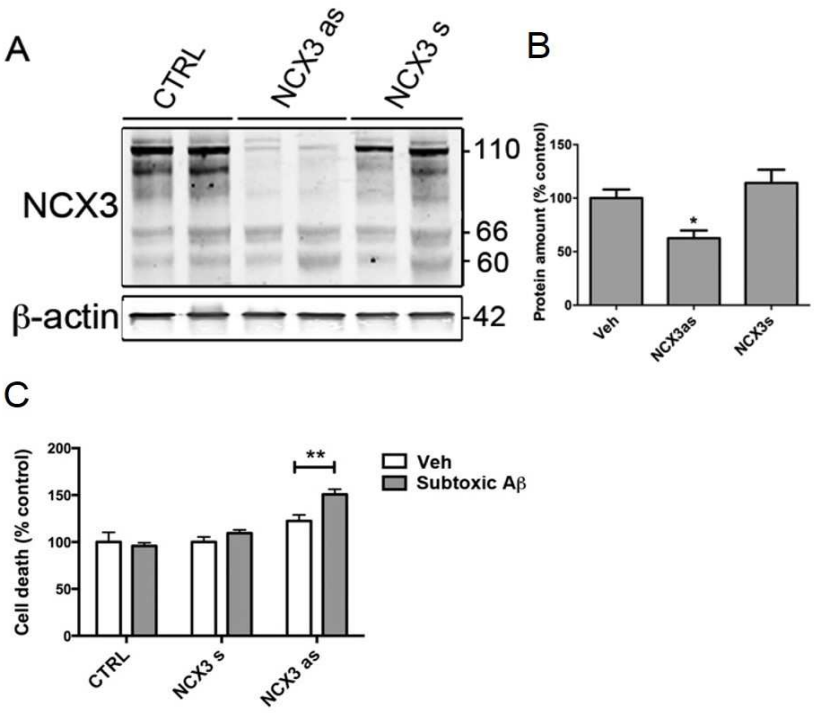

Fig. 3.2 Knockdown of NCX3 expression sensitizes cortical neurons to Aβ. Rat primary cortical cultures were transfected with antisense (as) or sense (s) oligonucleotides against NCX3 for 24 h followed by treatment with a subtoxic dose (1μM) of oligomeric Aβ for a further 16 h. (A) Representative immunoblots of cortical lysates probed with antibodies detecting NCX3 holoprotein at 110 kDa and cleaved fragments at, 60-66 kDa. Blots were also probed with an anti-β-actin antibody (42 kDa) as a loading control. Bar graphs show (B) total NCX3 protein amounts standardized to β-actin and (C) proportion of neuron death as measured by live/dead assay following treatment with 1μM Aβ, Aβ and antisense NCX3 oligonucleotides, 1μM Aβ and sense NCX3 oligonucleotides, or oligonucleotides alone, all expressed as a percentage of neuron death in control cultures. Data are mean ± SEM (n = 3). *$p < 0.05$, **$p < 0.01$

3.2.5 Characterization of biochemical changes in AD-relevant proteins in post mortem brains of different AD stages

Alterations in Ca^{2+} homeostasis are proposed to occur during the very earliest stages of AD development (Chakroborty 2012; Chakroborty et al. 2012). Since

calpain is a Ca^{2+}-activated protease, assessment of calpain activity in early stage AD brain was used as an indicator of changes in Ca^{2+}, and how these relate to changes in other important disease proteins. Therefore, postmortem human frontotemporal cortex was obtained from Braak stage II-VI AD brain and compared to age- and post mortem delay (PMD)-matched controls that showed no clinical or histopathological evidence of neurodegenerative diseases. It was important to first confirm the Braak staging of these tissues. The microtubule-associated protein tau accumulates in a hyperphosphorylated form in NFTs in affected regions of AD brain (Hanger et al., 2009). The accumulation of phosphorylated tau is associated with synaptic and neuronal dysfunction in AD (Crimins et al., 2013), and therefore tau is a promising target for new dementia therapies (Noble et al., 2011).

Post mortem brain homogenates were probed with antibodies against total tau (DAKO), detecting bands ranging from 37 to 75 kDa in size, and tau phosphorylated at the PHF1 epitope (Ser396/404), which yields bands ranging from 50-68 kDa in size, corresponding to full-length tau in the adult human CNS (Fig. 3.3A). The intensity of tau bands were normalized to those for NSE in the same sample. Quantification of band densities showed that, compared to control brain, there is an increase in total tau protein amounts in early AD stages that is sustained throughout AD progression. The increase in total tau was significant in Braak stage II, IV and VI brains compared to control ($p < 0.05$), with Braak stage III and VI elevated, but not significantly, which likely reflects the small sample

number and/or variation within groups (Fig. 3.3B). Immunoblotting of postmortem brain lysates with the PHF1 antibody revealed bands only in late stage AD brain, suggesting that the amounts of tau phosphorylated at these sites in early to mid-AD are quite low, certainly below the level of detection of immunoblotting. Quantitative analysis of tau phosphorylated at PHF1 sites following normalization to total tau amounts in the same sample showed that tau is significantly more phosphorylated at Ser396/404 in late stage AD (Braak stage VI) when compared to earlier stages of AD and control brain ($p < 0.001$; Fig. 3.3C). This trend was also observed when samples were immunoblotted with an antibody against tau phosphorylated at Ser202 (CP13; data not shown). These findings are in support of previous reports of increased total tau protein in degenerating AD cortical regions (Khatoon et al., 1994), and may represent accumulation of degradation-resistant aggregated tau in tissue homogenates. The results are unlikely to reflect increases in tau expression since previous reports have failed to identify any changes in total tau mRNA in AD brain when compared to control brain (Boutajangout et al., 2004; Hyman et al., 2005). To further confirm Braak staging of post mortem brain samples, immunohistochemistry was performed on fixed tissue using an antibody against phosphorylated tau (AT8) which recognises NFTs in AD brain. These studies revealed the expected and well-characterized progressive appearance of tangle-like structures in Braak IV-VI sections (Fig. 3.3D). NFTs were absent from age-matched control brain.

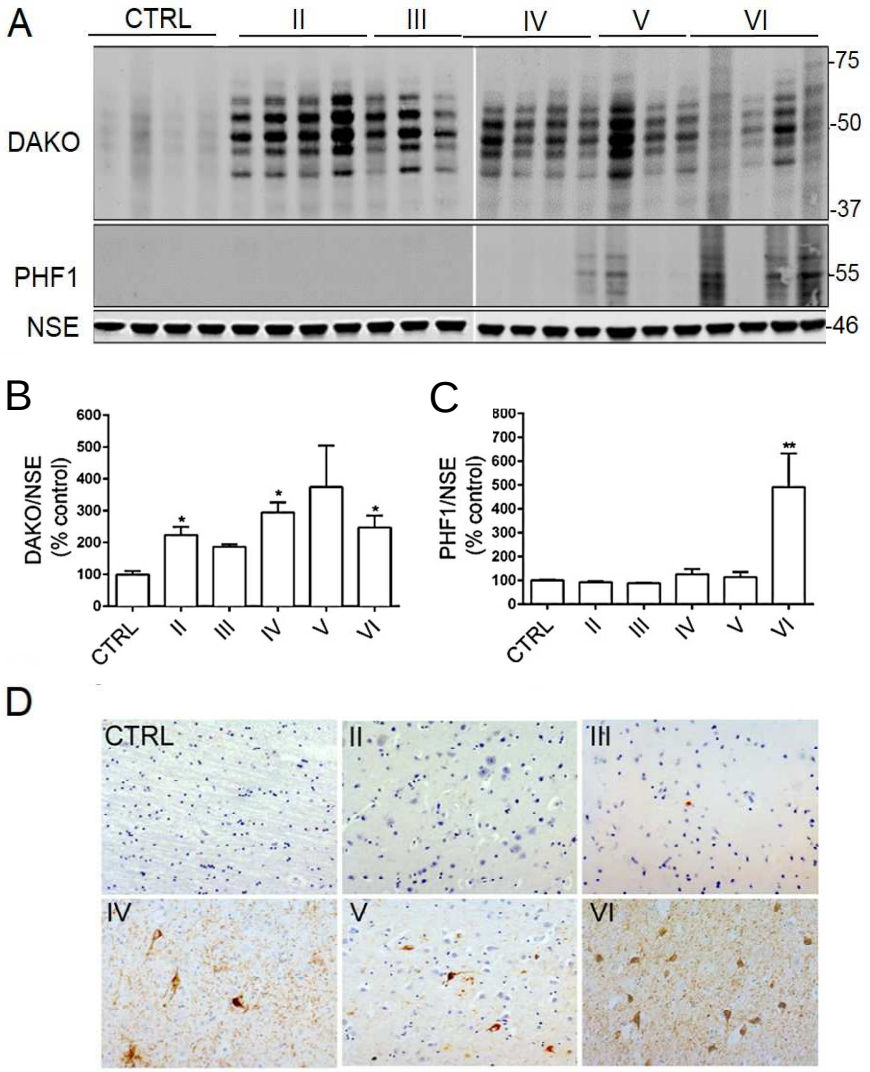

Fig. 3.3 Tau accumulates throughout AD development and is hyperphosphorylated in end-stage disease. (A) Representative immunoblots of post mortem cortical lysates from control and Braak II-VI AD brain. Blots were probed with antibodies against total tau (DAKO) at 40 to 75 kDa and tau phosphorylated at Ser396/404 (PHF1) which detected defined bands of 50 to 62 kDa. Blots were also probed with an antibody against 46 kDa neuron-specific enolase (NSE) as a loading control. Bar graphs show amounts of (B) Total tau (DAKO) and (C) tau phosphorylated at PHF1 sites, both standardized to NSE amounts in each sample. (D) Post mortem cortical sections immunostained with an antibody against phosphorylated tau (AT8) that labels neurofibrillary tangles (NFTs). CTRL: control (n = 7), Braak II: early AD (n = 4), Braak III: early AD (n = 3), Braak IV: moderate AD (n = 4), Braak V: advanced AD (n = 3), Braak VI: severe AD (n = 4). Data shown are mean ± SEM.*$p < 0.05$, **$p < 0.01$.

3.2.6 APP processing is altered in early AD brain

Amyloid precursor protein (APP) is a large type 1 transmembrane protein that is proteolytically cleaved to yield toxic Aβ peptides in AD (Dawkins and Small, 2014). To assess changes in APP cleavage in post mortem AD brain, samples were immunoblotted with an antibody specific for C-terminal APP (6E10), which recognizes 3 bands at 106, 113, and 130 kDa, characteristic of the 3 major isoforms of human APP holoprotein (Fig. 3.4A; Nordstedt et al., 1991; Delvaux et al., 2013). When standardized to NSE, quantification of western blot band intensities showed that there are significantly increased amounts of total APP holoprotein in Braak stages II and III AD brain lysates ($p < 0.01$) when compared to those from control brain, with late stage AD brain showing approximately equivalent levels to that observed in control tissue (Fig. 3.4B). This findings are in line with and extend previous studies which have reported no differences in the amounts of total APP holoprotein between control, non-demented and end-stage AD brains (Nordstedt et al., 1991).

The major Aβ isoforms produced from pathological APP cleavage in AD are the 40 and 42 residue variants, the latter possessing a higher propensity to aggregate and induction of neurotoxicity *in vitro* (Gouras et al., 2000; Butterfield, 2002). To assess changes in amount of secreted Aβ1-40 and Aβ1-42 in post mortem control and AD tissue, specific amounts of each peptide were measured in these samples using Invitrogen Aβ ELISAs, as previously described (Vagnoni et al., 2011, 2012).

These experiments revealed no significant difference in the amounts of Aβ1-40 in lysates from AD of any stage and control tissues (Fig. 3.4C). In contrast, there was a significant increase in Aβ1-42 tissue burden in Braak stage IV ($p < 0.05$), Braak V ($p < 0.01$, Braak V) and Braak VI ($p < 0.05$, Braak VI) AD brain when compared to that measured in control lysates (Fig. 3.4D). Similar findings were previously reported following analysis of cortical lysates from sporadic AD individuals (Shinohara et al., 2014).

Immunohistochemical analysis of fixed post mortem cortical sections with an antibody against Aβ (6E10) confirmed the expected presence of diffuse amyloid plaques in Braak II and III tissue, and dense core and neuritic plaques in Braak IV and VI tissue, none of which were observed in control sections (Fig. 3.4E).

The above findings reveal transient elevations in APP holoprotein amounts in early stage AD brain, which may signify an, as yet unestablished, compensatory mechanism in response to early pathological changes in AD brain. Moreover, the changes in APP processing identified here were found to precede increases in Aβ1-42 production and the senile plaque deposition detected in moderate to end stage AD brain. Interestingly, the presence of diffuse plaques in immunostained cortical tissue was observed prior to accumulation of Aβ as measured by ELISA, and reflect the inability of the ELISA technique to detect aggregated Aβ.

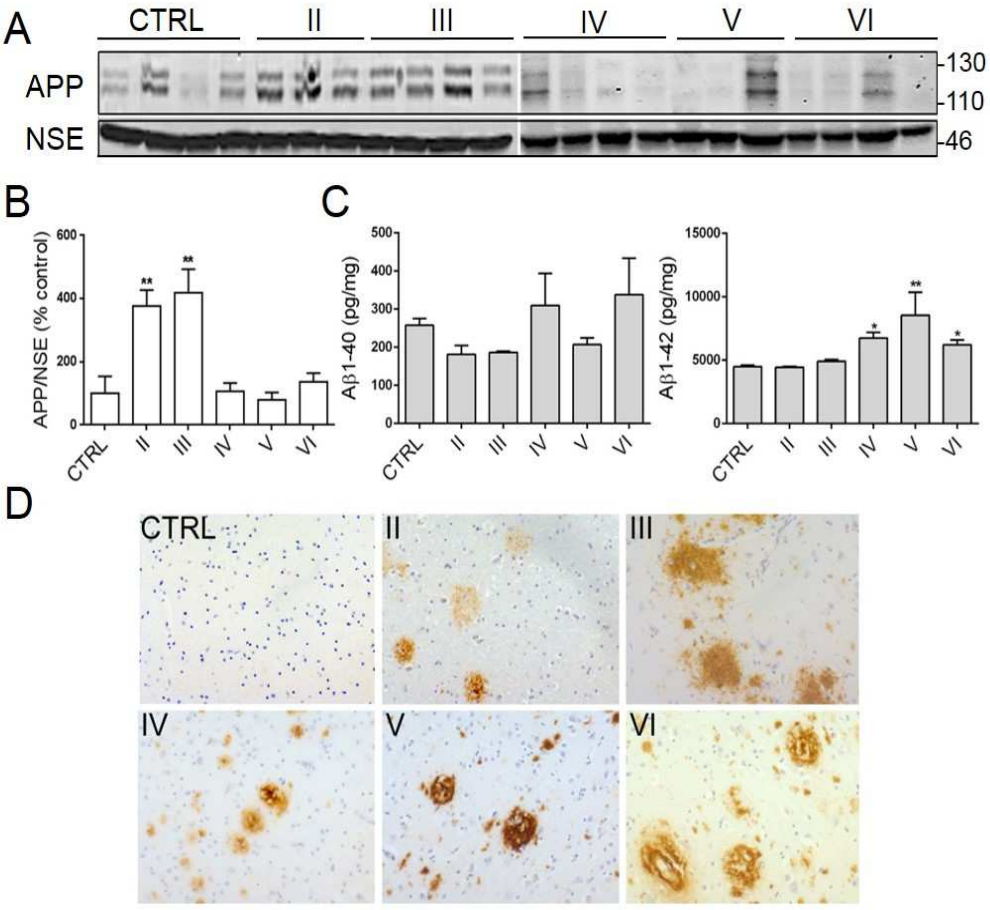

Fig. 3.4 Transient elevations of total APP amounts occur in the early stages of AD, and persistent accumulations of Aβ1-42 are observed in end-stage disease. (A) Representative immunoblots of post mortem cortical lysates from control and Braak II-VI AD brain. Blots were probed with an antibody against the major forms of full-length APP (110-130 kDa) and NSE was used as a loading control (46 kDa). Bar graphs show amounts of (B) APP standardized to NSE and (C) Aβ1-40 and Aβ1-42 as measured by quantitative ELISA. (D) Immunostaining of post mortem cortex sections with an antibody against Aβ (6E10) that labels diffuse and senile plaques. CTRL: control (n = 7), Braak II: early AD (n = 4), Braak III: early AD (n = 3), Braak IV: moderate AD (n = 4), Braak V: advanced AD (n = 3), Braak VI: severe AD (n = 4). Data shown are mean ± SEM. *p < 0.05, **p < 0.01.

3.2.7 Calpain-1 activity is increased in early AD brain and sustained throughout disease

Calpain-1 is activated by prolonged intracellular Ca^{2+} elevations, which are postulated to occur in the early, asymptomatic stages of AD (Chakroborty and Stutzmann, 2011; Chakroborty et al., 2012). To investigate temporal changes in Ca^{2+} throughout AD course, post mortem frontotemporal lysates were probed with an antibody against the active subunit of calpain-1, yielding a single prominent band at 76 kDa (Fig. 3.5A). Quantitative analysis of western blot band intensities, following normalization to NSE, showed significantly elevated calpain-1 activity in lysates from Braak stage III AD brain ($p < 0.05$) relative to controls, that was sustained in Braak IV ($p < 0.05$), Braak V ($p < 0.01$) and Braak VI ($p < 0.001$) lysates (Fig. 3.5B). These findings indicate that calpain overactivation is prolonged throughout AD development.

3.2.8 CAST activity is upregulated in early, but not late AD brain

CAST activity is decreased in end stage AD brain (Fig. 3.1). Here, this work was extended by examining changes in CAST activity in different AD stages by immunoblotting post mortem cortical lysates with an antibody that detects active CAST (holoprotein at 110 kDa and fragments at 37-75 kDa) and inactive CAST (< 25 kDa; Fig. 3.5A). When standardized to NSE, quantification of band intensities for full length and active CAST as a proportion of total CAST revealed that levels

of active CAST are significantly increased in Braak III AD brain ($p < 0.05$) compared to control (Fig. 3.5C). Although CAST levels also appeared to be increased in Braak stage IV and V tissue lysates, these were found to be not significantly different from controls. No significant differences in inactive CAST amounts were observed between any AD brain lysates and controls (Fig. 3.5D).

3.2.9 Caspase-3 activity is unaltered throughout AD progression

Multiple studies point to a crosstalk between calpains and caspases (Nakagawa and Yuan, 2000), and activation of neuronal caspase-3 by apoptotic and non-apoptotic stimuli has been linked to neurodegenerative processes in the brain (Porter and Jänicke, 1999; de Calignon et al., 2010). Caspase-3 is a 32 kDa proenzyme that is activated upon caspase-8- and caspase-9-mediated cleavage into 17 and 19 kDa active fragments, respectively.

To assess caspase-3 activity, post mortem lysates were immunoblotted with an antibody against caspase-3 that labels pro-caspase-3 and its active fragments. This antibody detected a 17 kDa active caspase-3 band, as previously found in post mortem brain (Atherton et al., 2014; Fig. 3.5A). Following normalization to NSE, the densities of caspase-3 bands were quantified. The results showed that there were no significant differences in caspase-3 activity in lysates from any AD stage brain when compared to control tissue (Fig. 3.5E). This finding supports

previous results from this group (Atherton et al., 2014) and others (Jellinger and C. Stadelmann, 2000).

3.2.10 Proteolytic processing of α-spectrin increases with advancing AD stages

A common substrate of both calpain-1 and caspase-3 is the cytoskeletal protein α-spectrin. To determine if cleavage of α-spectrin corresponds with increased activity of calpain in AD brain, immunoblots of post mortem brain lysates were probed with an anti-α-spectrin antibody that detects holoprotein at 240 kDa, calpain- and caspase-cleaved fragments (145 to 150 kDa) and caspase-3-cleaved fragments (110 to 125 kDa; Fig. 3.5A). Calpain- and caspase-cleaved species were separately quantified and normalized to NSE. The results of this analysis showed a trend of increasing calpain- and caspase-cleaved α-spectrin fragments (145-150kDa) with advancing disease stage. The increases in calpain/caspase-cleaved α-spectrin cleavage were significant in lysates from Braak stage III ($p < 0.05$) and VI ($p < 0.01$) brain tissues (Fig. 3.5F). No significant differences in the amounts of caspase-3-cleaved α-spectrin species were found between any AD group and control (Fig. 3.5G). These findings are in support of earlier analyses of calpain-1 and caspase-3 activities (Fig. 3.5B-E), and suggest that, unlike caspases, there is sustained activation of calpains in AD brain.

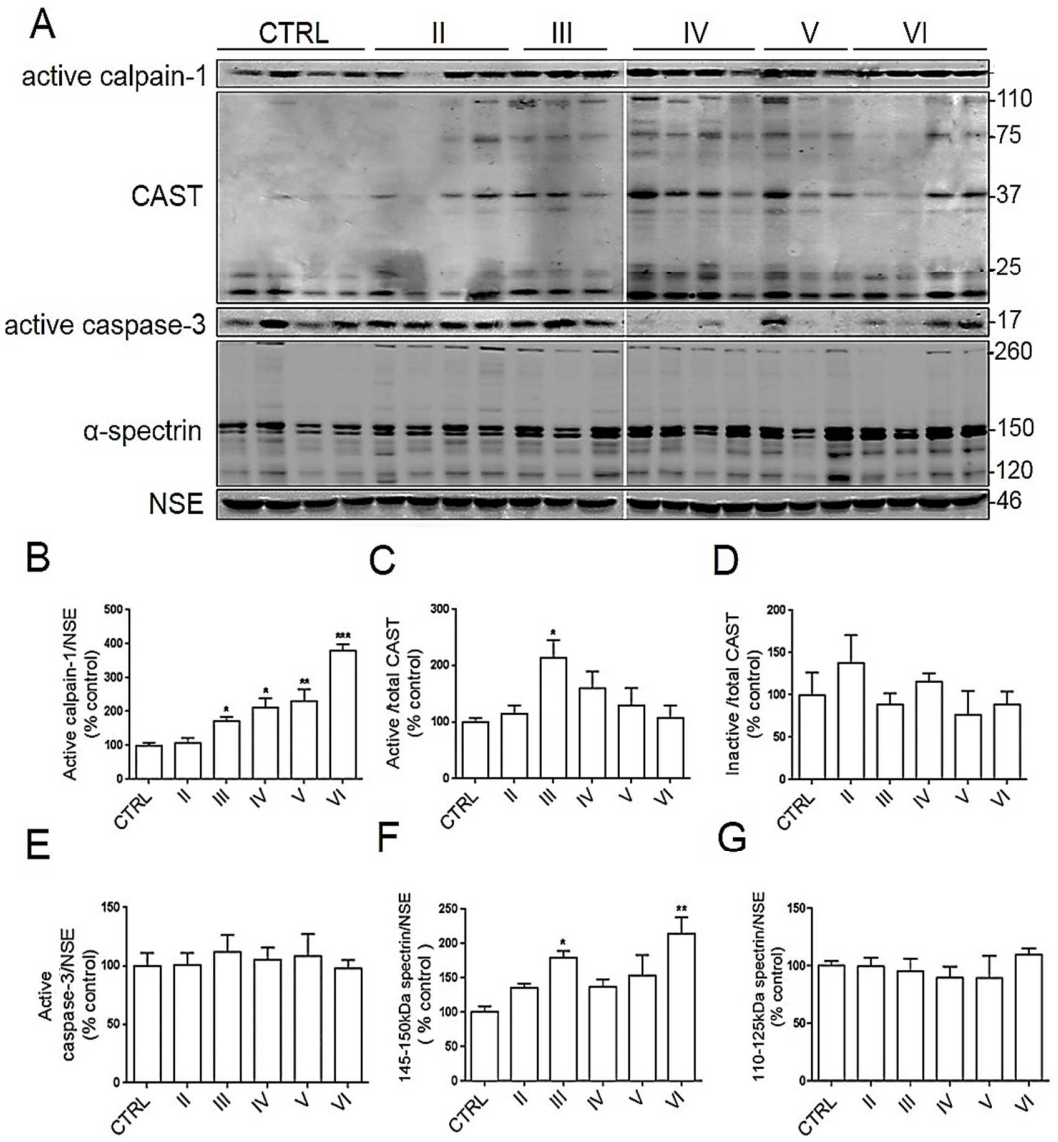

Fig. 3.5 Calpain-1 activity is elevated in early AD brain and is sustained in late stage disease. (A) Representative blots of post mortem cortical lysates from control and Braak II-VI AD individuals. Blots were probed with antibodies that detect active calpain-1 at 76 kDa and active caspase-3 at 17 kDa. An anti-calpastatin (CAST) antibody detects full-length CAST at 110 kDa, active CAST at > 25 kDa and inactive CAST at < 25 kDa. An antibody against α-spectrin detects holoprotein at 240 kDa, calpain- and caspase-cleaved fragments at 140 to 150 kDa and caspase-cleaved fragments at 110 to 125 kDa. Blots were also probed with an antibody against neuron-specific enolase (NSE) antibody (46 kDa), as a loading control. Bar graphs show amounts of (B) active calpain-1 following normalisation to NSE (C) active CAST and (D) inactive CAST as a proportion of total CAST, (E) active caspase-3 following normalisation to NSE, (F) calpain-cleaved α-spectrin and (G) caspase-cleaved α-spectrin standardized to NSE. CTRL: control (n = 7), Braak II: early AD (n = 4), Braak III: early AD (n = 3), Braak IV: moderate AD (n = 4), Braak V: advanced AD (n = 3), Braak VI: severe AD (n = 4). Data is mean ± SEM. *$p < 0.05$, **$p < 0.01$, ***$p < 0.001$

3.2.11 Cdk5 activity is elevated in early AD brain and its activity is sustained throughout disease progression

Cdk5 is a proline-directed serine/threonine kinase that phosphorylates several serine and threonine residues on tau in AD brain (Hanger et al., 2009). However, the specific contribution of cdk5 to AD pathogenesis is somewhat controversial (Patrick et al., 1999; Taniguchi et al., 2001; Giese, 2014). Cdk5 activation requires complex formation with one of its neuronal activators, p35 or p25. P35 is subject to cleavage by calpain into a smaller fragment, p25, which is a more stable and potent cytoplasmic activator of cdk5. Prolonged activation of cdk5 as a result of p25 over-expression leads to increased tau phosphorylation, aggregation and NFT formation, Altered APP processing and enhanced Aβ production, synaptic and neuronal demise in transgenic mice (Noble et al. 2003; Cruz et al. 2003; Cruz et al., 2005).

To examine the activation of cdk5 in these brain samples, blots were probed with an antibody against cdk5 holoprotein, detecting a 33 kDa band, and an antibody against p35 which detects both p35 and p25 at 35 and 25 kDa, respectively (Fig. 3.6A). Quantitative analysis of band densities in these blots revealed no significant changes in the amounts of cdk5 or p35 in any AD group compared to control (Fig.3.6B). In contrast, when measuring p25 as a proportion of p35, there was a significant increase in p25/p35 ratio in Braak stage III that was sustained in all later Braak stages ($p < 0.01$; Fig. 3.6D). These results are indicative of increased

calpain-mediated degradation of p35 to p25 and, therefore, indicate increased cdk5 activity from an early stage in AD that is sustained throughout mid- and late-stage disease.

3.2.12 GSK3 expression and activity are increased in late stage AD brain

GSK3 is a proline-directed serine/threonine kinase that is widely recognized to play a a pivotal role in AD pathogenesis (Hooper et al. 2008; Hanger et al., 2009). GSK3 exists as two species, GSK3α and GSK3β, which are respectively phosphorylated at Ser21 and Ser9 to inhibit kinase activity. GSK-3 is constitutively active, with the addition of phosphate to Ser21/9 acting to inhibit kinase activity (Hanger et al., 2009). Activation of GSK3 can be induced upon calpain cleavage of GSK3 at its N-terminus, which acts to removes inhibitory phosphorylation at Ser21/9 residues (Goñi-Oliver et al., 2007).

To examine the activity of GSK-3 in AD brain, post mortem blots were probed with an antibody against total GSK3, detecting two bands at 51 and 47 kDa which represent GSK3α and GSK3β, respectively (Fig. 3.6A). Blots were also probed with an antibody against GSK3 phosphorylated at Ser21/9 (pGSK3), which yielded a single prominent band in these samples (Fig. 3.6A). This band is likely to represent GSK3β phosphorylated at Ser9, since our group has previously

observed that this antibody has higher affinity for GSK3β. For this reason, quantitative analysis of pGSK3 did not differentiate between GSK3α and GSK3β. When normalized to NSE, analysis of GSK3 protein bands revealed significantly increased amounts of total GSK3α ($p < 0.01$) and GSK3β ($p < 0.001$) in end stage AD (Braak VI) brain when compared to control brain (Fig. 3.6E, F). Quantification of pGSK3 showed significantly reduced phosphorylation of GSK3 in Braak stage V and VI AD brain lysates when compared to those from control tissue, indicating that GSK3 activity is significantly increased in the later stages of AD.

3.2.13 Synaptic proteins are upregulated in early Braak stages and lost in end-stage AD brain

AD is characterized by widespread synaptic dysfunction and loss that is believed to be mediated by alterations in Ca^{2+}, calpain activity and tau phosphorylation (Wu and Lynch, 2006; Crimins et al., 2013). To begin to understand changes in synaptic activity in the brain samples used in this study, lysates of post mortem brain were immunoblotted were with antibodies against major pre- and postsynaptic markers. Synapsin I was selected as a pre-synaptic marker. Synapsin I is a neuronal phosphoprotein localized to small presynaptic vesicles that plays a vital role in neurotransmitter release (Bähler et al., 1990). The antibody against synapsin I yielded an approximately 80 kDa doublet, likely reflecting differential phosphorylation of full-length synapsin I (Fig. 3.7A). To assess changes in

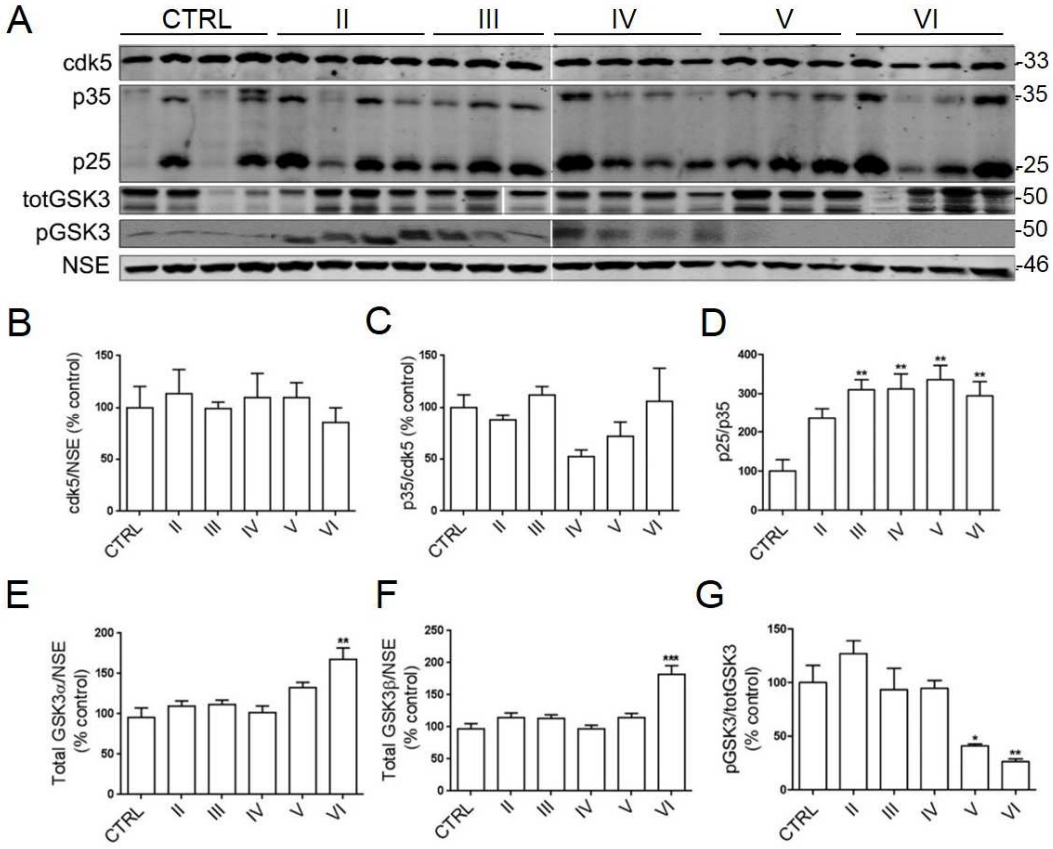

Fig. 3.6 Cdk5 and GSK3 activities are increased in AD brain. (A) Representative blots of post mortem cortical lysates from control and Braak II-VI AD brain. Blots were probed with antibodies against cyclin dependent kinase 5 (cdk5) holoprotein at 33 kDa, p35 at 35 kDa and the calpain-cleaved fragment, p25 (25 kDa). Blots were also probed with antibodies detecting glycogen synthase kinase 3 (totGSK3) -α and -β at 52 and 47 kDa, respectively, and GSK3 phosphorylated at Ser9 (pGSK3) at 52 kDa. Anti-neuron-specific enolase (NSE) antibody was used as a loading control (46 kDa). Bar graphs show amounts of (B) cdk5 following normalisation to NSE, (C) p35 as a proportion of cdk5, (D) p25/p35 ratio, (E) totGSK3α and (F) totGSK3β following normalisation to NSE, and (G) pGSK3 standardised as a proportion of total GSK3. CTRL: control (n = 7), Braak II: early AD (n = 4), Braak III: early AD (n = 3), Braak IV: moderate AD (n = 4), Braak V: advanced AD (n = 3), Braak VI: severe AD (n = 4). Data is mean ± SEM. *p < 0.05, **p < 0.01, ***p < 0.001.

postsynaptic markers, antibodies specific to postsynaptic density-95 protein (PSD95) and the NR2B subunit of NMDARs were used. These yielded bands at the

expected sizes of approximately 95 and 170 kDa, respectively (Fig. 3.7A). PSD95 is commonly used as a marker for synaptic loss as it comprises an integral portion of the postsynapse (Dorostkar et al., 2014). NR2B is an extrasynaptic Ca^{2+}-permeant ionotropic glutamate receptor that mediates excitotoxicity and is subject to calpain cleavage in AD (Ittner et al., 2010).

The density of protein bands were measured and normalized to NSE content in the same sample. Quantitative analysis of these findings showed that there was a common pattern of expression for all synaptic markers, where protein amounts increased in early AD stages, followed by recovery to control levels and/or protein loss in late stage AD. The amounts of both synapsin I and NR2B were significantly increased in early AD ($p < 0.05$; Braak III and II respectively), followed a reduction to levels close to control in Braak IV to VI tissue (Fig. 3.7B, C). Levels of PSD95 protein were also significantly elevated in Braak III tissue ($p < 0.05$), and returned to levels below control in Braak VI lysates (Fig. 3.7D). The reduction in PSD-95 in Braak stage VI tissues was clearly apparent, but was not statistically significant, which may result from variation within small sample sets. Nevertheless, these findings suggest that there is an increase in synaptic activity or synapse number in the early stages of AD, which is eventually followed by synapse loss as the brain atrophies in end-stage disease. Furthermore, it is possible that increased NR2B expression in the early Braak stages could have contributed to glutamate excitotoxicity extrasynaptically.

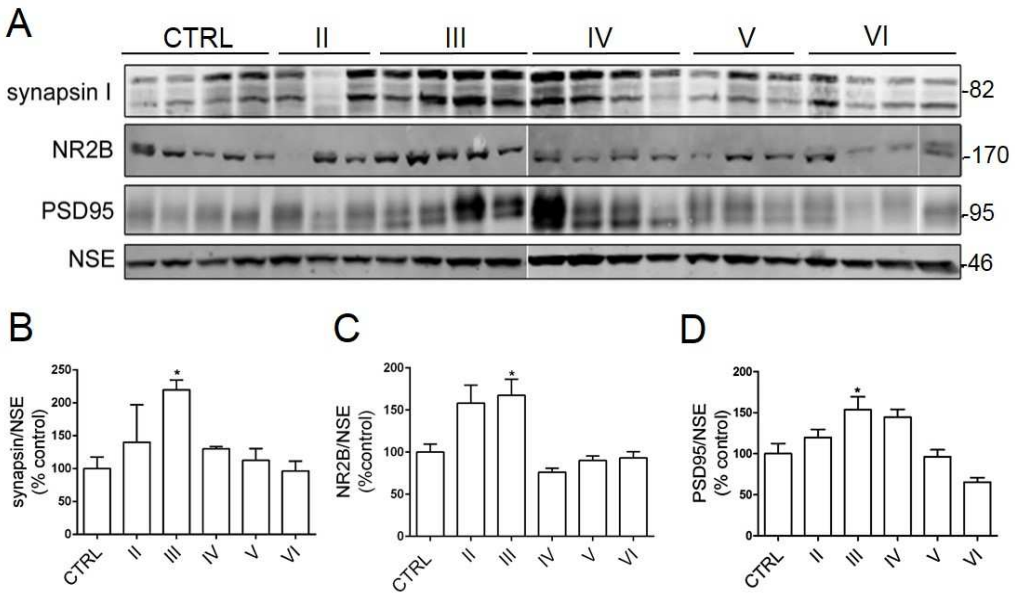

Fig. 3.7 Pre- and post-synaptic markers are elevated in early Braak stages. (A) Representative blots of post mortem cortical lysates from control and Braak II-VI AD brain. Blots were probed with antibodies that detect synapsin I at 80-85 kDa, the NR2B subunit of NMDARs (NR2B) at 170 kDa, and post-synaptic density 95 protein (PSD95) at 95 kDa. An antibody against anti-neuron-specific enolase (NSE) provided a loading control (46 kDa). Bar graphs show amounts of (B) synapsin I, (C) NR2B and (D) PSD95 all standardized to NSE. CTRL: control (n = 7), Braak II: early AD (n = 4), Braak III: early AD (n = 3), Braak IV: moderate AD (n = 4), Braak V: advanced AD (n = 3), Braak VI: severe AD (n = 4). Data is mean ± SEM. *p < 0.05

3.2.14 Calpain-1 activity correlates with Aβ1-42 load, tau kinase activity and tau accumulation

Considerable research links alterations in neuronal Ca^{2+} to Aβ overproduction, tau phosphorylation and synaptic changes in AD (LaFerla and Oddo, 2005; Zempel et al., 2010). Therefore, it was important to determine if there is any correlation between active calpain-1 amounts and disease-relevant changes in the postmortem brain lysates examined here (Fig. 3.8).

These analyses revealed a significant positive correlation between active calpain 1 and Aβ1-42 ($p < 0.001$; Fig. 3.8A), confirming findings previously reported by this group (Atherton et al., 2014) in sporadic AD brain, and also reports from others in experimental models of AD (Mathews et al., 2002; Town et al., 2002). These findings support evidence showing that calpain may be induced by and/or regulate Aβ production. Active calpain-1 amounts were also significantly correlated with amounts of calpain- and caspase-cleaved α-spectrin fragments ($p < 0.001$; Fig. 3.8B) and p25 amounts ($p < 0.05$; Fig. 3.8C), as would be expected for calpain substrates, with this data acting as further confirmation that there is increased calpain-1 activity in AD brain. Notably, amounts of active calpain-1 showed a significant negative correlation with levels of GSK3 phosphorylated at the inhibitory residues Ser21/9 (pGSK3) ($p < 0.001$; Fig. 3.8D). These findings are likely to be indicative of N-terminal cleavage of GSK3 by calpain (Goñi-Oliver et al., 2007), which cleaves these N-terminal phosphorylation sites to activate GSK-3. These findings are in keeping with recent reports of calpain-mediated GSK3 regulation in end-stage AD brain (Jin, Yin, Yu, et al., 2015). Interestingly, active calpain-1 levels also showed a significant positive correlation with amounts of total tau ($p < 0.05$; Fig. 3.8E) in AD brain. Tau is subject to N-terminal truncation by calpain-1 to yield neurotoxic fragments (Garg et al., 2011a; Liu et al., 2011), for which reason the correlation between calpain-1 and accumulation of tau could signify increased calpain-mediated generation of these tau fragments. Finally, correlation analyses between tissue Aβ burden and synaptic markers showed a

significant negative correlation between Aβ1-42 and NR2B amounts ($p < 0.01$; Fig. 3.8G), but no correlation between Aβ1-42 and synapsin-1 or PSD95 (Fig. 3.8F, H). These findings indicate that in conditions where Aβ1-42 is elevated, there is loss of NR2B, likely reflecting previously reported synaptotoxic effects of Aβ at NMDA receptors (Ittner et al., 2010).

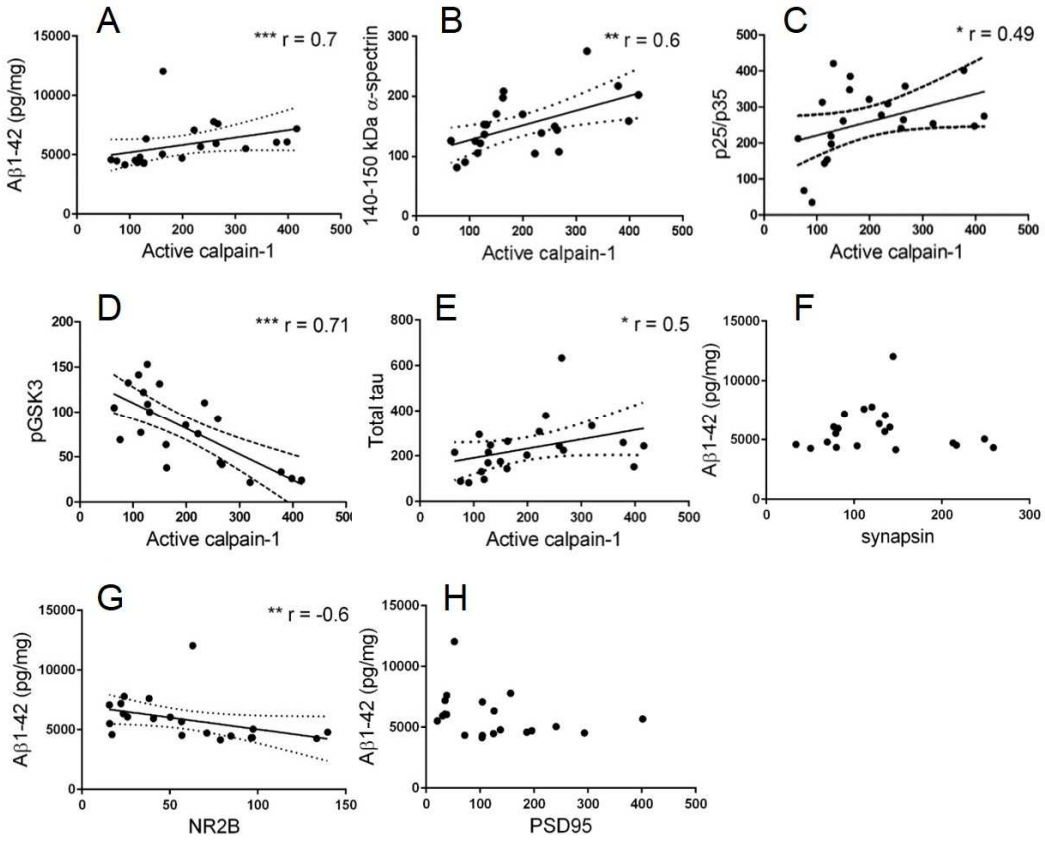

Fig. 3.8 Calpain-1 activity correlates with Aβ burden, kinase activities and tau amounts in AD brain. Scatter plots show the correlation between levels of active calpain-1 and (A) Aβ1-42, (B) calpain- and caspase-cleaved α-spectrin fragments, (C) p25/p35 and (D) phosphorylated (inactive) GSK3 (pGSK3) in lysates from control and AD brain. Aβ tissue burden as measured by ELISA was also correlated with (F) synapsin, (G) NR2B and (H) PSD95 protein amounts. Parametric correlation analysis was used to generate correlation coefficients (r values) and significance. *$p < 0.05$, **$p < 0.01$, ***$p < 0.001$.

3.3 Summary and Discussion

The main findings of this chapter are:

- Elevated calpain-1 activity in the cortex of end-stage AD and other neurodegenerative brain relative to controls.
- Increased calpain-mediated cleavage of NCX3 in end-stage AD brain, but not that from other tauopathies, compared to controls.
- Reducing NCX3 expression sensitizes rat primary neurons to subtoxic concentrations of Aβ, suggesting a functional link between NCX3 function and Aβ-induced neurotoxicity.
- Progressive accumulation of tau from early- to late-stage AD brain, and increased tau phosphorylation in end-stage disease.
- Increased APP holoprotein amounts in early Braak stage AD brain, prior to increased production of Aβ1-42 in late-stage disease.
- Calpain-1 activity is elevated in early stages of AD tissue and this is sustained throughout disease progression.
- Elevations in amounts of active calpain-1 preceded increased activities of the key tau kinases ckd5 and GSK3.
- Increased expression of synaptic proteins in early AD brain, followed by a return to control levels or loss in end-stage disease.

- Positive correlations between active calpain-1 amounts, Aβ1-42, activities of cdk5 and GSK3, and tau accumulation.

3.3.1 Calpain-1 activity is elevated in neurodegenerative disease brain

Altered neuronal Ca^{2+} homeostasis causes the induction of intracellular signaling cascades that have the capacity to mediate the neurodegenerative changes seen in AD (LaFerla, 2002). The data presented in this chapter demonstrates that there are marked increases in the activity of the Ca^{2+}-activated cysteine protease calpain-1 in late-stage AD brain, confirming findings previously reported by many other groups (Saito et al., 1993; Tsuji et al., 1998). This increase in calpain activity was also observed in brain tissue from patients with PSP, CBD and FTD. This is consistent with previous reports of calpain activation in end-stage PSP and CBD brain (Ferreira and Bigio, 2011).

The increase in calpain-1 activity observed in these tissues was associated with reduction of active CAST, the endogenous calpain inhibitor that is itself a substrate of calpain and which has previously been shown to be depleted in AD brain (Rao et al., 2008). When taken together, these results suggest that elevated calpain-1 activity is a common neurodegenerative disease feature, suggesting that there is accumulation of intracellular Ca^{2+} in affected brain regions in all of these

diseases. Moreover, calpain-mediated suppression of CAST inhibitory activity implies that calpain activity is exacerbated in end-stage AD in a positive-feedback manner, thereby accelerating degradation of cytoskeletal substrates and disease-relevant proteins such as α-spectrin and tau (Ferreira and Bigio, 2011; Huh et al., 2001).

3.3.2 NCX3 is cleaved by calpain in AD brain and confers neuronal vulnerability to Aβ in primary culture

NCX3 belongs to a family of plasmalemmal exchangers that provide a route of Ca^{2+} efflux during conditions of high intracellular Ca^{2+}, thereby serving a vital homeostatic function. Reduction of NCX3 holoprotein amounts was observed here in late-stage AD brain relative to control, and this was accompanied by increases in the amounts of calpain-cleaved, inactive, NCX3 fragments. While depletion of functional NCX3 in AD brain was previously reported (Sokolow et al., 2011), demonstration of increased calpain-cleaved NCX3 in this AD tissue here is a novel finding. Moreover, generation of these cleaved NCX3 species correlates with Aβ1-42 burden (Atherton et al., 2014) and is absent in tissue from other neurodegenerative conditions. This suggests that calpain-mediated NCX3 cleavage is induced by Aβ1-42 in a mechanism specific to AD, and therefore that analysis of NCX3 processing could have potential as a biomarker for AD. This is particularly relevant since NCX3 can be detected in plasma (Atherton et al., 2014).

Of interest, proteolytic inactivation of NCX3 was not associated with compensatory upregulation of NCX1, as shown by this group (Atherton et al., 2014) and others (Sokolow et al., 2011); however, changes in the expression of other Ca^{2+} transport proteins such as plasma membrane Ca^{2+}-ATPases were not assessed in these studies. Calpain-mediated cleavage and inactivation of NCX3 has been previously shown in an in *vitro* model of ischaemia. In these studies, inactivation of NCX3 upon calpain proteolysis resulted in glutamate-induced excitotoxicity associated with impaired extrusion of excess cellular Ca^{2+} (Bano et al., 2005). Moreover, NCX3 knockout mice exhibit delayed clearance of excess resting Ca^{2+} and diminished LTP, implying a crucial role for NCX3 in learning and memory. These findings have led to the current hypothesis that altered NCX3 function contributes to AD. In support of this idea, knockdown of NCX3 with antisense oligonucleotides was shown here to sensitize primary neurons to a normally subtoxic dose of oligomeric Aβ. These data suggests that NCX3 could mediate neuronal dysfunction and loss in AD, with calpain-mediated inactivation of NCX3 in response to Aβ preventing neuronal Ca^{2+} clearance, thereby promoting intracellular cytotoxic Ca^{2+} overload and neuronal death.

3.3.3 Calpain-1 activation precedes Aβ overproduction, tau phosphorylation and synaptic loss in AD

The temporal associations between key neurodegenerative processes during the course of AD are as yet unclear, and to begin to understand these, changes in proteins were studied here using post mortem cortical tissue exhibiting pathological changes consistent with early, mid and late disease stages. It is demonstrated here that calpain-1 activity is elevated in the early stages of AD development (Braak stage III) and this is sustained in later stages of disease. The increase in calpain-1 activity was found to precede activation of the tau kinases cdk5 and GSK3, hyperphosphorylation of tau at disease-relevant sites, elevated Aβ production and loss of synaptic proteins (Fig. 3.9). These findings in post mortem brain complement multiple studies carried out in cell and animal models of sporadic AD, all of which suggest that aberrant Ca^{2+} signalling induced by Aβ mediates the neurodegenerative changes seen in disease (Khachaturian, 1989; LaFerla, 2002; Stutzmann et al., 2007; Thibault et al., 2007; Bezprozvanny and Mattson, 2008; Stutzmann and Mattson, 2011; Berridge, 2014).

In parallel to increased calpain-1 activity, this study demonstrates upregulation of the major synaptic proteins synapsin I, PSD95 and the NR2B subunit of NMDARs in the early stages of AD. These results may represent an initial compensatory response of neurons to the synaptic dysfunction that is proposed to occur as disease starts (Forero et al., 2006), as well as elevated Ca^{2+} and calpain

activities. Following these early increases, protein amounts of synapsin I and NR2B are reduced to approximately control levels in moderate to late Braak stages, whereas PSD95 amounts are decreased somewhat below control levels in Braak stage VI tissue.

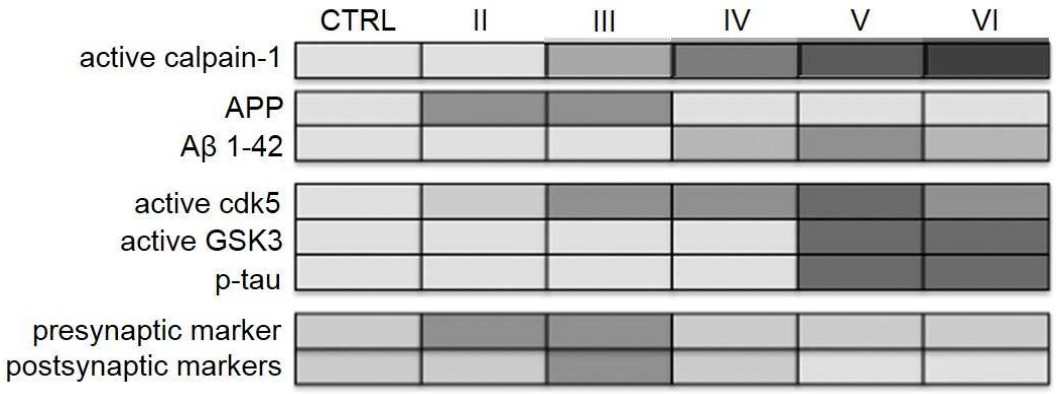

Fig. 3.9 The temporal association between calpain activity, APP processing and Aβ production, tau kinase activity, tau phosphorylation (p-tau) and pre- and postsynaptic markers. Diagram depicting protein amounts in different Braak stages using a scale of light grey (low protein amounts) to dark grey (high protein amounts). Calpain-1 activity is elevated in parallel to increases in amounts of APP holoprotein and synaptic markers. The increase in active calpain-1 is sustained throughout AD progression, and is followed by activation of tau kinases cdk5 and GSK3, tau phosphorylation and increased Aβ production.

The synapsin I protein expression pattern here is inconsistent with previous observations of significantly reduced synapsin I amounts in Braak V-VI AD posterior cingulate cortex compared to non-cognitively impaired controls (Scheff et al., 2015). However, this inconsistency is likely accounted by connectivity differences between the frontotemporal and posterior cingulate cortex (Pearson

et al., 2011). The depletion of PSD95 in end-stage AD tissue was expected since terminal stages of AD are characterized by widespread synaptic degeneration and neural atrophy (Arendt, 2009). Furthermore, PSD95 is subject to calpain cleavage in adult rat brain (Lu et al., 2000), and its reduction in late-stage AD post mortem tissue could be explained by calpain hyperactivity. The relatively small loss of synaptic protein amounts detected here in end-stage disease brain could also have been a reflection of the relative insensitivity of western blotting to detecting small changes in protein abundance.

NR2B is cleaved by calpain in primary neurons after excitotoxic glutamatergic activation and in *vivo* during ischaemia, giving rise to the presence of active NMDAR forms on the cell membrane (Simpkins et al., 2003). Calpain-cleaved NR2B products were not observed in any post mortem tissue here, which may be due to the effects of post mortem protein degradation or these species being below detectable levels. However, the early increases in NR2B holoprotein amounts could also be indicative of a neuroprotective response to calpain cleavage of this protein in early AD stages. Similarly, transient upregulation of CAST activity was seen here in Braak III tissue, and this could also be a result of compensatory mechanisms induced by increased calpain-mediated cleavage of its endogenous inhibitor.

There is growing evidence suggesting that not all Ca^{2+}-related changes in AD are harmful to neurons (reviewed by Supnet and Bezprozvanny, 2010), and it is

possible that the elevations in CAST and synaptic protein amounts observed here in Braak stage II to III AD brain may indicate cellular compensation mechanisms mediated by Ca^{2+} and calpain that are eventually overcome as disease severity increases, conveying the insufficiency of early neuroprotective mechanisms in light of widespread neural cell damage.

3.3.4 Limitations of this work

The use of post mortem brain in this study enabled a valuable analysis of biochemical and neuropathological changes associated with the progression of AD. However, there are many limitations associated with the use of post mortem tissue. First, there is a limited tissue availability, which limited the sample size of each group (n = 3 - 6). Early Braak stage tissue is especially hard to source since clinical diagnosis is more difficult at these stages. Since human brain is notoriously heterogeneous, it is possible that the results presented here are not wholly representative. There was frequent observation of significant variation within sample groups, which may have been exacerbated during the experimental procedures. For this reason, inferences concerning certain proteins of interest could not always be made confidently.

Other considerations include the effects of PMD on sample integrity, and freeze-thawing steps, conditions in which activate proteases can that degrade their cellular substrates. For example, calpain cleavage of GSK3 was found to correlate

with PMD in a previous study (Goñi-Oliver et al., 2007). However, variations in PMD between Braak stages did not exceed 10 h in this study, with the mean PMD (in h) for each group being: CTRL 43.5, II 33.8, III 33.7, IV 39.8, V 36.0, VI 33.9. Moreover, PMD did not correlate with calpain-1 or GSK3 activities in this study.

Control tissue is obtained from individuals with a variety of acute or chronic conditions, and it is possible that these co-morbidities could potentially affect brain health and therefore results obtained here. For example, calpains and caspases are activated during cerebral ischaemia (Pike et al., 2004). Furthermore, the controls were age-matched, and it is clear that certain neurodegenerative processes, including calpain activation, also occur naturally during ageing (Banay-Schwartz et al., 1994; Arsene and Ardeleanu, 2010; Rodriguez-Arellano et al., 2015). Another factor to take into account is the likelihood of secondary or compensatory effects during the course of primary disease in control and AD subjects, such as medication, smoking and chronic illnesses. It is possible that any CNS changes mediated by these factors may underlie some of the observed changes in post mortem tissue, and these are difficult to distinguish from pathological changes intrinsic to AD. Post mortem analyses of brain obviously prevents the possibility of manipulation (e.g. pharmacological or genetic) of the tissue, therefore any data is merely descriptive or correlational and is insufficient for mechanistic inferences. For this reason, further experiments in tractable models are required to determine the pathogenic role of protein changes observed in AD brain.

Finally, following use of the anti-NCX3 antibody in initial experiments (sections 3.2.3/4), this antibody (and others) then failed to detect NCX3 in subsequent Braak II-IV AD studies. The NCX3 antibody was provided by a collaborator with limited stocks, and it was not possible to obtain additional reagents to continue this work. It would have been useful to examine other changes in NCX3 in these tissues since calpain cleavage of NCX3 during early Aβ-induced Ca^{2+} elevations are shown to give rise to hyperfunctional forms of NCX3 that correct Ca^{2+} dyshomeostasis in cell lines (Pannaccione et al., 2012). Identification of this or other NCX3 fragments in early Braak brains would have provided further insight into the neuroprotective effects of Ca^{2+} and calpain activities.

3.3.5 Conclusions

The findings presented in this chapter suggest that calpain-1 overactivation is a common feature of neurodegenerative tauopathies that in AD occurs in early disease stages, preceding pathological changes in tau and increased production of Aβ. The following chapter extends these results by investigating the importance of calpain-1 in Aβ-mediated neurotoxicity, Ca^{2+} dysregulation and tau changes using cell models.

CHAPTER 4

Aβ causes elevation of Ca^{2+} in SH-SY5Y cells and induces calpain-dependent signalling and neurotoxicity in neurons

4.1 Introduction

Ca^{2+} dysregulation is believed by many to play a crucial neurodegenerative role in AD and is seen to occur adjacent to amyloid plaques in neurites of APP transgenic mice (Pascale and Etcheberrigaray, 1999; Kuchibhotla et al., 2008; Lim et al., 2014; Grolla et al., 2013) and in neurons containing abnormal disease-related tau species (Decker et al., 2015). Multiple studies have shown that dysfunction and degeneration of synapses are induced by soluble Aβ oligomers through cytotoxic elevations of dendritic Ca^{2+} (Wu et al. 2010; Selkoe 2002; Ittner et al., 2010). These synaptic perturbations correlate with cognitive decline in transgenic mice (McLaurin et al., 2006; Cissé et al., 2011), and it is therefore proposed that the early cognitive deficits seen in the pre-symptomatic stages of AD are caused by early accumulation of soluble Aβ oligomers and synaptotoxicity

that is dependent on disruption of neuronal Ca^{2+} homeostasis (Chakroborty et al., 2012; Chakroborty, 2012).

The mechanisms through which Aβ-induced Ca^{2+} perturbations lead to synaptic dysfunction and neuronal degeneration remain to be fully elucidated. In cellular models of sporadic AD, application of Aβ has been shown to cause the formation of Ca^{2+}-permeable pores in bilayer membranes (Arispe et al., 1993) or thinning of membranes resulting in increased ion permeability (Kayed et al., 2004). Numerous studies demonstrate that Aβ can also stimulate dysregulated Ca^{2+} influx through interaction with native ion channels and/or receptors, including voltage-gated Ca^{2+} channels (VGCCs), NMDARs and transient receptor potential (TRP) channels (Small, 2009), which leads to rapid increases in neuronal Ca^{2+} content.

As described in the previous chapter, an abundance of evidence implicates the Ca^{2+}-sensitive cysteine protease calpain as a central mediator of numerous AD processes (Ferreira, 2012). Calpains are activated during conditions of high intracellular Ca^{2+}, which can be induced by Aβ in primary neural cell cultures (Town et al., 2002; Hanger et al., 2009) and in transgenic mice overexpressing mutant human APP (Vaisid et al., 2007a). Post mortem AD brain shows elevated calpain-1 activity, with associated increased proteolysis of cytoskeletal and Ca^{2+}-regulating proteins (Chapter 3; Atherton et al., 2014; Tsuji et al., 1998; Nixon, 2003). The work described in this thesis has shown that calpain-1 upregulation

occurs in the early, asymptomatic stages of AD and is sustained throughout disease progression (section 3.2.7). It was therefore important to investigate these findings in more detail in a tractable model where protein activities could be modulated. Therefore, the effects of Aβ on Ca^{2+}, calpain and associated neurodegenerative events were next investigated in rat primary neurons and a neuronal cell line.

The aims of this work were to 1) confirm the importance of calpain activity in mediating Aβ-induced neurotoxicity, 2) investigate the mechanistic relationship between Aβ, calpain, changes in tau and APP processing and synaptic function, and 3) begin to determine the mechanisms underlying Aβ-induced Ca^{2+} elevations in primary cortical cultures.

4.2 Results

It was necessary to first characterise the composition of the rat primary cortical cultures used in these studies. To establish the number and type of neural cells in primary cultures, cells were fixed after 10 DIV and labelled with antibodies to neurons (MAP2), and astrocytes (GFAP; Fig. 5.1). This laboratory has previously demonstrated that cultured prepared as used here contain negligible numbers of microglia and oligodendrocytes (Garwood et al., 2011). Hoechst-33342 nuclear stain was used to indicate the total number of cells present. Typical cortical

neuronal cultures primarily contained neurons, and 17 ± 1.9 %, (n=6, independent cultures) GFAP-positive astrocytes were detected (data not shown).

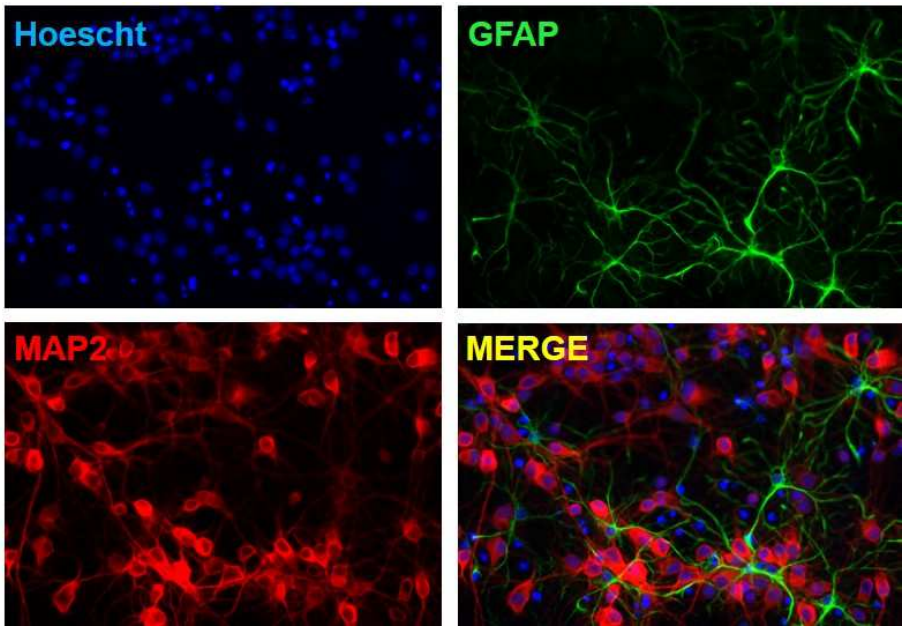

Fig. 4.1 Rat primary cortical cultures contain ~17 % astrocytes. Cultures were fixed at 10DIV and immunostained with antibodies against neurons (MAP2), astrocytes (GFAP) and cell nuclei (Hoescht-33342). GFAP-positive cells were quantified as a proportion of total nuclei. n=8. Scale bar = 75µm.

To investigate the contribution of calpain to Aβ neurotoxicity, the synthetic calpain inhibitor calpeptin was used to block calpain activity in primary cortical cultures treated with soluble oligomers of human Aβ1-42. The effect of calpain blockade on mechanisms shown to be induced by Aβ, including changes in APP processing, tau kinase activation, tau phosphorylation and synaptic damage

(Buxbaum et al., 1994; Garg et al., 2011b; Town et al., 2002; Hooper et al., 2008) were studied using immunoblotting with antibodies against proteins of interest. Using fluorescent live imaging, it was then determined whether or not Aβ induces elevations in intracellular Ca^{2+} prior to calpain activation. Finally, to investigate the mechanisms that contribute to Aβ-induced Ca^{2+} changes, neural cells were pre-treated with synthetic inhibitors of NMDARs, calpains, caspases and PARP.

4.2.1 Calpeptin dose-dependently inhibits calpain activity

Calpeptin is cell-permeable calpain-specific inhibitor that has previously been used by this laboratory (Atherton et al., 2014) and others (Bano et al., 2005; Yano et al., 1993) to abolish calpain activity in *vitro*. To establish the minimum effective calpeptin dose for use in the present study, a dose-response experiment was performed using a logarithmic range of calpeptin concentrations (0.1 μM, 1 μM and 10 μM).

Lysates from rat primary cortical cultures treated with different doses of calpeptin or vehicle for 3 h were immunoblotted using an antibody specific to the cytoskeletal protein α-spectrin, a known substrate of calpain. This antibody detected α-spectrin holoprotein at 240 kDa as well as calpain- and caspase-cleaved (140-150 kDa) and caspase-cleaved (110-125 kDa) fragments (Fig. 4.2A). Blots were also probed with an antibody against the housekeeping protein, β-actin. Amounts of full-length, cleaved and total α-spectrin were separately

quantified as a proportion of β-actin content in the same sample. This allowed normalisation of protein amounts to account for differences in protein loading and/or protein concentration in each sample. Quantitative analysis of band densities revealed that there were no significant difference in the amounts of total α-spectrin between control and calpeptin-treated cultures (Fig. 4.2B). Unexpectedly, amounts of full-length α-spectrin appeared to be reduced by calpeptin treatment (Fig. 4.2C) but this reduction was found to be not statistically significant from control, possibly reflecting variation within groups. Calpeptin treatment reduced amounts of calpain- and caspase-cleaved (140-150kDa) α-spectrin species in a dose-dependent manner (Fig. 4.2D), with approximately 50% of calpain-cleaved fragments reduced when 10 μM calpeptin was used ($p < 0.05$), as previously found in this and other laboratories (Atherton et al., 2014; Bano et al., 2007). Levels of caspase-cleaved α-spectrin were also dose-dependently reduced by calpeptin (Fig. 4.2E), significantly so at 10 μM concentrations (p 0.01), indicating reduced caspase proteolytic activity. This may be expected as calpains are shown to directly cleave and activate caspases (McCollum et al., 2002; Nakagawa and Yuan, 2000).

To ensure that calpeptin treatments of cultures were not cytotoxic, a live/dead cell assay was performed (section 2.2.5) and these experiments revealed no differences in cell death between untreated and calpeptin-treated neurons (Fig. 4.2F). Therefore, any neurotoxic effects of Aβ on primary culture in further experiments were not a result of calpeptin application. Based on these

experiments, 10 μM calpeptin was established as a dose at which calpeptin significantly inhibits calpain proteolytic activity without causing toxicity, and this concentration was used for all subsequent experiments described in this chapter.

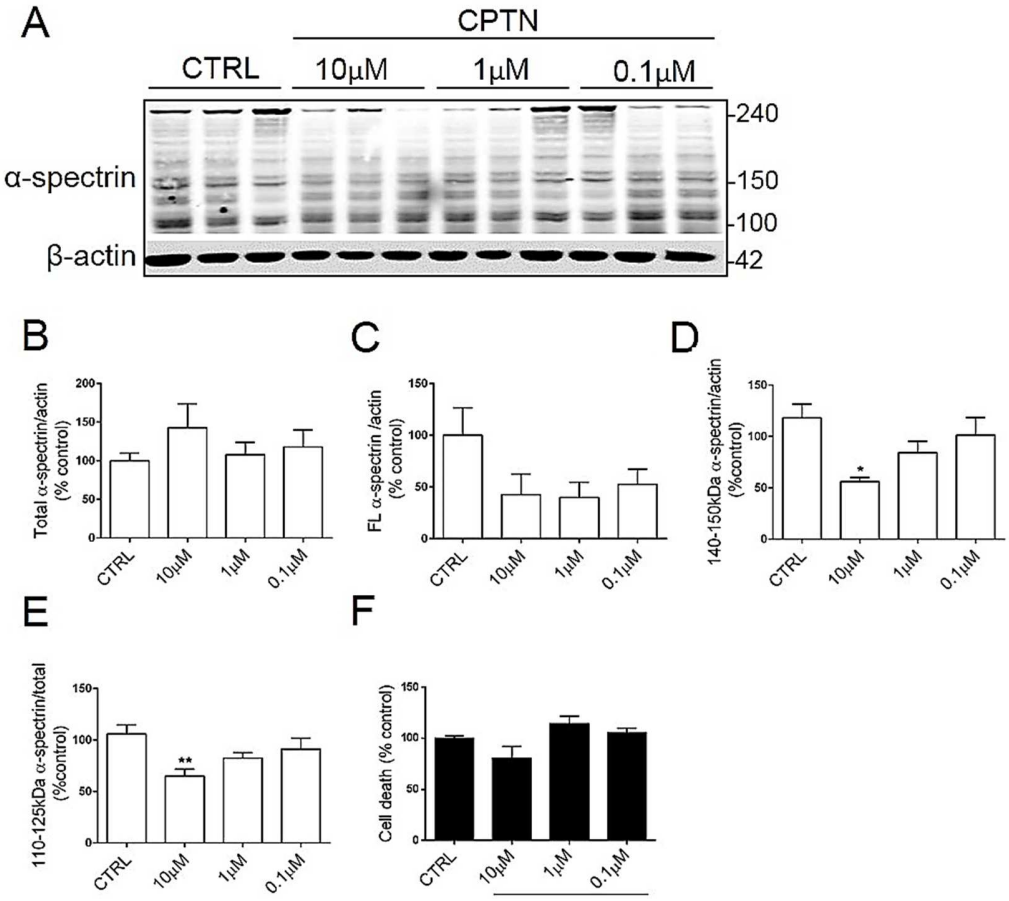

Fig. 4.2 Calpeptin dose-dependently inhibits calpain activity in primary cortical neurons. (A) Representative immunoblots of lysates from neurons treated with vehicle (CTRL) or 0.1, 1, 10 μM calpeptin (CPTN). Blots were probed with an antibody against α-spectrin which detects holoprotein at 240 kDa, calpain- and caspase-cleaved fragments at 140-150 kDa and caspase-cleaved fragments at 110-125 kDa. Blots were also probed with an antibody against β-actin (42 kDa), as a loading control. Bar graphs show amounts of (B) total α-spectrin, (C) full-length α-spectrin, (D) calpain- and caspase-cleaved α-spectrin, and (E) caspase-cleaved α-spectrin, all normalised to β-actin. (F) Bar graph shows % cell death in cultures with each treatment. n=9. Data is mean ± SEM. *$p < 0.05$, **$p < 0.01$.

4.2.2 Aβ-induced neurotoxicity is rescued by calpain inhibition in *vitro*

The amyloid hypothesis proposes that Aβ is directly toxic to neurons through mechanisms that may involve excess glutamate-mediated NMDA receptor activation and subsequent Ca^{2+} accumulation (Harkany et al., 2000a; Molnár et al., 2004; Mattson et al., 2000). Indeed, Aβ-induced cholinergic neurodegeneration was recently shown to be reversed by inhibiting calpain activity in rats (Granic et al., 2010). In order to investigate the role of calpain in Aβ-induced neurotoxicity in primary cortical cell cultures, it was first vital to determine whether calpain inhibition is neuroprotective in primary neurons exposed to a toxic dose of Aβ.

Synthetic human Aβ1-42 peptide was prepared as previously described by this group (Hanger et al., 2009; Garwood et al., 2011; Atherton et al., 2014). This Aβ preparation was previously described to consist of several species of soluble Aβ oligomers (Town et al., 2002) and provides physiological (nM) concentrations of peptide. This was an important consideration since there is substantial evidence that oligomers are likely responsible for Aβ-induced neurotoxicity (Walsh and Selkoe, 2007). To examine the Aβ preparation used in this work, recombinant peptide was assessed by SDS-PAGE and immunoblotting with an antibody against C-terminal APP that detected 3 major Aβ1-42 species: monomers at 4 kDa, dimers at 8 kDa and oligomers of greater than 12 kDa (Fig. 4.3A).

Primary cortical cultures were treated with 10 μM Aβ1-42, of which 500nM is active Aβ oligomers, for 48 h - conditions previously shown to be neurotoxic in primary cultures in this laboratory (Garwood et al., 2011; Atherton et al. 2014). A live/dead assay revealed that exposure of neurons to Aβ caused more than a 2-fold increase in cell death when compared to untreated cells ($p < 0.05$; Fig. 4.3B), in line with previous reports (Atherton et al., 2014; Garwood et al., 2011). To determine the importance of calpain activity in Aβ-induced neurotoxicity, Aβ-treated cultures were also pre-treated with 10 μM calpeptin for 3 hr. These cultures exhibited a cell death levels nearing those in control cells ($p < 0.05$; Fig. 4.3B.), indicating that calpain plays a key role in mediating Aβ neurotoxicity. These findings support previous reports by this group (Atherton et al., 2014), and provided a basis for the subsequent investigations into downstream calpain targets and their role in Aβ-induced cell death in this chapter.

4.2.3 Aβ-induced elevation of calpain proteolytic activity is prevented by calpain inhibition

Cortical Aβ1-42 burden correlates with calpain-1 activity in AD brain (section 3.2.14). To confirm previous reports that primary neurons exposed to Aβ show increased activation of calpain-1 (Atherton et al. 2014), lysates from primary cortical neurons treated with Aβ with and without calpeptin pre-treatment were immunoblotted with an anti-calpain-1 antibody that normally detects the 76 kDa

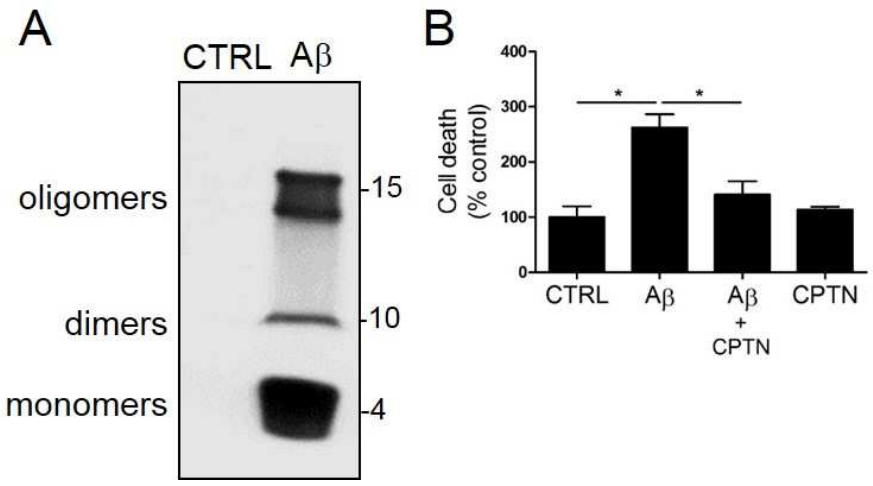

Figure 4.3 Aβ-induced neurotoxicity in primary cortical cultures is rescued by calpeptin (CPTN). Cultures were exposed to Aβ for 48 hours. (A) Western blot showing the Aβ species found in the soluble Aβ preparations used in this study. 5 μg Aβ was loaded in each lane of a 20 % polyacrylamide gel, and the resulting blots were probed with the 6E10 antibody, which primarily labels low molecular weight Aβ oligomers, as well as APP. The predominant species of Aβ detected were monomeric (approximately 4 kDa). nM concentrations of dimers (approximately 8kDa) and higher order oligomers of approximately 12 kDa and above were also apparent. (B) Bar graph shows % cell death in primary neurons treated with vehicle (CTRL), Aβ, Aβ in combination with calpeptin (CPTN), or calpeptin alone. n=9. Data is mean ± SEM. *p < 0.05

active subunit of calpain-1 (Fig. 4.4A). In these cell lysates, this antibody, and several other commercial antibodies against rat calpain-1 that were tested, failed to detect the active calpain-1 fragment; however, a calpain fragment of 28 kDa was labelled. This band is believed to represent the regulatory calpain-1 subunit that is known to heterodimerize with the 80 kDa subunit of calpain-1 in the presence of Ca^{2+} and optimize calpain proteolytic activity (Ravulapalli et al., 2009).

Following standardization of 28 kDa calpain bands to β-actin, quantitative analysis revealed a two-fold increase in the amount of the regulatory calpain-1 fragment in cultures treated with Aβ when compared to control ($p < 0.001$), suggesting that calpain activity is increased following Aβ treatment of primary cortical neurons. This suggestion is supported by findings that the presence of this calpain fragment was reduced by approximately 60 % when cells were treated with calpeptin prior to application of Aβ ($p < 0.01$; Fig. 4.4B).

Blots were also probed an antibody specific for α-spectrin, detecting holoprotein at 240 kDa, calpain- and caspase-cleaved fragments at 140-150 kDa and caspase-cleaved fragments at 110-125 kDa. An antibody against β-actin antibody was used as a loading control. Aβ treatment of cortical neurons was found to lead to a 4-fold increase in amounts of calpain- and caspase-cleaved α-spectrin fragments ($p < 0.001$; Fig. 4.4E) relative to control cultures, which were significantly reduced when cells were pre-treated with calpeptin ($p < 0.05$). Aβ treatment of cultures also resulted an approximately 4-fold increase in caspase-cleaved α-spectrin species ($p < 0.05$) which was also somewhat reduced by calpeptin pre-treatment (Fig. 4.4F). Amounts of total and full-length α-spectrin were not significantly altered with any treatment compared to control (Fig. 4.4C, D). Taken together, these findings suggest that calpain activity is increased in primary cultured neurons following treatment with soluble Aβ oligomers, corroborating previous findings (Town et al., 2002; Atherton et al. 2014).

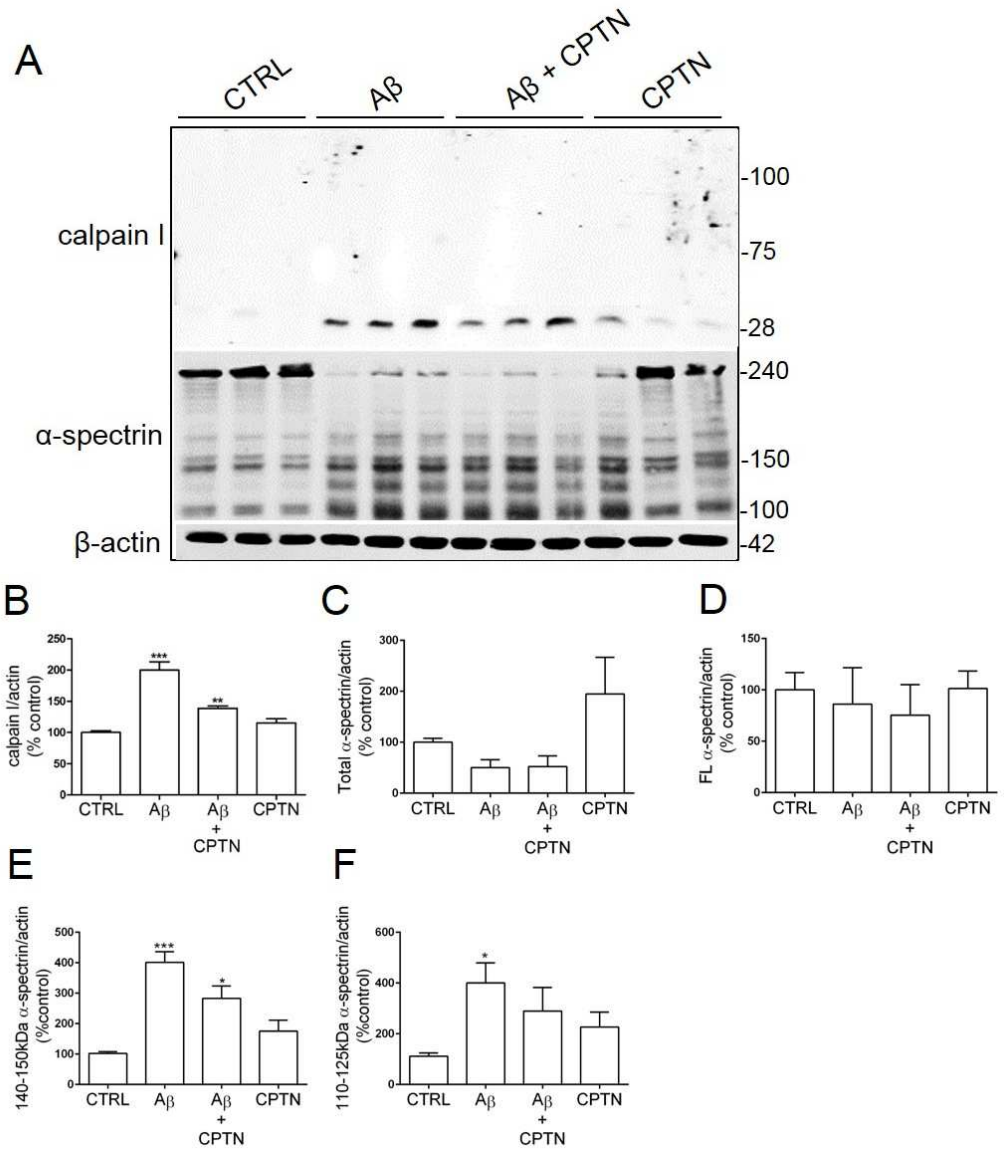

Fig. 4.4 Aβ-induced changes in calpain activity in primary cortical cultures. (A) Representative immunoblots of neurons treated with vehicle (CTRL), Aβ, Aβ in combination with calpeptin (CPTN), or calpeptin alone. Blots were probed with an antibody against active (76 kDa) calpain, which also detects the 28 kDa regulatory subunit of calpain that is required for calpain activation. Blots were also probed with an antibody against α-spectrin which detects holoprotein at 240 kDa, calpain- and caspase-cleaved fragments at 140-150 kDa and caspase-cleaved fragments at 110-125 kDa. An antibody against β-actin was used as a loading control. Bar graphs show amounts of (B) 28 kDa calpain-1, (C) total α-spectrin, (D) full-length α-spectrin, (E) calpain- and caspase-cleaved α-spectrin, and (F) caspase-cleaved α-spectrin, all following normalisation to β-actin amounts in the same sample n=9. Data is mean ± SEM. *p < 0.05, **p < 0.01, ***p < 0.001

4.2.4 Non-amyloidogenic APP processing is altered by Aβ and calpain

Calpain has been found to regulate the cell surface distribution and proteolytic processing of APP in cells (Mathews et al., 2002; Trinchese et al., 2008), therefore it was of interest to determine the effect of Aβ and calpeptin treatment on APP amounts in the cell system used here. APP is a type 1 membrane glycoprotein that has been widely researched in the context of AD, as it is pathologically cleaved to generate neurotoxic and pro-aggregatory species of Aβ (Zhang et al., 2011), and mutations in APP and PS1, the latter part of the γ-secretase complex that cleaves APP, cause familial forms of AD (Hardy et al., 2014). In addition, N-terminal processing of APP was recently found to release a series of small N-terminal fragments (NTFs) in the adult human CNS, which display key physiological and neurodevelopmental functions in mice (Portelius, Brinkmalm, et al., 2010; Hoshino et al., 2003; Vella and Cappai, 2012). In the present study, it was of interest to determine whether generation of these physiological NTFs is altered by Aβ- and/or calpain-dependent mechanisms.

Protein extracted from primary cortical cultures treated with Aβ and/or calpeptin was immunoblotted with an antibody against N-terminal APP (22c11), which detects mature full-length APP at 120 and 130 kDa, and immature (unglycosylated) APP at 110 kDa (Fig. 4.5A). Blots were also probed with the 42 kDa housekeeping protein β-actin for normalisation of data when taking into

account potential protein loading variations (Fig. 4.5A). Quantitative analysis of the intensity of bands in the resulting blots showed that there were no changes in total (Fig 4.5B), mature (Fig. 4.5C, D) or immature (Fig. 4.5E) APP following treatment of cells with either Aβ or calpeptin. The above findings suggest that neither Aβ nor calpain alter APP maturation or synthesis, at least not in the cell cultures used here. In contrast, cultures treated with calpeptin, whether in combination with Aβ or not, generated 17 kDa APP NTFs (Fig. 4.5A).

Recently, 17-28 kDa NTFs were detected in transgenic mouse and post mortem AD tissue, as well as SH-SY5Y cells, using the same antibody and these were shown to be protein kinase C-regulated and secretase-independent cleavage products of APP (Vella and Cappai, 2012). Preferentially expressed in the developing mouse brain, these NTFs were suggested by the authors to contribute to synaptogenesis and copper homeostasis. Since the NTFs identified here were not generated in control or Aβ-treated cultures, where calpain activity may be elevated by Aβ (section 4.2.3) or culture stress, but were detected following calpain inhibition, this suggests that calpain suppresses physiological N-terminal APP processing under basal conditions.

To further investigate potential effects of Aβ and calpeptin treatment on APP processing, blots were also probed with an antibody against the α-secretase protein a disintegrin and metalloproteinase domain-containing protein 10 (ADAM10), which yielded two prominent bands at 75 and 68 kDa, respectively

characteristic of the proenzyme and active protease. This band profile was expected since this enzyme is constitutively active in primary neurons (Kuhn et al., 2010). Treatment of cultures with Aβ significantly reduced levels of active (68kDa) ADAM10 compared to control ($p < 0.001$; Fig. 4.5F). This could either signify that 1) Aβ directly shifts the equilibrium from non-amyloidogenic to amyloidogenic (α-secretase-independent) APP processing in a positive feedback mechanism, or 2) other mechanisms activated by Aβ alter ADAM10 activity and APP processing. For example, Aβ-induced oxidative stress was shown to stimulate amyloidogenesis in human vascular smooth muscle cells (Coma et al., 2008). Surprisingly, treatment of cultures with calpeptin alone also significantly reduced levels of ADAM10 ($p < 0.005$; Fig. 4.5F), which suggests that calpain activity may be required for non-amyloidogenic processing that does not yield 17-28 kDa NTFs. Indeed, the combination of calpain inhibition and Aβ exposure reduced levels of ADAM10 in cultures to a greater extent than either treatment alone ($p < 0.001$; Fig. 4.5F). As pre-treatment of Aβ-treated cultures with calpeptin did not recover ADAM10 activity to control levels, it can be deduced that the mechanism through which Aβ regulates ADAM10 activity does not involve calpain. Together, these findings suggest that Aβ and calpain independently and differentially regulate non-amyloidogenic APP processing, with calpain inhibition 1) promoting generation of APP NTFs through an Aβ- and secretase-independent pathway or 2) suppressing α-secretase-dependent non-amyloidogenic processing, and Aβ

suppressing non-amyloidogenic processing of APP by α-secretase through a calpain-independent mechanism.

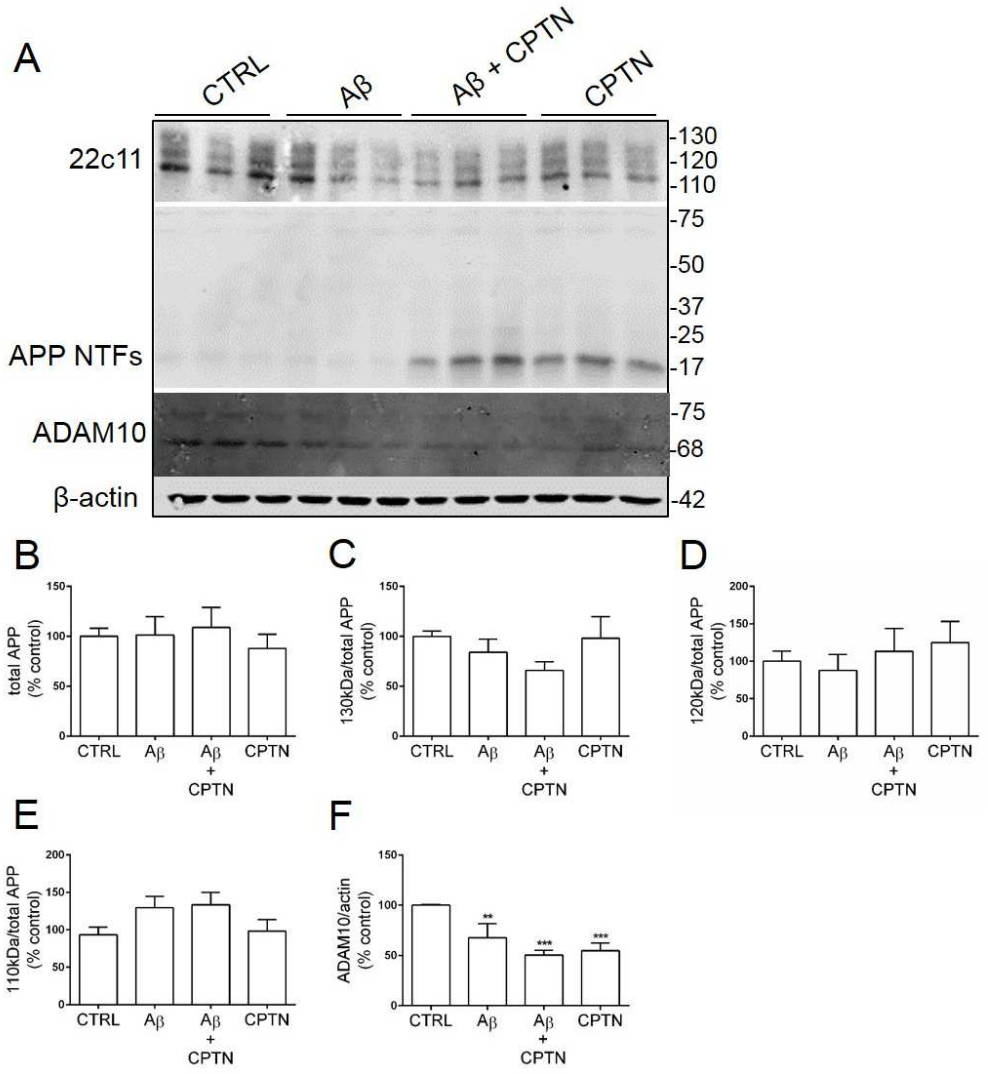

Fig. 4.5 Aβ and calpain differentially suppress non-amyloidogenic APP processing. (A) Representative immunoblots of neurons treated with vehicle (CTRL), Aβ, Aβ in combination with calpeptin (CPTN), or calpeptin alone. Blots were probed with an antibody against N-terminal APP (22c11), detecting bands at 110 to 130 kDa representative of mature and immature APP isoforms, and proteolytically generated N-terminal fragments (NFTs) at 17 kDa. Blots were also probed with an antibody against a disintegrin and metalloproteinase 10 (ADAM10), detecting holoprotein at 75 kDa and 68 kDa active ADAM10. An antibody against β-actin was used as a loading control. Bar graph shows amounts of (B) total APP, (C) 130 kDa mature APP, (D) 120 kDa mature APP, (E) 110 kDa immature APP and (F) active (68kDa) ADAM10, with all bands normalised to β-actin n=9. Data is mean ± SEM. **p < 0.01, ***p < 0.001

4.2.5 Exogenous Aβ promotes amyloidogenic APP processing and intracellular generation of Aβ

It was important to also examine the effects of Aβ and calpain inhibition on Aβ production through the amyloidogenic pathway since there is emerging evidence that 1) extracellular Aβ stimulates further intracellular Aβ synthesis in astrocytes, possibly via inflammatory signaling pathways (Dal Pra et al., 2011), and 2) calpain inhibition reduces Aβ production in 3xTg-AD mice (Medeiros et al., 2012). The contribution of exogenously applied Aβ to neuronal APP processing and Aβ production was therefore investigated here.

Neuronal lysates of cultures treated with Aβ and/or calpeptin were immunoblotted with an antibody that labels APP C-terminal fragments (CTFs) generated by β- and γ-secretases during amyloidogenic processing in AD (Fig 4.6A). This antibody recognized a single prominent band around 15 kDa in size, representing the membrane-bound C99 fragment (C99), generated by the action of β-secretase, and a 4 kDa band characteristic of Aβ monomers. Blots were also probed with antibodies against the beta-site amyloid precursor protein cleaving enzyme (BACE-1), which revealed a band at 70 kDa representative of BACE holoprotein, and nicastrin, which forms part of the γ-secretase protein complex and yields a band at 78 kDa. For standardization purposes, blots were also probed with an antibody against the housekeeping protein β-actin. Following standardization of the above bands to β-actin, quantitative analysis showed that

Aβ treatment did not significantly alter BACE levels in neurons (Fig. 4.6B), although small increases in total BACE levels were apparent relative to control cells. In accordance with this, Aβ treatment of cells did not significantly alter amounts of the C99 fragment (Fig. 4.6C), which is proteolytically generated by BACE during the initial step of APP metabolism (Zhang et al., 2011), likely due to variations within the treatment group. Generation of the C99 fragment was significantly increased by combined Aβ and calpeptin treatments compared to control ($p < 0.05$; Fig. 4.6C), which was inconsistent with the lack of effect of treatment with calpeptin alone on BACE activity or C99 fragment production, suggesting that these effects are likely to be mediated by Aβ rather than being modulated by inhibition of calpain activity. Furthermore, the measurement of BACE protein expression does not reflect activity of the enzyme; thus, it is possible that BACE activity is increased in the cultures that show accumulation of C99 fragment.

Notably, treatment of cultures with Aβ significantly increased protein amounts of nicastrin ($p < 0.05$), which was recovered to control by calpeptin pre-treatment ($p < 0.05$; Fig 4.6D). This suggest that Aβ promotes γ-secretase activity through increased nicastrin expression - as seen in active astrocytes and microglia following neuronal insults (Nadler et al., 2008) - and further amyloidogenesis through calpain signalling. Indeed, cultures treated with Aβ increased displayed Aβ in cell lysates when compared to control cultures (Fig. 4.6A), further suggesting a positive feedback loop whereby increased extracellular Aβ promotes

further Aβ production, possibly by inhibiting non-amyloidogenic APP cleavage (Fig. 4.6A). However, pre-treatment of cultures with calpeptin did not prevent accumulation of Aβ in lysates, which is inconsistent with the reduction of nicastrin levels in these samples, and perhaps reflects the additional presence of exogenous Aβ that has been internalized following treatment - as seen in neurons lacking ApoE (Saavedra et al., 2007).

Aβ is widely recognised as being notoriously sticky, therefore it was important to establish that the Aβ detected in lysates was intracellular and not residual synthetic peptide harvested together with the protein. Thus, primary cultures treated with Aβ were immunostained with an antibody that recognizes C-terminal APP and CTFs (6E10; Fig. 4.7). Cells were also stained with an antibody against microtubule-associated protein 2 (MAP2), which labels the neuronal cytoskeleton, and the nuclear stain Hoescht-33342. The staining protocol included a permeabilization step which ensured that access of the antibody to its intracellular protein antigen.

Neurons exposed to Aβ showed high 6E10 immunoreactivity in addition to many degenerating dendrites, in contrast to a lack of 6E10 labelling in control cultures (Fig. 4.7). Cultures were also treated with H_2O_2, which is used to model oxidative stress in AD (Dávila and Torres-Aleman, 2008), as a positive control for neuronal damage. These cells exhibited DNA fragmentation consistent with oxidative DNA damage during apoptosis. The absence of a 6E10 signal in control cultures

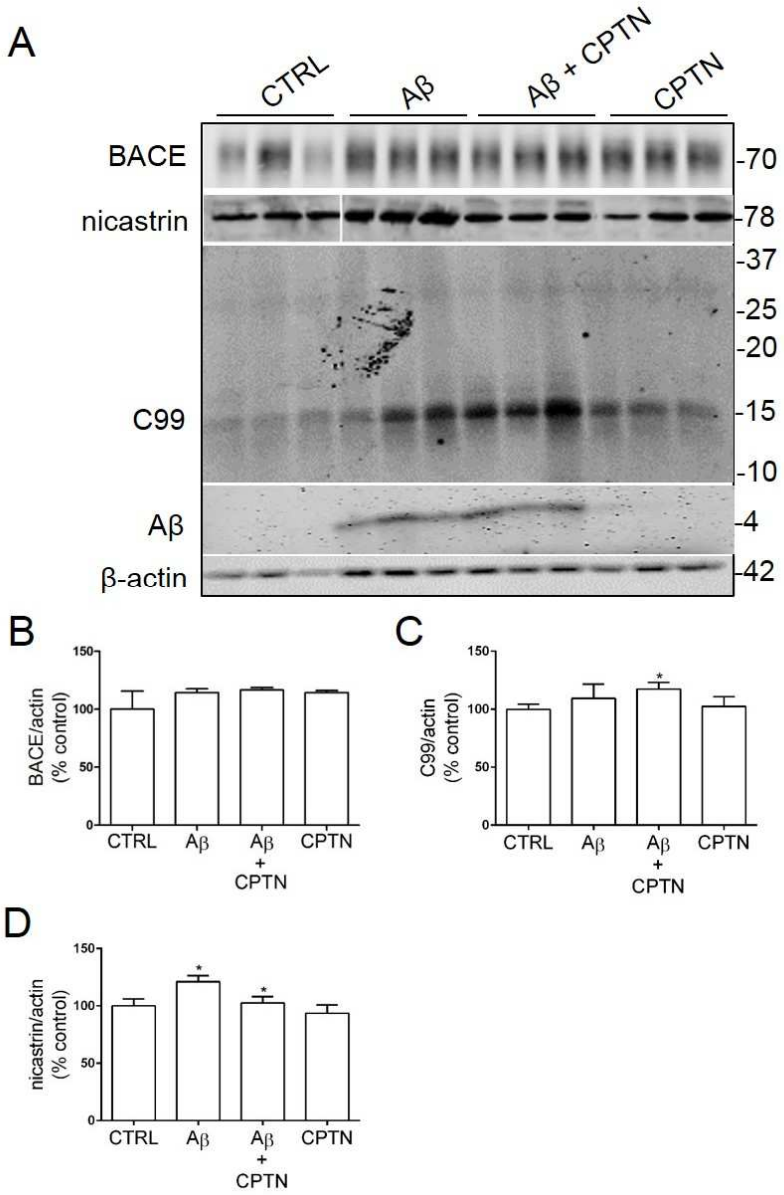

Fig. 4.6 Aβ promotes amyloidogenic APP processing and intracellular accumulation of Aβ. (A) Representative immunoblots of neurons treated with vehicle (CTRL), Aβ, Aβ in combination with calpeptin (CPTN), or calpeptin alone. Blots were probed with an antibody against C-terminal APP fragments, detecting a single prominent band at 15 kDa, indicative of the C99 APP fragment. Blots were also probed with antibodies against BACE and nicastrin, detecting holoprotein at 70 kDa and 78 kDa, respectively. An antibody against β-actin was used as a loading control. Bar graphs show amounts of (B) BACE, (C) C99 and (D) nicastrin, with all bands normalised to β-actin. n=6. Data is mean ± SEM. *$p < 0.05$

indicates that this antibody recognizes Aβ rather than APP, since APP is constitutively expressed on the cell surface of neurons and would not be labelled using these methods (Zhang et al., 2011). Furthermore, there was no Aβ immunoreactivity in H_2O_2-treated cultures, indicating that Aβ generation is a result of extracellular Aβ-mediated mechanisms and not general stress responses (Paola et al., 2000). High magnification (X63) of labelled cells (Fig. 4.8) showed that some Aβ was not associated with cells, and appeared to be simply stuck to the glass coverslips, or had accumulated following degeneration of the associated neuronal processes. However, there were also Aβ puncta that co-localized with neuronal processes (Fig. 4.8) as previously described by this group (Williamson et al., 2008). Together, these findings suggest that the application of exogenous Aβ1-42 peptides to rat primary cortical cultures results in inhibition of α-secretase mediated non-amyloidogenic APP processing, calpain-dependent stimulation of γ-secretase, subtle increases in β-secretase cleavage of APP, and elevated intracellular production of Aβ in a positive feedback loop. This is in agreement with and extends previously published findings (Dal Pra et al., 2011). Alternatively, these findings might suggest that exogenous Aβ is taken up by neuronal cells, although the relationship of this to altered APP processing is not clear.

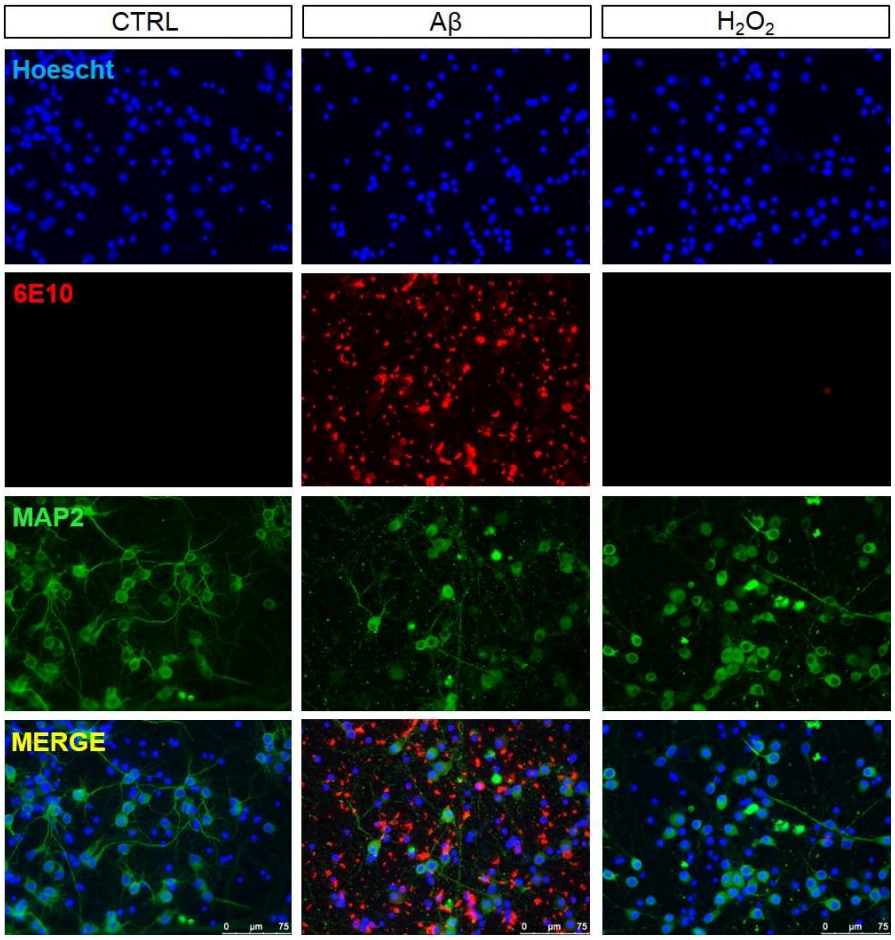

Fig. 4.7 Exposure of primary cortical cultures to Aβ causes neuronal damage associated with increased Aβ immunoreactivity. Neurons treated with vehicle (CTRL), Aβ, or H_2O_2, which is used to stimulate oxidative stress in culture, were immunostained with antibodies against C-terminal APP (6E10), which detects Aβ, neuronal microtubule-associated protein 2 (MAP2), and the nuclear stain Hoescht-33342. Scale bars are 75µm. n=8

4.2.6 Aβ-induces mild alterations in tau phosphorylation that are reduced upon inhibition of calpain

Calpain is known to promote tau phosphorylation through N-terminal cleavage and activation of tau kinases, including cdk5 and GSK3 (Goñi-Oliver et al., 2007;

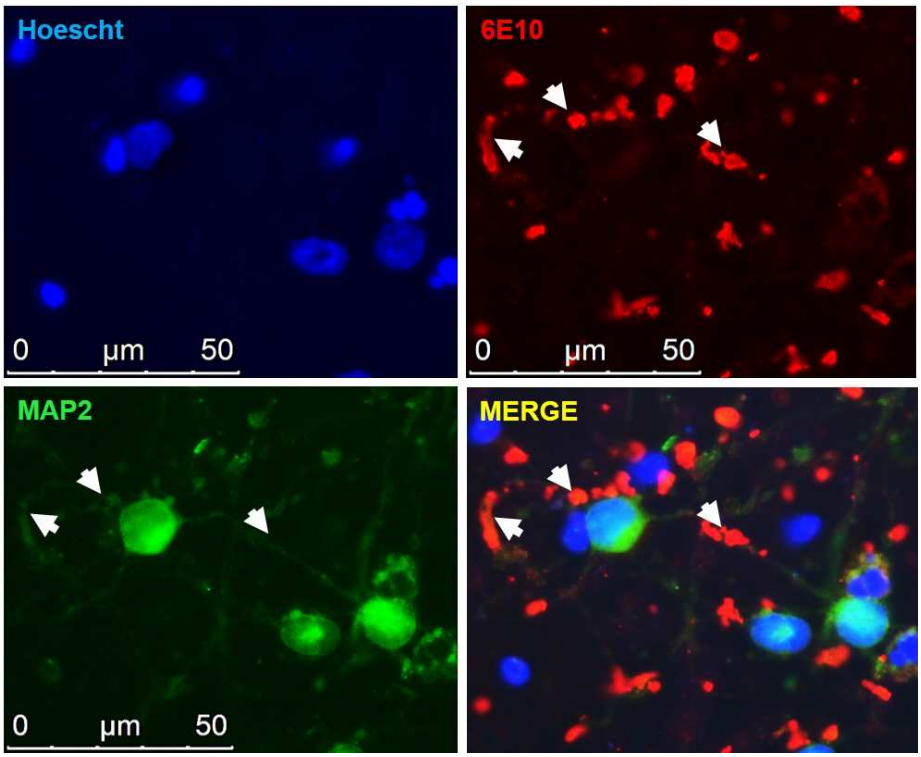

Fig. 4.8 Exposure of primary cortical cultures to Aβ causes neuronal damage associated with increased dendritic accumulation of Aβ (white arrows). Neurons treated with vehicle (CTRL), Aβ, were immunostained with antibodies against C-terminal APP (6E10), which detects Aβ, neuronal microtubule-associated protein 2 (MAP2), and the nuclear stain Hoescht-33342. Cultures were viewed under X63 magnification to determine co-localization of Aβ puncta with neuronal structures. Scale bars are 75µm, n=6

Taniguchi et al., 2001; Jin et al., 2015). Calpains and tau kinases are activated by Aβ (Town et al., 2002; Zheng et al. 2002; Lloret et al. 2011; Liang et al. 2010); therefore, it is hypothesized that tau phosphorylation occurs downstream of Aβ and is mediated by calpain activation.

To examine this process, cell lysates from primary cortical cultures treated with Aβ and/or calpeptin were probed with antibodies detecting total tau bands, independent of phosphorylation state, (DAKO) at approximately 55 kDa, tau phosphorylated at the AD-relevant epitopes Ser396/404 (PHF1) and Ser202 (CP13), and tau dephosphorylated at Ser199/202/Thr205 (tau-1). Blots were also probed with an antibody against β-actin for standardization purposes (Fig. 4.9A). Following standardization of total tau (DAKO) amounts to β-actin, and phosphorylated (PHF1 and CP13 immunoreactive) tau to total tau (DAKO) amounts, quantitative analysis revealed no changes in total tau amounts (Fig. 4.9B) or tau phosphorylated at Ser396/404 or Ser202 (Fig. 4.9D, E) following treatment with Aβ or calpeptin relative to controls. In contrast, Aβ-treated cultures showed significantly reduced amounts of dephosphorylated (Tau-1) tau ($p < 0.05$), an effect reduced upon pre-treatment of cultures with calpeptin ($p < 0.001$; Fig. 4. 9C).

The findings that tau is not phosphorylated at the CP13 and PHF1 epitopes in response to Aβ is a somewhat unexpected result since these epitopes have previously been shown to be phosphorylated under similar conditions (Garwood et al., 2011). However, the cultures used here were of an older developmental stage than those reported by Garwood et al. (2011), which may account for some of these differences. Nevertheless, these experiments showed that phosphorylation of the Tau-1 epitope (Ser199/202/Thr205) is significantly elevated following Aβ treatment via a calpain-dependent mechanism. Increased

calpain activity upon Aβ treatment of primary cells has also been described to lead to the generation of a neurotoxic 17 kDa calpain-cleaved tau fragment (Park and Ferreira, 2005). However, this fragment was not observed in Aβ-treated neurons in this study (Fig. 4.9A). Furthermore, the relevance of this fragment for Aβ-induced toxicity remains uncertain (Garg et al., 2011b).

4.2.7 Aβ-induced activation of GSK3 is prevented by calpain inhibition

It was important to examine the mechanisms by which increased calpain activity might lead to tau phosphorylation in response to Aβ treatment. GSK3 is a key tau kinase that phosphorylates tau at multiple disease-relevant epitopes (Hanger and Noble, 2011) and is central to multiple neurodegenerative pathways in AD (Hooper et al., 2008). GSK3 can be activated by calpain, which removes the N-terminal portion of the kinase which contains inhibitory phosphorylation epitopesSer21 (GSK3α) and Ser9 (GSK3β). It is therefore possible that GSK3 is involved in Aβ-mediated tau phosphorylation and neurotoxicity as a downstream effector of calpain.

Aβ- and/or calpeptin-treated primary neuronal lysates were immunoblotted using antibodies against total GSK3 which detected two bands at 51 and 47 kDa representing GSK3α and GSK3β, respectively (Fig. 4.10A). Blots were also probed

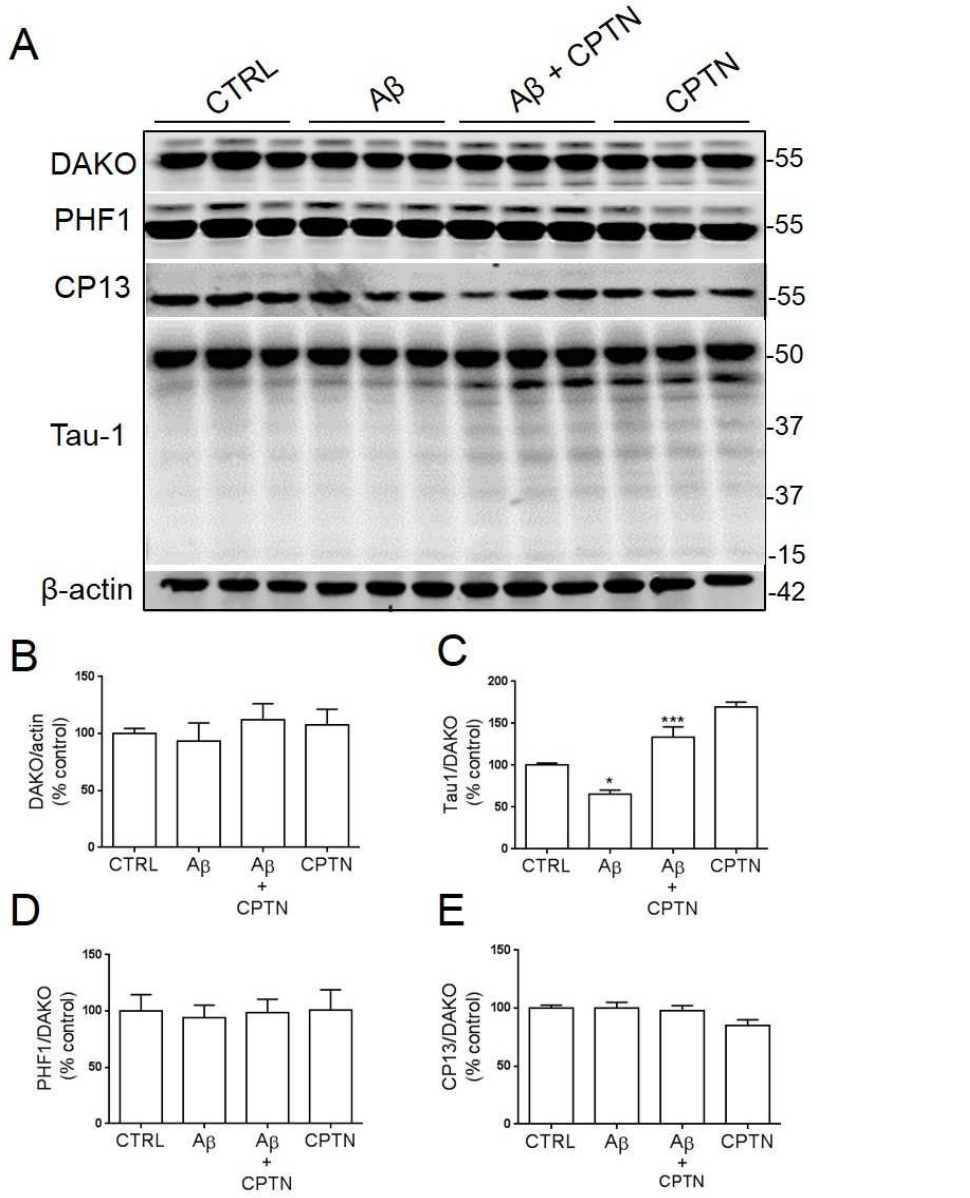

Fig. 4.9 Aβ-induced tau phosphorylation at the Tau-1 epitope is attenuated by calpain inhibition. (A) Representative immunoblots of neurons treated with vehicle (CTRL), Aβ, Aβ in combination with calpeptin (CPTN), or calpeptin alone. Blots were probed with antibodies against total tau (DAKO) at approximately 55 kDa, tau phosphorylated at Ser396/404 (PHF1) and at Ser202 (CP13), both detecting bands at 50-61 kDa and tau dephosphorylated at Ser199/202 (tau1) which detects bands at 17 to 55 kDa. Blots were also probed with an antibody against β-actin (42 kDa) as a loading control. Bar graphs show amounts of (B) DAKO following normalisation to β-actin amounts in each sample, and (C) tau dephosphorylated at tau1 sites, and tau phosphorylated at (D) PHF1 and (E) CP13 epitopes, all of which were standardized to total tau (DAKO) amounts in each sample. n=9. Data is mean ± SEM. *$p < 0.05$, ***$p < 0.001$

with an antibody against GSK3 phosphorylated at Ser21/9 (pGSK3), yielding two bands at 51 and 47 kDa representing GSK3 phosphorylated at Ser21 and Ser9, respectively. An antibody against β-actin was used as a loading control. Following standardization of the intensity of protein bands, quantitative analysis revealed no change in total protein amounts of GSK3α (Fig. 4.10B) and a significant increase in GSK3β amounts in cultures treated with Aβ ($p < 0.05$; Fig. 4.10C). These findings are in support of evidence of upregulated GSK3 expression in post mortem AD hippocampal tissue (Blalock et al., 2004) and synaptosomes (Pei et al., 1997), and suggest that GSK3 expression is regulated is regulated by Aβ.

In addition, there was a significant reduction in the amounts of GSK3 phosphorylated at Ser21/9 in Aβ-treated cultures ($p < 0.05$), which was reduced to control levels by calpeptin pre-treatment ($p < 0.01$; Fig. 4.10D). These findings indicate an increase in the activity of GSK3 in response to Aβ, which was attenuated by inhibition of calpain. Aβ has been previously reported to increase GSK3β activity through inhibition of PI3-kinase in primary neurons (Takashima et al., 1993), the effect of AD pathology on GSK3 activity is still controversial, with numerous studies reporting no change in activity (Pei et al., 1997) or reduced activity (Swatton et al., 2004) of GSK3 in AD brain. The findings shown here are, therefore, in support of pathogenic increases in GSK3 expression and activity in AD.

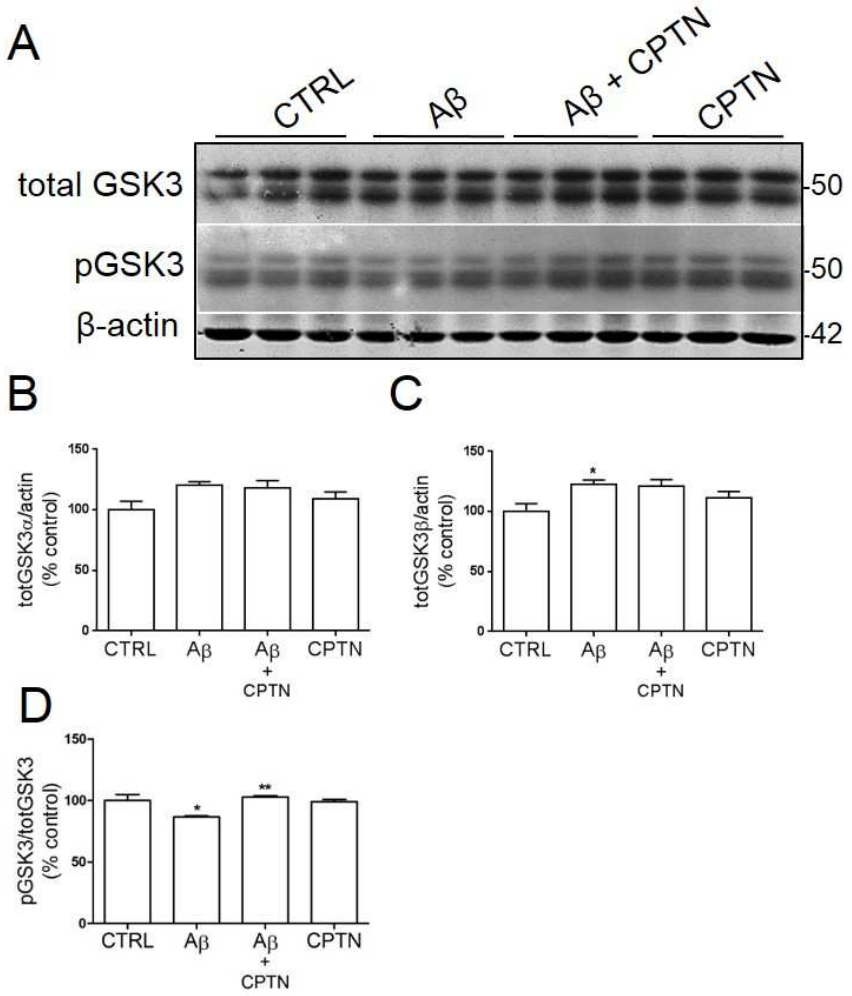

Fig. 4.10 Aβ-induced GSK3 activation is reduced by calpain inhibition. (A) Representative immunoblots of neurons treated with vehicle (CTRL), Aβ, Aβ in combination with calpeptin (CPTN), or calpeptin alone. Blots were probed with antibodies against GSK3, detecting GSK3α and GSK3β at 51 and 47 kDa, respectively, and GSK3 phosphorylated at Ser21/9 (pGSK3), yielding two bands at 51 and 47 kDa respectively representing GSK3 phosphorylated at Ser21 and Ser9. Blots were also probed with an antibody against β-actin (42 kDa) as a loading control. Bar graphs show amounts of (B) total GSK3α and (C) total GSK3 β, both standardized to β-actin and (D) total phosphorylated GKS3 (pGSK3), standardized to total GSK3. n=6. Data is mean ± SEM. *$p < 0.05$, **$p < 0.01$

4.2.8 Aβ increases Cdk5 activity through elevated calpain-mediated cleavage of p35 to p25

Cdk5 is a tau kinase that in AD is aberrantly regulated to result in tau phosphorylation, tangle formation and early memory deficits (Cruz et al., 2003; Giese, 2014). Cdk5 activity depends on physical association with one of its activators, p35, which can be truncated by Ca^{2+}-activated calpain to form p25, which is a more potent activator of cdk5 and results in sustained hyperactivity of the kinase (Goñi-Oliver et al., 2007). Lysates from primary cortical neurons treated with Aβ and/or calpeptin were immunoblotted with antibodies against cdk5 holoprotein, detecting a single prominent band at 33 kDa, and the cdk5 activator p35 which detects a single band at 35 kDa and a calpain-cleaved p25 fragment at 25 kDa (Fig. 4.11A). Blots were also probed with an anti-β-actin antibody for use as a loading control. Quantification revealed that Aβ did not alter levels of cdk5 holoprotein or p35 amounts from those detected in control conditions (Fig. 4.11B, C); although calpeptin-treated cells unexpectedly showed significantly elevated amounts of cdk5 ($p < 0.01$; Fig. 4.11B).

Aβ treatment induced an approximately 35 % increase in p25 amounts, when quantified as a proportion of cdk5 (p 0.05; Fig. 4.11D), which were notably reduced following calpeptin pre-treatment, but this reduction did not reach statistical significance. When quantified as a proportion of p35, p25 fragments showed a similar pattern of an increased p25/p35 ratio following Aβ treatment,

with slight reductions in this ratio following pre-treatment with calpeptin (Fig. 4.11E). These findings indicate that Aβ stimulates the calpain/p35-p25/cdk5 signalling pathway, via mechanisms that are likely to at least partially involve increased activation of calpain.

4.2.9 Aβ and calpain reduce amounts of PSD95 and synapsin, respectively

Aβ accumulation is implicated in the early synaptic dysfunction and loss seen in the early stages of AD in humans and in transgenic mice (Shankar and Walsh, 2009; Cummings et al., 2015). In recent reports, Aβ oligomers were shown to downregulate key pre- and postsynaptic proteins through actions on Ca^{2+} excitotoxicity mediated via NMDARs (Liu et al. 2010; Ittner et al., 2010). It is therefore postulated here that calpain is involved in Aβ–induced synapse loss.

To begin to gain an insight into the effects of Aβ and calpain on synapse health, primary neuronal lysates treated with Aβ and/or calpeptin were immunoblotted with antibodies against PSD95 and the presynaptic protein synapsin I, yielding bands at approximately 95 and 80 kDa, respectively (Fig. 4.12A). Blots were also probed with an antibody against β-actin to use as a loading control. Standardization to β-actin and quantification revealed that protein amounts of PSD95 were not altered by Aβ or calpeptin treatments (Fig. 4.12B). This finding is

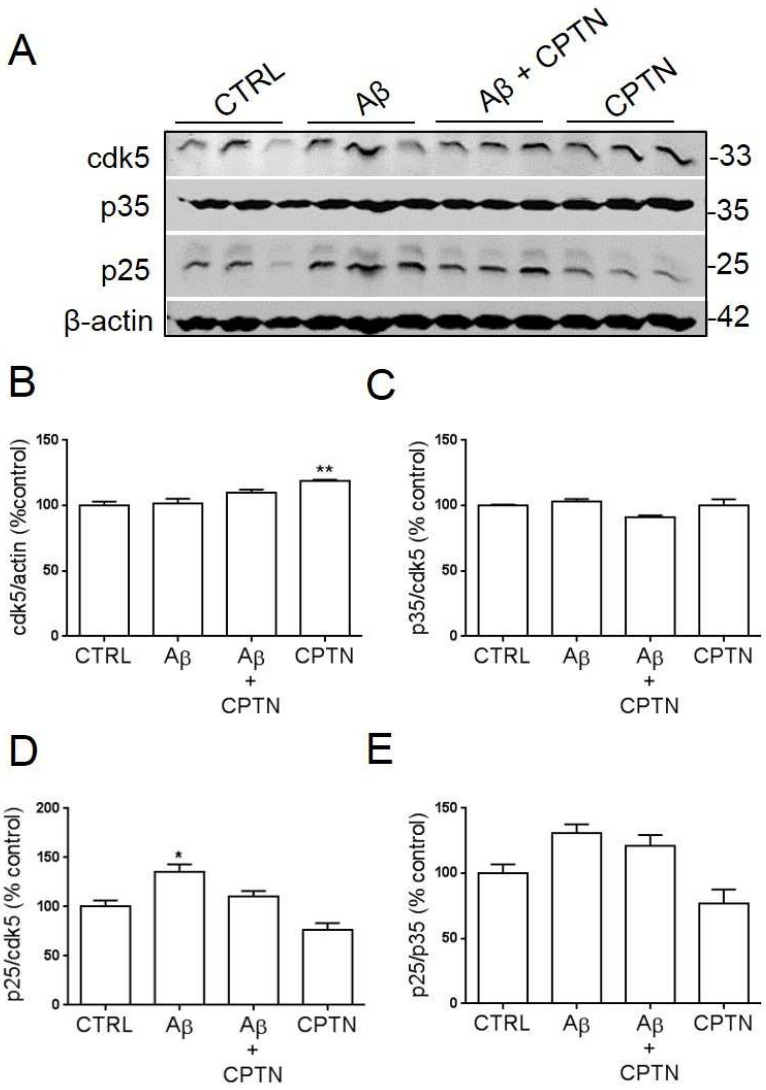

Fig. 4.11 Aβ-induced cdk5 activation is reduced by calpain inhibition. (A) Representative immunoblots of neurons treated with vehicle (CTRL), Aβ, Aβ in combination with calpeptin (CPTN), or calpeptin alone. Blots were probed with antibodies against cyclin dependent kinase 5 (cdk5), detecting holoprotein at 33 kDa, and an antibody against cdk5 activator p35, detecting a band at 35 kDa, and the calpain-cleaved p25 fragment at 25 kDa. Blots were also probed with an antibody against β-actin (42 kDa) as a loading control. Bar graphs show amounts of (B) cdk5 standardized to β-actin, (C) p35 and (D) p25 standardized to cdk5, and (E) p25 standardized to p35. n=6. Data is mean ± SEM. *$p < 0.05$, **$p < 0.01$

inconsistent with previous evidence of reduced PSD95 amounts in conditions of high Aβ, but these difference may be attributed to normalization of PSD95 amounts to β-actin, which is also expressed in astrocytes.

In contrast, levels of synapsin I were significantly increased in cultures treated with calpeptin, either alone or in the presence of Aβ ($p < 0.01$), while Aβ had no effect on the amounts of this presynaptic marker (Fig. 4.12C). These findings may also reflect that the cultures used in these experiments are still relatively immature (10 DIV). Although synapses are considered to be relatively mature by this time, not all receptors may be fully functional. Unfortunately, attempts to culture neurons for longer periods of time were not successful due to issues with $C0_2$ regulation across the whole Institution. Synapsin I is cleaved by calpain during activity-dependent calpain-mediated regulation of presynaptic activity in neurons (Murrey et al., 2006a; Khoutorsky and Spira, 2009). Moreover, synapsin I is upregulated in concert with elevated calpain activity in early AD brain, in what is likely a compensatory response to increased calpain cleavage of synapsin (section 3.2.13). The findings here in primary culture indicate that inhibition of calpain activity promote expression of synapsin I, thereby supporting the role of calpain as a regulator of synaptic activity.

To further investigate the role of Aβ on the postsynapse, primary neurons exposed to Aβ were immunostained with the 6E10 antibody that recognises C-terminal APP fragments, including Aβ (Fig. 4.13A). Cultures were also stained

with an antibody against microtubule-associated protein 2 (MAP2), which is predominantly found in neuronal dendrites, and the nuclear stain Hoescht-33342. These markers were expressed in both untreated and Aβ-treated cultures; however, cultures exposed to Aβ displayed abnormal dendritic morphology and cell loss (Fig. 4.13A). Cultures were then assessed under higher magnification so as to better visualize individual PSD95 puncta located on dendrites (Fig. 4.13B). PSD95 intensities were quantified separately in dendrites and somata as a proportion of MAP2 intensity, using the 'RGB measure' plugin in ImageJ, Quantification of immunostaining revealed that Aβ reduced dendritic PSD95 signals by more than 50% ($p < 0.01$), indicating that there is likely synapse loss in these cultures (Fig. 4.13C). Aβ also diminished somal PSD95 signals, however this reduction was not statistically significant likely due to variation between cells. These findings corroborate extensive reports of the synaptotoxic effects of Aβ (Lue et al., 1999; Kelly et al., 2005; Lacor et al., 2004; Shankar and Walsh, 2009), and in addition, indicate that western blotting is not a sufficiently sensitive method with which to examine the amounts of pre- and postsynaptic markers in this type of experiment.

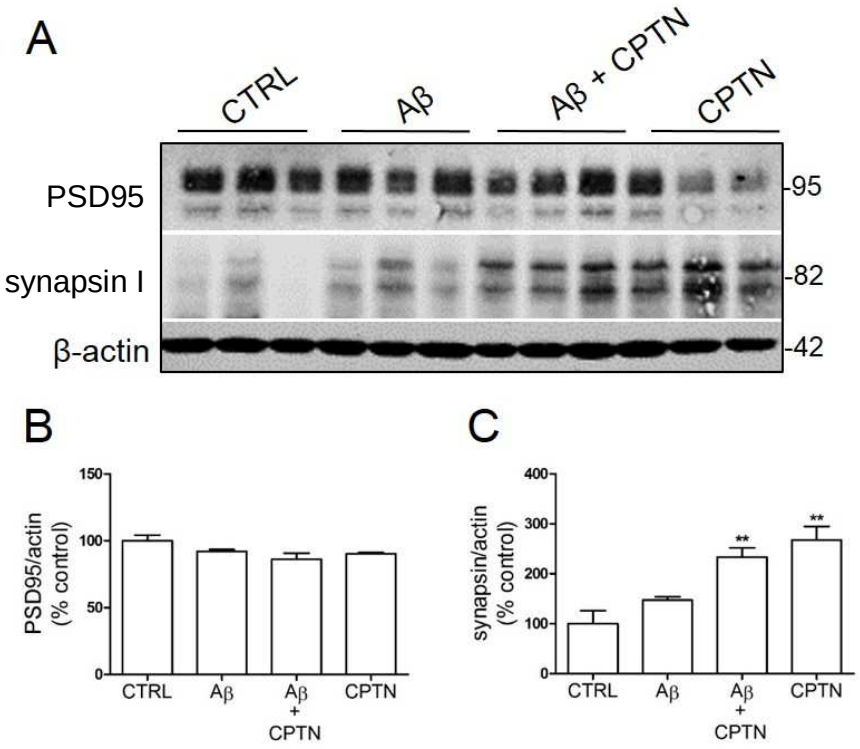

Fig. 4.12 Synapsin I protein expression is regulated by calpain. (A) Representative immunoblots of neurons treated with vehicle (CTRL), Aβ, Aβ in combination with calpeptin (CPTN), or calpeptin alone. Blots were probed with antibodies against the postsynaptic marker post synaptic density 5 (PSD95), detecting holoprotein at 95 kDa, and the presynaptic marker synapsin I, which detects two bands around 80 kDa. Blots were also probed with an antibody against β-actin (42 kDa) as a loading control. Bar graphs show amounts of (B) PSD95 and (C) synapsin I standardized to β-actin. n=3. Data is mean ± SEM. **p < 0.01

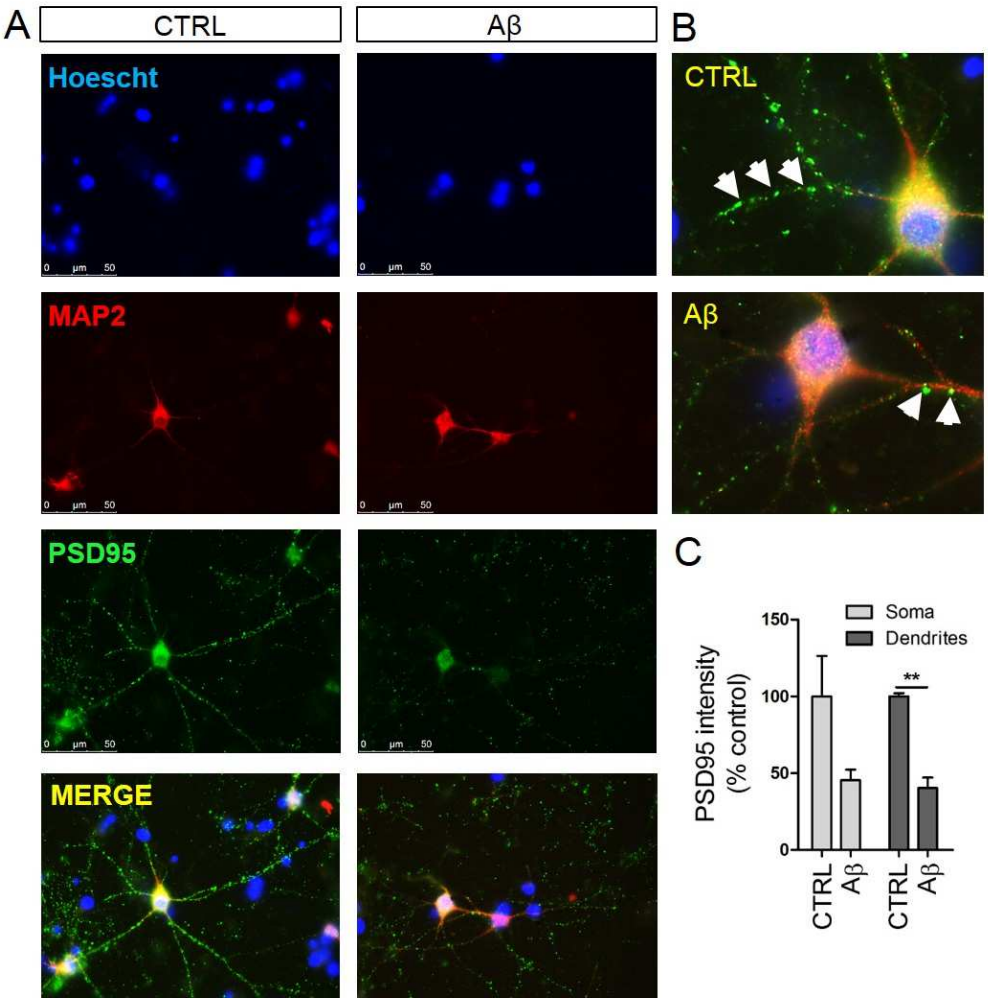

Fig. 4.13 Primary cortical cultures exposed to Aβ show reduced dendritic PSD95 puncta. (A) Neurons treated with Aβ were stained with antibodies against the major postsynaptic marker, post synaptic density 95 (PSD95), microtubule associated protein 2 (MAP2) which selectively labels neurons, and the nuclear stain Hoescht-33342. (B) Individual PSD95 puncta (white arrows) were visualized under X65 magnification. (C) Bar graph shows PSD95 intensity as a proportion of MAP2. Scale bar = 50 μM. n=4

4.2.10 Naturally secreted human Aβ oligomers do not alter calpain activity or tau phosphorylation in primary neurons

Synthetic human Aβ oligomers are commonly used at nM concentrations to model the effects of Aβ accumulation observed in AD in *vitro*, since this allows examination of the effects of different human Aβ species. However, it is argued that these Aβ preparations are not physiological and therefore may lack relevance for the study of human disease. In addition, the reporting of such Aβ preparation in the literature is a matter of controversy because of insufficient details concerning peptide size, concentration, species and aggregation state.

A naturally-derived source of Aβ oligomers has been reported to inhibit LTP and impair cognition in *vivo,* and this has been presented as a potential solution to the above obstacles associated with synthetic peptide (Walsh et al., 2002b; Cleary et al., 2005). Therefore, the well-characterized source of natural human Aβ oligomers from Chinese hamster ovary (CHO) cells stably expressing mutant APP (7PA2 cells; Walsh et al., 2002b) was also examined in this study. Conditioned medium from 7PA2 CHO cells contains secreted oligomeric Aβ that is SDS-stable and, importantly, is found at the same concentrations (0.1-2 nM) as detected in human cerebrospinal fluid.

Lysates of primary neurons treated with 7PA2 Aβ for 48 h and/or calpeptin were immunoblotted using an antibody against α-spectrin, detecting holoprotein at

240 kDa, calpain- and caspase-cleaved α-spectrin species at 140-150 kDa and caspase-cleaved α-spectrin species at 110-125 kDa (Fig. 4.14A). Blots were also probed with antibodies against total tau (DAKO) which detects multiple bands around 55 kDa, tau Ser199/202/Thr205 (tau-1), total GSK3 that detects a doublet at 51 and 47 kDa, respectively representing GSK3α and -β, and GSK3 phosphorylated at Ser21/9 that detects two bands at 51 and 47 kDa, respectively indicating GSK3 phosphorylated at Ser21 (GSK3α) and Ser9 (GSK3β) (Fig. 4.15A). An antibody specific for β-actin was used as a loading control.

Quantification of bands revealed no changes in total or full-length α-spectrin (Fig. 4.14B, C) or calpain- and caspase-cleaved fragments (Fig. 4.14D, E), between 7PA2 cell medium-treated and wild-type CHO cell-treated (control) cells. These findings show that treatment of primary cultures with natural Aβ for the same duration as synthetic Aβ does not elevate calpain activity or cause calpain-mediated cytoskeletal degradation. Amounts of total tau (Fig. 4.15B) or tau Ser199/202/Thr205 (tau-1; Fig. 4.15C) were also unchanged between any treatment group and control. In accordance, there was no change in GSK3 expression or activity in response to natural Aβ and/or calpeptin treatment (Fig. 4.15D, E). The concentrations of synthetic Aβ oligomers used here exceed those of naturally secreted Aβ oligomers by approximately 500-fold. Therefore, it is possible that synthetic Aβ is more fast-acting in *vitro*, and may be preferred for short-term studies of Aβ mechanisms in primary cell culture. The time course of naturally-derived Aβ effects, on the other hand, may recapitulate the slow Aβ-

mediated toxicity observed over long periods of time in transgenic animal models and in human AD.

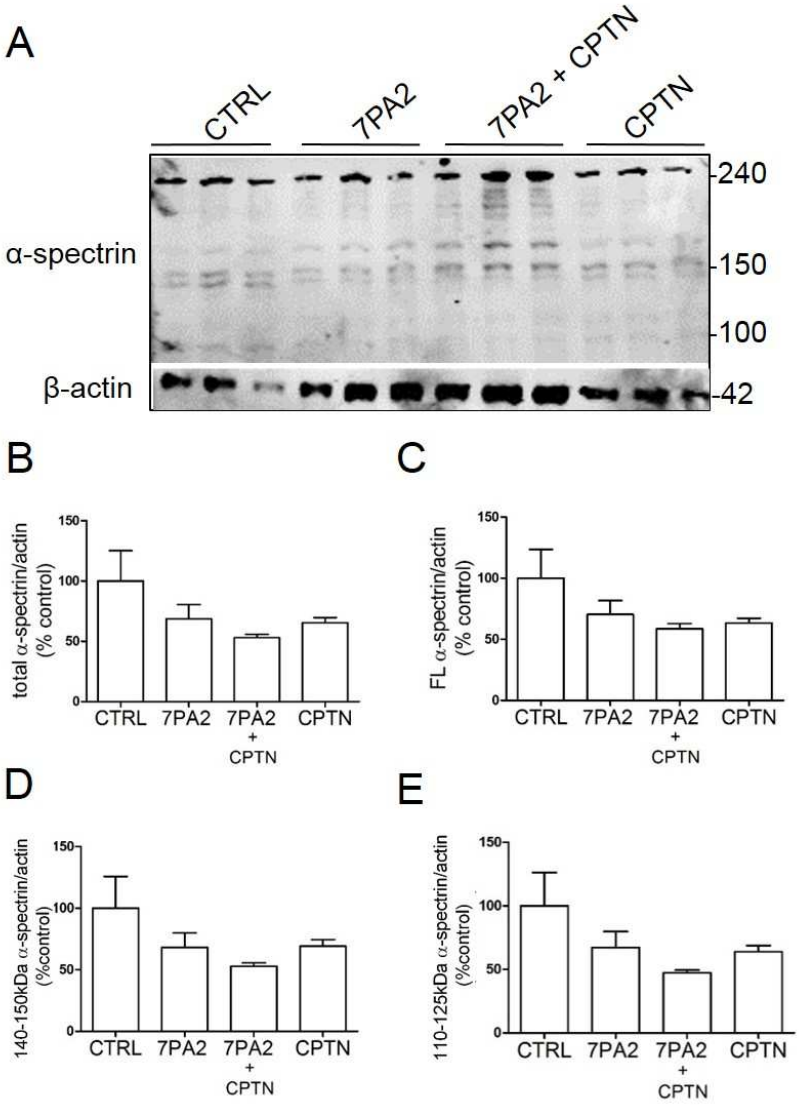

Fig. 4.14 Natural human Aβ oligomers do not alter activity-spectrin cleavage in primary cortical cultures (A) Representative immunoblots of lysates from neurons treated with vehicle (CTRL), 7PA2 CHO cell conditioned medium, 7PA2 medium with calpeptin (CPTN), or calpeptin alone. Blots were probed with an antibody against α-spectrin which detects holoprotein at 240 kDa, calpain- and caspase-cleaved fragments at 140 to 150 kDa and caspase-cleaved fragments at 110 to 125 kDa. Blots were also probed with an antibody against β-actin (42 kDa), as a loading control. Bar graphs show amounts of (B) total α-spectrin (C) full-length (D) calpain- and caspase-cleaved α-spectrin, and (E) caspase-cleaved α-spectrin, with all species normalised to β-actin. n=9. Data is mean ± SEM.

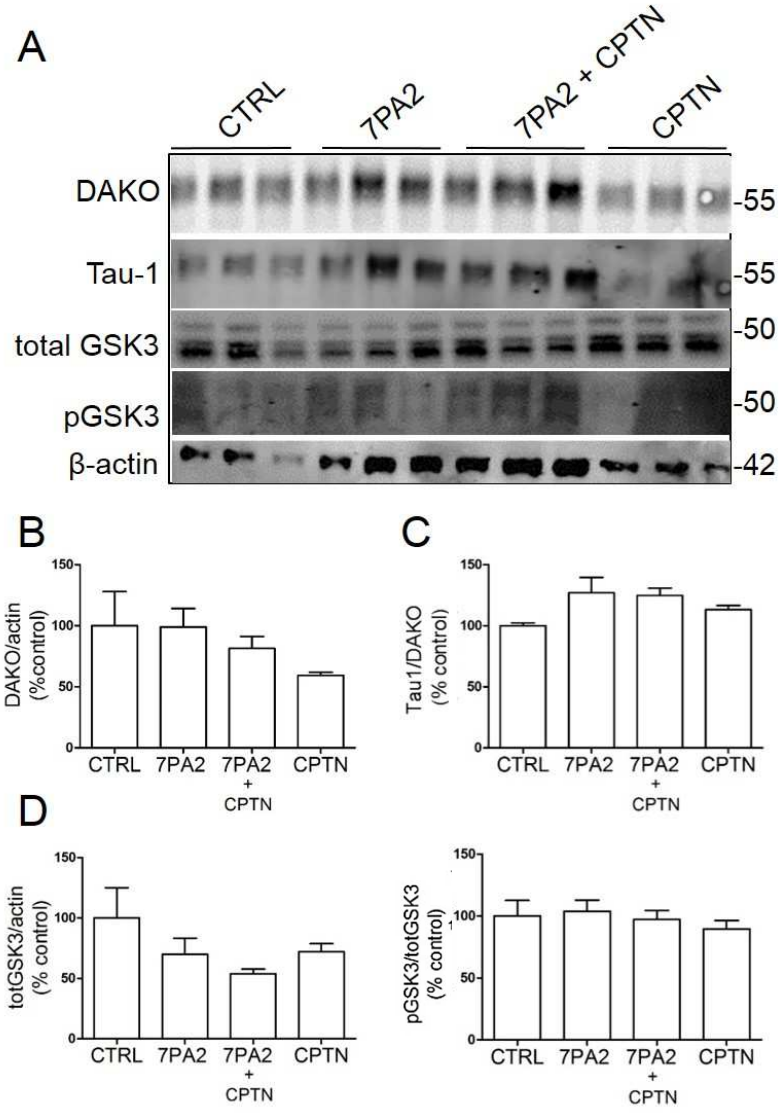

Fig. 4.15 Naturally secreted human Aβ oligomers do not alter tau kinase activity or tau phosphorylation in primary cortical cultures (A) Representative immunoblots of lysates from neurons treated with vehicle (CTRL), Aβ derived from 7PA2 Chinese Hamster Ovary cells (7PA2), 7PA2 Aβ with calpeptin (CPTN) or calpeptin alone. Blots were probed with an antibody against total tau (DAKO) and tau phosphorylated at Ser396/404 (PHF1), both of which detect a single band around 55 kDa. Blots were also probed with antibodies against total glycogen synthase kinase 3 (totGSK3), detecting bands at 51 and 47 kDa, representing GSK3α and -β, respectively and GSK3 phosphorylated at Ser21 and Ser9 (pGSK3), detecting two bands at 51 and 47 kDa, respectively. An antibody against β-actin (42 kDa) was sued as a loading control. Bar graphs show amounts of (B) DAKO standardized to β-actin, (C) PHF1 as a proportion of DAKO, (D) total GSK3, and (E) pGSK3 normalised to β-actin. n=3. Data is mean ± SEM.

4.2.11 Lithium suppresses calpain activity through inhibition of GSK3

In a recent study, treatment of primary hippocampal neurons with lithium was found to reduce calpain activity, tau phosphorylation and excitotoxicity mediated by kainic acid (Crespo-Biel et al., 2010). Lithium is a mood-stabilizer that has emerged as a promising neuroprotective agent in AD since it inhibits GSK3 activity, reduces tau phosphorylation and prevents neuronal apoptosis in *vitro* and *in vivo* (Hong et al., 1997; Song et al., 2002). In the study by Crespo-Biel et al. (2010), calpain activity was reduced after 3-5 days of lithium treatment, suggesting that calpain is reciprocally regulated by its downstream effector GSK3. Since a close correlation between GSK3 and calpain activities has been observed in the work presented here, it was deemed important to investigate the effects of GSK3 inhibition by lithium on calpain activity.

To test the effect of acute GSK3 inhibition on calpain activity, primary cortical cultures were treated with 5, 10 and 20mM lithium chloride (LiCl) or sodium chloride (NaCl) control for 4 h. Cortical lysates were first immunoblotted with antibodies against GSK3α and -β, detecting two respective bands at 51 and 47 kDa, and GSK3 phosphorylated at Ser21 and Ser9 (pGSK3) which also detects a doublet at 51 and 47 kDa, respectively (Fig. 4.16A). Blots were then probed with an antibody against the calpain substrate α-spectrin, which labels holoprotein at 240 kDa, calpain- and caspase-cleaved fragments at 140-150 kDa and caspase-cleaved

fragments at 110-125 kDa (Fig. 4.17A). For normalization purposes, an antibody against β-actin was used.

Quantitative analysis of immunodetected band intensities confirmed a dose-dependent inhibition of GSK3 following LiCl treatment, since there were significantly increased amounts of GSK3 phosphorylated at Ser21/9 in cultures treated with 10 mM ($p < 0.05$) and 20 mM ($p < 0.01$) LiCl (Fig 4.16B). At these concentrations, LiCl also significantly reduced the expression of GSK3 ($p < 0.05$; Fig. 4.16C). Increased GSK3 protein amounts are observed in late stage AD brain (section 3.2.12); thus LiCl treatment may potentially counteract the detrimental effects of increased GSK3 expression in these stages of disease. LiCl treatment was also found to reduce the amounts of total α-spectrin by 50% when used at 20 mM (Fig. 4.17B). Treatment also caused significantly increased amounts of α-spectrin holoprotein at 20mM concentration ($p<0.05$) and also when used at 10 mM ($p < 0.001$Fig. 4.17C). In accordance with this, the amounts of calpain- and caspase-cleaved fragments were reduced by more than 50% with 10 mM ($p < 0.05$) and 20 mM ($p < 0.01$) LiCl (Fig. 4.17D), indicating suppression of calpain proteolytic activity. The amounts of caspase-cleaved α-spectrin also showed a trend towards reduction following lithium treatment of neurons (Fig. 4.17E); however, these decreases did not reach significance likely due to the variation within the control group. These results therefore support previous reports that calpain inhibition can be induced upon treatment with LiCl. As the mechanisms of action of lithium on calpain activity are as yet undetermined, it is possible that alterations in

calpain activity are not directly mediated by GSK3, but may, for instance, result from modulation of Ca^{2+} entry (as suggested by Crespo-Biel et al., 2010). Nevertheless, this data suggests another possible mechanistic link between Ca^{2+} signalling and tau phosphorylation that is mediated by GSK3 and calpain signalling pathways.

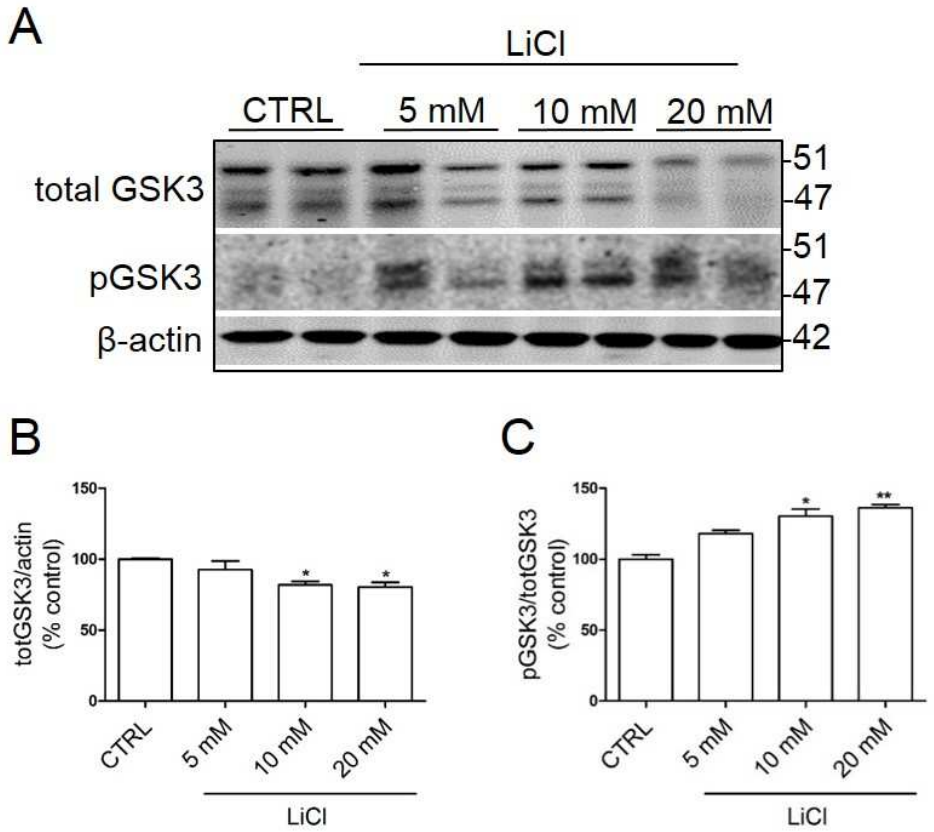

Fig. 4.16 Lithium dose-dependently reduces GSK3 expression and activity in primary cortical cultures. (A) Representative immunoblots of lysates from neurons treated with NaCl vehicle (CTRL), and lithium chloride (LiCl) at 5, 10 and 20 mM doses. Blots were probed with antibodies against total glycogen synthase kinase 3 (totGSK3), detecting bands at 51 and 47 kDa, representing GSK3α and -β, respectively and GSK3 phosphorylated at Ser21 and Ser9 (pGSK3), detecting two bands at 51 and 47 kDa, respectively. An antibody against β-actin (42 kDa) was used as a loading control. Bar graphs show amounts of (B) total GSK3 normalised to β-actin, and (C) pGSK3 normalised to total GSK3. n=3. Data is mean ± SEM. * $p < 0.05$, ***$p < 0.001$.

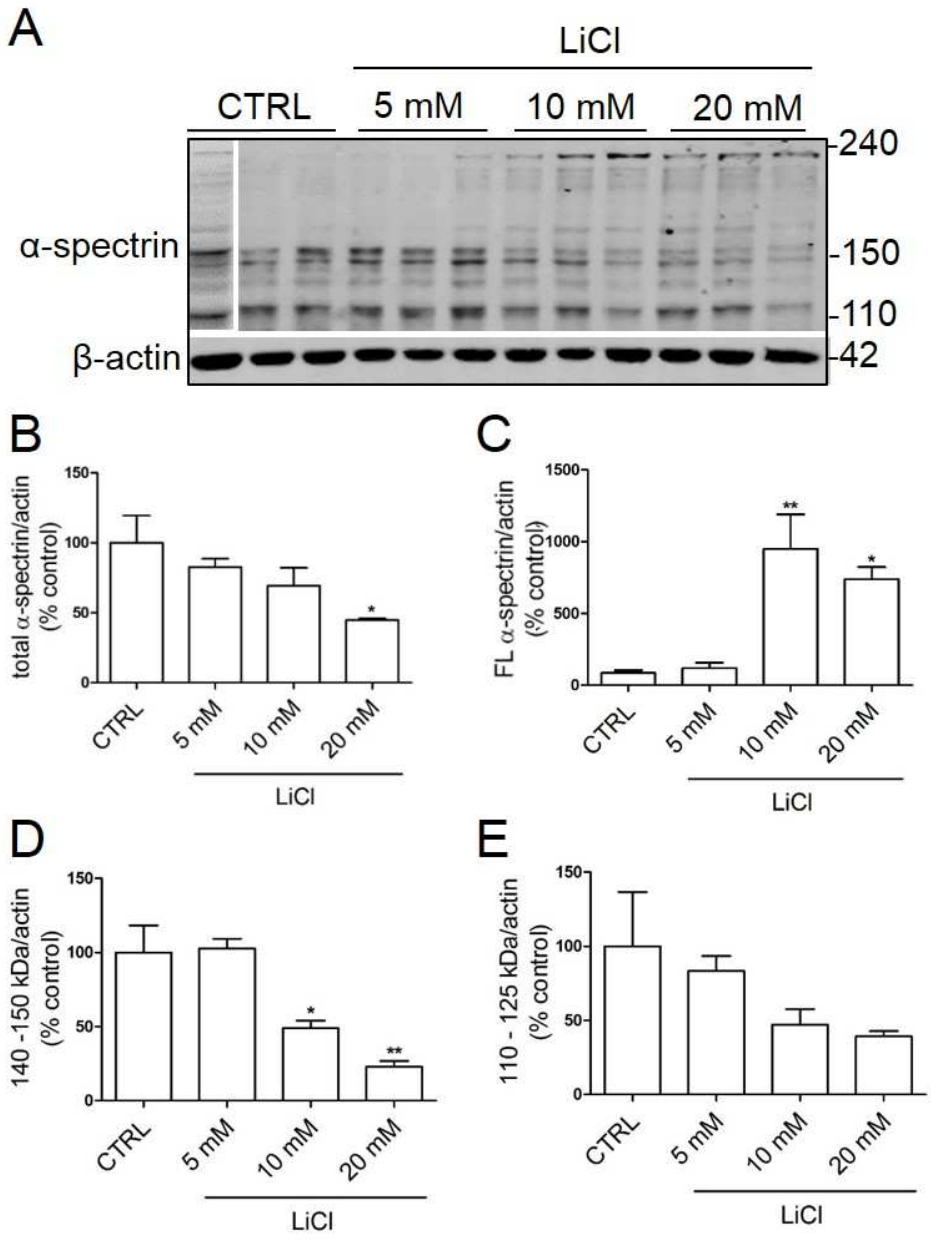

Fig. 4.17 Lithium dose-dependently decreases calpain activity in primary cortical cultures. (A) Representative immunoblots of lysates from neurons treated with vehicle (CTRL), and lithium chloride (LiCl) at 5, 10 and 20 mM doses. Blots were probed with antibodies against α-spectrin, which detects holoprotein at 240 kDa, calpain- and caspase-cleaved fragments at 140-150 kDa and caspase-cleaved fragments at 110-125 kDa. Blots were also probed with an antibody against β-actin (42 kDa), as a loading control. Bar graphs show amounts of (B) total α-spectrin (C) full-length (D) calpain- and caspase-cleaved α-spectrin, and (E) caspase-cleaved α-spectrin, with all species normalised to β-actin. n=9. Data is mean ± SEM. *$p < 0.05$, **$p < 0.01$

4.2.12 Aβ does not alter neuronal Ca^{2+} dynamics in primary cortical culture

Aβ is believed to mediate synaptic dysfunction and neuronal loss by causing cytotoxic elevations of intracellular Ca^{2+} (Kuchibhotla et al., 2008; Supnet and Bezprozvanny, 2010). Human and rodent primary neurons (10 to 21 DIV) undergo rapid increases in intraneuronal Ca^{2+} within minutes of exposure to Aβ (Atherton et al. unpublished; Mattson et al., 1992; De Felice et al., 2007). Therefore, it was hypothesized that the AD-relevant protein changes induced by calpain in this chapter occur downstream of intraneuronal Ca^{2+} accumulation in response to Aβ. To determine whether Aβ modulates intracellular Ca^{2+} in primary cortical neurons, it was first important to distinguish neurons from other cell types, as cultures used here were established as predominantly neuronal but containing ~17 % astrocytes and a negligible (0.01 %) proportion of microglia (Garwood et al., 2011). Neurons were identified under bright-field based on dendritic and axonal morphology and stasis in culture, while astrocytes showed stellate morphology and motility over time. As this thesis examines neuronal mechanisms of Ca^{2+} dysregulation, only neurons were selected for live imaging. Soluble oligomeric Aβ1-42 was applied to primary cultures incubated in fluo-4 AM Ca^{2+} indicator (section 2.1.6) immediately prior to imaging. Standard fluorescence live microscopy was used to measure changes in fluo-4 signal intensity, thereby indicating changes in cytosolic Ca^{2+}. Images were taken over the course of 10 min, at a 1 s interval and were analysed as described in section 2.2.7.

Application of Aβ oligomers did not evoke a detectable change in neuronal fluo-4 signal over 10 min from baseline (Fig. 4.18). Cultures were checked for neuronal viability by application of 50 mM KCl, which is known to induce rapid neuronal depolarization in healthy neurons (Franklin et al., 1995). The observed Ca^{2+} peak increase of $\Delta F/F = 1.6 \pm 0.6$ (S.E; Fig. 4.18.C) immediately after treatment with KCl confirmed the viability of these cultures, signifying that neuronal health was not a factor in the absence of a Ca^{2+} response to Aβ. Although these results are inconsistent with previous findings in this group, it is likely that variations in Aβ and culture preparations or differential effects of exogenous and intracellular Aβ could account for this discrepancy.

4.2.13 Aβ-induced Ca^{2+} elevations in SH-SY5Y cells are mediated by influx of extracellular Ca^{2+}

Human SH-SY5Y cells commonly replace neuronal culture as an in *vitro* model for neurodegenerative disorders as they are morphologically similar to primary neurons, express a number of mature neuronal markers and are immortal (Kovalevich and Langford, 2013). Importantly, these cells express Ca^{2+} channels, receptors and pumps known to be dysregulated in AD by Aβ (Kulikov et al., 2007; Morton et al., 1992; Magi et al., 2005). Thus, SH-SY5Y cells were used here to model Aβ mechanisms of Ca^{2+} dysregulation in the absence of results in primary neurons (section 4.2.12).

Aβ was applied to SH-SY5Y cells loaded with fluo-4 Ca^{2+} dye (section 2.1.6) immediately before recording was started (Fig. 4.19). Intracellular fluo-4 signal

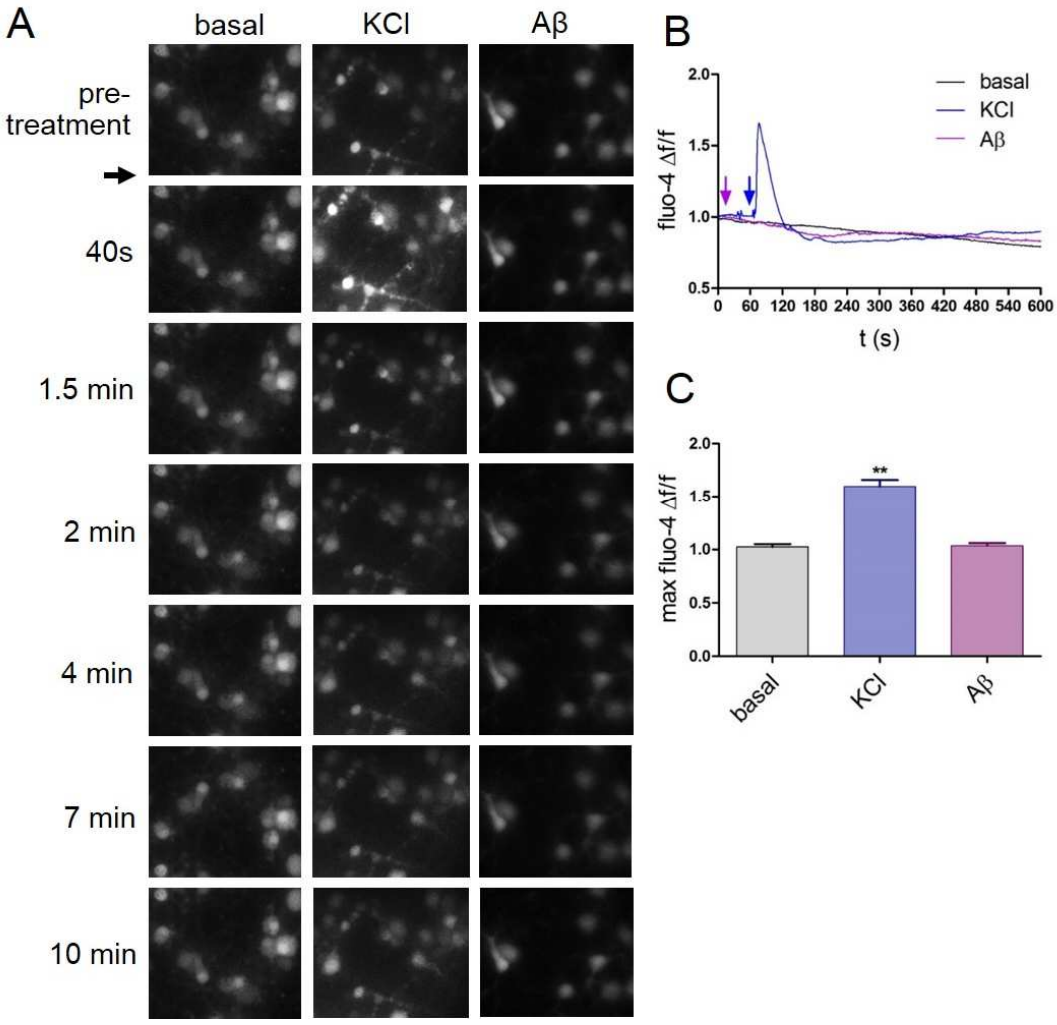

Fig. 4.18 Synthetic human Aβ does not alter intracellular Ca^{2+} concentration in primary cortical cultures. (A) Cultures loaded with fluo-4 Ca^{2+} dye were imaged at 1 s intervals for a period of 10 min immediately after application of Aβ or KCl. (B) Representative Ca^{2+} traces from cultures imaged prior to application of either Aβ (purple arrow) or 50 M KCl (blue arrow). Ca^{2+} signal was calculated as change in fluo-4 fluorescence as a proportion of original fluorescence (ΔF/F). (C) Bar graph shows maximum intracellular Ca^{2+} in resting cultures (basal) and cultures treated with KCl or Aβ. Data is mean ± SEM. **p < 0.01

was measured by standard live fluorescence microscopy, with changes in signal intensity representing changes in intracellular Ca^{2+}. Images were captured at 1 s intervals for a total of 10 min, and were analysed as described in section 2.2.7.

Fluo-4 signal was measured from multiple cells on each coverslip so as to determine the proportion of cells responding to Aβ and derive an average Ca^{2+} trace. Interestingly, while Aβ induced a Ca^{2+} response in > 90 % (n = 120) of cells, there was variability between cells in the patterning of the response. The majority of cells displayed large Ca^{2+} transients, while less than 20 % (n = 24) responded with prolonged elevations and minor increases in Ca^{2+} (Fig. 4.20A). Differences in the temporal patterning of Ca^{2+} signals is likely to indicate execution of different Ca^{2+}-sensitive cellular processes under physiological conditions (Berridge et al., 2000). On the other hand, the differential Ca^{2+} dynamics evoked here by Aβ may possibly indicate intercellular communication or propagation of the Aβ response.

On average, cells that were exposed to Aβ displayed elevated Ca^{2+} transients that lasted around 60 s and dampened over time, with an initial highest peak increase of $\Delta F/F = 3.3 \pm 0.2$ (S.E) at 60 s after treatment (Fig 4.19 and 4.20B). These Ca^{2+} transients significantly exceeded the Ca^{2+} response to depolarization by KCl ($p < 0.05$; Fig 20.C), supporting the hypothesis that Aβ destabilizes neuronal Ca^{2+} homeostasis (Mattson et al., 1992). Moreover, the amplitudes of these Ca^{2+} transients were previously reported as characteristic of Aβ oligomer action in SH-SY5Y cells (Demuro et al., 2005).

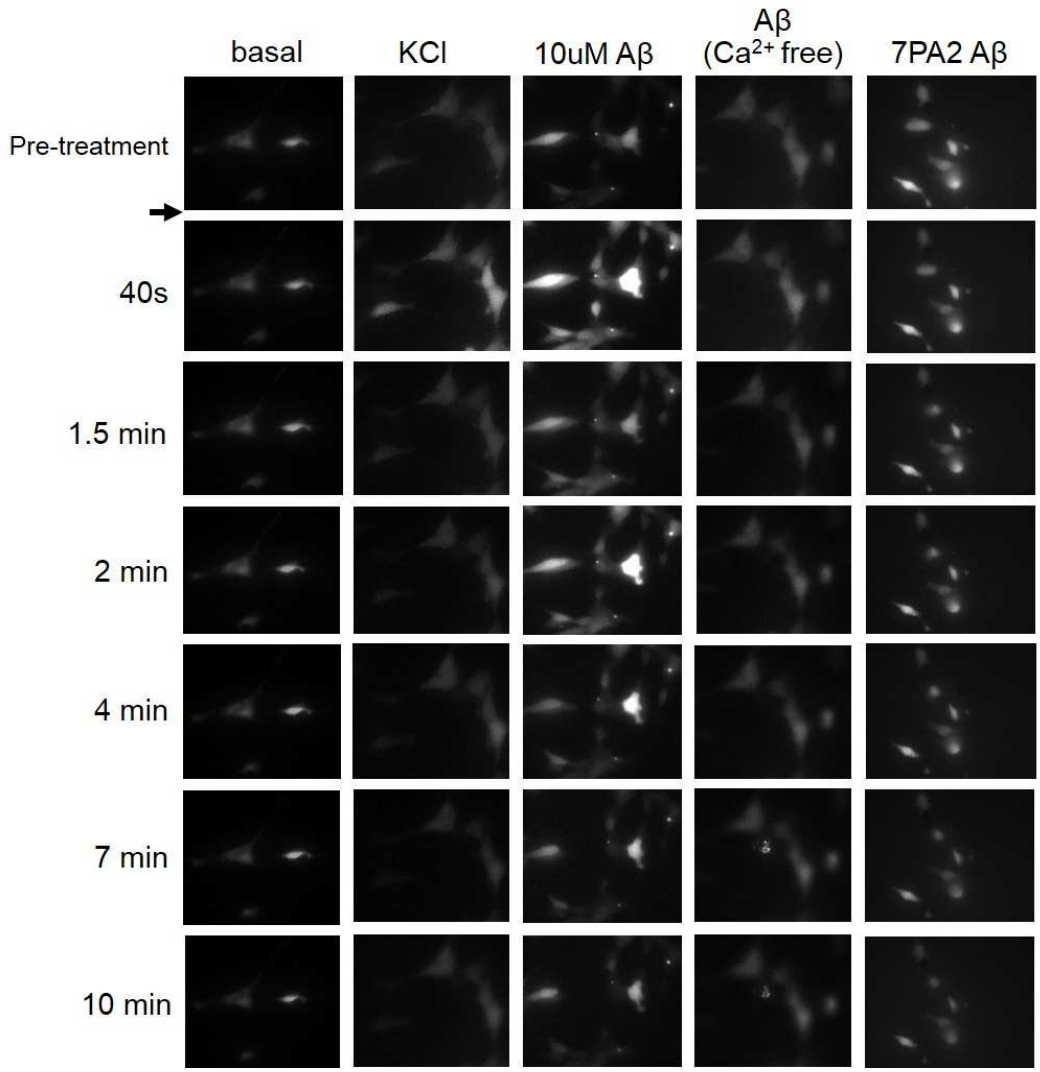

Fig. 4.19 Aβ transiently elevates intracellular Ca^{2+} concentrations via influx of extracellular Ca^{2+} in SH-SY5Y cells. Cultures loaded with fluo-4 Ca^{2+} dye were imaged at 1 s intervals for a period of 10 min immediately after application of either KCl, Aβ, Ca^{2+} Aβ in free solution or natural Aβ derived from 7PA2 Chinese hamster ovary cells (7PA2 Aβ).

The Ca^{2+} response to Aβ was abolished when cells were imaged in Ca^{2+}-free solution (Fig. 4.19 and 4.20B, C), thereby indicating that Aβ-induced cytosolic Ca^{2+} elevations are mediated by influx of extracellular Ca^{2+}, in line with numerous

reports (Supnet and Bezprozvanny, 2010; Bezprozvanny and Mattson, 2008; Demuro et al., 2011; Brorson et al., 1995; Mark et al., 1995).

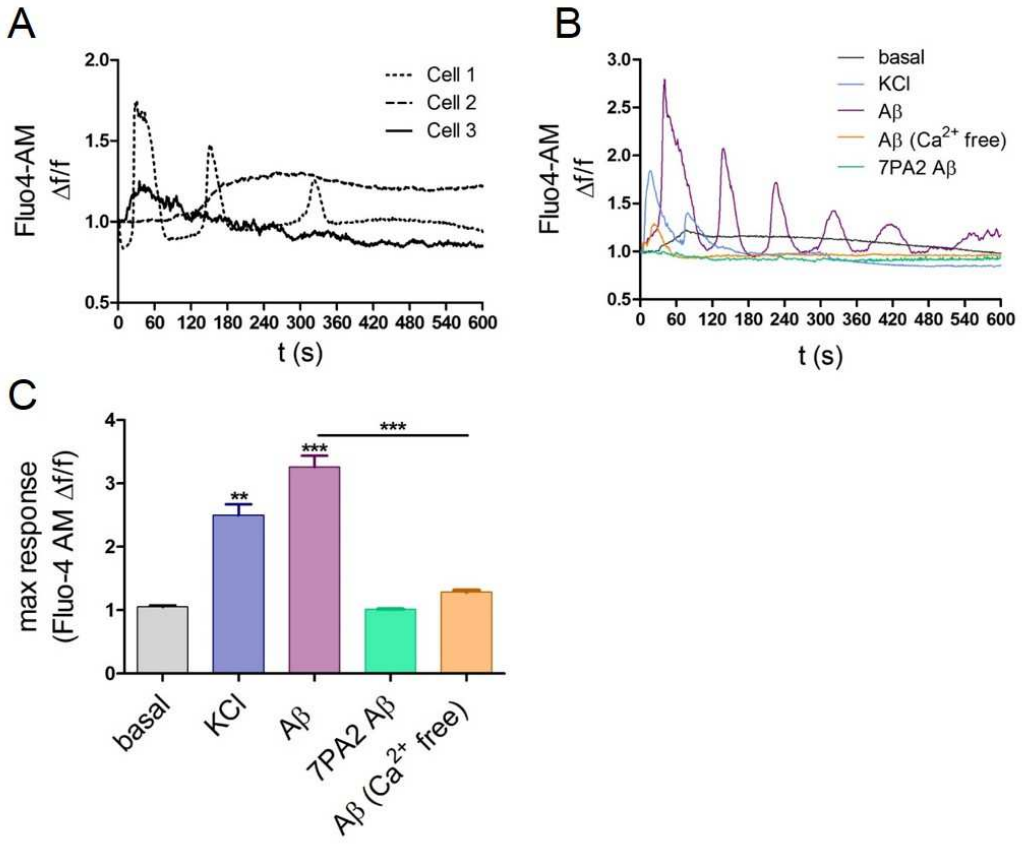

Fig. 4.20 Aβ transiently elevates intracellular Ca^{2+} concentrations via influx of extracellular Ca^{2+} in SH-SY5Y cells. (A) Representative Ca^{2+} traces from different cells in a single culture treated with Aβ and (B) cultures treated with either KCl, Aβ, Aβ in Ca^{2+}-free solution or 7PA2 CHO cell media (7PA2 Aβ). Ca^{2+} signal was calculated as change in fluo-4 fluorescence as a proportion of original fluorescence (ΔF/F). (C) Bar graph shows maximum intracellular Ca^{2+} in resting cultures (basal) and cultures treated with KCl, Aβ, Aβ in Ca^{2+} free solution and 7PA2 Aβ. Data is mean ± SEM. **p < 0.01, ***p < 0.001

However, there was evidence of a small Ca^{2+} peak occurring immediately after Aβ application to cells in Ca^{2+}-free solution (Fig. 4.20C), measuring $\Delta F/F = 1.28 \pm 0.3$ (S.E) above basal, and possibly signifying release of Ca^{2+} from intracellular stores. Pharmacological modulation of ER Ca^{2+} release has previously been shown to significantly reduce the cytosolic Ca^{2+} increases induced by Aβ (Suen et al., 2003). This suggests that Aβ mediates neuronal Ca^{2+} insults partially through stimulation of ER stores, which may account for the Ca^{2+} response seen here in the absence of extracellular Ca^{2+}. However, the small size of this observed Ca^{2+} peak implies that it does not play a major role in the overall Aβ-induced Ca^{2+} response, and the role of ER Ca^{2+} signalling in Aβ neurotoxicity remains unclear, at least in the model used here.

4.2.14 Physiological Aβ does not alter short-term Ca^{2+} dynamics in SH-SY5Y cells

As described in section 4.2.10, an important aim of this chapter was to compare the effects of naturally secreted Aβ oligomers derived from 7PA2 cells to those elicited by synthetic Aβ oligomers in primary neurons (section 4.2.12). Since 7PA2 Aβ did not increase activity of Ca^{2+}-sensitive calpain-1 after 48 h (section 4.2.10), this suggested that 7PA2 Aβ would also not affect Ca^{2+} dynamics over the same time period.

Indeed, when measured by standard fluorescence microscopy in fluo-4-loaded SHSY-5Y cells, treatment of cells with 7PA2 cell medium prior to recording did not increase cytosolic Ca^{2+} from baseline over 10 min (Fig. 4.19 and 4.20B, C), in contrast to the prolonged Ca^{2+} elevations observed in response to synthetic Aβ (section 4.2.13). Again, this might reflect the differences in Aβ concentration between these two preparations, as discussed above.

4.2.15 Aβ-induced Ca^{2+} elevations in SH-SY5Y cells are blocked by inhibition of calpains, caspases and PARP

Aβ has shown to dysregulate neuronal Ca^{2+} by modulating a variety of mechanisms that form the Ca^{2+} signalling toolkit, including activation of NMDARs (Molnár et al., 2004) and calpains (Atherton et al., 2014). Accumulating evidence also implicates PARP in Aβ-mediated neurotoxicity, since PARP is activated during the oxidative stress induced by Aβ (Fonfria et al., 2005), Aβ-induced NMDAR activation (De Felice et al., 2007) and elevations in neuronal Ca^{2+} (Virág et al., 1999). PARP initiates apoptosis through activation of caspase-3 and calpain-1 (Chaitanya et al., 2010), which in turn respectively activate and inhibit PARP. Therefore, the contribution of calpain, caspase and PARP activities in Aβ-induced Ca^{2+} elevations were next investigated in live neurons.

Prior to Ca^{2+} imaging, cultures were pre-treated for 3 h with calpain inhibitor calpeptin (CPTN), NMDAR antagonist MK-801 (MK), pan-caspase inhibitor VI (CI VI) and PARP inhibitor SB750139 (SB). Synthetic Aβ was prepared as described in section 2.2.7 and was directly added to fluo-4-loaded SH-SY5Y cells immediately prior to imaging using standard live fluorescence microscopy (Fig. 4.21). Images were captured at 1 s intervals for a duration of 10 min and fluo-4 signal intensity was used as an arbitrary measure of intracellular Ca^{2+} concentration.

Treatment of cells with Aβ produced a series of large Ca^{2+} transients as described in section 4.2.13. These transients were suppressed in the presence of all compounds, with a marked variation in the patterning of Ca2+ signals depending on which compound was used (Fig. 4.22A, B). Treatment with MK-801 (MK) reduced the initial Aβ-evoked Ca^{2+} peak by approximately 42 % ($p < 0.05$; Fig. 4.22B), followed by a steady decline in intracellular Ca^{2+} concentrations that was punctuated by minor oscillations that temporally synchronized with the diminishing transients elicited by Aβ alone (Fig. 4.22A). These results are in agreement with the literature, indeed the role of NMDARs in Aβ oligomer-induced Ca^{2+} dysregulation in AD is widely supported (Texidó et al., 2011; Alberdi et al., 2010; Ferreira et al., 2012; Francis, 2008; Ferreira et al., 2015; De Felice et al., 2007).

Exposure of Aβ-treated cells to SB750139 (SB) reduced the Ca^{2+} peak evoked by Aβ by approximately 25 % (Fig. 4.22B) but this did not reach statistical significance, likely due to variation between experiments. However, SB abolished the later Ca^{2+} oscillations seen with Aβ, instead causing a steady decline of Ca^{2+} to basal levels (Fig. 4.22A). These findings imply that PARP signalling may play a key secondary role in the Ca^{2+} response to Aβ, following an initial Ca^{2+} influx via NMDARs as previously described (Virág et al., 1999; Vosler et al., 2009).

Treatment of cells with a cocktail of Aβ and calpeptin (CPTN) caused an almost 3-fold reduction of the initial Aβ-induced Ca^{2+} transient to levels slightly elevated from basal ($p < 0.001$, Fig 4.22), which were only completely recovered after 6 min of imaging (Fig. 4.22A). These findings suggest that calpain activity plays a key role in mediating the prolonged Ca^{2+} increase induced by Aβ, as proposed in this thesis and previous work by this group (Atherton et al., 2014). Calpain cleaves and inactivates NCX3 in AD brain, which in primary culture confers neurotoxicity (Chapter 3). NCX3 is responsible for clearing excess Ca^{2+} from cells to protect neurons. These findings therefore support the hypothesis that calpain inhibition may relieve the toxic effects of Ca^{2+}-mediated calpain-induced NCX3 cleavage and inactivation of NCX3 in response to Aβ.

Imaging of cells treated with Aβ in the presence of pan-caspase inhibitor VI (CI VI) revealed a 62 % reduction in the initial Ca^{2+} spike evoked by Aβ ($p < 0.001$; Fig. 4.22B), following which Ca^{2+} levels were further reduced to basal for the duration

of the experiment (Fig. 4.22A). Elevations in intracellular Ca^{2+} were previously shown to upregulate expression and activity of caspases (Juin et al., 1998; Gong et al., 2007).

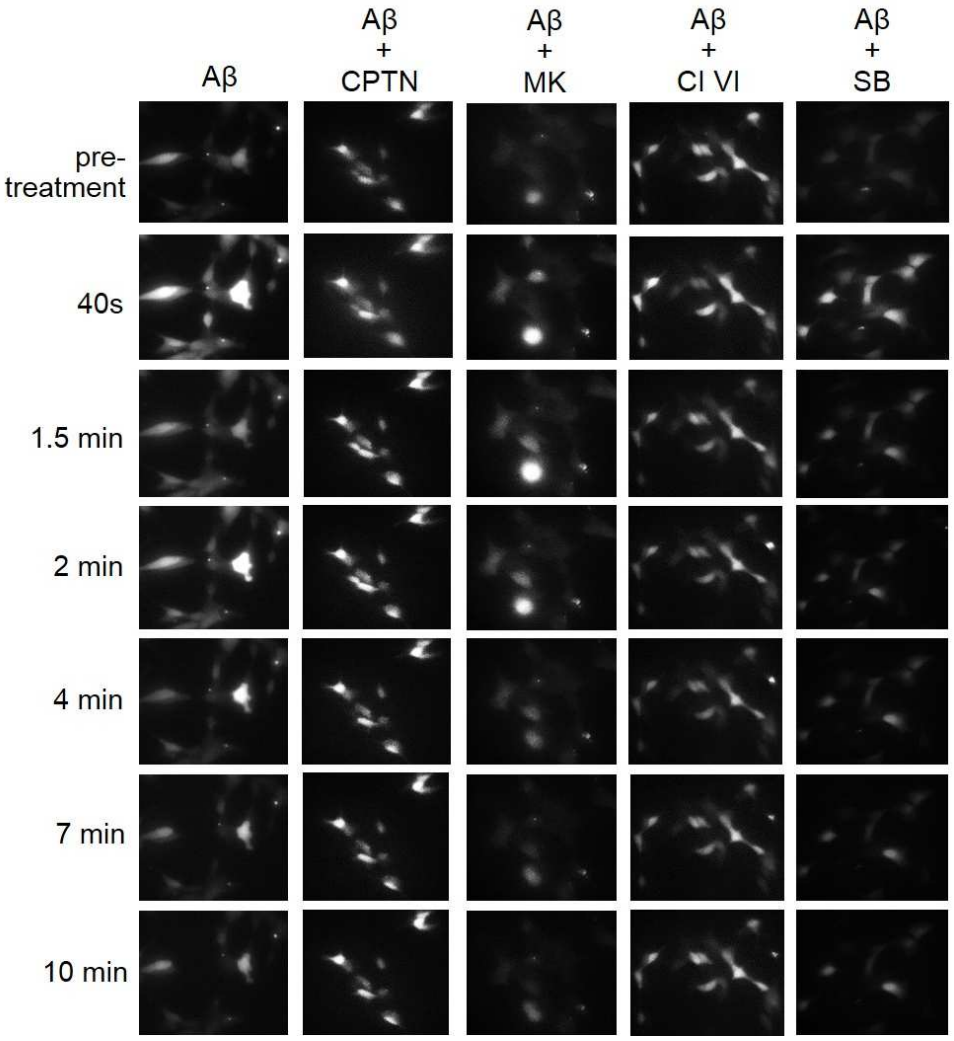

Fig. 4.21 Aβ-induced transient elevations of intracellular Ca^{2+} are modulated by inhibition of N-methyl-D-aspartate receptors (NMDAR), calpain, caspase, and poly(ADP)ribose polymerase (PARP) activities. Prior to imaging, cultures were pre-treated for 3 h with calpain inhibitor calpeptin (CPTN), NMDAR antagonist MK-801 (MK), pan-caspase inhibitor VI (CI VI) and PARP inhibitor SB750139 (SB). Cultures were loaded with fluo-4 Ca^{2+} dye and imaged at 1 s intervals for a period of 10 min immediately after application of Aβ.

The tight interrelationship between caspases and calpains (Nakagawa and Yuan, 2000) suggests that caspases could also play a role in calpain-mediated mechanisms of Ca^{2+} overload. Elevated caspase-3 activity has been found to mediate synaptic dysfunction in APP_{SWE} mice, suggesting that caspase activity is activated by Aβ (Kuwako et al., 2002). However, these authors also showed that caspase-3 downregulates glutamatergic transmission, by removing the GluR1 subunit of AMPARs, and that caspase-3 is not involved in NMDAR signalling. Therefore, the degree to which caspases appear to contribute to the Aβ-induced Ca^{2+} response in these experiments was somewhat unexpected, but could simply imply activation of caspases other than caspase-3 since the inhibitor used here is not specific to caspase-3 alone.

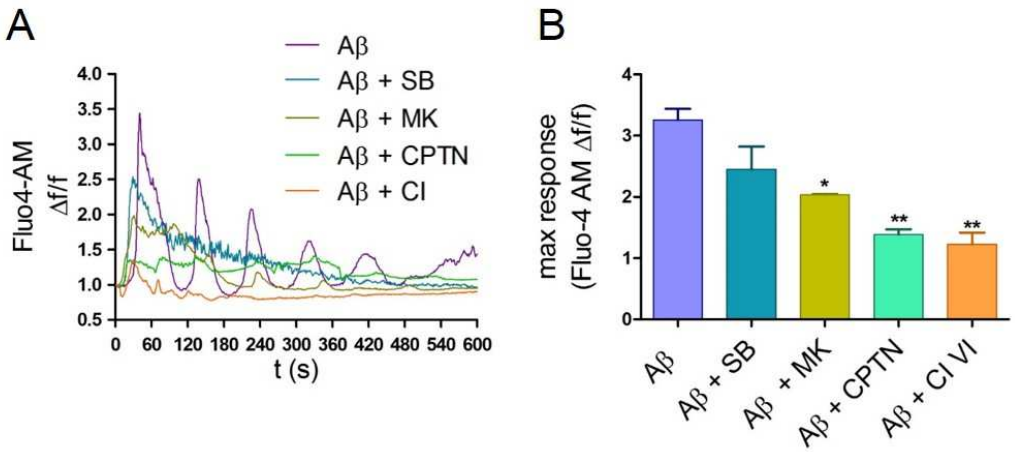

Fig. 4.22 Aβ-induced transient elevations of intracellular Ca^{2+} are abolished by inhibition of N-methyl-D-aspartate receptors (NMDAR), calpain, caspase, and poly(ADP)ribose polymerase (PARP) activities. (A) Representative Ca^{2+} traces from cultures pre-treated for 3 h with calpain inhibitor calpeptin (CPTN), NMDAR antagonist MK-801 (MK), pan-caspase inhibitor VI (CI VI) and PARP inhibitor SB750139 (SB). Ca^{2+} signal was calculated as change in fluo-4 fluorescence as a proportion of original fluorescence (ΔF/F). (C) Bar graph shows maximum intracellular Ca^{2+} in cultures treated with Aβ only or with Aβ in combination with CPTN, MK, CI VI and SB. Data is mean ± SEM. *$p < 0.05$, **$p < 0.001$

4.3 Summary and Discussion

The main findings of this chapter are:

- Aβ induces neuronal death and calpain proteolytic activity in primary culture, which is reduced by inhibition of calpain
- Aβ and calpain have independent and differential effects on non-amyloidogenic and amyloidogenic processing of APP to influence intracellular Aβ production
- Aβ alters tau phosphorylation via a mechanism at least partly dependent on calpain and which likely involves alterations in GSK3 and cdk5 activities
- Calpain-activated GSK3 reciprocally upregulates calpain activity
- Aβ and calpain affect synaptic markers suggesting effects on synapse health
- Aβ stimulates intracellular accumulation of Ca^{2+} through influx of extracellular Ca^{2+}
- Naturally secreted human Aβ oligomers does not alter Ca^{2+} homeostasis, calpain activity or tau phosphorylation in the cell models used here
- Aβ-induced elevation of cytosolic Ca^{2+} is rescued by inhibition of NMDAR, PARP, calpain and caspase activities

4.3.1 Calpain plays a significant role in Aβ mechanisms of neurotoxicity

In this chapter, exposure of primary cortical neurons to Aβ caused a significant increase in cell death, which was rescued by pharmacological inhibition of calpain (section 4.2.2). These findings were previously observed by this group and others (Atherton et al., 2014; Kelly et al., 2005; Kelly and Ferreira, 2006; Nicholson and Ferreira, 2009), and suggest a key role for calpain in Aβ-induced neurotoxicity.

Calpain-1 is predominantly expressed in neurons and regulates a variety of vital physiological processes by catalysing proteolytic degradation of more than a 100 protein substrates (Ferreira, 2012). These include cytoskeletal proteins (including α-spectrin and tau), signal transduction proteins, synaptic markers, glutamate receptors and transcription factors. It is thus unsurprising that, under physiological conditions, calpain activity is tightly regulated by intracellular Ca^{2+} levels, the endogenous calpain-specific inhibitor calpastatin, and a number of protein kinases (Goll et al., 2003; Kiss et al., 2008). Calpains are primarily inactivated by homoestatic cytosolic Ca^{2+} concentrations in the nM range, and are activated by discrete elevations of Ca^{2+} to μM concentrations (in the case of calpain-1). It may therefore be expected that prolonged activation of calpain-1 induced by chronically elevated Ca^{2+} would result in significant cellular damage due to massive proteolytic activity.

Indeed, the Aβ-induced neuronal death seen here was associated with increased calpain-mediated cleavage of α-spectrin, indicating elevated calpain proteolytic activity and cytoskeletal degradation. This was accompanied by increased generation of cleaved (active) caspase species, indicating that Aβ signals apoptosis through caspase activity, which is likely calpain-dependent (Warren et al., 2007; Nakagawa and Yuan, 2000). Inhibition of calpain activity attenuated calpain-mediated breakdown of α-spectrin and was neuroprotective to cultures. Therefore, these findings support previous evidence that Aβ mediates neuronal death through calpain-dependent cellular damage.

Aβ-induced neuronal death in primary culture is accompanied by synaptic damage (Shankar and Walsh, 2009; Sivanesan et al., 2013). Depletion of dendritic spines by Aβ oligomers is mediated by elevations of spine Ca^{2+} and occurs prior to localized activation of tau kinases and tau phosphorylation (Zempel et al., 2010). Calpain-1 is enriched between synaptic vesicles, where it regulates vesicular trafficking and neurotransmitter release (Khoutorsky and Spira, 2009; Murrey et al., 2006b); therefore, it is likely that Aβ-induced synaptic loss involves local calpain dysregulation mediated by local Ca^{2+} elevations. In this study, Aβ-induced neurotoxicity and calpain upregulation was associated with loss of synaptic markers, particularly significantly reduced PSD95 immunoreactivity in neuronal dendrites (section 4.2.9). However, inhibition of calpain did not recover PSD95 protein expression, which is inconsistent with previous reports (Lu et al.,

2000) and does not add further support for a role of calpain in synaptic loss, at least in the culture model used here.

4.3.2 Aβ and calpain differentially promote amyloidogenic APP processing and Aβ production

Although many consider Aβ as the initial pathogenic trigger in AD, there is growing evidence that Ca^{2+} dyshomeostasis occurs upstream of and contributes to aberrant APP processing and Aβ production (Buxbaum et al., 1994; Hoey et al., 2009). Mutations in the Ca^{2+} channel CALHM1 in patients with sporadic AD lead to Aβ overproduction (Dreses-Werringloer et al., 2008), and PS mutations in animal models of familial AD increase Aβ generation through dysregulated ER Ca^{2+} signalling (Green et al., 2008).

The observations here of Aβ accumulation in neurons exposed to synthetic Aβ (section 4.2.5) was somewhat surprising since 1) Aβ is classically secreted extracellularly following proteolytic cleavage of plasma membrane APP (Zhang et al., 2011), and 2) current literature lacks evidence on the role of Aβ in modulating APP processing. However, a number of studies have demonstrated that intracellular pools of Aβ are generated from APP located within intraneuronal compartments in transgenic animals and AD brain (LaFerla et al., 2007; Vetrivel and Thinakaran, 2006; Tomita et al., 1998), and intracellular Aβ1-42 was shown

to be synthesized *de novo* in normal human cerebral astrocytes exposed to Aβ25-35 - a surrogate of Aβ1-42 (Dal Pra et al., 2011). Axonal and dendritic Aβ has been shown to disrupt synaptic plasticity and reduces dendritic spine numbers (Wei et al., 2010), which causes cognitive and memory impairment (Lacor et al., 2004). When taken together, these findings suggest that Aβ may mediate memory loss and neuronal death in AD through synaptotoxic mechanisms that involve further overproduction of Aβ and intracellular accumulation of the peptide.

Several lines of evidence suggest that Ca^{2+} mediates changes in APP processing through calpain activation and signalling. Calpain activation increases BACE expression, amyloidogenesis and plaque formation in mice expressing mutant APP either alone or together with mutant PS1 (Liang et al., 2010). Moreover, BACE is shown to be elevated in brain tissue and CSF from patients with early AD (Evin et al., 2010). On the other hand, inhibition of calpain by calpeptin in murine L cells has shown to dose-dependently increase Aβ1-42 secretion (Mathews et al., 2002). Thus, the role of calpain in APP processing remains controversial. The calpain-mediated modulation of physiological APP processing observed in the current study (section 4.2.4) suggests that calpain shifts APP homeostasis towards amyloidogenesis; however calpain inhibition had no effect on BACE expression, or Aβ production (section 4.2.5). Therefore, it is possible that Aβ and calpain promote aberrant APP processing via separate mechanisms, independent of each other. On the other hand, the marked increase in the BACE-cleaved C99 fragment in cultures treated with calpeptin may signify increased BACE proteolytic activity

(which was not directly measured in this study). As these cultures also showed increases in Aβ peptide, which requires both β- and γ-secretase proteolytic activity, it is therefore possible that calpain inhibition increased BACE activity, without altering BACE expression, in primary neurons.

Importantly, the finding of increased Aβ accumulation in lysates from cultures exposed to exogenous Aβ was accompanied by increased expression of nicastrin in these samples. Nicastrin is essential for secretase activity, and CHO cells overexpressing nicastrin display increased γ-secretase proteolytic activity and Aβ production (Marlow et al., 2003). Therefore, the increase in nicastrin expression in Aβ-treated primary neurons implies that the Aβ detected in these lysates is indeed intracellularly generated as a result of increased APP proteolysis. The increase in nicastrin expression was recovered by calpeptin treatment, supporting previous evidence by Liang et al. (2010) that calpain stimulates Aβ production. However, the amounts of Aβ peptide found in lysates were unaltered by calpeptin, which may suggest the additional presence of exogenously applied Aβ in these samples.

Table 4.1 illustrates the differential effects of Aβ and calpain on the secretases and cleavage fragments involved in amyloidogenic and non-amyloidogenic APP proteolysis.

Protein	*CTRL*	*Aβ*	*Aβ + CPTN*	*CPTN*
ADAM10	-	↓	↓	↓
BACE	-	-	-	-
nicastrin	-	↑	↓	-
FL APP	-	-	-	-
N-APP (17 kDa)	-	-	↑	↑
C-APP (C99)	-	↑	↑	-
Aβ	-	↑	↑	-

Table 4.1 Aβ and calpain differentially affect amyloidogenic and non-amyloidogenic APP processing in primary cortical neurons. Cultures were treated with vehicle (CTRL), Aβ, Aβ together with the calpain inhibitor calpeptin (CPTN), or calpeptin alone. The effect of treatments on APP processing was assessed by examining changes in protein amounts of ADAM10, BACE and nicastrin, indicating activities of α, β, and γ-secretases, respectively. Changes in protein amounts of full-length (FL) APP, N-terminally cleaved (N-APP) and C-terminally cleaved (C-APP) species, including Aβ were also assessed. '-' indicates no effect; ↑ indicates increased protein amounts and ↓ indicates decreased protein amounts.

The alteration of APP processing by calpain shown in this study supports the upstream role of Ca^{2+} signalling in regulating APP homeostasis, and suggests an enhancing effect of calpain on Aβ production. Furthermore, as calpain is shown here to be activated by Aβ (section 4.2.3), this study may support emerging evidence of a bidirectional relationship between Ca^{2+} signalling pathways and Aβ production, where Aβ-induced cytotoxic Ca^{2+} elevations lead to further generation of Aβ in a vicious cycle (Kyratzi and Efthimiopoulos, 2014).

4.3.3 Calpain mediates Aβ-induced tau phosphorylation

It is shown here that calpain plays a role in Aβ-induced tau phosphorylation, as Aβ treatment caused reduced amounts of dephosphorylated tau in primary neurons, an effect reduced by calpain inhibition (section 4.2.6).

Substantial evidence implicates Aβ as an upstream trigger of tau pathology seen in AD (reviewed by Stancu et al., 2014). Aβ phosphorylates tau in degenerating cholinergic neurons in *vitro* and in APP and tau mutant rodents (Zheng et al., 2002; Zempel et al., 2010; Huang and Jiang, 2009; Götz et al., 2001; Lewis et al., 2001). Tau processing is also subject to modification by Ca^{2+}, and this has been strongly implicated in neurodegeneration. In cultured neurons, Ca^{2+} influx stimulated by membrane depolarization leads to transient phosphorylation of tau by GSK3 and cdk5 (Pierrot et al., 2006). Similarly, in SH-SY5Y cells, prolonged Ca^{2+} influx stimulated by treatment of cells with a Ca^{2+} ionophore increased levels of phosphorylated tau, which was reversed upon inhibition of Ca^{2+}-dependent kinases (Shea and Ekinci, 1999).

Since Aβ increases concentrations of neuronal Ca^{2+} it is highly plausible that Aβ may induce pathological changes in tau through aberrant Ca^{2+} signalling. In support of this, marked calpain immunoreactivity in dystrophic neurites associated with NFTs and amyloid plaques are observed in patient AD hippocampal tissue (Adamec et al., 2002). Indeed, Aβ is known to phosphorylate tau through activation of calpain and mitogen-activated protein kinase, both of

which differentially stimulate tau kinases, as well as downregulation of calcineurin-dependent tau dephosphorylation (Zheng et al., 2002; Lloret et al., 2011). Therefore, the attenuation of Aβ-induced tau phosphorylation by calpain inhibition seen here supports the hypothesis that Aβ influences tau phosphorylation through Ca^{2+}-dependent calpain activity and downstream tau kinase activation.

It may have been expected that Aβ would increase tau phosphorylation at PHF1 and CP13 epitopes, which are implicated in AD (Hanger et al., 2009) and are sites phosphorylated by GSK3 in *vivo* (Noble et al., 2005). However, phosphorylation at these sites was unaltered by Aβ in the present study, perhaps indicating that these sites are only involved upon aggregation of tau into PHF in progressed stages of AD, as seen in animal models. Alternatively, activation of calpain by glutamate in hippocampal neurons was shown to decrease tau phosphorylation due to concomitant activation of the Ca^{2+} -dependent phosphatase, calcineurin (Kerokoski et al., 2002), and it is possible that these opposing effects would counteract each other to result in no overall effect of Aβ on tau phosphorylation in the experiments shown here.

In addition to phosphorylation, tau is pathologically truncated by calpains and caspases to generate 17-50kDa species, argued by some to be neurotoxic and trigger NFT formation (de Calignon et al., 2010; Liu et al., 2011; Park and Ferreira, 2005). Aβ was shown here to activate both proteases (section 4.2.3), and it was

expected that generation of caspase- and/or calpain-cleaved tau species might be detected in Aβ treated neurons. However, these tau fragments were not observed in Aβ-treated cultures, despite being described to be induced by Aβ in hippocampal neurons (Park and Ferreira, 2005). This discrepancy may be explained by the use of different Aβ preparations of different concentrations, and a difference in neuronal type and age between previously reported studies and the current work.

4.3.4 Aβ elevates neural Ca^{2+} through activation of NMDARs, calpains, caspases and PARP

In this chapter, primary neurons did not show any response to synthetic Aβ treatment, which likely reflected ongoing problems with primary neuron health in the host institution. As an alternative model, SH-SY5Y cells were used, and when exposed to Aβ these displayed rapid increases in cytosolic Ca^{2+} in the form of prolonged Ca^{2+} transients or sustained elevations. The Ca^{2+} responses to Aβ were abolished by removal of Ca^{2+} from extracellular solution and were reduced in the presence of inhibitors of NMDARs, calpains, caspases and PARP. Together, these findings show that Aβ elevates neural Ca^{2+} through a mechanism that involves influx of extracellular Ca^{2+}, followed by dysregulated activation of signalling cascades that lead to sustained intracellular Ca^{2+} overload. These Ca^{2+}

events occur prior to the changes in APP, tau phosphorylation and neurotoxicity seen in primary cultures.

Multiple studies have shown that Aβ-induced synaptic and neuronal loss is mediated by excitotoxic increases in Ca^{2+} (Harkany et al., 2000a; Boehm, 2013; Liu et al., 2008). Excitotoxicity in primary culture is dependent on overactivation of NMDARs either by glutamate or Aβ, and occurs in three steps (Brustovetsky et al., 2010a). There is an initial Ca^{2+} spike triggered by NMDARs, followed by a transient decrease to levels above resting Ca^{2+}. After some delay, this is followed by a large and sustained Ca^{2+} increase, termed 'delayed calcium deregulation' (DCD), which is required to induce neurotoxicity (Nicholls and Budd, 1998). The varied Ca^{2+} responses to Aβ in the current study did not fit the described pattern (section 4.2.13) and may be specific to SH-SY5Y cells, which may be less vulnerable to Aβ toxicity and may not share an identical Ca^{2+} toolkit with neurons. Nevertheless, the Aβ-induced Ca^{2+} elevations were NMDAR-dependent, and exceeded physiological increases both in amplitude and duration, indicating Ca^{2+} dysregulation. The mechanisms underlying DCD remain unclear due to conflicting evidence. In striatal neurons, excitotoxic cell death depends on calpain activation and cleavage of NCX3 (Bano et al., 2005), which is also observed in post mortem brain from end stages of AD (section 3.2.3) where increases in neuronal Ca^{2+} reach excitotoxic levels (Berridge, 2014). It was therefore postulated that calpain is vital for Aβ-induced Ca^{2+} dysregulation. Indeed, the transient Ca^{2+} elevations elicited here by Aβ were immediately abolished by calpain inhibition (section

4.2.15). This suggests that calpain is activated during the initial NMDAR-dependent Ca^{2+} rise in Aβ excitotoxicity, and contributes to DCD via mechanisms that may include NCX3 inactivation (illustrated in Fig 4.23).

Aβ-induced oxidative stress in primary neurons causes Ca^{2+} accumulation through aberrant PARP signalling (Halliwell, 2006). PARP is a nuclear enzyme that catalyzes production of ADPR during its primary function of DNA repair. ADPR activates plasmalemmal TRPM2 - a heat-sensitive subtype of Ca^{2+}-permeable TRP channels. Earlier reports in this laboratory, and others (Fonfria et al., 2005; Miller, 2004; Xie et al., 2010), have shown that PARP-mediated TRPM2 activation is important in mediating neuronal Ca^{2+} overload in AD. The findings shown here are in support of this hypothesis, as blockade of TRPM2-gated Ca^{2+} entry by inhibition of PARP attenuated the Aβ-induced Ca^{2+} response (section 4.2.15). However, the initial Ca^{2+} rise was not significantly reduced by PARP blockade, suggesting that PARP-TRPM2 signalling occurs secondary to NMDAR and calpain activation. Therefore, it is possible that TRPM2-mediated entry could play a role in DCD, in response to intracellular mechanisms stimulated by the initial Ca^{2+} influx (Fig 4.23). To support this idea, Aβ-induced Ca^{2+} elevations were completely abolished by inhibiting caspases, which are activated downstream of calpains (Nakagawa and Yuan, 2000) and are known to cleave PARP in NMDAR-induced excitotoxicity and apoptosis (Chaitanya et al., 2010). The role of the PARP-TRPM2 pathway in Aβ neurotoxicity is investigated further in the next chapter.

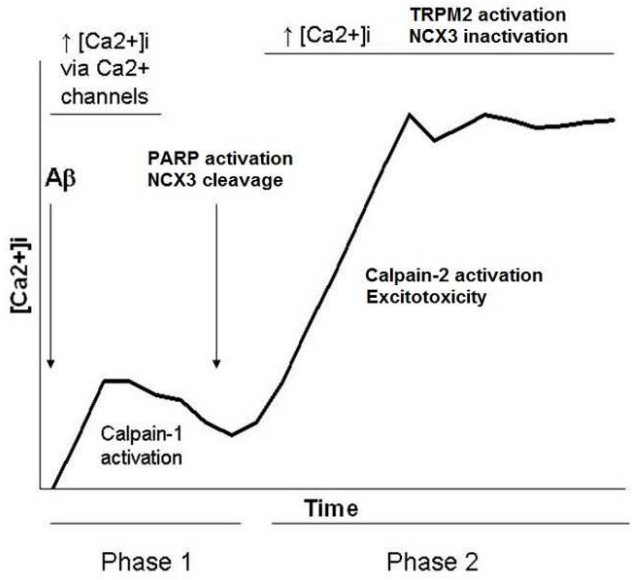

Fig. 4.23 A hypothetical model of the mechanisms underlying Aβ-induced excitotoxic elevations in neural Ca^{2+} based on the findings described in this chapter. Aβ mediates excitotoxicity in neurons through initial activation of N-methyl-D-aspartate receptors (NMDAR) and other native Ca^{2+} channels (Harkany et al., 2000b). The resulting Ca^{2+} elevations are shown to occur in two phases (Brustovetsky et al., 2010a). Phase 1 is characterized by small increases in Ca^{2+}, which stimulate the Ca^{2+}-sensitive protease calpain-1. This is followed by a fall in to levels elevated from basal, during which calpain and caspase signalling may lead to cleavage of the sodium calcium exchanger 3 (NCX3) and activation of poly(ADP)ribose polymerase (PARP), respectively. After a delay, these events may contribute to the sustained and irreversible Ca^{2+} elevations seen during excitotoxicity prior to neuronal demise.

4.3.5 Physiological Aβ oligomers do not recapitulate disease processes in *vitro*

As described above, the source of Aβ used in cell culture studies is a subject of great debate in the field. Therefore, in addition to synthetic Aβ, conditioned media from 7PA2 cells was used as a well-characterized natural source of human Aβ

oligomers. Exposure of primary neurons to physiological (2-500nM) concentrations of 7PA2 Aβ did not differentially alter calpain activity, tau kinase activities or tau phosphorylation in primary neurons or SHSY5Y cells. Moreover, these Aβ oligomers had no effect on short-term neural Ca^{2+} dynamics.

The worsening of cognitive symptoms in AD have been linked with a gradual and progressive rise in intracellular Ca^{2+} over the time-course of the disease (Berridge, 2014). Hypothesized to be stimulated by early Aβ deposition, these Ca^{2+} elevations start during the early pre-clinical stages of AD and only reach concentrations that impair synaptic function and plasticity years later, when the first cognitive and memory symptoms appear (section 1.2). Furthermore, excitotoxic intracellular Ca^{2+} levels above 300 nM are only reached in terminal stages of AD, at which point this contributes to global neuronal atrophy (Berridge, 2014).

Aβ oligomers found in 7PA2 cell medium are highly similar in molecular mass and amounts to SDS-stable oligomers derived from human AD cortex. In adult rats, 7PA2 Aβ blocked LTP 3 hours after stimulation (Walsh et al., 2002a), and disrupted cognitive function 3 days after microinjection (Cleary et al., 2005). In this study, 7PA2 Aβ was applied to primary culture and neural cells for 10 min to 48 h. Therefore, use of cell models and relatively short incubation periods may have prevented 7PA2 Aβ from exerting the pathological effects seen in *vivo* in human AD brain. This suggests that cell-derived natural Aβ oligomers may not be

suitable for modelling mechanisms of Aβ neurotoxicity in *vitro*. However, treatment of hippocampal neurons with 7PA2 for 5 days previously triggered spine and synapse loss (Shankar et al., 2007). Thus, longer treatments with 7PA2 may have to be carried out before conclusions can be made about its ability to alter AD-relevant proteins in *vitro*.

4.3.6 Limitations of this work

There are several limitations to the experiments performed in this chapter. As the chapter focuses on the role of calpain in Aβ mechanisms, it was first important to establish the effect of Aβ on calpain activity by means of immunoblotting with an antibody that labels the 76-78 kDa active calpain fragment. Multiple anti-calpain-1 antibodies were tested, none of which detected this fragment. However, these antibodies consistently revealed a 28 kDa band (section 4.2.2), which represents the regulatory subunit of calpains (Cong et al., 1993). This 28 kDa subunit is required for autolysis and, hence, proteolytic activation of the 80 kDa catalytic subunit of calpain. Therefore, the increase in the presence of the 28 kDa calpain subunit observed here after Aβ treatment likely signify increased calpain-1 proteolytic activity, although this cannot be stated with certainty. Increased calpain activity was confirmed by the increased generation of calpain-cleaved fragments of α-spectrin. Immunoblotting for detection of cleaved α-spectrin was previously used in multiple studies to indirectly assess calpain and caspase

activities in the absence of calpain blots (Warren et al., 2007; Axelsson et al., 2006; Trinchese, Liu, et al., 2008). However, a direct and more accurate measurement of calpain activity would require detection of the 76-78 kDa active calpain subunit or a calpain activity assay.

In the current study, Aβ application to neurons did not alter Ca^{2+} homeostasis over 10 min. The effects of soluble Aβ oligomers on neuronal Ca^{2+} dynamics have been extensively researched, yet are inconsistent. There are numerous reports of Aβ inducing Ca^{2+} overload in primary neurons prior to their demise (Bezprozvanny and Mattson, 2008; Ramsden et al., 2002; Price et al., 1998). However, Aβ has also shown to decrease intraneuronal Ca^{2+}, selectively alter astrocytic Ca^{2+} or have no effect at all (Abramov et al., 2004; Chin et al., 2006). Since the effects of Aβ on calpain activity, APP processing, tau phosphorylation and synaptic health were studied here in primary neurons, it was important to show that Aβ aberrantly alters these processes through dysregulated Ca^{2+} signalling in the same cell model. Earlier findings in this group and others suggest that excitotoxic Ca^{2+} elevations in primary neurons induced by glutamate and Aβ are seen after 20 min to 1 h (Bano et al. 2005; Brustovetsky et al. 2010; Atherton et al., unpublished). Furthermore, Aβ induced neurotoxic calpain activity in primary neurons after 48 h, but had no effect on calpain activity or cell death after shorter treatments. Therefore, longer imaging experiments and Aβ incubations may have been required to see aberrant Ca^{2+} changes. However, exposure of fluo-4-labelled neurons to fluorescent light for longer than 10 min caused photobleaching, during

which Ca^{2+} spikes evoked by KCl depolarization were not detected by the software. This limitation is likely specific to the dye used, and may have been avoided by using a ratiometric dye, such as fura-2, which minimizes the effects of photobleaching.

Aβ transiently elevated cytosolic free Ca^{2+} in SH-SY5Y cells to levels that were higher than those detected under basal conditions or induced by KCl (section 4.2.13). The discrepancy between these findings and earlier results in primary neurons may be accounted for by phenotypic differences between the two cell types. It is suggested that enrichment of tau in primary neurons regulates dendritic Ca^{2+}, whereas SH-SY5Y cells contain smaller amounts of tau and may, therefore, respond more readily to Aβ (Eva-Maria Mandelkow, personal communication). Excitotoxic increases in Ca^{2+} that are associated with NMDAR overactivation are characterized by prolonged, irreversible elevations in Ca^{2+}. However, the Ca^{2+} elevations in SH-SY5Y cells did not follow this pattern, instead showing a series of diminishing transients not previously characterized in this cell type, that suggest processes which may follow from or protect against acute Ca^{2+} dysregulation. Further studies would be required to uncover these mechanisms and could, for example, investigate receptor internalization and recycling in excitotoxic conditions (Waxman et al., 2007). Furthermore, as calpain proteolytic activity has shown to cause cytoskeletal degradation in response to Aβ here (section 4.2.3), it may have been worth determining whether the cytoskeletal

structures degraded by calpain included membrane portions containing Ca^{2+}-permeable receptors or channels.

Finally, the findings reported in section 4.2.15 and earlier work performed in this group suggest that TRPM2 Ca^{2+} gating is important in shaping the dysregulated Ca^{2+} response to Aβ. This could be further investigated either by overexpression of functional TRMP2 channels in primary neurons or transfecting them with a C-terminally truncated isoform of TRPM2 which inhibits Ca^{2+} influx and excitotoxicity (Zhang et al., 2003). Equally, genetically manipulating NCX3 expression in neurons would confirm whether calpain-mediated cleavage and loss of NCX3 function (described in Chapter 3) mediates the calpain-dependent Ca^{2+} accumulation induced by Aβ in section 4.2.15.

4.3.7 Conclusions

The findings presented in this chapter suggest that Aβ neurotoxicity in primary neurons involves calpain-mediated degradation of the cell cytoskeleton, synaptic degeneration, increased activation of tau kinases and tau phosphorylation, apoptotic caspase signalling and Aβ accumulation. In SH-SY5Y cells, Aβ may induce Ca^{2+} elevations via activation of TRPM2 channels and cleavage of NCX3.

CHAPTER 5

PARP-TRPM2 signalling influences Aβ neurotoxicity

5.1 Introduction

The limited efficacy of NMDAR antagonists, such as memantine, in preventing excitotoxic neurodegeneration in AD patients (Lipton, 2004) and clinical stroke models (Ikonomidou and Turski, 2002) suggests the involvement of additional Ca^{2+} influx pathways. Oxidative stress occurs early in AD, alongside alterations in intraneuronal Ca^{2+}, and is acknowledged to contribute to neuronal death during AD progression (Halliwell, 2006). Studies show that soluble Aβ oligomers cause neuronal insults by directly binding intraneuronal metal ions and lipoproteins, leading to generation of ROS, energy depletion, mitochondrial dysfunction and apoptosis (Su et al., 2008). This process results in increased expression of BACE1 and PS1, which sequentially metabolise APP to yield Aβ, thereby promoting further Aβ production and neurotoxicity (Mouton-Liger et al., 2012; Oda et al., 2010). Of interest for this research, experiments in primary neurons have shown that oxidative stress-induced DNA damage triggers activation of nuclear PARP-1, which belongs to a family of 17 enzymes that play multiple roles in cytoskeletal regulation, cell division and cell viability (Luo and Lee Kraus, 2012). PARP-1 is the major enzyme in this family that determines cell fate, depending on stress stimulus, by catalyzing repair of single and double stranded DNA breaks or

signalling apoptosis. PARP-1 uses nicotinamide adenine dinucleotide (NAD+) as a substrate to synthesize PAR, which are added to nuclear and cytoplasmic proteins during PARP signalling (Schreiber et al., 2006).

Substantial evidence suggests that PARP activity is aberrantly increased in AD, and that it signals apoptosis in response to Aβ-induced oxidative stress (Love et al., 1999; Abeti et al., 2011; Strosznajder et al., 2000; Wang et al., 2010). For example, exposure of aged rat hippocampus to Aβ oligomers upregulates PARP activity by 80 %, causing depletion of NAD+, mitochondrial respiratory stress and release of apoptosis inducing factor (AIF) from mitochondrial pores inserted by PAR (Strosznajder et al., 2000). PAR has also been shown to be directly neurotoxic, and to contribute to NMDAR-dependent excitotoxicity in cortical neurons (Andrabi et al., 2006). In addition, aging of APP and PS1 mutant mice is associated with accumulation of PAR (Abeti et al., 2011), and both PAR and PARP immunoreactivity is increased in post mortem AD cortex (Love et al., 1999). In the experiments described here in section 4.2.15, pharmacological inhibition of PARP was found to attenuate neural Ca^{2+} elevations that are elicited by oligomeric Aβ. This data further suggests that oxidative stress induced by Aβ may trigger downstream Ca^{2+} dyshomeostasis through PARP upregulation.

Recently, a new non-selective Ca^{2+}-permeable channel, TRPM2, was found to mediate neuronal death in response to oxidative stress (McNulty and Fonfria, 2005a; Perraud et al., 2003). TRPM2 belongs to family of heat-sensitive TRP

channels that are widely expressed in the CNS, in both neurons and glia. The primary physiological activator of TRPM2 is ADPR, which is proteolytically cleaved from PAR by PARG, leading to PAR accumulation in the cytoplasm (Blenn et al., 2011). ADPR binds to the Nudix hydrolase moiety of TRPM2, causing opening of the channel pore and entry of Ca^{2+} along an electrochemical gradient (Naziroğlu, 2011). TRPM2 is also gated by intracellular Ca^{2+}, which accumulates following Aβ activation of NMDARs (section 4.2.15) and ADPR-stimulated Ca^{2+} release from the ER (Naziroğlu, 2011). Therefore, PARP-induced activation of TRPM2 channels may play a role in Aβ-induced Ca^{2+} dysregulation and neurotoxicity in AD. Indeed, TRPM2 is reported to contribute to Aβ-induced oxidative stress induced in striatal neurons (Fonfria et al. 2005), and suppressing TRPM2 function prevented Aβ-induced increases in neuronal Ca^{2+} and rescued cell death (Fonfria et al., 2005). TRPM2 activation has also been shown to activate caspases and induce translocation of mitochondrial AIF to the nucleus in response to PARP-1, thereby triggering apoptosis (Blenn et al., 2011). Despite efforts to establish the importance of the PARP-TRPM2 pathway in AD, there is as yet no evidence of TRPM2 alterations in AD brain and further studies are required to determine the relationship between PARP-TRPM2 signalling and other degenerative mechanisms in AD.

The aims of the current chapter were to determine if 1) There are alterations in PARP or TRPM2 protein expression during the progression of AD, 2) Aβ-induced neurotoxicity is mediated by PARP hyperactivity, 3) TRPM2 expression is altered

in response to PARP upregulation or Aβ treatment and 4) PARP mediates Aβ-induced changes in tau phosphorylation.

5.2 Results

Post mortem tissue from control and AD brain was first used to examine changes in PARP and TRPM2 expression at different stages of AD. To investigate the contribution of PARP-TRPM2 signalling to Aβ neurotoxicity, the synthetic PARP inhibitor SB750139 was used to block PARP activity in primary cortical cultures treated with soluble oligomers of human Aβ1-42. The effect of PARP inhibition on mechanisms shown to be induced by Aβ, including calpain activation, PAR synthesis and tau phosphorylation, were studied using immunocytochemistry and immunoblotting with antibodies against proteins of interest. The effect of PARP inhibition on Aβ-induced neurotoxicity was determined using a cell death assay.

5.2.1 PARP cleavage is increased in moderate and late stages of AD

PARP-1 is known to orchestrate different types of cell death, including apoptosis, necrosis and parthanatos, during which it is differentially cleaved by suicide proteases such as caspases and calpains (Chaitanya et al., 2010). Cleavage of

PARP-1 by these proteases generates characteristic fragments, which serve as signatures of different modes of cell death, and can also provide insight into signalling cascades activated during neurodegeneration (Chaitanya et al., 2010; O'Brien et al., 2001). Animal and cell models of AD feature activation of both apoptotic and necrotic pathways prior to neuronal loss (Behl, 2000), and PARP-1 activity has previously been shown by immunohistochemistry to be increased in AD brain (Love et al., 1999). It was therefore of interest to characterize PARP-1 amounts and cleavage at different stages of AD. Importantly, this would also provide an insight into the cell death mechanisms involved in the development of AD.

Post mortem brain homogenates from control brains and those from different AD Braak stages (II-VI) were immunoblotted with an antibody against PARP-1, which detects intact PARP-1 at 116 kDa and an 89 kDa caspase- and cathepsin-cleaved fragment, which is generated during apoptosis (Fig. 5.1A). These PARP species were detected here, along with additional bands at 75 kDa, characteristic of PARP-1 cleavage by cathepsins during necrosis, and 100 kDa, which has not been characterized in literature and may indicate non-specific binding of the antibody. Blots were also probed with an antibody against NSE, which was used to control for protein amounts in each sample. Since the levels of the75 kDa PARP-1 fragment were not sufficiently intense to allow quantification, this fragment was excluded from quantitative analysis. Full-length PAPR-1 (116 kDa) and the apoptosis-related PARP-1 fragment (89 kDa) were separately quantified as a

proportion of NSE. This quantification revealed no significant difference in the amounts of full-length PARP-1 in any AD stage compared to control (Fig. 5.1B). The 89 kDa PARP-1 fragment was not detected in control or early (Braak II-III) AD brain (Fig. 5.1A, C). In contrast, amounts of the 89 kDa PARP-1 fragment were significantly increased in moderate stage (Braak IV; $p < 0.01$), and further increased in end stage disease AD brain homogenates (Braak V-VI; $p < 0.001$) when compared to control samples (Fig. 5.1C).

These findings of increased cleaved PARP in moderate to late stages of AD but not in early disease, suggest that caspase-dependent apoptotic cell death is induced in later AD stages. These findings may be related to the accumulation of Aβ1-42 that was also found to accumulate in moderate to late stages of AD (section 3.2.6). The 89 kDa C-terminal catalytic subunit of PARP-1 generated by caspase cleavage, shown here to be increased during AD progression, has previously been found to inhibit PARP-1 activity and PAR synthesis in multiple studies (D'Amours et al., 2001; Boulares et al., 1999; Chaitanya et al., 2010; Cohen, 1997). Thus, these findings are inconsistent with evidence of increased PARP activity in AD brain (Love et al., 1999) and in rat striatal neurons undergoing apoptosis in response to Aβ (Fonfria et al., 2005). Thus, the role of PARP-1 in AD appears to be complex and it is clear that its relationship to neurodegeneration is not yet fully understood.

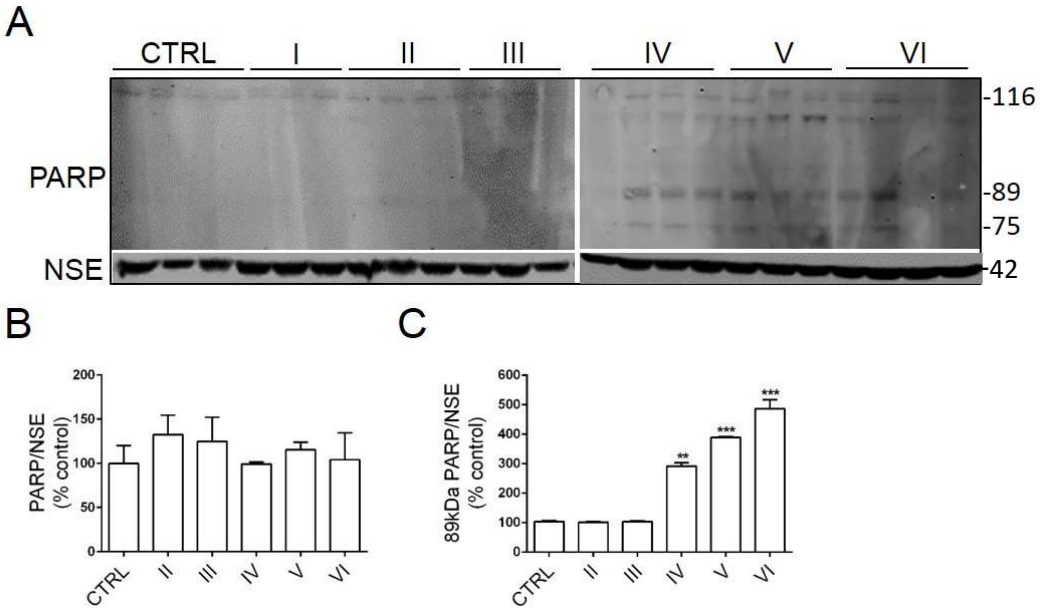

Fig. 5.1 PARP-1 is progressively cleaved throughout AD development by caspases and cathepsins. (A) Representative immunoblots of post mortem homogenates from control and Braak II-VI AD brains. Blots were probed with an antibody against poly(ADP)ribose polymerase (PARP-1), detecting holoprotein at 116 kDa, caspase- and cathepsin- cleaved PARP-1 at 89 kDa, and cathepsin- and calpain-cleaved PARP-1 at 75 kDa. Blots were also probed with an antibody against NSE to control for protein loading. Bar graph shows amounts of (B) PARP-1 holoprotein and (C) caspase- and cathepsin- cleaved (89 kDa) PARP-1, with all bands normalised to NSE. CTRL: control (n = 7), Braak II: early AD (n = 4), Braak III: early AD (n = 3), Braak IV: moderate AD (n = 4), Braak V: advanced AD (n = 3), Braak VI: severe AD (n = 4). Data is mean ± SEM. **p < 0.01, ***p < 0.001

5.2.2 TRPM2 expression is unaltered in AD brain

TRPM2 is a non-selective Ca^{2+}-permeable channel that is activated in response to PARP-1 and that confers susceptibility to cell death in models of AD (McNulty and Fonfria, 2005a; Fonfria et al., 2005; Miller, 2004). TRPM2 channels are widely

expressed in the CNS, although their expression pattern and function are poorly understood. It is also, so far, unknown whether TRPM2 expression is altered in response to or triggers neurodegenerative processes in AD. Studies in human bone marrow, monocytes and other immune cells have identified a naturally occurring short TRPM2 splice variant (TRPM2-S) which lacks the entire C terminus of the channel, including the channel pore (Zhang et al., 2003, 2006). This TRPM2-S variant is non-functional and exerts a dominant-negative effect on Ca^{2+} gating by functional long TRPM2 variants (TRPM2-L) in *vitro*. The relative expression levels of the two TRPM2 variants, as well as the function of TRPM2-S, in neurodegenerative disease have yet to be investigated. Therefore, protein expression of both TRPM2-L and TRPM2-S was compared here in control and AD post mortem brain, including early Braak stages of AD.

Post mortem lysates from control and end-stage (Braak stage VI) AD frontal cortex were immunoblotted with an antibody against functional TRPM2 (TRPM2-L), which label the N-terminus of TRPM2 at 171 kDa, and also detects the short TRPM2 isoform (TRPM2-S) at 95 kDa (Fig. 5.2A). The antibody specific to TRPM2-L also revealed multiple bands from 35 to 40 kDa in size, which may represent TRPM2 cleaved fragments. Blots were also probed with an antibody against NSE, for standardisation of protein amounts in each sample. Normalisation of the density of bands of each TRPM2 variant to NSE in the same sample and quantification of these results revealed no differences in protein amounts of TRPM2-L and TRPM2-S between control and end-stage (Braak stage VI) AD brain

(Fig. 5.2B). However, there was a visible increase in bands measuring 35 to 40 kDa in AD samples when compared to control (Fig. 5.2A). TRPM2 fragments of this size have not been described in literature and were not shown in previous studies using these and other TRPM2 antibodies. Since these bands were consistently absent in control tissue, it is likely that they represent cleaved species of TRPM2 rather than non-specific binding of the antibody. There are no reports of TRPM2 cleavage; however, a related TRP channel, TRPML1, is known to undergo cathepsin-mediated cleavage in lysosomes under physiological conditions (Kiselyov et al., 2005). As TRPM2 is also localized to lysosomes (Sumoza-Toledo and Penner, 2011), it may also be subject to proteolysis by lysosomal enzymes. Moreover, elevated calpain activity in AD brain (shown here in Chapter 3) is thought to lead to lysosomal membrane rupture and dysfunction, which may involve cleavage of TRP channels, including TRPM2 (McBrayer and Nixon, 2013).However, although potentially interesting, it is not possible to determine if there is any functional relevance of these cleaved TRPM2 species and these bands were excluded from analysis. Since there were no apparent changes in the amounts of TRMP2-L or TRPM2-S in late stage AD brain, the amounts of these proteins were not assessed further in tissue from earlier Braak stage brain.

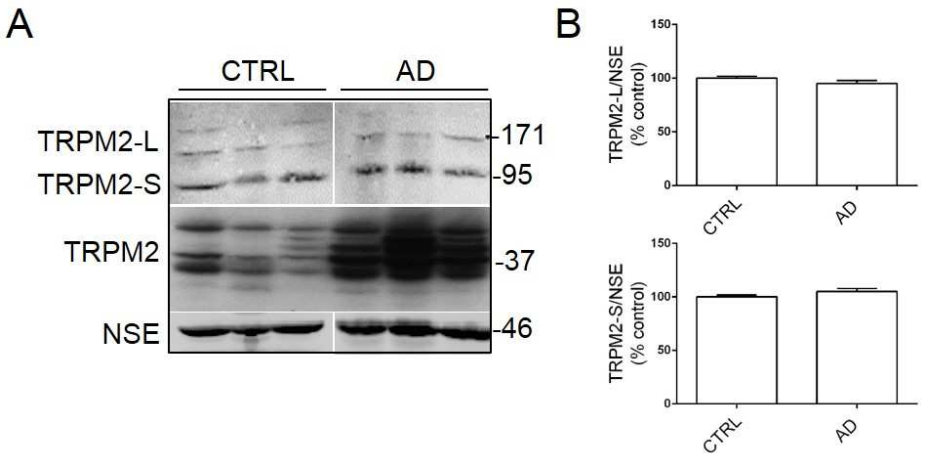

Fig. 5.2 TRPM2 expression is not altered in end-stage AD brain compared to control. (A) Representative immunoblots of post mortem homogenates from control and end-stage (Braak stage VI) AD brain. Blots were probed with an antibody against the N-terminal portion of TRPM2, which detects both functional TRPM2-L holoprotein at 171 kDa and non-functional TRPM2-S holoprotein at 95 kDa. The antibody also detected bands at 37-50kDa which may represent cleaved species of TRPM2. Blots were also probed with an antibody against NSE to control for protein loading. Bar graphs shows amounts of (B) TRPM2-L and TRPM2-S, with all bands normalised to NSE CTRL: control (n = 7), Braak II: early AD (n = 4), Braak III: early AD (n = 3), Braak IV: moderate AD (n = 4), Braak V: advanced AD (n = 3), Braak VI: severe AD (n = 7).

5.2.3 Increased PARP-1 activity in primary neurons undergoing oxidative stress does not alter TRPM2 expression

To gain some insight into potential roles of PARP and TRPM2 in AD, additional experiments were performed in cell cultures. Oxidative stress-induced DNA damage has been shown to upregulate activity of nuclear PARP-1 prior to cell death in a variety of disease models, including AD (Luo and Lee Kraus, 2012; Boesten et al., 2013; Love et al., 1999). Therefore, it was first important to confirm that PARP activity is increased in response to oxidative stress in rat primary

cortical neurons. It was also of interest to investigate whether expression of TRPM2, an effector of PARP-1, is altered in response to oxidative stress and elevated PARP-1 activity.

Rat primary cortical cultures were briefly treated with H_2O_2, which is used to induce oxidative stress reminiscent of that which occurs in AD (Dávila and Torres-Aleman, 2008) and cause deterioration of neuron health in primary cultures (Whittemore et al., 1995; Haraguchi et al., 2012). To confirm this, a cell death assay revealed significantly increased cell death in cultures exposed to 1mM H_2O_2 for 1 h compared to vehicle-treated cells ($p < 0.05$; Fig. 5.4A). It was important to observe oxidative stress under neurotoxic conditions, as the role of PARP in Aβ neurotoxicity, which involves induction of oxidative stress, will be investigated in this chapter. Cultures were pre-treated for 3 h with the PARP inhibitor SB750139 (SB), which was shown to abolish TRPM2-mediated Ca^{2+} influx in section 4.2.15. Following treatment, cells were washed, fixed and immunostained with antibodies specific for PAR and the N-terminal region of TRPM2, which recognizes both TRPM2-L and TRPM2-S variants (Fig.5.2A). Cells were also stained with the nuclear marker, Hoescht-33342. The staining protocol included a permeabilization step which ensured access of the antibody to its intracellular protein antigen.

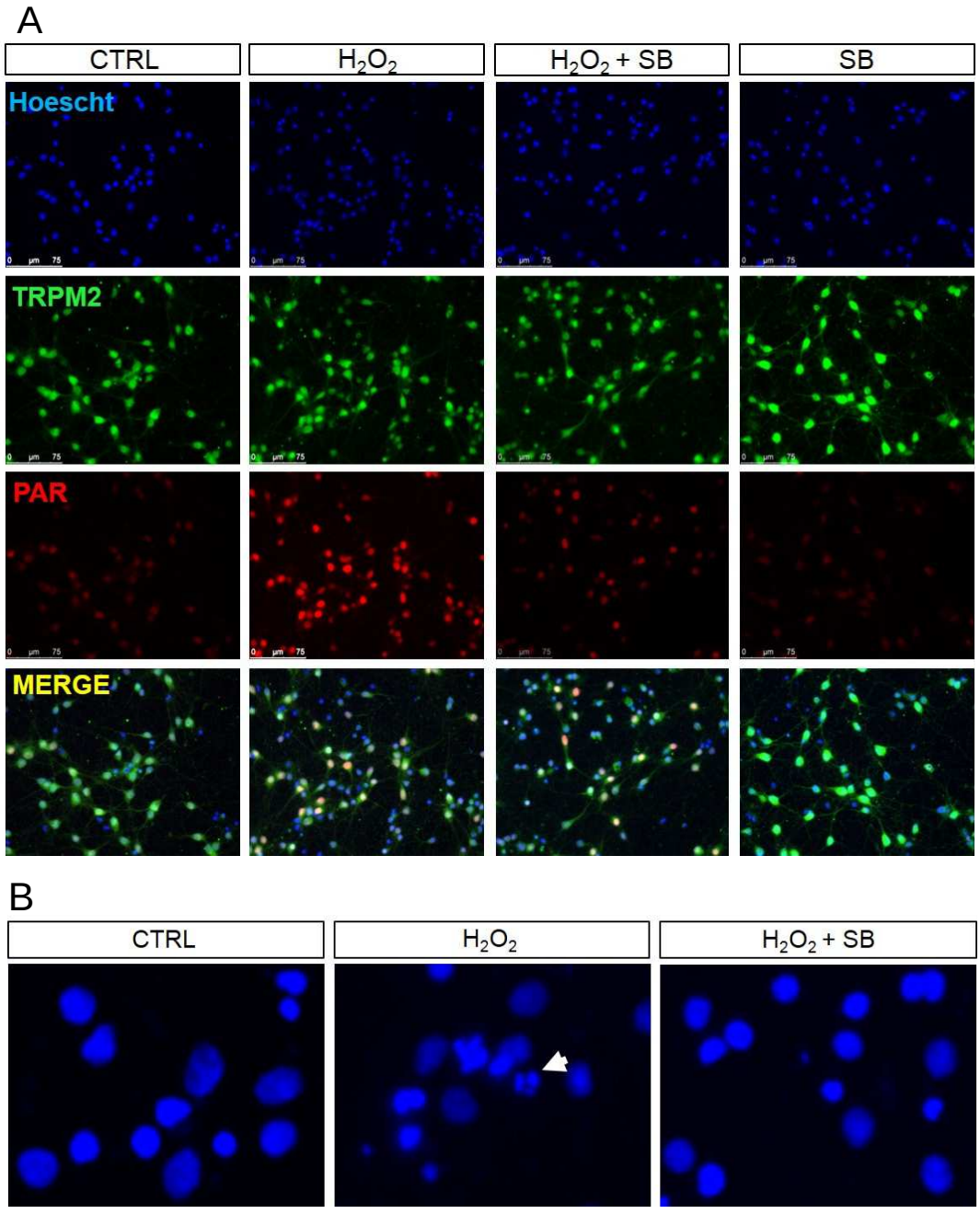

Fig. 5.3 Exposure of primary cortical cultures to H_2O_2 causes oxidative DNA damage and increased nuclear PAR immunoreactivity, which are reversed by PARP inhibition. (A) Neurons treated with vehicle (CTRL), 1 mM H_2O_2 for 1 h, which is used to stimulate oxidative stress in culture, and/or 1 µM of the PARP inhibitor SB750139 (SB) for 3 h were immunostained with antibodies against poly(ADP)ribose (PAR), the N-terminal portion of TRPM2 channels, and the nuclear stain Hoescht-33342. (B) X63 magnification of Hoescht-positive nuclei was used to visualize nuclear fragmentation (white arrow). Scale bars are 75µm. n=8

Neurons exposed to H_2O_2 exhibited nuclear condensation and fragmentation (Fig. 5.3B), indicative of reduced cell viability and cell death and consistent with previous observations in neurons during oxidative stress (Higgins et al., 2009). In addition, H_2O_2-treated neurons displayed significantly increased PAR immunoreactivity compared to control ($p < 0.001$), as measured by numbers of PAR-positive cells, indicating increased PARP-1 activation in response to oxidative stress. Pre-treatment of neurons with SB markedly reduced PAR accumulation, as expected ($p < 0.001$; Fig. 5.4B), and oxidative DNA damage-associated nuclear fragmentation induced by H_2O_2 (Fig. 3.B). Interestingly, when applied on its own, SB visibly reduced PAR immunoreactivity compared to control (Fig. 5.4B), implying that PARP inhibition may be neuroprotective, even under basal conditions. Quantification of TRPM2 immunoreactivity using the 'Measure RGB' plugin in ImageJ revealed no alterations in TPPM2 expression with either H_2O_2 or SB treatment (Fig. 5.4C).

These findings show that nuclear PARP-1 activity is upregulated during oxidative stress induced by H_2O_2, as evidenced by increased nuclear accumulation of PARP-synthesized PAR. This findings is in agreement with previous reports (Luo and Lee Kraus, 2012; Szenczi et al., 2005). Reduction of nuclear PAR immunoreactivity by pre-treatment of cultures with SB indicates suppression of PARP activity by this compound, in line with previous evidence (Fonfria et al., 2005). TRPM2 immunoreactivity in rat primary cortical neurons was found to be localized to neuronal somata and processes, as previously shown (Lee et al., 2013; Bai and

Lipski, 2010), and was unaltered during oxidative stress or following PARP inhibition.

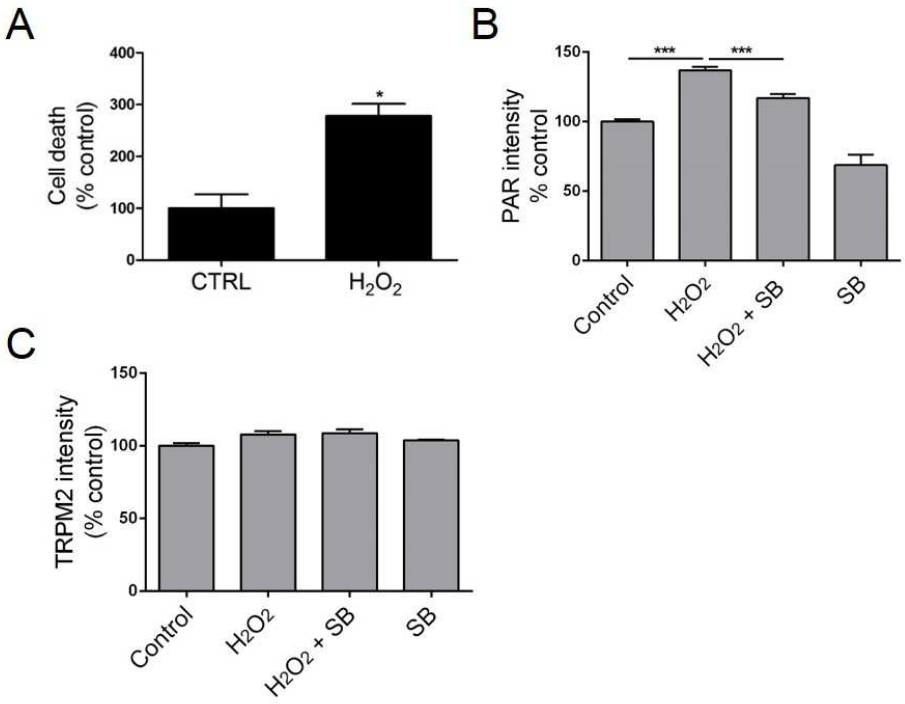

Fig. 5.4 Exposure of primary cortical cultures to a neurotoxic dose of H_2O_2 causes increased nuclear PAR immunoreactivity, which is reversed by PARP inhibition. Neurons treated with vehicle (CTRL), 1mM H_2O_2 for 1 h, which is used to stimulate oxidative stress in culture, and/or 1uM of the PARP inhibitor SB750139 (SB) for 3 h, were immunostained with antibodies against poly(ADP)ribose (PAR), the N-terminal portion of TRPM2 channels, and the nuclear stain Hoescht-33342. Bar graphs show (A) % cell death in cultures treated with vehicle or H_2O_2, and immunoreactivity of (B) PAR and (C) TRPM2 in cultures treated with control H_2O_2 and/or SB. Data is mean ± SEM. ***$p < 0.001$. n=8

5.2.4 Increased PARP activity mediates Aβ-induced neurotoxicity in primary cultures without altering TRPM2 expression

It was important to next determine the effects of Aβ on PARP-1 activity and TRPM2 channel amounts and localisation. The data shown in this thesis has demonstrated that the PARP inhibitor SB suppresses Aβ-induced intraneuronal Ca^{2+} elevations (section 4.2.15), supporting the hypothesis that PARP-1 activates Ca^{2+}-permeable TRPM2 channels through production of its primary physiological activator, ADPR (Blenn et al., 2011; Fonfria et al., 2005). In addition, TRPM2 channels have been implicated in the pathways leading to cell death in neurons undergoing oxidative stress (Kaneko et al., 2006) and following exposure to Aβ (Fonfria et al., 2005), which implies a vital role for PARP/TRPM2 channel signalling in AD. Therefore, PARP activity and its contribution to Aβ neurotoxicity in the cell model used here was investigated.

Rat primary cortical cultures treated with Aβ +/- SB as described above were washed, fixed and immunostained with antibodies specific for PAR and the N-terminal region of TRPM2, which recognizes both TRPM2-L and TRPM2-S variants (Fig. 5.5). Cells were also stained with the nuclear marker, Hoescht-33342. The staining protocol included a permeabilization step which allowed access of antibodies to their intracellular protein antigen. Neurons treated with 10 μM Aβ for 3 h showed higher numbers of fragmented nuclei, indicating

deterioration of culture health consistent with previous reports of Aβ-induced neurotoxicity in primary neuron cultures (Garwood et al., 2011, and observed in section 5.2.3). In addition, measurement of PAR-positive cells revealed that Aβ treatment significantly increased nuclear PAR immunoreactivity when compared to control cultures (Fig. 5,6A; $p < 0.01$). Aβ-induced elevations in PAR immunoreactivity were significantly reduced upon pre-treatment of cultures with 1 μM SB for 3 h ($p < 0.05$; Fig. 5.6A). These findings indicate that Aβ upregulates PARP activity, as indicated by the accumulation of nuclear PAR, and that these effects are effectively reduced upon PARP-1 inhibition with the PARP inhibitor SB.

In contrast, TRPM2 immunoreactivity was not altered by treatment with Aβ or SB when compared to control (Fig. 5.6B). Moreover, colocalization analysis using the Intensity Correlation Quotient plugin in ImageJ revealed no significant spatial correlation of PAR and TRPM2 signals (Fig. 5.6C), indicating that Aβ-induced upregulation of PAR signal does not alter TRPM2 expression in the same neurons. Cultures treated with SB showed decreased co-localization of PAR with TRPM2; however, this is due to a decrease of PAR signal intensity upon SB treatment of neurons, conditions where TRPM2 expression remained unaltered. SB appeared to protect from Aβ-induced neurotoxicity and to exert a neuroprotective effect on neuronal health under basal conditions when compared to control cultures (Fig. 5.6A), consistent with the findings in section 4.2.3. Therefore, it was next of interest to determine if Aβ neurotoxicity could be rescued by PARP inhibition. A cell death assay, of cultures treated with Aβ +/- SB, using a fluorescent stain that

incorporates into dead cells, revealed an almost 3-fold increase in neuronal death induced by Aβ ($p < 0.05$) was recovered by SB treatment to control levels ($p < 0.05$; Fig. 5.6D). Treatment of cultures with SB alone reduced levels of death below those of control neurons; however, this was not statistically significant (Fig. 5.6D).

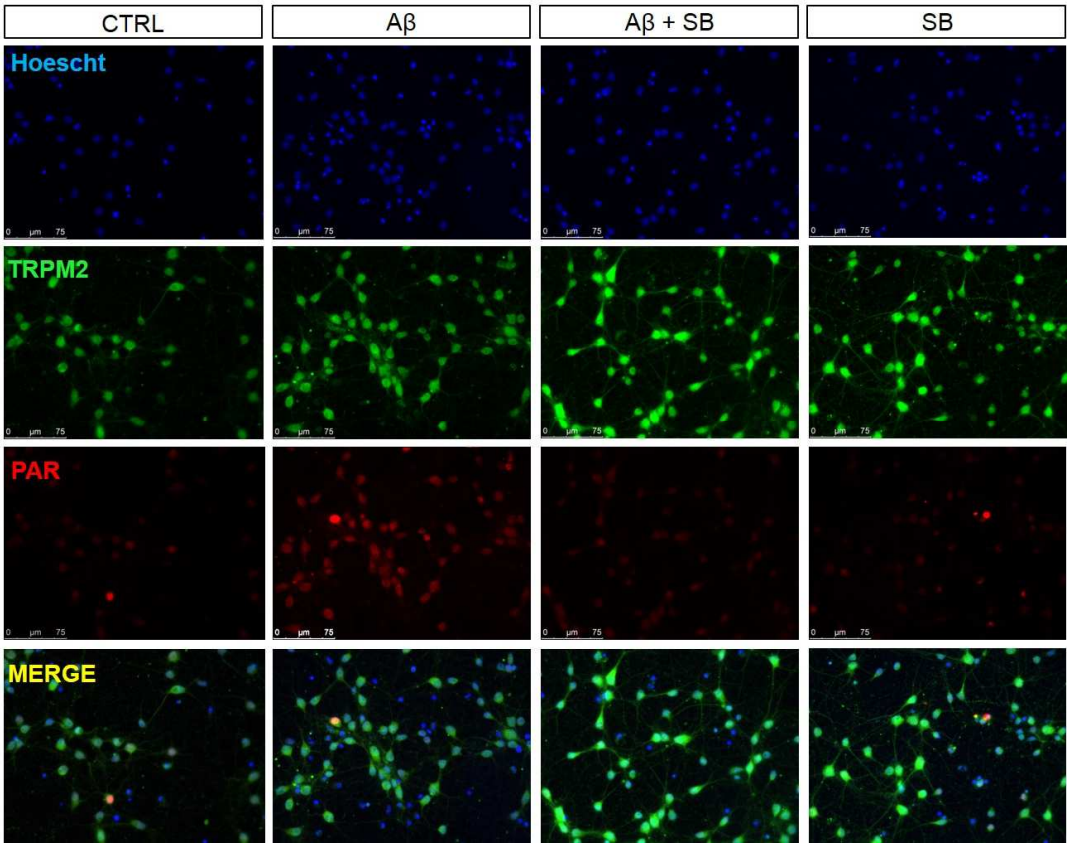

Fig. 5.5 Exposure of primary cortical cultures to Aβ causes neuronal damage and increases nuclear PAR immunoreactivity, which is reversed by PARP inhibition. Neurons treated with vehicle (CTRL), 10 μM Aβ for 48 h, and/or 1 μM of the PARP inhibitor SB750139 (SB) for 3 h, were immunostained with antibodies against poly(ADP)ribose (PAR), the N-terminal portion of TRPM2 channels, and the nuclear stain Hoescht-33342. Scale bars are 75μm. n=8

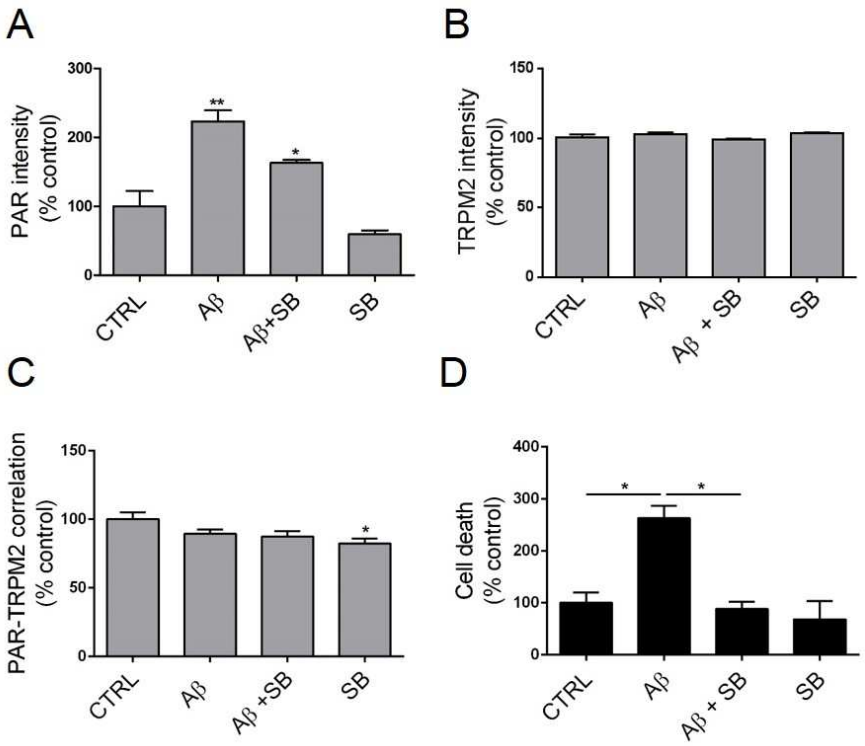

Fig. 5.6 Exposure of primary cortical cultures to Aβ causes increased nuclear PAR immunoreactivity and neurotoxicity, which are reversed by PARP inhibition. Neurons treated with vehicle (CTRL), 10 μM Aβ for 48 h and/or 1 μM of the PARP inhibitor SB750139 (SB) for 3 h, were immunostained with antibodies against poly(ADP)ribose (PAR), the N-terminal portion of TRPM2 channels, and the nuclear stain Hoescht-33342. Bar graphs show (A) Intensity of PAR immunoreactivity, (B) Intensity of TRPM2 immunoreactivity, (C) spatial correlation of PAR and TRPM2 and (D) Cell death, as assessed by live/dead assay, in cultures treated with Aβ and/or SB. Data are expressed as a proportion of death in control cultures. Data is mean ± SEM. *$p < 0.05$, **$p < 0.005$. n=8

The data presented above showing that increased PARP activity is found in cultures exposed to Aβ confirm that Aβ is a pro-oxidant and causes DNA damage. To support this, previous studies have shown that the induction of oxidative stress requires Aβ peptide oligomerization and a high (μM) concentration

(Iversen et al., 1995; Kontush, 2001), in line with the Aβ preparation and treatment protocol used here and previously reported by this group (Garwood et al., 2011; Atherton et al., 2014). The increase in PARP activity in response to Aβ observed here has been previously shown by this group and others (Fonfria et al., 2005; McNulty and Fonfria, 2005b; Love et al., 1999), and supports a pathogenic role for PARP in AD. Moreover, the work presented in this thesis shows that inhibition of PARP activity with SB prevents Aβ-induced intraneuronal Ca^{2+} elevations in neural cells (section 4.2.15) and protects from Aβ neurotoxicity in primary neurons (Fig. 5.6D), in line with previous evidence (Abeti et al., 2011). Together, these findings suggest that PARP-mediated activation of TRPM2 channels is likely a mechanism that contributes to neuronal death induced by Aβ.

TRPM2 expression was not altered in response to Aβ-induced neurotoxicity, consistent with observations in neurons undergoing oxidative stress induced by H_2O_2. This suggests that TRPM2 expression is not altered in models of AD, and specifically that upregulation of TRPM2 may not be a mechanism that contributes to increased TRPM2 channel activity, Ca^{2+} accumulation and toxicity seen in models of AD, as previously suggested by Xie et al. (2010).

5.2.5 Aβ induces PARP activation in neurons and not astrocytes

In AD post mortem cortex, PARP immunoreactivity and accumulation of PAR is predominantly localized to neurons, although a small proportion of astrocytes

also show some immunoreactivity (Love et al., 1999). However, PARP is also reported to be upregulated in astrocytes in response to Aβ, causing mitochondrial metabolic failure which plays a key role in Aβ-induced neuronal death (Abeti et al., 2011; Tang et al., 2010). This suggests that mechanisms of Aβ neurotoxicity may involve induction of oxidative stress in astrocytes and resultant astrocytic PARP hyperactivity. Therefore, it was important to investigate astrocytic PARP activity in these cultures in response to Aβ.

Primary cultures treated with vehicle or 10 μM Aβ for 3 h were immunostained with antibodies against the astrocyte-specific marker glial fibrillary acidic protein (GFAP), PAR and were labelled with the nuclear stain Hoescht-33342 (Fig. 5.7A). Cultures treated with Aβ showed PAR immunoreactivity, consistent with results in sections 5.2.3 and 5.2.4, while control cultures did not exhibit any signal above background, as previously reported (Abeti et al., 2011). High magnification (X63) of labelled cells showed that PAR-positive nuclei do not colocalize with astrocytic nuclei (Fig. 5.7B), indicating that Aβ causes PAR accumulation in neurons and not astrocytes. These findings are inconsistent with previous evidence of astrocytic PAR accumulation in cortical astrocytes co-cultured with hippocampal neurons which were exposed to lower concentrations of Aβ (Abeti et al., 2011), although the PAR immunoreactivity detected in these experiments was predominantly cytoplasmic. In addition, astrocytes show higher PAR immunoreactivity than neurons in post mortem spinal cord tissue from patients with amyotrophic lateral sclerosis - a related neurodegenerative disorder (Kim et al., 2003). However,

these findings are consistent with many other reports of nuclear PAR accumulation in neurons in primary culture.

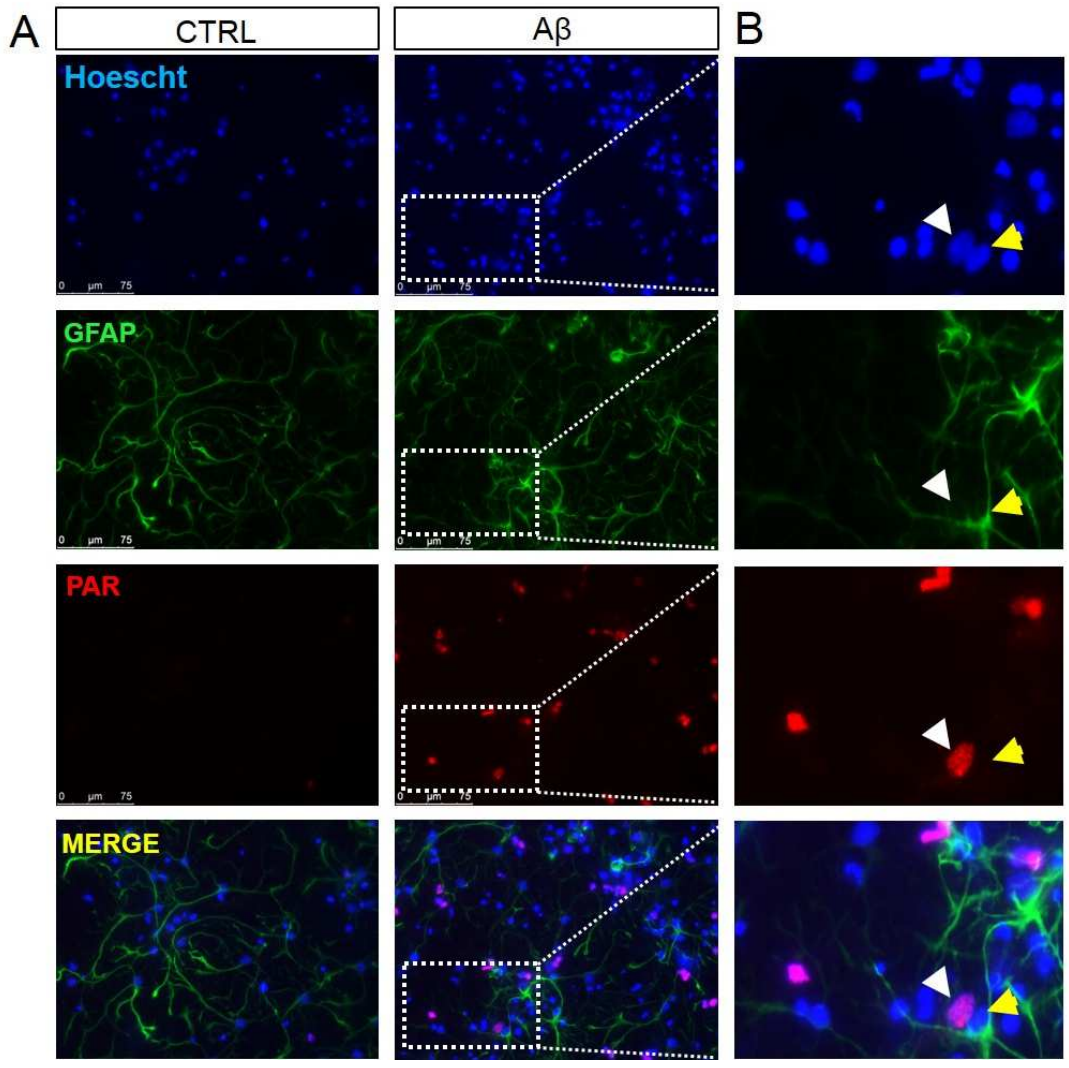

Fig. 5.7 PAR immunoreactivity in primary cortical cultures exposed to Aβ is localized to neurons. (A) Neurons treated with vehicle (CTRL), or 10 μM Aβ for 48 h were immunostained with antibodies against poly(ADP)ribose (PAR), astrocytic glial acidic fibrillary protein (GFAP), and the nuclear stain Hoescht-33342. (B) Higher magnification (X63) of neurons was used to visualize co-localization between PAR-positive nuclei (white arrow) and astrocytic nuclei (yellow arrow). Scale bar = 75 μm n=8

In addition, the neural cell localisation of TRPM2 was examined following immunohistochemical labelling of control cultures with antibodies specific to astrocytes (GFAP), neurons (MAP2) and TRPM2 (Fig 5.8). These preliminary experiments suggest that TRPM2 is predominantly localized to neurons in primary culture, since TRPM2 was detected in cells also labelled with MAP2 more readily than those labelled with GFAP (Fig. 5.8) which suggests that PARP-mediated TRPM2 signalling is more dominant in neurons, at least in the age of rat primary cortical cultures (10 DIV) used for these experiments. It is likely that variations in model systems, Aβ preparations, age of neurons and treatment times could account for the contradictory results obtained in the current study and others (for instance, treatments with 5 μM Aβ25-35 by Abeti and colleagues (2011) for 1 h as opposed to 10 μM Aβ1-42 for 3 h here.

5.2.6 PARP does not mediate Aβ-induced tau phosphorylation

Aberrant activation of TRPM2 by upon increased activity of PARP-1 has been suggested to contribute to Aβ neurotoxicity in animal and cell models of AD (Abeti et al., 2011; Fonfria et al., 2005; Xie et al., 2010). However, the downstream effects of PARP-TRPM2 signalling remain to be fully understood. In the model systems used here, Aβ-induced Ca^{2+} elevations were dependent on PARP-mediated neuronal Ca^{2+} influx (section 4.2.15), which is likely to lead to activation of calpain-1 (section 4.2.3), which could promote neurotoxic tau phosphorylation.

Tau is a requirement for Aβ-mediated toxicity in cultured neurons (Rapoport et al., 2002) and tau hyperphosphorylation and/or caspase cleavage of tau is well established to be important in neurodegeneration in AD (Noble et al., 2013). It was therefore of interest to determine the calcium-activated signalling pathways that occur downstream of PARP-TRPM2 signalling.

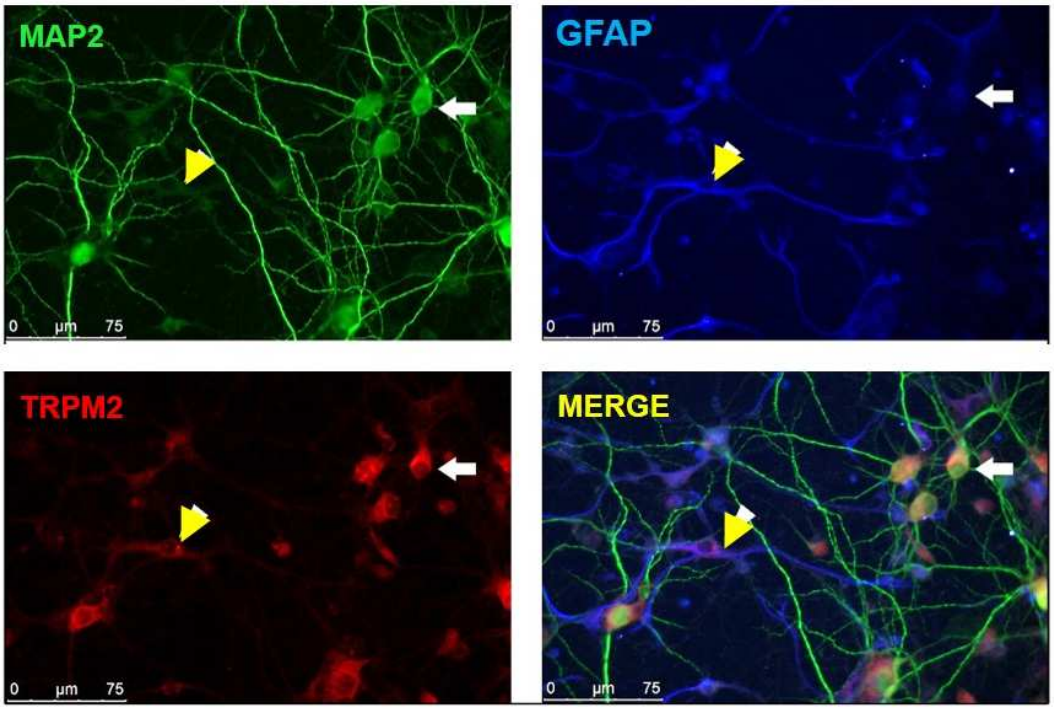

Fig. 5.8 TRPM2 channels are primarily localized to neurons in the current cell system. Control cortical cultures were immunostained with antibodies against astrocytic astrocytic glial acidic fibrillary protein (GFAP), neuronal microtubule-associated protein 2 (MAP2) and TRPM2. High magnification (X63) of cultures was used to visualize co-localization of TRPM2 with MAP2-positive neurons (white arrows) and GFAP-positive astrocytes (yellow arrows). Scale bar = 75 µm. n=4

Lysates from primary neurons treated with Aβ +/- SB were next immunoblotted with antibodies detecting total tau, independent of phosphorylation state (DAKO), which detects bands at approximately 55 kDa, tau phosphorylated at the AD-relevant epitope Ser396/404 (PHF1) and which labels bands at 55-61 kDa, and tau dephosphorylated at Ser199/202/Thr205 (tau-1) which labels species of tau at approximately 55 kDa (Fig. 5. 9A). Blots were also probed with an antibody against β-actin for standardization purposes. Following standardization of total tau (DAKO) amounts to β-actin in the same sample, and the amounts of tau phosphorylated at PHF1 to total tau (DAKO) amounts, quantitative analysis revealed no changes in total tau amounts (Fig. 5.9B) or tau phosphorylated at PHF1 (Fig. 5.9C) following treatment with Aβ and/or SB relative to controls. In contrast, Aβ-treated cultures showed significantly reduced amounts of dephosphorylated (Tau-1) tau ($p < 0.05$), indicating tau phosphorylation at these sites in response to Aβ treatment. However, Aβ-induced phosphorylation at Ser199/202/Thr205 was not reduced upon pre-treatment of cultures with SB (Fig. 5. 9D). These results suggest that the capacity of SB to reduce Aβ-induced tau phosphorylation is limited. Recently, a calpain-cleaved 17kDa N-terminal tau fragment has been reported to be generated after Aβ treatments in neurons (Park et al., 2005; Nicholson and Ferreira, 2009; Ferreira and Bigio, 2011). This fragment may be toxic to cells (Nicholson and Ferreira, 2009), although its relevance for AD is controversial (Garg et al., 2011). The tau-1 antibody which

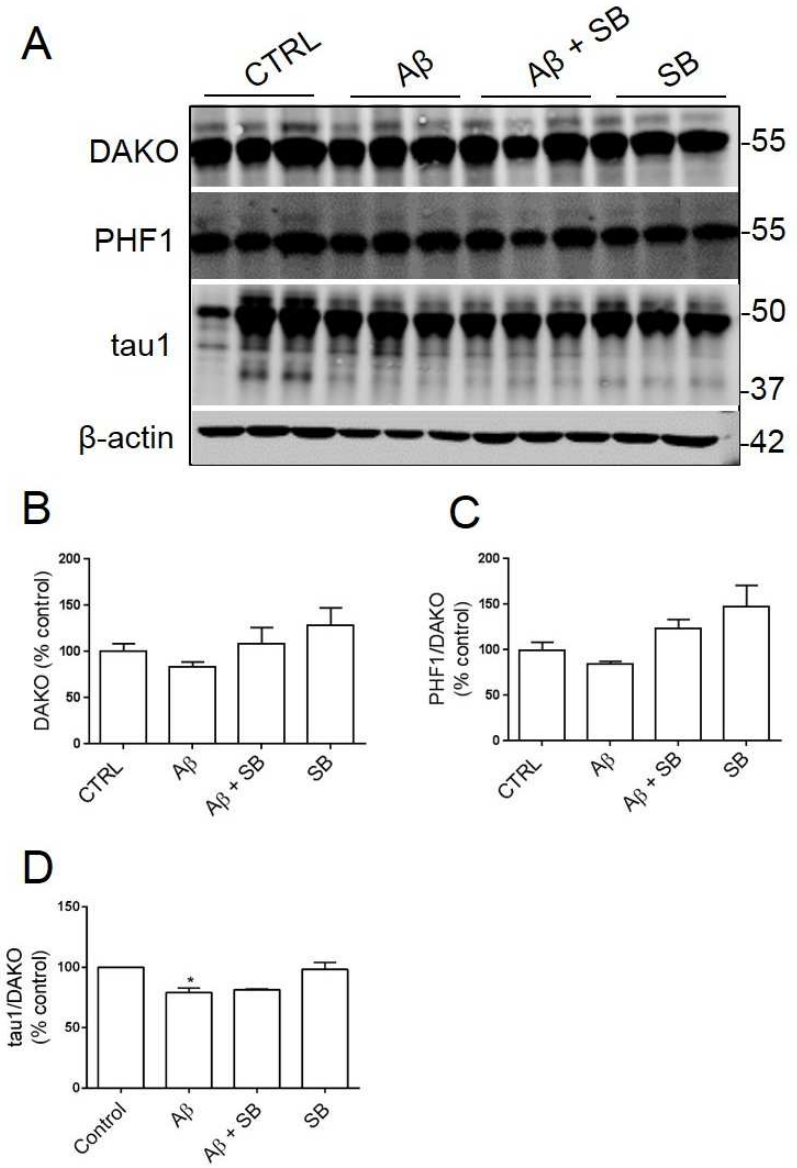

Fig. 5.9 PARP does not influence tau phosphorylation in cultures treated with Aβ. (A) Representative immunoblots of lysates from neurons treated with vehicle (CTRL), 10μM Aβ for 48 hours, 1μM of the PARP inhibitor SB750139 (SB) for 3 hours, or SB alone. Blots were probed with antibodies against total tau, independent of phosphorylation state (DAKO), which yields bands around 55 kDa in size, tau phosphorylated at the AD-relevant epitope Ser396/404 (PHF1), which yields bands from 55 to 61 kDa, and tau dephosphorylated at Ser199/202/Thr205 (tau-1), which yields bands of approximately 55 kDa in size. n=9. Data is mean ± SEM. *$p < 0.05$

labels tau dephosphorylated at Ser202/205 has previously been found by this laboratory to detect calpain-cleaved tau under certain conditions. However, scanning of tau-1 immunolabelled membranes at high intensity did not detect this fragment in the lysates of the cells treated here. Therefore, it can be concluded that the protective effects of PARP-1 inhibition that were found in the experiments described in this chapter are likely not related to tau-associated neurodegeneration in response to elevated Aβ concentrations. The mechanisms of PARP-1/TRPM2-mediated neuronal toxicity in Aβ treated cultures requires further investigation since it may represent a novel target for developing new AD therapeutics that have the capacity to modify disease course.

5.3 Summary and Discussion

The main findings of this chapter are:

- Caspase-dependent PARP cleavage occurs in moderate to late AD brain
- TRPM2 expression is not altered in severe AD brain when compared to control, however, TRPM2 is likely to be degraded in moderate to late-stage AD brain
- PARP activity is upregulated in neurons undergoing H_2O_2-induced oxidative stress and following Aβ treatment

- Inhibition of PARP activity protects from H_2O_2- and Aβ-induced neuron death
- Aβ-induced PARP activation is localized to neurons and not astrocytes
- PARP-TRPM2 signalling does not influence Aβ-induced tau phosphorylation in primary neurons

5.3.1 Aβ-induced neurotoxicity involves upregulation of PARP-TRPM2 signalling

In this chapter, exposure of primary neurons to Aβ resulted in neuronal death, confirming previous experiments (Chapter 4). Here, the data show that Aβ-induced neurotoxicity is associated with an upregulation of PARP activity neuronal, as evidenced by accumulation of nuclear PAR in neurons (section 5.2.6). Inhibition of PARP activity by treatment of neurons with SB-750139 rescued neurons from Aβ-induced neurotoxicity (section 5.2.6), which is associated with decreased calpain activation (section 5.2.6) and attenuation of Aβ-induced TRPM2 channel mediated Ca^{2+} elevations in neural cells (section 4.2.15). These cell culture-based findings suggest that PARP-1/TRPM2 may play an important role in Aβ-induced degenerative pathways and these data were complemented by observation of increasing PARP-1 cleavage by apoptotic caspases in moderate to late stage AD brain (section 5.2.1). Expression of functional (TRPM2-L) and non-functional (TRPM2-S) TRPM2 isoforms were unaltered in AD brain (section 5.2.2)

and in neurons undergoing oxidative stress induced by H202 or following Aβ treatment (sections 5.2.3 and 5.2.4).

Plentiful evidence supports a role for PARP in Ca^{2+} signalling and AD. PARP activity and PARylation (attachment of PAR polymers onto target proteins) are required for long-term memory (Cohen-Armon et al., 2004; Wang et al., 2012), which is known to be governed by Ca^{2+} dynamics in dendritic spines (Berridge, 2014). In addition, a deficiency in PARP-1 is associated with aging (Piskunova et al., 2008), which is also characterized by altered Ca^{2+} homeostasis in numerous models (Thibault et al., 2007; Oh et al., 2013; Nikoletopoulou and Tavernarakis, 2012). Furthermore, PARP-1 is known to regulate many transcription factors that are involved in modulating the function of Ca^{2+} handling proteins and Ca^{2+} pumps in myocardial cells (Szenczi et al., 2005), and PARP-1 is activated under excitotoxic conditions in a type of PARP-mediated cell death, termed parthanatos (Wang et al., 2010).

Of particular relevance for this work, PARP-1 activity is increased as a result of oxidative stress, which is promoted in aging (Boesten et al., 2013) and is triggered by Aβ in AD (Su et al., 2008; De Felice et al., 2007). In primary neurons exposed to Aβ, oxidative stress-induced DNA damage activates PARP-1 and activates downstream TRPM2 channels to cause dysregulated Ca^{2+} accumulation (Fonfria et al., 2005). Importantly, TRPM2 signalling occurs prior to, and is shown to be required for, neurodegeneration in multiple studies (Zhang et al., 2003; McNulty

and Fonfria, 2005b; Kaneko et al., 2006; Fonfria et al., 2005). Together, these findings support the current work, which shows that PARP-1 is upregulated by Aβ and mediates Aβ neurotoxicity in primary neurons. Moreover, the attenuation of Aβ-induced Ca^{2+} increases by treatment of cells with SB (section 4.2.15) suggests that PARP mediates neuronal death through TRPM2-mediated Ca^{2+} influx. Indeed, TRPM2 also appears to be required for increased NMDAR signalling induced by H_2O_2 in guinea pig midbrain slices (Lee et al., 2013). This implies a key role for TPRPM2 in oxidative stress and excitotoxicity, both of which occur in AD and feature TRPM2 activation (Takahashi et al., 2011; Xie et al., 2010). Therefore, the upregulation of PARP-1 observed here in response to H_2O_2 and Aβ is likely to be indicative of TRPM2 activation in these conditions.

The above findings are supported by observations of increased caspase-3-mediated PARP cleavage products in post mortem brain tissue from individuals with different stages of AD. Caspase-3 activation and proteolytic cleavage of PARP is a hallmark feature of apoptosis (Chaitanya et al., 2010), and therefore could indicate progressive brain atrophy at these stages, although this cannot be stated with any certainty due to the limited area of tissue examined in this work. The increased caspase-mediated proteolysis of PARP-1 was found to occur in parallel with the accumulation of toxic and pro-aggregatory Aβ1-42 into neuritic plaques in these samples (section 3.2.6), and supports the much discussed hypothesis that Aβ triggers neurodegenerative processes in AD (Hardy and Higgins, 1992).

PARP cleavage by caspases is featured as an important step in the apoptotic cascade, and is preceded by activation of PARP, which itself signals caspase activation and release of mitochondrial AIF. Therefore, caspase-mediated PARP cleavage in moderate to late AD tissue serves as indirect evidence of PARP activation at these stages. While TRPM2 protein expression was not altered in AD brain compared to control, caspase cleavage of PARP may also indicate increased TRPM2 signalling, as TRPM2 channels are shown to activate caspases prior to apoptosis in endothelial cells (Sun et al., 2012).

5.3.2 Aβ selectively upregulates neuronal PARP activity in primary neurons

In this chapter, H_20_2 and Aβ treatment of primary cortical cultures resulted in accumulation of PAR in nuclei, indicating that these treatments cause activation of PARP-1. PAR immunoreactivity in Aβ-treated primary cortical cultures was localized to neuronal nuclei, and was not present in astrocytic nuclei. This was associated with significantly increased cell death, and both nuclear PAR accumulation and cell death were rescued by pre-treatment of cells with the PARP-1 inhibitor, SB-750139. These findings suggest that Aβ neurotoxicity is, at least in part, mediated by selective activation of neuronal, and not astrocytic, PARP signalling.

There is a discrepancy between the current findings and some previous observations in AD brain and cell models of AD. In AD cortical sections, PARP and PAR immunoreactivity was mostly detected in small pyramidal neurons in laminae 3 and 5 (Love et al., 1999). However, the authors also reported occasional PAR-labelling of GFAP-positive astrocytes, although the exact proportion of astrocytes expressing PAR was not given. Moreover, astrocytes and microglia surrounding plaques show high inducible nitric oxide synthase, which is indicative of oxidative activation (Akama and Van Eldik, 2000), and Aβ triggers oxidative stress in both types of glia via production of ROS (García-Matas et al., 2010; Schilling and Eder, 2011). In a study by Abeti et al. (2011), Aβ1-42 and Aβ25-35 treatment of hippocampal neurons co-cultured with cortical astrocytes resulted in predominantly neuronal death, which was associated with upregulation of PARP-1 in astrocytes. The increase in astrocytic PARP-1 activity was triggered by oxidative stress resulting from Aβ-induced depletion of astrocytic nicotinamide adenine dinucleotide phosphate oxidase (a mitochondrial substrate) and subsequent loss of mitochondrial membrane potential. This was accompanied by rises in astrocytic Ca^{2+}, which might imply PARP-mediated activation of TRPM2 channels in astrocytes, although this is not examined by these authors. Whether TRPM2 is expressed in astrocytes is disputed, and the neural cell localisation of TRPM2 has been shown to vary between brain regions (Xie et al., 2010). Nevertheless, TRPM2 activation was found to confer necrosis and swelling of primary astrocytes induced by ammonium toxicity in a recent

study (Sai et al. 2013). When taken together, evidence of TRPM2 expression in astrocytes, Aβ-induced upregulation of astrocytic PARP and resultant Ca^{2+} elevations in astrocytes suggests that an astrocytic PARP-TRPM2 pathway may also play a role in Aβ neurotoxicity. On the other hand, expression of TRPM2 was previously shown to be predominantly found in neurons here (Section 5.2.5) and by others (Bai & Lipski 2010).

The lack of astrocytic PAR signal in Aβ-treated primary cultures in the current study, which is in disagreement with some previous reports, may be explained by experimental inconsistencies between laboratories, such as different Aβ incubation periods. Abeti et al. (2011) observed an increase in cytoplasmic astrocytic PAR immunoreactivity approximately 8 h post Aβ treatment, whereas here cultures were examined for PAR signal after 3 h, and the PAR signal was predominantly nuclear. It is possible that astrocytic responses to Aβ occur prior to neurons; for instance, preliminary experiments in this group have shown that Aβ elevates astrocytic Ca^{2+} prior to large elevations in neuronal Ca^{2+} (Atherton et al. unpublished). This was also seen in early experiments in rat forebrain cultures, where stimulation of astrocytes caused an elevation of Ca^{2+} that propagated from astrocyte to astrocyte, and triggered increases in cytosolic Ca^{2+} in neighbouring neurons (Nedergaard, 1994). Indeed, astrocytic Ca^{2+} signalling was later shown to induce Ca^{2+} responses in neurons, either through propagation of signal through gap junctions or release of transmitters such as glutamate (Verkhratsky and Kettenmann, 1996). Furthermore, exocytotic release of glutamate from astrocytes

requires elevation of astrocytic Ca^{2+}, and is in turn required for stimulation of neuronal NMDARs, which raise neuronal Ca^{2+} (Parpura et al., 2011). It is also possible that differences in model systems between studies could account for the contradictory observations here and in the literature. For instance, astrocytes only comprise approximately 17 % of total cells in the current model, whereas previous studies show PARP activation in cultured astrocytes (Abeti et al., 2011) and AD brain (Love et al., 1999), where the phenotype of the astrocyte population is likely considerably different. Indeed, astrocytes in the hippocampus and entorhinal cortex display different Ca^{2+} responses to Aβ, which may in turn differentially affect PARP (as proposed in section 4.3.4).

5.3.3 Limitations to this work

There are several limitations to the work carried out in the current chapter that are worth mentioning. First, it would have been interesting to compare PARP and PAR immunoreactivity in post mortem brain sections from control and Braak II-VI AD brains, so as to further previous studies by Love et al. (1999) and investigate any changes in PARP activity and expression during the progression of AD (similar to the studies in Chapter 3). Second, aside from PARP, PARG also plays a role in TRPM2-mediated Ca^{2+} influx as it catalyzes hydrolysis of PAR into ADPR monomers prior to their translocation to the nucleus and activation of TRPM2 channels (Blenn et al., 2011; Andrabi et al., 2006). Immunoblotting of post

mortem control and AD tissue or primary cortical cultures with an antibody specific to PARG would have provided further insight into the role of PARG in AD progression and Aβ-induced neurotoxicity. These analyses were attempted; however, the commercial antibodies purchased against PAR, PARP-1 and PARG showed limited detection of proteins in post mortem homogenates or rat cortical lysates. Another way of determining the contribution of PARG activity to Aβ neurotoxicity and TRPM2-mediated Ca^{2+} signalling would have been to treat primary neurons with a PARG inhibitor and observe changes in PAR synthesis, Ca^{2+} dynamics and cell death. For instance, Andrabi et al. (2006) showed that knockdown of PARG in neurons made them more sensitive to NMDAR-mediated excitotoxicity compared to wild-type cultures, and mice overexpressing PARG showed reduced infarcts following focal ischaemia.

Emerging evidence suggests a role for neuroinflammation in PARP-TRPM2 signalling, and vice versa, in AD. PARP-1 activity is shown to activate inflammation-related genes, including inflammatory cytokine 1 (IL-1) and tumour necrosis factor α (TNFα; Ba and Garg, 2011). These pro-inflammatory factors were shown to stimulate neuronal PARP and TRPM2 activities and subsequent Ca^{2+} elevations in response to Aβ in preliminary experiments in this group (Atherton et al., unpublished) and others (Fonfria et al., 2006; Zhang et al., 2003). Furthermore, these neuronal effects were preceded by increases in astrocytic Ca^{2+} and changes in astrocytic morphology. It is, therefore, important to consider the role of neuroinflammatory processes in Aβ-induced PARP-TRPM2

signalling and neurotoxicity. Future work could determine whether soluble inflammatory factors released from astrocytes contribute to alterations in AD-related mechanisms in neurons (e.g. calpain activation and tau phosphorylation) through elevations of TRPM2-mediated Ca^{2+} in neurons.

The inhibition of PARP by SB was found to prevent Aβ-induced Ca^{2+} elevations in neural cells (section 4.2.15), suggesting an important contribution of TRPM2 channels in shaping cellular responses to Aβ. This could be confirmed by direct pharmacological inhibition of TRPM2 using commercially available TRPM2 antagonists, such as flufenamic acid and clotrimazole (CLA). However, these agents are not specific to TRPM2 and show cell-specific efficacy; for example, CLA does not block ADPR-activated TRPM2 in rat hippocampal neurons (Naziroğlu, 2011). Furthermore, these agents are difficult to utilize as they are lipophilic and irreversible. The use of TRPM2-L and TRPM2-S clones to modulate TRPM2 function in transfected cells is another approach to directly determine the role of TRPM2 in neuronal Ca^{2+} signalling. In addition, electrophysiological studies have shown that PARP inhibition does not prevent TRPM2 activation by ADPR, as ADPR is also produced by mitochondria (Naziroğlu, 2011), and this is worth further exploration. Finally, further studies could investigate the role of TRPM7, a close relative of TRPM2 channels, in Aβ-induced neurotoxicity and Ca^{2+} elevations as this channel has higher Ca^{2+} permeability than TRPM2 and is also involved in apoptosis induced by oxidative stress (Yamamoto et al., 2007). Unfortunately,

time restrictions meant that it was not possible to complete these additional studies during this PhD.

5.3.4 Conclusions

In summary, the results presented in this chapter describe a pathway by which Aβ induces PARP-1 activity, resulting in cell death through a pathway not involving aberrant phosphorylation or cleavage of tau. Further experiments may identify the precise mechanisms of cell death involved in these events, and may find further evidence in support of PARP-1 inhibitors as novel neuroprotective agents for the treatment of AD. Since PARP-1 inhibitors are currently in clinical trials for some types of cancer, a successful outcome of these trials would mean that they are suitable for drug repositioning which may lead to an accelerated path for their clinical use in the treatment of AD.

CHAPTER 6

Discussion

The main aims of this thesis were to investigate: 1) the association between Ca^{2+}-dependent pathways and neurodegenerative processes during the progression of AD, and 2) novel mechanisms contributing to Ca^{2+} dyshomeostasis in AD.

The studies presented here corroborate the hypothesis that aberrant increases in Ca^{2+} occur early during the development of AD, features that can be replicated in cells. Moreover, the findings of this work suggest the involvement of novel signalling pathways that contribute to Ca^{2+} dysregulation and neurodegeneration in AD. In particular, increased activity of the Ca^{2+}-activated cysteine protease calpain-1 was found to be a common feature of post-mortem AD and other neurodegenerative brain, and was associated with calpain-mediated cleavage and inactivation of NCX3 in end-stage (Braak VI) disease. The reduction of functional NCX3 by knockdown of NCX3 with antisense oligonucleotides was found to sensitize primary neurons to subtoxic concentrations of Aβ. Together, these findings suggest that aberrant activation of calpain and calpain-mediated degradation of functional NCX3 may be a mechanism that contributes to the toxic accumulation of intraneuronal Ca^{2+} in neurons in affected regions of AD brain.

An important finding was the presence of elevated active calpain-1 amounts in early (Braak II) AD brain, increases that were sustained throughout disease progression. The early increases in calpain-1 activity were associated with upregulation of the endogenous calpain inhibitor, calpastatin, and preceded activation of the prominent tau kinases cdk5 and GSK3, elevated tau phosphorylation and loss of synaptic markers. Moreover, the progressive increases in calpain-1 activity correlated with increased Aβ1-42 production and proteolysis of the cytoskeletal protein α-spectrin. Many of these events had previously been shown in isolation in cell or animal model studies, but this is the first direct evidence in support of this neurodegenerative cascade in human AD brain.

In cell studies, increased calpain-1 activity resulted from prolonged Ca^{2+} elevations that were induced by oligomeric species of Aβ1-42, and neurotoxicity under these conditions was closely associated with activation of tau kinases, tau phosphorylation, loss of synaptic markers and altered APP processing. Increased PARP signalling and activation of TRPM2 channels was found to contribute to Aβ-induced Ca^{2+} elevations and neurotoxicity, and this was supported by evidence for altered PARP processing and signalling in AD brain. Again, there has been some previous evidence for PARP-1 involvement in AD, but to the best of our knowledge, this thesis provides the first evidence to link altered PARP signalling and Ca^{2} influx through TRPM2 channels in response to AD, with alterations in tau and neurotoxicity.

To summarise, the primary findings of this thesis are:

- **Calpain-1 activity is increased in early stages of AD and this is sustained throughout disease progression.** Increases in active calpain-1 protein amounts are associated with increased calpain-mediated proteolysis of α-spectrin and Aβ1-42 accumulation
- **Increased calpain-1 activity precedes increased tau kinase activity, tau phosphorylation and synaptic loss in AD.** Aβ-induced neurotoxicity is dependent on calpain activation, tau phosphorylation and synaptic degeneration in primary neurons
- **Calpain-mediated NCX3 cleavage is a feature of end-stage AD brain and confers Aβ neurotoxicity.** Calpain cleavage of NCX3 was a prominent feature of AD brain, but was not apparent in brain from a group of related neurodegenerative disorders. Knockdown of NCX3 causes neurotoxicity in primary neurons exposed to normally subtoxic concentrations of Aβ.
- **PARP hyperactivity mediates Aβ-induced neurotoxicity.** Aβ induces abnormal Ca^{2}increases in neural cells, which are abolished by blockade of Ca^{2} influx through TRPM2 ion channels using specific PARP inhibitors. The physiological relevance of this process is supported by evidence for altered PARP signalling in moderate to late AD brain, suggesting a neurodegenerative role for PARP/TRPM2 signalling in AD.

6.1 Ca^{2+} and calpain dyshomeostasis in AD

6.1.1 Increased calpain signalling in AD

Abnormal calpain activation occurs during conditions of prolonged intracellular Ca^{2+}elevation, such as during excitotoxicity and Wallerian degeneration following neuronal injury (Nixon et al., 1994). In AD brain, increased calpain-1 and calpain-2 activities are a consistent and prominent feature of diseased brain, and is associated with increased calpain-mediated proteolysis of key signalling and cytoskeletal proteins (Nixon et al., 1994; Nixon, 2003; Saito et al., 1993; Grynspan et al., 1997; Rao et al., 2008; Atherton et al., 2014). Interestingly, increased levels of active calpains were recently observed in CSF from AD patients, and positively correlated with Aβ1-42 levels and cognitive impairment in these patients (Laske et al., 2015). Increased proteolytic activity of calpain-1 and calpain-2 are also observed in double mutant APP and APP/PS1 mutant mice, which overproduce Aβ (Vaisid et al., 2007a; Trinchese, Liu, et al., 2008). This work supports these previous findings from post-mortem AD brain and transgenic mouse models of AD by demonstrating 1) elevated amounts of active calpain-1 and associated calpain-mediated cleavage of several calpain substrates in AD brain compared to controls, 2) a strong positive correlation between Aβ1-42 burden and calpain-1 activity in AD brain, and 3) increased calpain-1 activity in Aβ-treated primary cortical neurons. Together, these results indicate a close association between Aβ production and elevated calpain activity.

However, elevated active calpain-1 amounts were also observed here in several other neurodegenerative tauopathies, which are not characterized by a prominent Aβ phenotype (Boeve, 2012; Wadia and Lang, 2007; Lee et al., 2001). Upregulation of calpain-1 in many of these disorders was previously reported (Adamec et al., 2002; Vosler et al., 2008), and is thought to either suggest the involvement of other mechanisms besides Aβ overproduction in neurodegenerative calpain signalling, or that calpain activation occurs independently from/upstream of Aβ accumulation. The results in this work favour the latter hypothesis, and extend previous studies by demonstrating that calpain-1 activity progressively increases from an early stage in AD development, prior to significant Aβ burden. Since calpain-1 is a Ca^{2+}-activated protease, and is considered to be a good indicator of pathologically elevated intracellular Ca^{2+} levels, this finding suggests that changes in Ca^{2+} occur prior to early alterations in APP processing and Aβ accumulation in AD, as previously suggested by others (Buxbaum et al., 1994; Siman et al., 1990; Kyratzi and Efthimiopoulos, 2014). However, it is also possible that some Aβ species are present in early AD brain, and these were not detected by the methods used here. For instance, certain AD mouse models exhibit disruptions in Ca^{2+} homeostasis months before extracellular Aβ pathology is detected (LaFerla, 2002). Moreover, AD brain shows a higher increase in calpain-1 activity than other neurodegenerative conditions studied here and in previous reports (Nixon, 2003; Atherton et al., 2014; Adamec et al., 2002), which suggests that some form of Aβ species may lie upstream of

calpain activation. Indeed, moderate and late stages of AD, which are characterized by Aβ1-42 overproduction, also show higher calpain-1 activity compared to earlier stages where tissue Aβ levels do not differ from controls. Moreover, in the cell systems used here, oligomeric Aβ peptides induce abnormal increases in neural Ca^{2+} and subsequent calpain-1 activation, in line with previous reports suggesting that calpain activation is downstream of Aβ in AD (Demuro et al., 2011; De Felice et al., 2007; Park and Ferreira, 2005).

When considering the effects of Aβ production, it is important to also think about APP processing. The complex relationship between Ca^{2+} signalling and APP metabolism includes conflicting evidence on the role of calpain in Aβ production. Overproduction of Aβ in APP/PS1 mutant mice was shown to be associated with increased BACE-1 and calpain activities (Liang et al., 2010). Liang et al. (2010) showed that treatment of primary neurons with Aβ, or overexpression of calpain in neurons, acted to increase BACE expression, enhanced APP cleavage and promoted Aβ secretion. This was prevented in APP/PS1 mice by overexpression of the endogenous calpain inhibitor, calpastatin, which led to a reduced Aβ plaque load. These findings suggest that Aβ begets further Aβ production in a positive feedback loop, via mechanisms that may involve activation of calpain-1 and increased BACE-mediated APP cleavage.

In a cell-based study, primary neurons treated with Aβ demonstrated increased production and intracellular accumulation of endogenous Aβ (Dal Pra et al.,

2011), again supports the hypothesis of a positive feedback loop of Aβ production. However, the role of calpain and APP secretases in this cell system was unclear, as expression of BACE was unaltered by calpain or Aβ, and the inhibitory effect of Aβ on α-secretase-mediated non-amyloidogenic APP processing was shown to be independent of calpain activity. Interestingly, Aβ treatment of cells was found to induce a calpain-dependent increase in expression of the γ-secretase component, nicastrin. Furthermore, suppressing calpain activity promoted non-amyloidogenic processing of APP, although independently of Aβ treatment (Dal Pra, 2011). In another study, suppressing calpain activity in murine L cells increased C-terminal APP proteolysis and Aβ1-42 production, thereby indicating an inhibitory role for calpain in amyloidogenic APP processing (Mathews et al., 2002). Taken together, these findings suggest that Aβ and calpain may differentially regulate APP processing, either in concert or independently of each other, and the precise effects may be dependent upon the particular model system used in additional to other experimental parameters. Further studies in transgenic animals or AD brain are required to determine the mechanisms of APP regulation at different stages of disease. Interestingly, amounts of APP holoprotein are observed to be elevated in early Braak stage AD brain in this work, which suggests that the activation of calpain-1 in these stages may act to inhibit C-terminal APP metabolism and Aβ production.

Calpains are also implicated in the generation of pathological tau species, including abnormally phosphorylated and truncated tau, in multiple models of AD

(Ferreira, 2012; Jin, Yin, Yu, et al., 2015; Taniguchi et al., 2001). Active calpain-2 is localized to 'pre-tangle' tau aggregates in AD brain (Grynspan et al., 1997), and activation of calpain-1 and -2 in APP/PS1 mutant mice is associated with tau phosphorylation and cognitive deficits (Liang et al., 2010). Tau hyperphosphorylation in AD is causally linked to increased activity of several tau kinases, including GSK3, cdk5, mitogen-activated protein kinase (MAPK), DYRK1 and extracellular signal-regulated kinases (ERK1/-2), which are activated either directly or indirectly by calpain (Goñi-Oliver et al., 2007; Taniguchi et al., 2001; Veeranna et al., 2004; Qian et al., 2013; Jin, Yin, Gu, et al., 2015). In the work presented here, activation of calpain-1 was required for cdk5 and GSK3 activation and increased tau phosphorylation induced by Aβ in cultured cells, in agreement with previous reports (Hung et al., 2005; Jin et al., 2015; Huang and Jiang, 2009). Furthermore, calpain-1 activation occurred prior to increased tau phosphorylation at an AD-relevant epitope (pSer396/404, PHF1) and the appearance of mature NFTs in AD brain (Chapter 3). Moreover, the increase in calpain-1 activity showed a strong positive correlation with activities of GSK3 and cdk5 in AD brain, as assessed by measurement of the inhibitory phosphorylation sites (Ser21/9) on GSK-3 α/β and the amounts of the neuronal cdk5 activators p35 and p25, relative to cdk5 levels. These findings support data from cell and animal model studies by suggesting that elevations in calpain activity in the early stages of AD progression mediate downstream tau phosphorylation through increasing the activity of important tau kinases, in agreement with previous

findings (Jin et al., 2015; Hung et al., 2005). Therefore, this work supports a causal link between early Ca^{2+} dysregulation, calpain activation and pathological changes in tau.

Interestingly, despite both being activated by calpain-1, there were differences in the stage of disease at which increases in GSK3 and cdk5 activities were observed in AD brain. Activity of cdk5 was found to progressively increase in parallel with increasing calpain-1 activity, from an early (Braak III) stage in AD. In contrast, GSK3 activity was found only to be significantly increased in late (Braak V-VI) AD brain. The Cdk5 activator p25 was previously found to preferentially bind GSK3β in mouse neurons overexpressing GSK3, altering GSK3β substrate specificity to result in increased tau phosphorylation (Chow et al., 2014), independently of alterations in Ser21/9 phosphorylation. It is therefore possible, that the GSK3 contributed to tau phosphorylation from an earlier stage of disease development, but this was not apparent through analysis of inhibitory GSK3 phosphorylation, as examined here. Conversely, mice overexpressing p25 show increased cdk5 activity at a young age which is associated with a reduction in active GSK3 species, this effect resulting from increased phosphorylation of the inhibitory (Ser9) residue of GSK3β via the ErbB and downstream phosphatidylinositol 3-kinase/Akt pathways (Wen et al., 2008). Notably, these p25 overexpressing mice exhibited reduced tau phosphorylation and increased Aβ production at young ages. Therefore, the late activation of GSK3 seen here in AD brain could be a result of negative regulation of GSK3 by cdk5 in earlier disease stages. This may also

explain why accumulation of Aβ in AD brain corresponds to cdk5 activation, whereas tau phosphorylation occurs alongside increased GSK3 activity in end-stage AD brain. Since the cdk5 and GSK3 hypotheses of AD have mostly been studied in isolation, it has only been recently that evidence of a complex interrelationship between these two kinases has emerged (Engmann and Giese, 2009). Furthermore, aside from GSK3 and cdk5 influencing each other's activity, GSK3 is reported to reciprocally promote calpain activity in excitotoxic neurons (Crespo-Biel et al., 2010). This is also shown here in primary neurons, and indicates that the relative contribution of tau kinases and calpain to AD neurodegenerative pathways is very complex and not fully understood.

Other tau abnormalities are linked with calpain activity in neurodegeneration. Tau aggregates are reported to contain N- and C-terminally truncated tau species, generated as a result of abnormal activation of calpain and other proteases (García-Sierra et al. 2008). Moreover, APP mutant mice known to exhibit cognitive and behavioural deficits are shown to contain physiologically acetylated, ubiquitinated and lysine methylated tau species (Morris et al., 2015). There is substantial evidence that these post-translationally modified tau species accelerate tau polymerization, induce neurotoxicity and positively correlate with severity of dementia in AD (Gamblin et al., 2003; Amadoro et al., 2004; Morris et al., 2015). Indeed, Aβ-induced activation of calpain-1 results in the generation of 17 kDa tau species which leads to degeneration of neurites in hippocampal cells (Park and Ferreira, 2005). These 17 kDa tau fragments were also observed in AD

brain (Ferreira and Bigio, 2011), indicating that accumulation of calpain-cleaved tau species may be a neurodegenerative process induced by Aβ in AD. In another study, rat cortical neurons undergoing excitotoxicity displayed accumulation of 35 kDa tau fragments that were also generated upon cleavage of tau by calpain (Liu et al., 2011). Interestingly, neither 17 kDa nor 35 kDa calpain-cleaved tau species were observed in AD brain or cultures exposed to Aβ in the current study. It is possible that the 17 kDa tau species reported by Park and Ferreira (2005) and Ferreiro and Bigio (2011) may actually be much smaller (as demonstrated by Garg et al., 2011a), for which reason they may have not been detected here. As Garg et al. (2011) also questioned the pathological relevance of these species by showing that they do not mediate Aβ toxicity in neural cells, this may suggest that calpain-cleaved truncated tau fragments of that size may not be a consistent feature of AD. Moreover, as similar tau species have been identified in other neurodegenerative conditions, such as CBD and FTD (Ferreira and Bigio, 2011), they are likely to represent a common neurodegenerative feature that is not directly associated with Aβ.

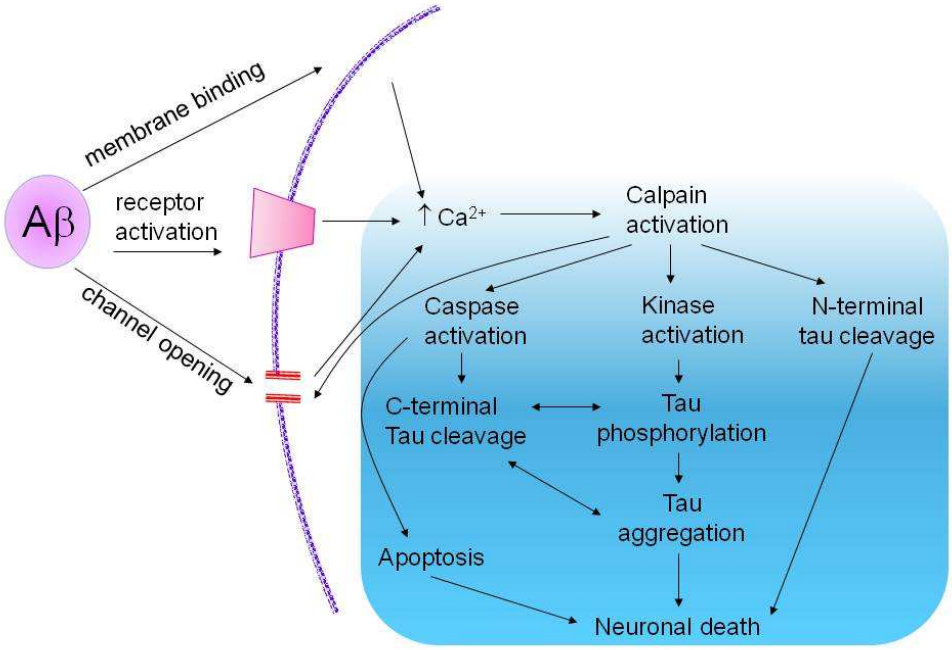

Fig. 6.1 The calpain hypothesis of AD. Prolonged elevations in intracellular Ca^{2+} concentrations, triggered by Aβ-mediated channel opening, receptor activation or membrane pore formation, lead to dysregulated activation of calpains. This in turn causes massive proteolytic cleavage of calpain substrates, including tau. Cleavage of tau kinases and pro-caspases leads to tau kinase and caspase activation, resulting in tau phosphorylation and truncation of tau into C-terminal toxic fragments, respectively. Both of these events are considered to promote tau aggregation, which leads to neuronal death. This is contributed to by caspase-dependent apoptotic signalling (Wray and Noble, 2009).

6.1.2 CAST, synapses and neuroprotection in AD

Calpain activity is endogenously regulated via its Ca^{2+}-dependent tripartite binding by the native specific calpain inhibitor, CAST, which is closely associated with calpain intracellularly (Goll et al., 2003). In turn, CAST is subject to

proteolytic inactivation by calpain and other calpain-activated proteases, including caspase-1 and -3. The ratio of functional CAST to calpain is an important factor in the control of calpain activity and this has been shown to be pathologically altered in various conditions, including AD (Vaisid et al., 2007). APP mutant mice exhibit diminished CAST and increased calpain-1 activity, and show increased calpain-dependent proteolysis in affected regions of AD brain such as the hippocampus and cortex (Vaisid et al., 2007). As CAST expression is physiologically lower in these areas compared to other brain regions such as the cerebellum (Vaisid et al., 2007), it is likely that calpain is therefore activated more readily by modest intracellular Ca^{2+} increases in these areas, where its aberrant activity contributes to AD neuropathology. Indeed, genetic deficiency of CAST or overexpression of calpain-1 were shown to augment Aβ production, tau phosphorylation, cognitive impairment and mortality in *vivo*, all of which was rescued by overexpression of CAST (Higuchi et al., 2012; Liang et al., 2010).

The work presented here demonstrates that there is depletion of active CAST in the cortex of AD brain when compared to controls. The inactivation of CAST is closely associated with increased calpain-1 activity and severity of Aβ and tau pathology in these tissues. Similar findings have previous been reported in end-stage AD brain (Nilsson et al., 1990; Rao et al., 2008). However, it was shown here that reduced CAST activity is also observed in other neurodegenerative conditions which lack Aβ pathology such as PSP and CBD. Therefore, such reductions of CAST activity are not always downstream of Aβ, but might result

from overactivation of calpain-1 via poorly understood mechanisms, and calpain-mediated cleavage CAST. This would result in a reduction in the ratio of active CAST to calpain, further exacerbating calpain activity in neurodegenerative disease brain.

The work presented here also investigated the regulation of CAST activity at different AD stages. The data revealed an initial increase in CAST activity in association with elevated calpain-1 activity in early-mid stage AD brain compared to control. The increase in CAST activity was temporary (limited to Braak stage III), and was followed by a progressive decline in active CAST amounts in brain from later stages of disease. Therefore, these early increases in CAST activity may represent a neuroprotective mechanism initiated in response to neural cell damage as a result of the pathological activation of calpain-1 in early AD, which is, in time, overcome as calpain-1 activity and calpain-mediated degradation of CAST increase above a certain threshold in later disease stages. In support of this idea, subtle alterations in neuronal Ca^{2+} regulation are observed early in transgenic models of AD, and these are hypothesized to be neuroprotective responses to early pathogenic changes in the brain, such as Aβ accumulation or increased neuronal excitability (Supnet and Bezprozvanny, 2010). For instance, 3xTg-AD mice show increases RyR-mediated ER release in the pre-symptomatic stages of disease at which time they exhibit normal synaptic activity (Chakroborty et al., 2009). In addition, many animal models of AD exhibit neuronal hyperexcitability (e.g. Busche et al., 2008), and it has been proposed that early alterations in ER Ca^{2+}

handling may act to prevent excitotoxicity in these animals by depressing membrane excitability (Chakroborty et al., 2009). However, these early protective responses by cells fail to halt disease progression and the animals go on to develop cognitive dysfunction and AD-like neuropathology (Chakroborty et al., 2009). Therefore, it is possible that the upregulation of CAST seen in the work presented here in early-mid stage AD brain represents a compensatory response to abnormal calpain-1 activation by early - possibly neuroprotective - elevations in neuronal Ca^{2+}. On the other hand, as CAST is normally activated during high cytosolic Ca^{2+}, the increase in CAST activity in early AD brain may be a physiological response, which is independent of changes in calpain activity.

It is also postulated that early compensatory changes in Ca^{2+} concentrations in AD neurons are only effective in protecting from cell death in the early stages of disease, and that these same responses may contribute to neurodegenerative cascades when they are sustained over the duration of AD progression (Supnet and Bezprozvanny, 2010; Maltsev et al., 2014). With this in mind, it is possible that the early increase in CAST activity observed here may have only been effective at protecting the CNS while levels of active calpain-1 were low enough to balance out CAST inhibitory activity. However, sustained increases in intraneuronal Ca^{2+} concentrations likely increased the ratio of active calpain to CAST, thereby increasing calpain-mediated proteolytic inactivation of CAST and stimulating further calpain activation in a vicious cycle. Indeed, brain from the terminal stages of AD features a more than 3-fold increase in calpain-1 activity, in

line with previous reports (Nixon et al., 1994). It is clear that further investigation into active CAST-calpain dynamics and downstream signalling events are required to determine their relative neurodegenerative roles throughout the development of AD. For instance, while calpains are shown to be co-localized with CAST and widely distributed in quiescent human 103H cells, stimulation of cells with Ca^{2+} ionophore causes redistribution of calpains to predominately plasma membranes, without affecting CAST localization (Goll et al., 2003). This suggests that calpain-1 overactivation may be at least in part due to the inability of CAST to directly interact with and inhibit calpains, which may explain the limited effectiveness of CAST upregulation in early AD brain.

Increased protein expression of pre- and post-synaptic markers was observed here in early AD brain, and this may serve as further evidence that a compensatory response occurs in response to increased calpain-1 activity in the early stages of disease. Synaptic dysfunction is argued by many to occur during the prodromal stages of AD (Arendt, 2009), where it is thought to be promoted by early alterations in Ca^{2+} signalling and synaptic excitotoxicity (Chakroborty, 2012). Ca^{2+} influx can cause long-term changes in synaptic efficacy and plasticity, with abnormal increases in synaptic Ca^{2+} - for instance, as a result of insertion of Aβ pores - leading to diminished spine density, aberrant dendritic sprouting and synaptic dysfunction (Koffie et al., 2009). In addition, abnormal Ca^{2+} overload in neurites and deficits in synaptic integration observed in APP transgenic mice

were shown to be dependent on the presence of amyloid plaques (Kuchibhotla et al., 2008).

However, aberrant Ca^{2+} regulation is also seen to occur prior to the development of substantial Aβ pathology in other transgenic mouse models of AD. For example, young 3xTg-AD mice display reduced hippocampal plasticity due to altered RyR-mediated ER Ca^{2+} release (Parent et al., 1999). Several lines of evidence demonstrate that abnormal calpain activity could contribute to early Ca^{2+} dysregulation and synaptic dysfunction in AD. In AD brain, increased calpain-1 activity causes increased degradation of protein kinase A, which is a positive regulator of cAMP-response element binding protein (CREB) - an important transcription factor in synaptic plasticity and memory (Liang et al., 2007). In hippocampal slices prepared from transgenic mice overexpressing mutant human APP and PS1, and in Aβ-treated hippocampal cultures, pharmacological inhibition of calpain activity rescued synaptic dysfunction and cognitive and memory deficits by preventing calpain cleavage of CREB (Trinchese, Liu, et al., 2008). These findings suggest that Ca^{2+}-dependent synaptic abnormalities in AD may involve alterations in calpain activity and calpain-mediated degradation of key synaptic proteins. Several calpain substrates that are relevant for this process have been identified, including synapsin I (Khoutorsky and Spira, 2009) and NR2B (Simpkins et al., 2003), both of which are modulated by calpain to regulate synaptic activity. The calpain-dependent degradation of NR2B subunits of NMDARs is controlled by PSD95 in cortical neurons (Yuen et al., 2008).

Furthermore, Trinchese et al. (2008) have shown that immunoreactive clusters of synapsin-I, PSD95 and α-spectrin are increased during normal synaptic function and plasticity. Therefore, it is possible that the upregulation of synaptic proteins seen in this study in early-mid stage AD brain signifies accelerated protein synthesis and reduced turnover to compensate for 1) increased calpain-1 activity and degradation of these proteins and/or 2) Ca^{2+}-dependent disruption of synaptic plasticity. In summary, it is possible that the transient upregulation of CAST and synaptic proteins that occur in parallel to increases in calpain-1 activity in early to mid-stage AD brain represent compensatory responses to dysregulated calpain proteolysis of key cellular proteins. These findings may also serve as an indication of early synaptic dysfunction at these disease stages, thereby corroborating the hypothesis that aberrant Ca^{2+} homeostasis and synaptic dysfunction occur in the prodromal stages of AD, prior to the development of substantial Aβ and tau pathology in AD (Chakroborty and Stutzmann, 2011; Selkoe, 2002). It is also important to consider that changes in calpain activity are triggered by pre-fibrillar or soluble species of tau or Aβ which are not routinely examined in AD brain. Soluble oligomeric species of both Aβ and tau are closely linked with synaptic and neuronal loss in models of AD (Welzel et al., 2014; Castillo-Carranza et al., 2015). In this work, loss of synaptic markers, in particular PSD95, is observed in late Braak stage AD brain, which also shows increased Aβ1-42 burden, soluble tau and tau phosphorylated at PHF1. Therefore, these findings support previous studies by suggesting a link between Aβ, tau and synaptic loss.

The loss of synaptic markers did not significantly correlate with amounts of Aβ1-42, total tau and phosphorylated tau in this study; however, this is likely due to the increase in synaptic protein numbers in early Braak stages.

6.1.3 Calpain perturbs NCX3 function in AD

The native NCX pumps - NCX1, NCX2 and NCX3 - are widely expressed in the brain, where they are predominantly localized to the cell surface and mitochondrial membranes of neurons, glia and endothelial cells (Gobbi et al., 2007). During conditions of abnormally high cytosolic Ca^{2+}, such as during excitotoxicity, ischaemia or multiple sclerosis (Bano et al., 2005; Brustovetsky et al., 2010b; Kurnellas et al., 2007), NCXs clear excess Ca^{2+} by providing the major route of Ca^{2+} extrusion out of the cell, (1 Ca^{2+} in exchange for 3 Na^{+}), and by sequestering Ca^{2+} into mitochondria stores (Wood-Kaczmar et al., 2013). Thus, the so-called 'forward' mode of NCX ion exchange plays a critical role in maintaining neuronal and glial Ca^{2+} homeostasis and function (Parpura and Verkhratsky, 2012; Gleichmann and Mattson, 2011). During neuronal depolarization or conditions of high intracellular Na^{+}, NCXs switch to 'reverse' mode to allow Ca2+ entry into the cell; this is also important for astrocytic release of glutamate and its utilization by neuronal synapses (Reyes et al., 2012). NCX3 undergoes proteolytic cleavage by calpains and caspases, which prevents binding of Ca^{2+} to the NCX Ca^{2+} regulatory domain and inactivates the exchanger (Bano et al., 2005, 2007). In striatal and

hippocampal cell models of ischemia, calpain cleavage and inactivation of NCX3 mediated glutamate-induced excitotoxicity and neuronal death (Bano et al., 2005; Brustovetsky et al., 2010a). In striatal cultures, cell death was rescued by overexpression of CAST or calpain-resistant NCX2; moreover, downregulation of NCX3 using NCX3 siRNA sensitized neurons to non-excitotoxic glutamate concentrations, resulting in lethal Ca^{2+} overload (Bano et al., 2005). Together, these findings indicate that abnormal calpain-mediated cleavage of NCX3 plays a pivotal role in excitotoxic neurodegeneration.

As discussed above, calpains are overactive in post-mortem AD brain and in the brain of relevant AD models, where they are associated with the proteolytic degradation of multiple substrates. In a recent study, loss of NCX3 holoprotein was observed in AD parietal cortex compared to controls, suggesting that NCX3 function is impaired in AD (Sokolow et al., 2011). Moreover, NCX3 knockout mice exhibit AD-like deficits in learning and memory, while primary cortical cultures obtained from these mice show reduced LTP, elevated neuronal Ca^{2+} concentrations and reduced Ca^{2+} clearance from neurons (Molinaro et al., 2011, 2013). It was therefore hypothesized here that increased calpain cleavage and disruption of NCX3 function could contribute to neuronal Ca^{2+} overload and death in AD. In support of this hypothesis, increased generation of cleaved NCX3 fragments was observed here in end-stage AD brain compared to control. These NCX3 fragments were characteristic of calpain and caspase cleavage, indicating that NCX3 degradation in AD results from direct calpain proteolysis, and likely

calpain-induced activation of proteolytic caspases (Nakagawa and Yuan, 2000). Interestingly, calpain cleavage of NCX3 was not increased in other neurodegenerative conditions such as PSP, CBD and FTD (Chapter 3), suggesting that calpain-mediated cleavage and inactivation of NCX3 exchangers is somehow selective to AD and may be casually linked to Aβ overproduction. Moreover, NCX1 and NCX2 amounts were found to be unaltered in AD brain, suggesting that other Ca^{2+} transporters are not upregulated to compensate for loss of functional NCX3 in AD.

In addition, the generation of calpain-cleaved NCX3 species was found here to show a strong positive correlation with Aβ burden in AD brain, suggesting that NCX3 cleavage may mediate Aβ neurotoxicity or vice versa. Indeed, NCX3 knockdown in neurons led to their susceptibility to normally subtoxic concentrations of Aβ, resulting in cell death. This was associated with prolonged neuronal Ca^{2+} elevations elicited by Aβ that were abolished in the presence of the calpain inhibitor calpeptin. These findings indicate that calpain-cleavage of Ca^{2+}-regulating proteins, such as NCX3, may contribute to neuronal Ca^{2+} responses to increased Aβ concentrations. When taken together, these findings suggest that calpain cleavage of NCX3 may occur downstream of Aβ and contribute to Ca^{2+} overload in AD. Since calpain is initially activated by high intracellular Ca^{2+}, calpain cleavage of NCX3 could represent an additional step in the vicious cycle of Ca^{2+} dysregulation that occurs in AD whereby reduced clearance and therefore accumulation of excess cytosolic Ca^{2+} stimulates further calpain activation,

cleavage of NCX3 and sustains cellular Ca^{2+} overload. Indeed, NCX3 function is reduced during aging (Michaelis et al., 1984), which together with progressive increases in neuronal Ca^{2+} with aging (Berridge, 2014), could mean that reduced Ca^{2+} clearance mechanisms increase neuronal susceptibility to excitotoxicity and neurodegeneration, particularly in the elderly. Perturbations in glial and neuronal Ca^{2+} are well documented in AD (Lim et al., 2014; Smith et al., 2005); therefore, the results of this work suggest that Aβ-induced calpain activation and cleavage of NCX3 is a novel mechanism that contributes to Ca^{2+} dyshomeostasis in AD.

It is worth mentioning that NCXs may also be disrupted in AD by mechanisms other than increased proteolytic degradation. For instance, NCX3 protein amounts were shown to be reduced in AD parietal cortex, without evidence of increased proteolytic cleavage of NCX3 (Sokolow et al., 2011). The same authors demonstrated that NCX1, NCX2 and NCX3 co-localized with Aβ in synaptic terminals of AD tissue, suggesting a close association between NCXs and Aβ. Indeed, Aβ was found to directly interact with the extracellular hydrophobic loops of NCXs, and resulted in reduced forward mode NCX-mediated Ca^{2+} transport (Wu and Colvin, 1994). Furthermore, NCX3 expression is shown to be subject to specific downregulation via Ca^{2+}-dependent binding of the transcriptional repressor DREAM (also known as calsenilin and KChIP3) to the NCX3 promoter (Naranjo and Mellström, 2012). Physiologically, DREAM corrects intracellular Ca^{2+} levels by inhibiting or promoting Ca^{2+} entry via L-VGCCs or NCX3. Overexpression of DREAM mRNA is a feature of AD brain, the cortex of APP

transgenic mice (APP_{SWE}) and Aβ-treated primary neurons (Jo et al., 2004). The overexpression of DREAM has been shown to lead to apoptosis in cerebellar neurons, at least in part through suppression of NCX3 expression and perturbation of Ca^{2+} homeostasis (Gomez-Villafuertes et al., 2005). These findings suggest that DREAM overexpression in AD brain may account for reductions in NCX3 amounts, and therefore reduced NCX3 function, in AD brain.

There is also some evidence that alterations in NCX function may be neuroprotective in AD. The observation of increased NCX1-3 isoforms by Sokolow et al. (2011) in Aβ-laden synaptosomal preparations of AD tissue, and increased NCX currents in plasma membrane vesicles extracted from AD cortex by Colvin et al. (1994), could signify compensatory responses to Aβ-induced inactivation of NCX-mediated Ca^{2+} transport in diseased brain. In a recent study using PC-12 cells, early Ca^{2+} fluxes induced by Aβ1-42 led to calpain activation and cleavage of NCX3, generating a hyperfunctional form of the antiporter and increased reverse mode NCX currents (Pannaccione et al., 2012). This was paralleled by an increased Ca^{2+} content in the ER, and was suggested to protect cells from the detrimental effects of prolonged Aβ exposure, including depletion of ER Ca^{2+}, ER stress and activation of apoptotic caspases. This adds further support to the hypothesis that rapid and early changes in intracellular Ca^{2+} concentrations and signalling in AD are neuroprotective. Since calpain-1 activity is shown here to be elevated in early stage AD brain, it is possible that these stages also feature cleavage of NCX3 into fragments that either 1) inactivate NCX-mediated Ca^{2+}

clearance or 2) generate neuroprotective NCX currents. Due to the experimental limitations of this study (section 6.2.5), the latter could not be further investigated.

6.1.4 Therapeutic targeting of calpains and NCXs for AD

The findings described in sections 6.1 and 6.2 suggest that modification of calpains and NCX activities, in particular calpain-1 and NCX3, could have therapeutic benefit for the treatment of AD - a possibility which is already avidly discussed in the literature (Rao et al., 2014; Annunziato et al., 2004; Getz, 2012; Noble and Herchuelz, 2007a). Multiple studies, including this work, have demonstrated that inhibiting calpain in cell models of AD rescues Aβ toxicity, through attenuation of several Aβ-induced mechanisms including prevention of protein degradation, excitotoxicity, tau phosphorylation, Aβ production and pro-apoptotic caspase activation (Atherton et al., 2014; Liang et al., 2010; Park and Ferreira, 2005; Hung et al., 2005; Jin et al., 2015; Bano et al., 2007). Moreover, calpain ablation prevents similar neurodegenerative events in mouse models of AD including the 3xTg-AD line and strains of APP mutant mice that all have a well-established AD-like phenotype (Trinchese, Fa et al., 2008; Liang et al., 2010; Getz, 2012). As a result of genetic or pharmacological reduction of calpain activation, these mice display reduced Aβ secretion and plaque load, attenuation of neuroinflammation, and amelioration of synaptic and cognitive deficits. This

indicates that new neuroprotective strategies for the treatment of AD could involve targeting mechanisms upstream of calpain activation in AD (e.g. NMDAR activity, Aβ), calpains directly and/or signalling cascades activated downstream of calpain activation (e.g. caspase activation; Yildiz-Unal et al., 2015). The results of this work also support the hypothesis that calpain activation occurs early in AD, even prior to the deposition of Aβ in plaques and the induction of recognised neurodegenerative cascades. Therefore, detecting and targeting calpain activity during these early disease stages may also have potential as a biomarker for AD diagnosis or for tracking the effectiveness of preventative therapies. However, despite numerous attempts to develop effective calpain inhibitors, none have so far been approved for clinical use (Yuan, 2009). This is likely due to the lack of specificity of existing synthetic calpain inhibitors among other proteolytic enzymes which may not be involved in AD pathogenesis. Moreover, effective calpain therapy would require modification of calpain inhibitors to allow their passage through the blood brain barrier and, most importantly, the specific targeting of brain calpains (Saez et al., 2006). Furthermore, since calpains play numerous vital physiological roles in the CNS and periphery, such as synaptic regulation and cardiac and skeletal muscle function (Sorimachi and Ono, 2012; Wu and Lynch, 2006; Goll et al., 2003), efficacious calpain inhibitors may have serious on-target toxicity leading to many unwanted side-effects. A similar situation arose when trying to develop GKS3 inhibitors as AD therapies (Noble et al., 2013). Furthermore, several studies report increased Aβ production

(Mathews et al., 2002) and depressed synaptic activity (Khoutorsky and Spira, 2009) in response to calpain inhibition, which would also be highly undesirable.

Targeting NCXs for AD therapy may be even less feasible as any potential protective effects from their modulation will depend on the mode of operation (forward or reverse) that predominates. NCX mode is electrochemically driven by relative intracellular Ca^{2+} and Na^{+} concentrations, both of which are altered during normal physiological responses and in neurodegenerative diseases (LaFerla, 2002; Vitvitsky et al., 2012). However, the findings presented in this work, as well as in previous studies (Bi et al., 2012; Iwamoto and Kita, 2006; Brustovetsky et al., 2010a; Brittain et al., 2012), suggest that pharmacologically targeting NCXs may be of therapeutic benefit to AD and, therefore, warrant further investigation. The results demonstrated here in Chapter 3, and previous work by this group (Atherton et al., 2014; Sokolow et al., 2011), indicate that inactivation of forward mode NCX3 exchange by overactive calpain-mediated NCX3 proteolysis may, in part, contribute to Aβ-induced Ca^{2+} dysregulation in AD. In support of this, NCX3 knockout mice show AD-like cognitive and memory phenotypes, as well as disrupted regulation of neuronal Ca^{2+} homeostasis (Molinaro et al., 2011). These findings suggest that restoring forward mode NCX3 function may be neuroprotective in AD. However, inhibition of upstream calpain activity to prevent NCX3 degradation may be more feasible than directly modulating NCX3 protein expression. Furthermore, as NCX3 transcription is regulated by the pro-apoptotic transcriptional repressor DREAM - which is

overexpressed in AD and downregulates NCX3 expression (Jo et al., 2004; Gomez-Villafuertes et al., 2005) - another strategy for restoring normal NCX3 function in AD may be to block DREAM transcriptional repressor activity.

Increased reverse mode NCX activity has been documented to pathologically increase intracellular Ca^{2+} in models of cardiac and neuronal ischaemia, multiple sclerosis and other excitotoxic conditions (Araújo et al., 2007; Gomez-Villafuertes et al., 2005; Noble and Herchuelz, 2007b). NCXs are known to switch to reverse mode in response to membrane depolarization and accumulation of high intracellular Na^{+}, leading to Ca^{2+} entry into the cell. Neuronal hyperexcitability and abnormalities in Na^{+} regulation have been described in AD brain and animal models of disease (Supnet and Bezprozvanny, 2010; Vitvitsky et al., 2012). Therefore, it is possible that increased reverse mode NCX-mediated Ca^{2+} entry could be a pathogenic feature of AD and could therefore represent a potential therapeutic target. However, effective therapy would have to ensure high selectivity for a specific mode of NCXs, which may be possible by designing antibodies or biologics to specific conformations of the receptor. However, the vital physiological functions of NCXs would have to be maintained. While NCX1 is more common in cardiac and kidney cells, it is also implicated in AD neuropathology and increased LOAD risk (Sokolow et al., 2011; Bi et al., 2012). NCX2 and NCX3 are highly expressed in the CNS and could therefore be selectively targeted for AD treatment. In summary, the role, and hence therapeutic potential of targeting NCX isoforms in AD appears to be too complex to be seriously

considered. Any treatment would require a precise balance of effect against forward and reverse mode NCX activities so as to prevent serious detrimental effects.

6.2 PARP and TRPM2 signalling in AD

6.2.1 Mechanisms of PARP-mediated cell death in AD

The PARP family comprises 17 nuclear and cytoplasmic enzymes that orchestrate a host of vital physiological functions, including DNA repair, genomic stability and cell fate (Schreiber et al., 2006). The importance of PARP to normal cell function and survival is demonstrated by its deficiency in the brain during aging - a process which is characterized by increased susceptibility of neurons and glia to DNA damage from oxidative stress, inflammation and metabolic stress (Piskunova et al., 2008; Bürkle et al., 2005; Altmeyer and Hottiger, 2009). In adult brain, moderate levels of oxidative DNA damage trigger activation of DNA-dependent PARP-1, which catalyzes repair of double and single stranded DNA breaks through NAD+-dependent addition of PAR polymers onto target nuclear proteins (PARylation; Luo and Lee Kraus, 2012). PARP-1 knockout mice exhibit hypersensitivity to DNA-damaging stimulants associated with reduced PARP-mediated protein PARylation in the brain (Altmeyer and Hottiger, 2009), and the neuroprotective functions of PARP-1 are compromised in animal models of aging

(Bürkle et al., 2005). However, many neuropathological conditions, including aging, excitotoxicity, inflammation, ischemia and neurodegeneration, feature abnormally increased stimulation of PARP-1 and subsequent induction of cell death mechanisms (Boesten et al., 2013; Mandir et al., 2000; Chaitanya et al., 2010; Ba and Garg, 2011; Strosznajder et al., 2000). The mechanisms by which PARP-1 differentially mediate neuronal death depends on the particular stress stimulus present as well as the metabolic status of the cell (Boulares et al., 1999; Berghe et al., 2010; Chaitanya et al., 2010). Multiple studies, including the work presented in this thesis, suggest that PARP-1 plays a critical role in mediating neuronal death in AD, through induction of both necrotic and apoptotic cell death cascades (Love et al., 1999; Fonfria et al., 2005; Abeti et al., 2011).

Necrosis is 'accidental' cell death, resulting from cellular damage and metabolic failure from oxidative insults (Golstein and Kroemer, 2007), and is observed in AD brain and models of AD-associated neurodegeneration (Behl, 2000). Immunohistochemical analysis of temporal and hippocampal tissue from terminal FAD patients bearing the PS1 E280A mutation shows morphological changes characteristic of necrotic cell death (Velez-Pardo et al., 2001), accompanied by severe plaque deposition, gliosis and NFTs. Moreover, Aβ is shown to induce both PARP activation, as shown here and in previous studies (Fonfria et al., 2005; Abeti et al., 2011), and necrotic cell death in PC-12 cells via activation of IL-1β converting enzyme (Suzuki, 1997). Therefore, these findings suggest that PARP-mediated necrosis can be a downstream effect of Aβ

accumulation in AD. Increased PARP-1 activity can also lead to necrosis upon depletion of the PARP substrate, NAD+, which requires excess consumption of cellular ATP for resynthesis, thereby leading to deficits in the available energy for remaining cellular functions (Ha and Snyder, 1999). Necrosis can also be initiated by dysregulated activation of cellular proteases, including cytosolic calpains and caspases and lysosomal cathepsins (Liu et al., 2004, 2009). Differential cleavage of PARP by proteases is reported to be an integral initiating step in necrotic and apoptotic cascades, and is therefore used experimentally to differentiate between these types of cell death (Table 6.1; Chaitanya et al., 2010).

In the data presented in this thesis, increased proteolytic cleavage of PARP-1 was observed in moderate to late stage AD brain, suggesting a potential role for PARP-1 in mediating the neuronal loss that occurs as AD progresses. Moreover, the fragments generated from full-length PARP-1 were 89 kDa, indicating caspase-3-/7- and cathepsin-B/-D cleavage, and 75 kDa - characteristic of cathepsin-G and calpain-1 cleavage, suggesting that a range of proteolytic enzymes are increased in AD brain. In support of this, age-related depletion of lysosomal and autophagic activities is link with programmed neuronal necrosis in LOAD, and is shown to be driven by calpain-mediated cleavage of lysosomal compartments to release proteolytic cathepsins (Yamashima, 2013). The findings here may therefore provide further support to previous publications reporting the activation of necrotic cell death pathways in AD (Velez-Pardo et al., 2001; Suzuki, 1997; Behl,

2000; Yamashima, 2013), and the involvement of several proteases for protein degradation in AD.

Calpains and caspases are also key mediators of apoptosis – programmed cell death that can be triggered by PARP in cases of irreparable oxidative DNA damage (Nakagawa and Yuan, 2000; Behl, 2000; Porter and Jänicke, 1999; Scovassi and Poirier, 1999; Boulares et al., 1999). Cleavage and inactivation of PARP-1 by caspases, and therefore inhibition of DNA repair, is important in preventing cell survival, and is considered to be a hallmark of apoptosis in these circumstances (Kaufmann et al., 1993). It is possible, therefore, that the increased generation of presumed caspase- and calpain-cleaved PARP species observed in this work in moderate to late stage AD brains may be indicative of apoptotic cell death in these samples. Previous findings have shown that caspase-3 cleavage of PAPR-1 is an important regulator of early synaptic dysfunction in AD (D'Amelio et al., 2011). However, the activity of caspase-3, as determined by measurement of cleaved caspase-3 species, was not globally altered here in any stage of AD brain when compared to control. This is in agreement with previous findings that only 'exceptional' neurons label with antibodies against active caspase-3 in AD brain (Jellinger and Stadelmann, 2000). Moreover, PARP cleavage products were not observed in early stage AD brain, although it is possible that the amounts of these cleavage fragments may have been below the detection threshold in these samples. Thus, it is possible that an increase in apoptotic cell death seen here during progression of AD - as suggested by generation of calpain-cleaved species

- may have occurred independently of caspase-3. Indeed, PARP-1 has been widely shown to play a pivotal role in a caspase-independent form of apoptosis, termed 'parthanatos' (Wang et al., 2009, 2010). This involves PAR polymer-mediated release of mitochondrial AIF and its translocation to the nucleus, which results in DNA fragmentation and neuronal death (Wang et al., 2009). PARP-dependent accumulation of nuclear AIF is observed in cerebral slice cultures treated with Aβ, suggesting that parthanatos may be important for Aβ neurotoxicity (Adamczyk et al., 2005). Although it was not possible to study AIF protein amounts or localization here in either AD brain or Aβ-treated neurons due to time restraints, Aβ and H_2O_2 neurotoxicity was found to be associated with DNA fragmentation, which suggests that Aβ-induced oxidative DNA damage may have triggered AIF and PARP-dependent parthanatos in these cultures.

Table 6.1 lists the proteolytically generated PARP fragments that are relevant to this work.

6.2.2 Mechanisms of Aβ-induced activation of PARP-1

Aβ has been shown to induce astrocytic and neuronal PARP-1 activation in animal and cell models of AD (Fonfria et al., 2005; Abeti et al., 2011; Strosznajder et al., 2000); however, the mechanisms by which Aβ activates PARP-1 are not fully understood. Multiple studies have demonstrated that Aβ induces oxidative DNA damage, which is coupled with lethal upregulation of PARP-1 in cultured neurons

Protease	*PARP fragment and size (kDa)*
Caspase-3 and -7	24 kD N-terminal fragment and 89 kD C-terminal fragments
Calpain-1	~70-40 kD N-terminal fragments
Cathespsin-B and -D	89, 74, 62 kD N-terminal fragments and 55, 44 kD C-terminal fragments
Cathespsin-G	74, 62 N-terminal fragments and 55, 44 kD C-terminal fragments

Table 6.1 Describing the cleavage products of PARP. PARP is subject to differential proteolytic cleavage by caspases, calpains and cathepsins during apoptotic and necrotic cell death. Generation of 89 and 75 kDa PARP fragments was observed here in AD brain, potentially implicating both necrotic and apoptotic mechanisms of cell death in AD. It is worth noting that PARP is also subject to cleavage by granzymes and matrix metalloproteases; however, characteristic PARP fragments generated by the action of these proteases were not observed in AD brain in this work (adapted from Chaitanya et al., 2010)

and astrocytes (Canevari et al., 2004; De Felice et al., 2007; Fonfria et al., 2005). These observations are corroborated by the current study, which shows that Aβ neurotoxicity features DNA fragmentation and accumulation of nuclear PAR - a marker of increased PARP activity. These effects were also observed here in H_2O_2-treated neurons, which could therefore suggest that Aβ-induced increased in PARP-1 activity are mediated by induction of oxidative stress responses. Indeed, oxidative DNA damage is considered as the primary trigger of PARP activity. Consistent with this, the activity of PARP and oxidative stress markers are reported to be significantly elevated in APP mutant mice which display

substantial Aβ over-production and develop amyloid pathology in old age, and in end-stage AD brain (Butterfield et al., 2001, 2010; Abeti et al., 2011; Love et al., 1999). Moreover, Butterfield et al. (2001) and others (Wang et al., 1999; McLean et al., 1999) have demonstrated that oxidative damage to DNA, neuronal lipids, and other proteins markers, are directly related to the presence of Aβ plaques, and also show strong positive correlations with soluble Aβ amounts. Therefore, Aβ-induced oxidative DNA damage is likely to be the primary cause of increased PARP-1 activity in AD.

Aβ-induced oxidative DNA damage and cell stress is proposed to occur through activation of neuronal and astrocytic NADPH oxidase, phospholipase A2 (Simonyi et al., 2010; Abeti et al., 2011) and nitric oxide synthase (Kim and Koh, 2002), as well as redox reactions between Aβ peptides and cellular transition metals, in particular Cu^{2+} (Su et al., 2008). The resultant generation of ROS and H_2O_2 disrupts cellular metabolism and causes DNA damage, which in turn triggers the activation of PARP-1. Of interest, Cu^{2+} dyshomeostasis has been widely observed in AD models as a correlate of oxidative stress (Eskici and Axelsen, 2012); therefore, it could be an important factor in PARP-1 signalling in AD.

There is substantial evidence to implicate oxidative stress pathways in PARP-1 mediated cell death. Treatment of mouse embryonic fibroblasts with H_2O_2 induces nuclear translocation of c-Jun-N-terminal kinase 1 (JNK1) and JNK1-mediated phosphorylation of PARP-1, followed by activation of parthanatos and cell death

(Zhang et al., 2007). Since Aβ neurotoxicity is associated with the activation of tau protein kinases such as GSK3 and cdk5 (Chapter 4; Zempel et al. 2010; Town et al. 2002), it may be interesting to investigate whether these kinases are also involved in the activation of PARP-1, which may reveal a novel neurodegenerative cascade in AD. In partial support of this idea, GSK3 is reported to phosphorylate and activate nuclear tankyrases - a family of PARPs involved in spindle assembly during mitosis (Yeh et al., 2006). On the other hand, tau kinases are possibly more likely to stimulate PARP-1 activation indirectly; for example, through GSK3-mediated activation of calpain-1 (Crespo-Biel et al., 2010), or signalling downstream respiratory stress and oxidative DNA damage (Brustovetsky et al., 2010a).

Importantly, Aβ oxidative DNA damage and subsequent PARP-1 overactivation appears to be important for Aβ-induced Ca^{2+} dyshomeostasis and neurotoxicity, since inhibition of PARP-1 by SB750139 here, and in previous studies (Atherton et al. unpublished; Fonfria et al., 2005; Vosler et al., 2009; Abeti et al., 2011), prevented abnormal Ca^{2+} elevations and neuronal death. Therefore, targeting Aβ-dependent mechanisms of PARP-1 activation may represent a promising therapeutic approach for the treatment of AD.

6.2.3 The role of PARP-mediated TRPM2 activation in Aβ excitotoxicity

Oxidative stress has been shown to induce Ca^{2+} dyshomeostasis through aberrant PARP signalling (Aarts and Tymianski, 2005; Uttara et al., 2009; Mattson, 2002). Increased PARP activity leads to accumulation of nuclear PAR, which is in turn hydrolysed by PARG into free ADPR and translocated to other cellular compartments (Blenn et al., 2011). Binding of free ADPR in the cytosol to the C-terminal cytoplasmic Nudix motif of the neuronally expressed TRPM2 channel (Peraud et al., 2001; Fonfria et al., 2004) is believed to be the most potent physiological activator of this non-selective and redox-sensitive cation channel (Fig. 6.2; Naziroğlu, 2011; Sumoza-Toledo and Penner, 2011). ADPR-mediated prolonged activation of TRPM2 channels then allows dysregulated influx of Ca^{2+} (Xie et al., 2010; Naziroğlu, 2011). Considerable research has implicated PARP-TRPM2 signalling in excitotoxic Ca^{2+} elevations in AD. Fonfria et al. (2005) have shown Aβ and H_2O_2 mediate cell death in rat striatal cultures endogenously expressing TRPM2. Transfection of cultures with the dominant negative TRPM2 isoform, TRPM2-S, which blocks TRPM2 function (Zhang et al., 2003), prevented Aβ-induced increases in intracellular Ca^{2+} and neurotoxicity in these cultures.

The same was observed when cultures were transfected with siRNA targeting TRPM2, which reduced TRPM2 mRNA levels and uncontrolled Ca^{2+} fluxes. Treatment of striatal neurons with the PARP inhibitor SB750139 also prevented

Aβ- and H_2O_2-induced excitotoxic Ca^{2+} elevations and cell death in this culture model. Therefore, increased PARP-mediated TRPM2 activation appears to play a key role in Ca^{2+}- mediated neuronal death that is triggered by Aβ- and H_2O_2-induced oxidative stress.

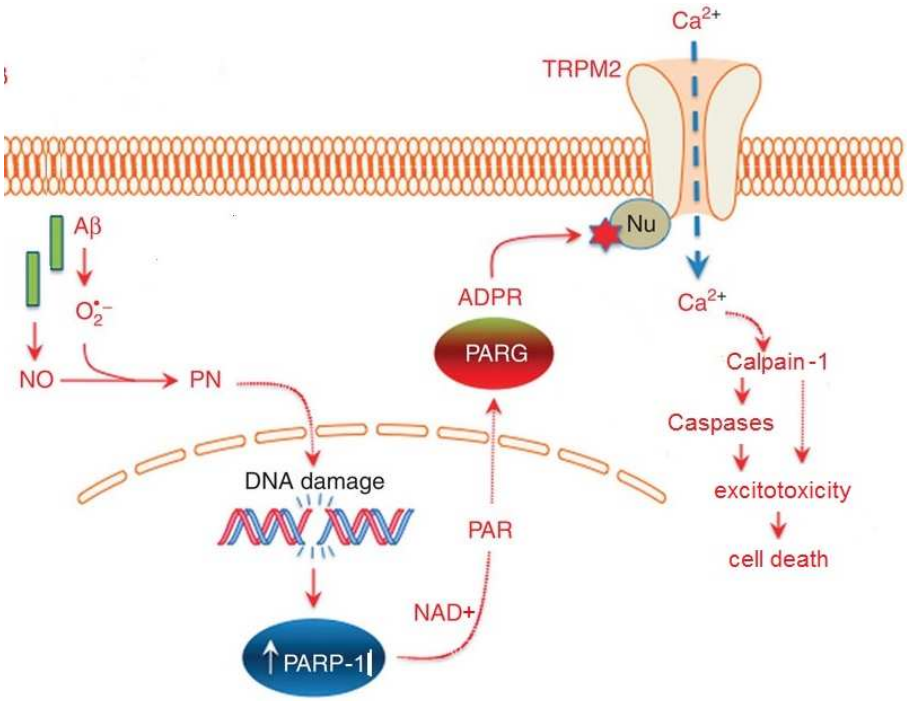

Figure 6.2 PARP-1 mediated TRPM2 channel opening leads to cell death. Aβ interaction with intracellular transition metals causes generation of reactive oxygen species, such as superoxide radicals (O_2-) which reacts with constitutive nitric oxide (NO), generating peroxynitrite (PN). PN causes DNA damage, which activates the nuclear DNA repair enzyme, PARP-1. PARP-1 utilizes nicotinamide adenine dinucleotide (NAD+) to catalyze polymerisation of PAR with nuclear target molecules. PAR is in turn hydrolysed by PARG into free ADPR, which in the cytoplasm activates plasma membrane TRPM2 channels by binding to the Nudix (Nu) moiety of TRPM2. Activation of TPRM2 causes channel opening and entry of Ca^{2+} into the cell. Prolonged activation of PARP and TRPM2 leads to accumulation of cytosolic Ca^{2+} and activation of calpain-1 and caspases, which further disrupt intracellular Ca^{2+} regulation to result in excitotoxicity and cell death(adapted from Park et al., 2014).

The work presented in this thesis confirms and extends these previous findings by showing that prolonged Ca^{2+} elevations induced by Aβ in neural cells are abolished by pre-treatment of cells with the PARP inhibitor SB750139. Interestingly, SB750139 did not appear to affect the initial Aβ-induced Ca^{2+} increase, which occurs within 60 seconds of treatment, but was effective in preventing subsequent elevations in Ca^{2+} that are seen to occur within 10 min of Aβ treatment. This profile of Ca^{2+} flux was not observed when cultured were pre-treated with inhibitors of NMDARs, calpains and caspases prior to application of Aβ - all of these agents significantly reduced the initial Aβ-elicited Ca^{2+} peak. It is therefore plausible that PARP and TRPM2 could be activated downstream of NMDAR-mediated induction of calpain and caspases during the initial phase of intracellular Ca^{2+} increases, and that they then contribute to the sustained Ca^{2+} elevations that are recognised to be required for neuronal death (Brustovetsky et al., 2010a; Brittain et al., 2012). On the other hand, activation of TRPM2 in human monocytes was previously shown to activate caspases and result in cleavage of PARP (Zhang et al., 2006). Moreover, increased TRPM2-mediated cytosolic accumulation is likely to trigger further calpain-1 activity and downstream signalling cascades that would lead to calpain-mediated cleavage of many important regulatory proteins (Chapter 4). It is therefore possible that aside from increasing Ca^{2+} influx, TRPM2 may also 1) mediate neuronal death through caspase-dependent or caspase-independent apoptotic signalling, 2) further increase NMDAR-induced calpain-1 activity or 2) prevent further activation of

TRPM2 through caspase-mediated cleavage and inactivation of nuclear PARP in AD. The latter may be suggested here by evidence of increased generation of 89 kDa caspase-cleaved PARP fragments in moderate and severe AD brain. However, protein expression of both functional and inactive (TRPM2-S) TRPM2 isoforms were unchanged in AD brain compared to control. Therefore, further investigation in cell and animal models of AD is required to ascertain the mechanisms by which PARP-TRPM2 signalling leads to neurodegeneration in AD.

Importantly, several studies have shown that activation of PARP and TRPM2 is important in glial inflammatory responses in AD. Perturbations of glial Ca^{2+} homeostasis and signalling are widely described in AD (Lim et al., 2014; Grolla et al., 2013; Alberdi et al., 2013; Verkhratsky et al., 2010), are shown to be induced by Aβ (Atherton et al. unpublished; Grolla et al. 2013; Abramov et al. 2004; Kuchibhotla et al., 2009), and involve activation of glial PARP and metabolic disruption (Abeti et al., 2011; Kauppinen et al., 2011). For instance, microglial PARP activity was shown to be important for Aβ-mediated microglial activation in double transgenic APP mutant/PARP knockout mice and in Aβ-treated mixed microglial and neuronal cultures (Kauppinen et al., 2011). This group has also shown that Aβ-induced activation of astrocytes leads to neuronal increases in tau phosphorylation and neuronal death through the action of astrocyte-secreted inflammatory cytokines and chemokines (Garwood et al., 2011). Moreover, Aβ-induced astrocytic secretion of TNFα was shown to be vital for Aβ toxicity and PARP-mediated neuronal Ca^{2+} overload (Chao and Hu, 1994; Boulares et al.,

2001). Therefore, the influence of glia in Aβ-induced neurotoxic Ca^{2+} overload cannot be discounted.

The primary cortical cultures used in this work contain negligible numbers of microglia (Chapter 4 and Garwood et al. 2011); therefore, it is unlikely that any Aβ mediated effects in neurons were mediated by microglial PARP in this work. On the other hand, characterization of primary cultures in this study showed approximately 17 % of cultured neural cells were astrocytes. Therefore, it is possible that treatment of cultures with Aβ could have triggered activation of astrocytic PARP and downstream neuronal damage, as shown by Abeti and colleagues (2011). However, Aβ-induced upregulation of PARP appeared to be selectively localized to neurons and was lacking in GFAP-positive astrocytes in the current study. Accordingly, TRPM2 immunoreactivity was also observed in neurons but not in astrocytes. Therefore, to ascertain whether astrocytic PARP may mediate Aβ neurotoxicity in this cell system, further work in astrocytic/neuronal co-cultures or in neurons treated with inflammatory factors, such as TNFα and IL-1β, would be required.

6.2.4 Therapeutic targeting of PARP-1 and TRPM2 in AD

The findings presented here suggest that inhibitors of PARP and TRPM2 may have therapeutic potential for the treatment of AD, since the PARP inhibitor SB750139

attenuated Aβ-induced DNA damage, intraneuronal Ca^{2+} elevations and neurotoxicity in the cell culture systems used here. Similar findings were also previously reported by Fonfria et al. (2005), who first demonstrated the importance of PARP-mediated TRPM2 activation for Aβ neurotoxicity. Therapies based on inhibiting PARP-1 may be especially relevant since numerous PARP-1 inhibitors have shown promise as cancer therapies. PARP-1 inhibitors show good safety and tolerability profiles, suggesting that the clinical use of such compounds is a possibility (Mégnin-Chanet et al., 2010; Davar et al., 2012).

It is likely that such therapies may be more effective in moderate and severe AD, since the pathogenic role of PARP in these stages appeared to be more prominent in the later stages of disease as judged by increased markers of PARP-mediated apoptotic and necrotic cell death in Braak IV-VI AD tissue compared to control. However, the benefits that could be gained from treating later stage disease, when much irreparable synaptic and neuron damage has already taken place is likely to be limited. Nevertheless, since previous studies have suggested a role for astrocytic and microglial PARP signalling in AD (Abeti et al., 2011; Tang et al., 2010; Kauppinen et al., 2011), PARP inhibition may represent a novel mechanisms by which neuroinflammatory processes may be attenuated in AD. However, due to evidence of both pathogenic and neuroprotective roles for neuroinflammatory responses in AD (Verkhratsky et al., 2010; Bélanger and Magistretti, 2009; Wyss-Coray, 2006), it is unclear whether targeting these responses is a viable strategy.

Another important consideration in targeting PARP for AD therapy is whether this treatment will be associated with any serious side effects since PARP carries out a plethora of important physiological functions including DNA repair, regulation of immune responses and suppression of tumorigenesis (Swindall et al., 2013; Davar et al., 2012; Bürkle et al., 2005; Chaitanya et al., 2010). However, SB750139, used here to inhibit PARP in cell models of AD, is already used for cancer therapy (Davar et al., 2012), without evidence of any adverse side effects. Moreover, the anti-inflammatory agent minocycline, also a potent inhibitor of PARP is currently used as an antibiotic and anti-acne treatment and, despite showing broad spectrum effects in the CNS, is not associated with any serious side effects (Plane et al., 2010). However, clinical testing of minocycline for neurodegenerative conditions, such as Parkinson's disease, have not yielded promising results (Plane et al., 2010). The reason for this could be a complex 'double-edged sword' role for PARP in conditions associated with neurodegeneration. PARP deficiency is shown to accelerate ageing (Piskunova et al., 2008; Bürkle et al., 2005); however, PARP is also shown to be hyperactive and accelerate neuronal death in response to excess oxidative stress in AD (Love et al., 1999; Abeti et al., 2011; Fonfria et al., 2005), for which ageing is the most prominent risk factor in sporadic cases. On the other hand, chronic oxidative stress and PARP-1 activation are also implicated in neuronal death in ageing (Boesten et al., 2013) and PARP is overactive in aged animals with endothelial dysfunction (Pacher et al., 2002). It is therefore clear that induction of PARP-mediated apoptotic cell death or DNA repair and cell

survival depends on multiple factors, such as the strength and type of stress stimulus, and therefore fine-tuning of PARP activity may be more beneficial for the treatment of AD rather than outright PARP inhibition.

As an alternative to PARP inhibition, another potential therapeutic strategy may be to directly target TRPM2 channels, either by blocking channel opening or reducing the levels of functional TPRM2s. Indeed, there is substantial evidence to support the role for TPRM2 in neuronal death induced by oxidative stress and Aβ in AD and other neurodegenerative disorders (McNulty and Fonfria, 2005a; Fonfria et al., 2005; Xie et al., 2010; Lee et al., 2013; Miller, 2004). Moreover, the neuroprotective effect of TRPM2 ablation together with the absence of an overt phenotype in TRPM2 knockout mice (Yamamoto et al., 2008) serves as evidence of the feasibility of anti-TRPM2 therapy in AD. However, none of the currently used TRPM2 inhibitors show TRPM2 specificity (Sumoza-Toledo and Penner, 2011; Naziroğlu, 2011) as the C-terminal Nudix domain (containing the channel activation site) is shared by TRPM2 and other TRP subtypes; thus, they may cause adverse side effects associated with inhibition of other TRP channels. Moreover, TRPM2 is shown to heterodimerize with other TRP subtypes, such as TRPM7; although the role of TRPM7 in AD is gaining interest (Naziroğlu, 2011). Therefore, development of more specific TRPM2 inhibitors and further investigation into the differential roles of different TRP subtypes to neuronal death may yield some promising new therapeutic targets.

6.2.5 Limitations of this work

Throughout this project, best efforts were taken to ensure that the experimental work carried out was well designed, planned and controlled. However, it is important to highlight some of the limitations of this work.

The relationship between Ca^{2+}-associated proteins and pathogenic mechanisms in AD was investigated here in post mortem tissue from individuals with different stages of AD, related neurodegenerative conditions (CBD, PSP, and FTD) and age-matched controls. While a relatively large number of end-stage AD cases were investigated, there were limited numbers (between 3 and 5) of samples available from early and moderate AD cases, CBD, PSP and FTD cases. Due to the high variability associated with LOAD pathology and post mortem tissue, analysis of larger sample sizes for each condition would yield more accurate results, by showing whether there is consistency in subtle protein changes between samples. Since less is currently known about the early neurodegenerative mechanisms in AD - which may be important for preventative and diagnostic strategies – having increased availability of early stage Braak tissue would have been especially helpful for this work. Furthermore, although no correlation between protein changes and post mortem delay in AD tissue was detected here, it is still possible that protein degradation during post mortem delay may have affected protein amounts in samples. For example, calpains are shown to be activated post mortem (Gandolfi et al., 2011) and amounts of calpain-cleaved cdk5 activator, p25, are

considered to be only accurate in tissue with a post mortem delay of less than 25 h (Engmann et al., 2011). However, although care was chosen to select cases in which tissue integrity was believed to be maintained as much as possible, the handling of post-mortem brain tissue was ultimately outwith the control of our group.

Western blotting of post-mortem brain and neuronal lysates treated with Aβ and/or compounds allowed the quantitative comparison of Ca^{2+}-associated protein amounts between different conditions, as well as identification of any post-translational modifications to proteins e.g. tau truncation and phosphorylation and APP glycosylation. However, this method did not allow for the assessment of changes in Ca^{2+} binding, protein-protein interactions, protein function or subcellular localization. For instance, it would be interesting to investigate whether the prolonged activation of calpains in AD brain or Aβ-treated neurons results from reduced interaction of calpains with CAST and increased calpain translocation to cell membranes, as suggested by Goll et al. (2003). Furthermore, since animal and cell models of AD feature increased TRPM2 activity, and hence Ca^{2+} overload, it would be worth investigating whether this alters TRPM2 localization - for instance, leading to compensatory TRPM2 internalization. TRPM2 and NCX3 currents are proposed to be altered in AD, which is indirectly evidenced here by the inhibition of Ca^{2+} transients in Aβ-treated neurons by the PARP inhibitor SB750139 and by the increased vulnerability of neurons to subtoxic Aβ concentrations following NCX3

knockdown. However, a more accurate and direct way of measuring changes in TRPM2 and NCX3 Ca^{2+} conductance in AD would be to perform electrophysiological analysis of post mortem AD tissue slices, which are shown to remain alive for several weeks in culture (Verwer et al., 2002). This could also be done in organotypic brain slices from APP mutant mice or in wild-type slices treated with Aβ and calpain inhibitors. Although the techniques required to make long-term organotypic slice cultures from transgenic animals (but not post-mortem AD brain) were available in the laboratory, these is a technically demanding and very time consuming technique, and unfortunately constraints with time and resources meant that such experiments could not be incorporated into this work.

The Ca^{2+} imaging experiments performed here provided direct measurement of Ca^{2+} dynamics in response to treatment with Aβ and compounds, including inhibitors of PARP, calpains, caspases and NMDARs. However, due to some technical difficulties, images could only be recorded for up to 10 min without photobleaching of the signal. This was associated with the use of Fluo-4 Ca^{2+} indicators here; use of another type of dye, such as Fura-2, was not possible due to issues with the live-imaging equipment with capabilities for ratiometric imaging. Unfortunately, these difficulties were not overcome in time for this equipment to be used in this work. If these technical issues had been surpassed, it would have been worth conducting longer term imaging experiments, as previous studies have reported important changes in Ca^{2+} concentrations in

neurons undergoing Ca^{2+}-mediated excitotoxicity from 15 minutes to 1 hour following treatment of cells with glutamate or Aβ (Atherton et al. unpublished; Brustovetsky et al., 2010a; Bano et al., 2005). Nevertheless, the data presented in this thesis were sufficient to demonstrate the effects of Aβ on neural cell Ca^{2+} dynamics.

6.3 Summary

In summary, the findings in this thesis yield some interesting insights into the role of Ca^{2+}-sensitive pathways during the progression of AD, and they also demonstrate a novel mechanism of Ca^{2+} dysregulation that may contribute to Aβ-induced neuronal death in AD. Investigation of protein changes in post mortem neurodegenerative and control brains confirmed previous reports of increased Ca^{2+}-activated calpain-1 activity in end-stage AD and other neurodegenerative conditions, such as CBD and FTD, when compared to age-matched control brain. These findings were then furthered by the demonstration that calpain-1 activity is aberrantly increased in early AD brain and that these elevations are sustained throughout the progression of AD. The early increases in calpain-1 activity were associated with increased protein amounts of the endogenous calpain inhibitor CAST and in major pre- and postsynaptic proteins. These changes may be indicative of a possible early neuroprotective response to excess calpain-1 activity in the very early stages of AD development. However, loss of CAST activity

and synaptic markers in end-stage AD brain, along with increased calpain-mediated degradation of the cytoskeletal protein α-spectrin and the Ca^{2+} extrusion pump NCX3, indicated sustained and prominent effects of calpain-1 activation and proteolysis of key signalling, structural and Ca^{2+}-regulating proteins in these tissues. Notably, calpain-mediated cleavage of NCX3 was only observed in AD tissue, in correlation with increased Aβ production, and knockdown of NCX3 conferred neuronal vulnerability to normally subtoxic concentrations of Aβ in primary cultures. Therefore, Aβ-induced calpain activation and cleavage of NCX3 may represent a novel mechanism by which elimination of excess cell Ca^{2+} is perturbed and contributes to neuronal Ca^{2+} dyshomeostasis in AD.

The early increase in calpain-1 activity in post mortem AD brain was also observed to occur prior to Aβ overproduction, activation of the tau kinases GSK3 and cdk5, increased tau phosphorylation, and synapse loss. Further investigations in cell systems, using the synthetic calpain inhibitor, calpeptin, were then carried out to show that calpain-1 activity is causally linked to these pathological changes. Inhibition of calpain with the chemical inhibitor calpeptin attenuated Aβ-induced Ca^{2+} elevations, GSK3 and cdk5 activation, tau phosphorylation and also altered APP processing, Aβ production and synaptic protein expression, independently of Aβ. Furthermore, Aβ-induced Ca^{2+} dysregulation and neurotoxicity were, at least in part, attributed to abnormal activation of PARP and TRPM2 signalling. The increased involvement of PARP in apoptotic cell death was also seen in moderate

and severe AD brain. To conclude, the data presented here add further support to the notion that Ca^{2+} dysregulation is an important early pathogenic event in AD, and that targeting key steps in Ca^{2+}-mediated neurodegenerative signalling cascades may have potential for the treatment of AD and related neurodegenerative diseases. Figure 6.3 summarizes the findings in this work.

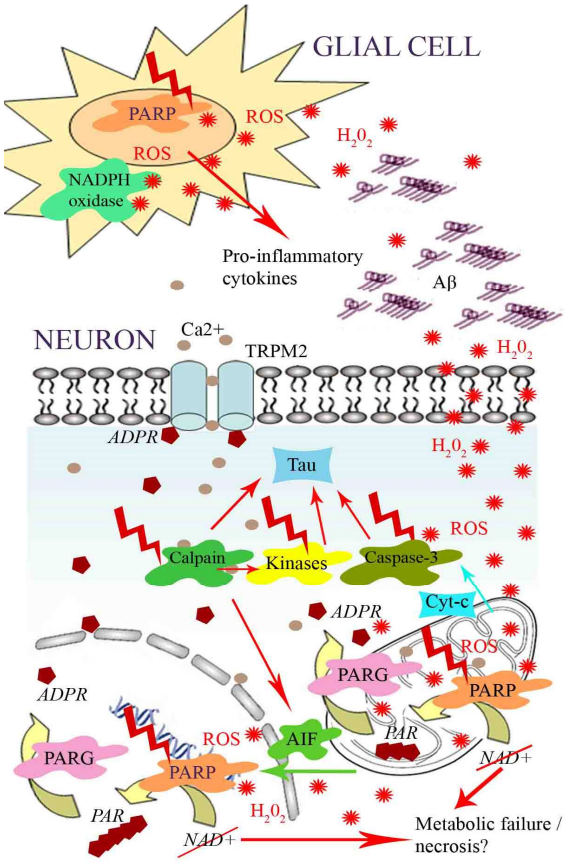

Figure 6.3. Proposed mechanisms of Ca^{2+}-mediated neurotoxicity in AD. Aβ induces astrocytic and neuronal DNA damage, which hyperactivates PARPs. In neurons, this leads to the production of PAR from NAD+, and subsequently ADPR via PARG hydrolysis of PAR. Free ADPR then mediates neuronal Ca^{2+} overload by excess stimulation of TRPM2. This causes prolonged calpain activation, mitochondrial Ca^{2+} overload and pro-apoptotic caspase signalling. Direct cleavage of tau is mediated by these proteases, and calpain-mediated AIF cleavage and translocation to the nucleus initiates 'parthanatos'. PARP activation could also result in excessive depletion of NAD+, which could mediate necrotic death through metabolic failure. PARP-mediated activation of glial cells could also exacerbate neuronal demise through promoting the production of pro-inflammatory cytokines.

References

Aarts, M. M. and Tymianski, M. (2005) TRPMs and neuronal cell death. *Pflugers Archiv European Journal of Physiology*. **451**, 243–249.

Abeti, R., Abramov, A. Y. and Duchen, M. R. (2011) Beta-amyloid activates PARP causing astrocytic metabolic failure and neuronal death. *Brain*. **134**, 1658–1672.

Abramov, A. Y., Canevari, L. and Duchen, M. R. (2004) Calcium signals induced by amyloid beta peptide and their consequences in neurons and astrocytes in culture. *Biochimica et Biophysica Acta - Molecular Cell Research*. **1742**, 81–87.

Ackerley, S., Grierson, A. J., Brownlees, J., Thornhill, P., Anderton, B. H., Nigel Leigh, P., Shaw, C. E. and Miller, C. C. J. (2000) Glutamate slows axonal transport of neurofilaments in transfected neurons. *Journal of Cell Biology*. **150**, 165–175.

Adamczyk, A., Czapski, G. A., Jęśko, H. and Strosznajder, R. P. (2005) Non-Aβ component of Alzheimer's disease amyloid and amyloid beta peptides evoked poly(ADP-ribose) polymerase-dependent release of apoptosis-inducing factor from rat brain mitochondria. *Journal of Physiology and Pharmacology*. **56**, 5–13.

Adamec, E., Mohan, P., Vonsattel, J. P. and Nixon, R. A. (2002) Calpain activation in neurodegenerative diseases: Confocal immunofluorescence study with antibodies specifically recognizing the active form of calpain 2. *Acta Neuropathologica*. **104**, 92–104.

Ahmed, M., Davis, J., Aucoin, D., Sato, T., Ahuja, S., Aimoto, S., Elliott, J. I., Van Nostrand, W. E. and Smith, S. O. (2010) Structural conversion of neurotoxic amyloid-beta(1-42) oligomers to fibrils. *Nature structural and molecular biology*. **17**, 561–567.

Akama, K. T. and Van Eldik, L. J. (2000) β-Amyloid Stimulation of Inducible Nitric-oxide Synthase in Astrocytes Is Interleukin-1β- and Tumor Necrosis Factor-α (TNFα)-dependent, and Involves a TNFα Receptor-associated Factor- and NFκB-inducing Kinase-dependent Signaling Mechanism. *Journal of Biological Chemistry* . **275**, 7918–7924.

Alberdi, E., Sánchez-Gómez, M. V., Cavaliere, F., Pérez-Samartín, A., Zugaza, J. L., Trullas, R., Domercq, M. and Matute, C. (2010) Amyloid β oligomers induce Ca2+ dysregulation and neuronal death through activation of ionotropic glutamate receptors. *Cell Calcium*. **47**, 264–272.

Alberdi, E., Wyssenbach, A., Alberdi, M., Sánchez-Gómez, M. V., Cavaliere, F., Rodríguez, J. J., Verkhratsky, A. and Matute, C. (2013) Ca2+-dependent endoplasmic reticulum stress correlates with astrogliosis in oligomeric amyloid β-treated astrocytes and in a model of Alzheimer's disease. *Aging Cell*. **12**, 292–302.

Alim, I., Teves, L., Li, R., Mori, Y. and Tymianski, M. (2013) Modulation of NMDAR subunit expression by TRPM2 channels regulates neuronal vulnerability to ischemic cell death. *The Journal of neuroscience : the official journal of the Society for Neuroscience*. **33**, 17264–17277.

Altmeyer, M. and Hottiger, M. O. (2009) Poly(ADP-ribose) polymerase 1 at the crossroad of metabolic stress and inflammation in aging. *Aging*. **1**, 458–469.

Amadoro, G., Serafino, A. L., Barbato, C., Ciotti, M. T., Sacco, A., Calissano, P. and Canu, N. (2004) Role of N-terminal tau domain integrity on the survival of cerebellar granule neurons. *Cell death and differentiation*. **11**, 217–230.

Andrabi, S. A., Kim, N. S., Yu, S.W., Wang, H., Koh, D. W., Sasaki, M., Klaus, J. A., Otsuka, T., Zhang, Z., Koehler, R. C., Hurn, P. D., Poirier, G. G., Dawson, V. L. and Dawson, T. M. (2006) Poly(ADP-ribose) (PAR) polymer is a death signal. *Proceedings of the National Academy of Sciences of the United States of America*. **103**, 18308–18313.

Annunziato, L., Pignataro, G. and Di Renzo, G. F. (2004) Pharmacology of Brain Na+/Ca2+ Exchanger: From Molecular Biology to Therapeutic Perspectives. *Pharmacological Reviews*. **56**, 633–654.

Araújo, I. M., Carreira, B. P., Pereira, T., Santos, P. F., Soulet, D., Inácio, A., Bahr, B. A., Carvalho, A. P., Ambrósio, A. F. and Carvalho, C. M. (2007) Changes in calcium dynamics following the reversal of the sodium-calcium exchanger have a key role in AMPA receptor-mediated neurodegeneration via calpain activation in hippocampal neurons. *Cell death and differentiation*. **14**, 1635–1646.

Arendt, T. (2009) Synaptic degeneration in Alzheimer's disease. Acta *Neuropathologica.* **118**, 167–179.

Arriagada, P. V, Growdon, J. H., Hedley-Whyte, E. T. and Hyman, B. T. (1992) Neurofibrillary tangles but not senile plaques parallel duration and severity of Alzheimer's disease. *Neurology*. **42**, 631–639.

Arsene, D. and Ardeleanu, C. (2010) Neurodegenerative changes in human aging brain. An autopsy study. *Rom.J.Morphol.Embryol.* **51**, 55–60.

Atherton, J., Kurbatskaya, K., Bondulich, M., Croft, C. L., Garwood, C. J., Chhabra, R., Wray, S., Jeromin, A., Hanger, D. P. and Noble, W. (2014) Calpain cleavage and inactivation of the sodium calcium exchanger-3 occur downstream of Aβ in Alzheimer's disease. *Aging Cell*. **13**, 49–59.

Atwood, C. S., Martins, R. N., Smith, M. A. and Perry, G. (2002) Senile plaque composition and posttranslational modification of amyloid-beta peptide and associated proteins. *Peptides*. **23**, 1343–1350.

Avila, J. (2006) Tau phosphorylation and aggregation in Alzheimer's disease pathology. *FEBS Letters.* **580**, 2922–2927.

Axelsson, V., Holback, S., Sjögren, M., Gustafsson, H. and Forsby, A. (2006) Gliotoxin induces caspase-dependent neurite degeneration and calpain-mediated general cytotoxicity in differentiated human neuroblastoma SH-SY5Y cells. *Biochemical and Biophysical Research Communications*. **345**, 1068–1074.

Ba, X. and Garg, N. J. (2011) Signaling mechanism of poly(ADP-ribose) polymerase-1 (PARP-1) in inflammatory diseases. *American Journal of Pathology.* **178**, 946–955.

Bähler, M., Benfenati, F., Valtorta, F. and Greengard, P. (1990) The synapsins and the regulation of synaptic function. *BioEssays : news and reviews in molecular, cellular and developmental biology*. **12**, 259–263.

Bai, J. Z. and Lipski, J. (2010) Differential expression of TRPM2 and TRPV4 channels and their potential role in oxidative stress-induced cell death in organotypic hippocampal culture. *NeuroToxicology*. **31**, 204–214.

Baki, A., Tompa, P., Alexa, A., Molnár, O. and Friedrich, P. (1996) Autolysis parallels activation of mu-calpain. *The Biochemical journal*. **318**. 897–901.

Banay-Schwartz, M., DeGuzman, T., Palkovits, M. and Lajtha, A. (1994) Calpain activity in adult and aged human brain regions. *Neurochemical research*. **19**, 563–567.

Bano, D., Munarriz, E., Chen, H. L., Ziviani, E., Lippi, G., Young, K. W. and Nicotera, P. (2007) The plasma membrane Na+/Ca2+ exchanger is cleaved by distinct protease families in neuronal cell death. *Annals of the New York Academy of Sciences*. 2007 **1099**, 451–455.

Bano, D., Young, K. W., Guerin, C. J., LeFeuvre, R., Rothwell, N. J., Naldini, L., Rizzuto, R., Carafoli, E. and Nicotera, P. (2005) Cleavage of the plasma membrane Na+/Ca2+ exchanger in excitotoxicity. *Cell*. **120**, 275–285.

Behl, C. (2000) Apoptosis and Alzheimer's disease. *Journal of Neural Transmission.* **107**, 1325–1344.

Bélanger, M. and Magistretti, P. J. (2009) The role of astroglia in neuroprotection. *Dialogues in Clinical Neuroscience.* **11**, 281–296.

Bergem, A. L., Engedal, K. and Kringlen, E. (1997) The role of heredity in late-onset Alzheimer disease and vascular dementia. A twin study. *Archives of general psychiatry*. **54**, 264–270.

Berghe, T. Vanden, Vanlangenakker, N., Parthoens, E., Deckers, W., Devos, M., Festjens, N., Guerin, C. J., Brunk, U. T., Declercq, W. and Vandenabeele, P. (2010) Necroptosis, necrosis and secondary necrosis converge on similar cellular disintegration features. *Cell death and differentiation*. **17**, 922–930.

Berridge, M. J. (2014) Calcium regulation of neural rhythms, memory and Alzheimer's disease. *The Journal of physiology*. [Online] **592**, 281–293.

Berridge, M. J., Lipp, P. and Bootman, M. D. (2000) The versatility and universality of calcium signalling. *Nature reviews. Molecular cell biology*. **1**, 11–21.

Bezprozvanny, I. and Mattson, M. M. P. (2008) Neuronal calcium mishandling and the pathogenesis of Alzheimer's disease. *Trends in neurosciences*. **31**, 454–463.

Bi, X. H., Lu, C. M., Liu, Q., Zhang, Z. X., Zhao, H. L., Yu, J. and Zhang, J. W. (2012) A 14 bp indel variation in the NCX1 gene modulates the age at onset in late-onset Alzheimer's disease. *Journal of Neural Transmission*. **119**, 383–386.

Bird, T. D. (1993) Early-Onset Familial Alzheimer Disease. *GeneReviews* (revised October 2012). Available at: http://www.ncbi.nlm.nih.gov/books/NBK1236/ [Accessed on 24 Mar 15]

Blalock, E. M., Geddes, J. W., Chen, K. C., Porter, N. M., Markesbery, W. R. and Landfield, P. W. (2004) Incipient Alzheimer's disease: microarray correlation analyses reveal major transcriptional and tumor suppressor responses. *Proceedings of the National Academy of Sciences of the United States of America*. **101**, 2173–2178.

Blenn, C., Wyrsch, P., Bader, J., Bollhalder, M. and Althaus, F. R. (2011) Poly(ADP-ribose)glycohydrolase is an upstream regulator of Ca 2+ fluxes in oxidative cell death. *Cellular and Molecular Life Sciences*. **68**, 1455–1466.

Bobinski, M., Wegiel, J., Tarnawski, M., Bobinski, M., Reisberg, B., de Leon, M. J., Miller, D. C. and Wisniewski, H. M. (1997) Relationships between regional neuronal loss and neurofibrillary changes in the hippocampal formation and duration and severity of Alzheimer disease. *Journal of neuropathology and experimental neurology*. **56**, 414–420.

Boehm, J. (2013) A 'danse macabre': Tau and Fyn in STEP with amyloid beta to facilitate induction of synaptic depression and excitotoxicity. *European Journal of Neuroscience.* **37**, 1925–1930.

Boesten, D. M. P. H. J., De Vos-Houben, J. M. J., Timmermans, L., Den Hartog, G. J. M., Bast, A. and Hageman, G. J. (2013) Accelerated aging during chronic oxidative stress: A role for PARP-1. *Oxidative Medicine and Cellular Longevity*. **2013**, 680414

Boeve, B. F. (2012) Progressive supranuclear palsy. *Parkinsonism and Related Disorders.* **18**, 192–S194.

Boulares, a. H., Yakovlev, A. G., Ivanova, V., Stoica, B. a., Wang, G., Iyer, S. and Smulson, M. (1999) Role of poly(ADP-ribose) polymerase (PARP) cleavage in apoptosis. Caspase 3-resistant PARP mutant increases rates of apoptosis in transfected cells. *Journal of Biological Chemistry*. **274**, 22932–22940.

Boulares, A. H., Zoltoski, A. J., Yakovlev, A., Xu, M. and Smulson, M. E. (2001) Roles of DNA Fragmentation Factor and Poly(ADP-ribose) Polymerase in an Amplification Phase of Tumor Necrosis Factor-induced Apoptosis. *Journal of Biological Chemistry*. **276** (41), 38185–38192.

Boutajangout, A., Boom, A., Leroy, K. and Brion, J. P. (2004) Expression of tau mRNA and soluble tau isoforms in affected and non-affected brain areas in Alzheimer's disease. *FEBS Letters*. **576**, 183–189.

Braak, H. and Braak, E. (1991) Neuropathological stageing of Alzheimer-related changes. *Acta neuropathologica*. **82**, 239–259.

Braak, H. and Braak, E. (1997) Staging of Alzheimer-related cortical destruction. *International psychogeriatrics / IPA*. **9**, 257–261; discussion 269–272.

Braak, H., Braak, E., Grundke-Iqbal, I. and Iqbal, K. (1986) Occurrence of neuropil threads in the senile human brain and in Alzheimer's disease: a third location of paired helical filaments outside of neurofibrillary tangles and neuritic plaques. *Neuroscience letters*. **65**, 351–355.

Brandt, R., Léger, J. and Lee, G. (1995) Interaction of tau with the neural plasma membrane mediated by tau's amino-terminal projection domain. *Journal of Cell Biology*. **131**, 1327–1340.

Bredesen, D. E., John, V. and Galvan, V. (2010) Importance of the caspase cleavage site in amyloid-beta protein precursor. *Journal of Alzheimer's Disease* **22**, 57–63.

Brittain, M. K., Brustovetsky, T., Sheets, P. L., Brittain, J. M., Khanna, R., Cummins, T. R. and Brustovetsky, N. (2012) Delayed calcium dysregulation in neurons requires both the NMDA receptor and the reverse Na+/Ca2+ exchanger. *Neurobiology of Disease*. **46**, 109–117.

Bronner, I. F., Ter Meulen, B. C., Azmani, A., Severijnen, L. A., Willemsen, R., Kamphorst, W., Ravid, R., Heutink, P. and Van Swieten, J. C. (2005) Hereditary Pick's disease with the G272V tau mutation shows predominant three-repeat tau pathology. *Brain*. **128**, 2645–2653.

Brorson, J. R., Bindokas, V. P., Iwama, T., Marcuccilli, C. J., Chisholm, J. C. and Miller, R. J. (1995) The Ca2+ Influx Induced by Beta-Amyloid Peptide-25-35 in Cultured Hippocampal-Neurons Results from Network Excitation. *Journal of Neurobiology*. **26**, 325–338.

Brosch, J. R. and Matthews, B. R. (2014) Journal Club: Comparison of symptomatic and asymptomatic persons with Alzheimer disease neuropathology. *Neurology*. **82**, 76-78

Brouwers, N., Van Cauwenberghe, C., Engelborghs, S., Lambert, J.-C., Bettens, K., Le Bastard, N., Pasquier, F., Montoya, A. G., Peeters, K., Mattheijssens, M., Vandenberghe, R., De Deyn, P. P., Cruts, M., Amouyel, P., Sleegers, K. and Van Broeckhoven, C. (2012) Alzheimer risk associated with a copy number variation in the complement receptor 1 increasing C3b/C4b binding sites. *Molecular Psychiatry.* **17**, 223–233.

Brunden, K. R., Trojanowski, J. Q. and Lee, V. M.-Y. (2009) Advances in tau-focused drug discovery for Alzheimer's disease and related tauopathies. *Nature reviews. Drug discovery*. **8**, 783–793.

Brustovetsky, T., Bolshakov, A. and Brustovetsky, N. (2010a) Calpain activation and Na+/Ca2+ exchanger degradation occur downstream of calcium deregulation in hippocampal neurons exposed to excitotoxic glutamate. *Journal of Neuroscience Research*. **88**, 1317–1328.

Brustovetsky, T., Bolshakov, A. and Brustovetsky, N. (2010b) Calpain activation and Na+/Ca2+ exchanger degradation occur downstream of calcium deregulation in hippocampal neurons exposed to excitotoxic glutamate. *Journal of Neuroscience Research*. **88**, 1317–1328.

Bürkle, A., Diefenbach, J., Brabeck, C. and Beneke, S. (2005) Ageing and PARP. *Pharmacological Research.* **52**, 93–99.

Busciglio, J., Lorenzo, A., Yeh, J. and Yankner, B. A. (1995) beta-amyloid fibrils induce tau phosphorylation and loss of microtubule binding. *Neuron*. **14**, 879–888.

Butterfield, A. (2002) Amyloid beta-peptide (1– 42)-induced Oxidative Stress and Neurotoxicity: Implications for Neurodegeneration in Alzheimer's Disease Brain. A Review*. *Free Radical Research*. **36**, 1307–1313.

Butterfield, D. A., Drake, J., Pocernich, C. and Castegna, A. (2001) Evidence of oxidative damage in Alzheimer's disease brain: central role for amyloid beta-peptide. *Trends in molecular medicine*. 7 (12), 548–554.

Butterfield, D. A., Galvan, V., Lange, M. B., Tang, H., Sowell, R. A., Spilman, P., Fombonne, J., Gorostiza, O., Zhang, J., Sultana, R. and Bredesen, D. E. (2010) In vivo oxidative stress in brain of Alzheimer disease transgenic mice: Requirement for methionine 35 in amyloid β-peptide of APP. *Free Radical Biology and Medicine*. **48**, 136–144.

Buxbaum, J. D., Ruefli, A. A., Parker, C. A., Cypess, A. M. and Greengard, P. (1994) Calcium regulates processing of the Alzheimer amyloid protein precursor in a protein kinase C-independent manner. *Proceedings of the National Academy of Sciences of the United States of America*. **91**, 4489–4493.

De Calignon, A., Fox, L. M., Pitstick, R., Carlson, G. a, Bacskai, B. J., Spires-Jones, T. L. and Hyman, B. T. (2010) Caspase activation precedes and leads to tangles. *Nature*. **464**, 1201–1204.

Canevari, L., Abramov, A. Y. and Duchen, M. R. (2004) Toxicity of Amyloid beta Peptide: Tales of Calcium, Mitochondria, and Oxidative Stress. *Neurochemical Research.* **29**, 637–650.

Castellani, R. J., Lee, H.-G., Zhu, X., Perry, G. and Smith, M. A. (2008) Alzheimer disease pathology as a host response. *Journal of neuropathology and experimental neurology*. **67**, 523–531.

Castellano, J. M., Kim, J., Stewart, F. R., Jiang, H., DeMattos, R. B., Patterson, B. W., Fagan, A. M., Morris, J. C., Mawuenyega, K. G., Cruchaga, C., Goate, A. M., Bales, K. R., Paul, S. M., Bateman, R. J. and Holtzman, D. M. (2011) Human apoE isoforms differentially regulate brain amyloid-β peptide clearance. *Science translational medicine*. **3**, 89ra57.

Celsi, F., Pizzo, P., Brini, M., Leo, S., Fotino, C., Pinton, P. and Rizzuto, R. (2009) Mitochondria, calcium and cell death: A deadly triad in neurodegeneration. *Biochimica et Biophysica Acta – Bioenergetics.* **1787**, 335–344.

Chaitanya, G. V., Steven, A. J. and Babu, P. P. (2010) PARP-1 cleavage fragments: signatures of cell-death proteases in neurodegeneration. *Cell communication and signaling: CCS*. **8**, 31.

Chakroborty, S. (2012) Early intracellular calcium disruptions in Alzheimer's disease: Setting the stage for synaptic dysfunction*. Science China Life Sciences.* **54**, 752-762

Chakroborty, S., Briggs, C., Miller, M. B., Goussakov, I., Schneider, C., Kim, J., Wicks, J., Richardson, J. C., Conklin, V., Cameransi, B. G. and Stutzmann, G. E. (2012) Stabilizing ER Ca2+ Channel Function as an Early Preventative Strategy for Alzheimer's Disease. *PLoS ONE*. **7**, e52056

Chakroborty, S., Goussakov, I., Miller, M. B. and Stutzmann, G. E. (2009) Deviant ryanodine receptor-mediated calcium release resets synaptic homeostasis in presymptomatic 3xTg-AD mice. *The Journal of neuroscience : the official journal of the Society for Neuroscience*. **29**, 9458–9470.

Chakroborty, S., Kim, J., Schneider, C., Jacobson, C., Molgo, J. and Stutzmann, G. E. (2012) Early Presynaptic and Postsynaptic Calcium Signaling Abnormalities Mask Underlying Synaptic Depression in Presymptomatic Alzheimer's Disease Mice. *Journal of Neuroscience.* **32**, 8341–8353.

Chakroborty, S. and Stutzmann, G. E. (2011) Early calcium dysregulation in Alzheimer's disease: Setting the stage for synaptic dysfunction. Science *China Life Sciences.* **54**, 752–762.

Chan, S. L. and Mattson, M. P. (1999) Caspase and calpain substrates: Roles in synaptic plasticity and cell death. *Journal of Neuroscience Research*. **58**, 167–190.

Chao, C. C. and Hu, S. (1994) Tumor necrosis factor-alpha potentiates glutamate neurotoxicity in human fetal brain cell cultures. *Developmental neuroscience*. **16**, 172–179.

Chen, J. X. and Yan, S. S. (2010) Role of mitochondrial amyloid-beta in Alzheimer's disease. *Journal of Alzheimer's disease: JAD*. **20**, 569–578.

Cheng, H., Wei, S., Wei, L. and Verkhratsky, A. (2006) Calcium signaling in physiology and pathophysiology. *Acta pharmacologica Sinica*. **27**, 767–772.

Chin, J. H., Tse, F. W., Harris, K. and Jhamandas, J. H. (2006) Beta-amyloid enhances intracellular calcium rises mediated by repeated activation of intracellular calcium stores and nicotinic receptors in acutely dissociated rat basal forebrain neurons. *Brain cell biology*. **35**, 173–186.

Chow, H.-M., Guo, D., Zhou, J.-C., Zhang, G.-Y., Li, H.-F., Herrup, K. and Zhang, J. (2014) CDK5 activator protein p25 preferentially binds and activates GSK3beta. *Proceedings of the National Academy of Sciences of the United States of America*. **111**, 4887–4895.

Chuckowree, J. A. and Vickers, J. C. (2003) Cytoskeletal and morphological alterations underlying axonal sprouting after localized transection of cortical neuron axons in vitro. *The Journal of neuroscience : the official journal of the Society for Neuroscience*. **23**, 3715–3725.

Cissé, M., Halabisky, B., Harris, J., Devidze, N., Dubal, D. B., Sun, B., Orr, A., Lotz, G., Kim, D. H., Hamto, P., Ho, K., Yu, G.-Q. and Mucke, L. (2011) Reversing EphB2 depletion rescues cognitive functions in Alzheimer model. *Nature*. **469**, 47–52.

Cleary, J. P., Walsh, D. M., Hofmeister, J. J., Shankar, G. M., Kuskowski, M. A., Selkoe, D. J. and Ashe, K. H. (2005) Natural oligomers of the amyloid-beta protein specifically disrupt cognitive function. *Nature neuroscience*. **8**, 79–84.

Cohen, G. M. (1997) Caspases: the executioners of apoptosis. *The Biochemical journal*. **326**, 11–16.

Cohen-Armon, M., Visochek, L., Katzoff, A., Levitan, D., Susswein, A. J., Klein, R., Valbrun, M. and Schwartz, J. H. (2004) Long-term memory requires polyADP-ribosylation. *Science (New York, N.Y.)*. **304**, 1820–1822.

Coma, M., Guix, F. X., Ill-Raga, G., Uribesalgo, I., Alameda, F., Valverde, M. A. and Muñoz, F. J. (2008) Oxidative stress triggers the amyloidogenic pathway in human vascular smooth muscle cells. *Neurobiology of Aging*. **29**, 969–980.

Cong, J., Thompson, V. F. and Goll, D. E. (1993) Effect of monoclonal antibodies specific for the 28-kDa subunit on catalytic properties of the calpains. *Journal of Biological Chemistry*. **268**, 25740–25747.

Conway, K., Baxter, E., K, F. and A, R. (2003) Emerging beta-amyloid therapies for the treatment of Alzheimer's disease. *Curr Pharm Des*. [Online] **9**, 427–447.

Corder, E. H., Saunders, A. M., Strittmatter, W. J., Schmechel, D. E., Gaskell, P. C., Small, G. W., Roses, A. D., Haines, J. L. and Pericak-Vance, M. A. (1993) Gene dose of apolipoprotein E type 4 allele and the risk of Alzheimer's disease in late onset families. *Science (New York, N.Y.)*. **261**, 921–923.

Creeley, C., Wozniak, D. F., Labruyere, J., Taylor, G. T. and Olney, J. W. (2006) Low doses of memantine disrupt memory in adult rats. *The Journal of neuroscience : the official journal of the Society for Neuroscience*. **26**, 3923–3932.

Crespo-Biel, N., Camins, A., Canudas, A. M. and Pallàs, M. (2010) Kainate-induced toxicity in the hippocampus: Potential role of lithium. *Bipolar Disorders*. **12**, 425–436.

Crimins, J. L., Pooler, A., Polydoro, M., Luebke, J. I. and Spires-Jones, T. L. (2013) The intersection of amyloid beta and tau in glutamatergic synaptic dysfunction and collapse in Alzheimer's disease. *Ageing Research Reviews* **12**, 757–763.

Cruts, M., Van Duijn, C. M., Backhovens, H., Van Den Broeck, M., Wehnert, A., Serneels, S., Sherrington, R., Hutton, M., Hardy, J., St George-Hyslop, P. H., Hofman, A. and Van Broeckhoven, C. (1998) Estimation of the genetic contribution of presenilin-1 and -2 mutations in a population-based study of presenile Alzheimer disease. *Human Molecular Genetics*. **74**, 3–51.

Cruts, M., Theuns, J. and Van Broeckhoven, C. (2012) Locus-specific mutation databases for neurodegenerative brain diseases. *Human Mutation*. **33**, 1340–1344.

Cruz, J. C., Tseng, H. C., Goldman, J. A., Shih, H. and Tsai, L. H. (2003) Aberrant Cdk5 activation by p25 triggers pathological events leading to neurodegeneration and neurofibrillary tangles. *Neuron*. **40**, 471–483.

Cummings, D. M., Liu, W., Portelius, E., Bayram, S., Yasvoina, M., Ho, S.-H., Smits, H., Ali, S. S., Steinberg, R., Pegasiou, C.-M., James, O. T., Matarin, M., Richardson, J. C., Zetterberg, H., Blennow, K., Hardy, J. A., Salih, D. A. and Edwards, F. A. (2015) First effects of rising amyloid-beta in transgenic mouse brain: synaptic transmission and gene expression. *Brain : a journal of neurology*. **138**, 1992–2004.

D'Amelio, M., Cavallucci, V., Middei, S., Marchetti, C., Pacioni, S., Ferri, A., Diamantini, A., De Zio, D., Carrara, P., Battistini, L., Moreno, S., Bacci, A., Ammassari-Teule, M., Marie, H. and Cecconi, F. (2011) Caspase-3 triggers early synaptic dysfunction in a mouse model of Alzheimer's disease. *Nature neuroscience*. **14**, 69–76.

D'Amours, D., Sallmann, F. R., Dixit, V. M. and Poirier, G. G. (2001) Gain-of-function of poly(ADP-ribose) polymerase-1 upon cleavage by apoptotic proteases: implications for apoptosis. *Journal of cell science*. **114**, 3771–3778.

Dal Pra, I., Whitfileld, J. F., Pacchiana, R., Bonafini, C., Talacchi, A., Chakravarthy, B., Armato, U. and Chiarini, A. (2011) The amyloid-beta(4)(2) proxy, amyloid-beta(25-35), induces normal human cerebral astrocytes to produce amyloid-beta(4)(2). *Journal of Alzheimer's disease : JAD*. **24**, 335–347.

Danysz, W. and Parsons, C. G. (2012) Alzheimer's disease, β-amyloid, glutamate, NMDA receptors and memantine--searching for the connections. *British journal of pharmacology*. **167**, 324–352.

DaRocha-Souto, B., Coma, M., Pérez-Nievas, B. G., Scotton, T. C., Siao, M., Sánchez-Ferrer, P., Hashimoto, T., Fan, Z., Hudry, E., Barroeta, I., Serenó, L., Rodríguez, M., Sánchez, M. B., Hyman, B. T. and Gómez-Isla, T. (2012) Activation of glycogen synthase kinase-3 beta mediates β-amyloid induced neuritic damage in Alzheimer's disease. *Neurobiology of Disease*. **45**, 425–437.

Davar, D., H. Beumer, J., Hamieh, L. and Tawbi, H. (2012) Role of PARP Inhibitors in Cancer Biology and Therapy. *Current Medicinal Chemistry.* **19**, 3907–3921.

Davies, C. A., Mann, D. M., Sumpter, P. Q. and Yates, P. O. (1987) A quantitative morphometric analysis of the neuronal and synaptic content of the frontal and temporal cortex in patients with Alzheimer's disease. *Journal of the neurological sciences*. **78**, 151–164.

Davies, P. (1976) SELECTIVE LOSS OF CENTRAL CHOLINERGIC NEURONS IN ALZHEIMER'S DISEASE. *The Lancet*. **2**, 1403.

Dávila, D. and Torres-Aleman, I. (2008) Neuronal death by oxidative stress involves activation of FOXO3 through a two-arm pathway that activates stress kinases and attenuates insulin-like growth factor I signaling. *Molecular biology of the cell*. **19**, 2014–2025.

Dawkins, E. and Small, D. H. (2014) Insights into the physiological function of the β-amyloid precursor protein: Beyond Alzheimer's disease. *Journal of Neurochemistry.* **129**, 756–769.

Deitmer, J. W., Verkhratsky, A. J. and Lohr, C. (1998) Calcium signalling in glial cells. *Cell Calcium.* **24**, 405–416.

Delvaux, E., Bentley, K., Stubbs, V., Sabbagh, M. and Coleman, P. D. (2013) Differential processing of amyloid precursor protein in brain and in peripheral blood leukocytes. *Neurobiology of Aging*. **34**, 1680–1686.

Demuro, A., Mina, E., Kayed, R., Milton, S. C., Parker, I. and Glabe, C. G. (2005) Calcium dysregulation and membrane disruption as a ubiquitous neurotoxic mechanism of soluble amyloid oligomers. *Journal of Biological Chemistry*. **280**, 17294–17300.

Demuro, A., Smith, M. and Parker, I. (2011) Single-channel Ca2+ imaging implicates Abeta 1-42 amyloid pores in Alzheimer's disease pathology. *Journal of Cell Biology*. **195**, 515–524.

DeWitt, D. A., Perry, G., Cohen, M., Doller, C. and Silver, J. (1998) Astrocytes regulate microglial phagocytosis of senile plaque cores of Alzheimer's disease. *Experimental neurology*. **149**, 329–340.

Dodson, S. E., Gearing, M., Lippa, C. F., Montine, T. J., Levey, A. I. and Lah, J. J. (2006) LR11/SorLA expression is reduced in sporadic Alzheimer disease but not in familial Alzheimer disease. *Journal of neuropathology and experimental neurology*. **65**, 866–872.

Dorostkar, M. M., Burgold, S., Filser, S., Barghorn, S., Schmidt, B., Anumala, U. R., Hillen, H., Klein, C. and Herms, J. (2014) Immunotherapy alleviates amyloid-

associated synaptic pathology in an Alzheimer's disease mouse model. *Brain : a journal of neurology*. **137**, 3319–3326.

Dreses-Werringloer, U., Lambert, J. C., Vingtdeux, V., Zhao, H., Vais, H., Siebert, A., Jain, A., Koppel, J., Rovelet-Lecrux, A., Hannequin, D., Pasquier, F., Galimberti, D., Scarpini, E., Mann, D., Lendon, C., Campion, D., Amouyel, P., Davies, P., Foskett, J. K., Campagne, F. and Marambaud, P. (2008) A Polymorphism in CALHM1 Influences Ca2+ Homeostasis, Aβ Levels, and Alzheimer's Disease Risk. *Cell*. **133**, 1149–1161.

Drubin, D. G. and Kirschner, M. W. (1986) Tau protein function in living cells. *The Journal of cell biology*. **103**, 2739–2746.

Duff, K., Eckman, C., Zehr, C., Yu, X., Prada, C. M., Perez-tur, J., Hutton, M., Buee, L., Harigaya, Y., Yager, D., Morgan, D., Gordon, M. N., Holcomb, L., Refolo, L., Zenk, B., Hardy, J. and Younkin, S. (1996) Increased amyloid-beta42(43) in brains of mice expressing mutant presenilin 1. *Nature*. **383**, 710–713.

Elder, G. A., Gama Sosa, M. A. and De Gasperi, R. (2010) Transgenic mouse models of Alzheimer's disease. *The Mount Sinai journal of medicine, New York*. **77**, 69–81.

Engmann, O. and Giese, K. P. (2009) Crosstalk between Cdk5 and GSK3beta: Implications for Alzheimer's Disease. *Frontiers in molecular neuroscience*. **2**, 2.

Engmann, O., Hortobágyi, T., Thompson, A. J., Guadagno, J., Troakes, C., Soriano, S., Al-Sarraj, S., Kim, Y. and Giese, K. P. (2011) Cyclin-dependent kinase 5 activator p25 Is generated during memory formation and is reduced at an early stage in Alzheimer's disease. *Biological Psychiatry*. **70**, 159–168.

Eskici, G. and Axelsen, P. H. (2012) Copper and oxidative stress in the pathogenesis of Alzheimer's disease. *Biochemistry*. **51**, 6289–6311.

Etcheberrigaray, R., Hirashima, N., Nee, L., Prince, J., Govoni, S., Racchi, M., Tanzi, R. E. and Alkon, D. L. (1998) Calcium responses in fibroblasts from asymptomatic members of Alzheimer's disease families. *Neurobiology of disease*. **5**, 37–45.

Evin, G., Barakat, A. and Masters, C. L. (2010) BACE: Therapeutic target and potential biomarker for Alzheimer's disease. *International Journal of Biochemistry and Cell Biology.* **42**, 1923–1926.

De Felice, F. G., Velasco, P. T., Lambert, M. P., Viola, K., Fernandez, S. J., Ferreira, S. T. and Klein, W. L. (2007) Aβ oligomers induce neuronal oxidative stress through an N-methyl-D-aspartate receptor-dependent mechanism that is blocked by the Alzheimer drug memantine. *Journal of Biological Chemistry*. **282**, 11590–11601.

Ferreira, A. (2012) Calpain dysregulation in Alzheimer's disease. *ISRN biochemistry*. **2012**, 728571.

Ferreira, A. and Bigio, E. H. (2011) Calpain-mediated tau cleavage: a mechanism leading to neurodegeneration shared by multiple tauopathies. *Molecular medicine (Cambridge, Mass.)*. **17**, 676–685.

Ferreira, I. L., Bajouco, L. M., Mota, S. I., Auberson, Y. P., Oliveira, C. R. and Rego, A. C. (2012) Amyloid beta peptide 1-42 disturbs intracellular calcium homeostasis through activation of GluN2B-containing N-methyl-d-aspartate receptors in cortical cultures. *Cell Calcium*. **51**, 95–106.

Ferreira, I. L., Ferreiro, E., Schmidt, J., Cardoso, J. M., Pereira, C. M. F., Carvalho, A. L., Oliveira, C. R. and Rego, A. C. (2015) Abeta and NMDAR activation cause mitochondrial dysfunction involving ER calcium release. *Neurobiology of aging*. **36**, 680–692.

Ferreiro, E., Resende, R., Costa, R., Oliveira, C. R. and Pereira, C. M. F. (2006) An endoplasmic-reticulum-specific apoptotic pathway is involved in prion and amyloid-beta peptides neurotoxicity. *Neurobiology of Disease*. **23**, 669–678.

Flores-Rodríguez, P., Ontiveros-Torres, M. A., Cárdenas-Aguayo, M. C., Luna-Arias, J. P., Meraz-Ríos, M. A., Viramontes-Pintos, A., Harrington, C. R., Wischik, C. M., Mena, R., Florán-Garduño, B. and Luna-Muñoz, J. (2015) The relationship between truncation and phosphorylation at the C-terminus of tau protein in the paired helical filaments of Alzheimer's disease. *Frontiers in Neuroscience.* **9**, 33

Fonfria, E., Marshall, I. C. B., Boyfield, I., Skaper, S. D., Hughes, J. P., Owen, D. E., Zhang, W., Miller, B. A., Benham, C. D. and McNulty, S. (2005) Amyloid beta-peptide(1-42) and hydrogen peroxide-induced toxicity are mediated by TRPM2 in rat primary striatal cultures. *Journal of Neurochemistry*. **95**, 715–723.

Fonfria, E., Mattei, C., Hill, K., Brown, J. T., Randall, A., Benham, C. D., Skaper, S. D., Campbell, C. A., Crook, B., Murdock, P. R., Wilson, J. M., Maurio, F. P., Owen, D. E., Tilling, P. L. and McNulty, S. (2006) TRPM2 is elevated in the tMCAO

stroke model, transcriptionally regulated, and functionally expressed in C13 microglia. *Journal of receptor and signal transduction research*. **26**, 179–198.

Forero, D. A., Casadesus, G., Perry, G. and Arboleda, H. (2006) Synaptic dysfunction and oxidative stress in Alzheimer's disease: Emerging mechanisms. *Journal of Cellular and Molecular Medicine.* **10**, 796–805.

Francis, P. T. (2008) 'Glutamatergic approaches to the treatment of cognitive and behavioural symptoms of Alzheimer's disease', in *Neurodegenerative Diseases*. **2008**, 241–243.

Franklin, J. L., Sanz-Rodriguez, C., Juhasz, A., Deckwerth, T. L. and Johnson, E. M. (1995) Chronic depolarization prevents programmed death of sympathetic neurons in vitro but does not support growth: requirement for Ca2+ influx but not Trk activation. *The Journal of neuroscience : the official journal of the Society for Neuroscience*. **15**, 643–664.

Frautschy, S. A., Yang, F., Irrizarry, M., Hyman, B., Saido, T. C., Hsiao, K. and Cole, G. M. (1998) Microglial response to amyloid plaques in APPsw transgenic mice. *The American journal of pathology*. **152**, 307–317.

Gagnon, L. G. and Belleville, S. (2011) Working memory in mild cognitive impairment and Alzheimer's disease: contribution of forgetting and predictive value of complex span tasks. *Neuropsychology*. **25**, 226–236.

Gamblin, T. C., Chen, F., Zambrano, A., Abraha, A., Lagalwar, S., Guillozet, A. L., Lu, M., Fu, Y., Garcia-Sierra, F., LaPointe, N., Miller, R., Berry, R. W., Binder, L. I. and Cryns, V. L. (2003) Caspase cleavage of tau: linking amyloid and neurofibrillary tangles in Alzheimer's disease. *Proceedings of the National Academy of Sciences of the United States of America*. **100**, 10032–10037.

Gandolfi, G., Pomponio, L., Ertbjerg, P., Karlsson, A. H., Nanni Costa, L., Lametsch, R., Russo, V. and Davoli, R. (2011) Investigation on CAST, CAPN1 and CAPN3 porcine gene polymorphisms and expression in relation to post-mortem calpain activity in muscle and meat quality. *Meat Science*. **88**, 694–700.

García-Matas, S., de Vera, N., Aznar, A. O., Marimon, J. M., Adell, A., Planas, A. M., Cristòfol, R. and Sanfeliu, C. (2010) In vitro and in vivo activation of astrocytes by amyloid-β is potentiated by pro-oxidant agents. *Journal of Alzheimer's Disease*. **20**, 229–245.

García-Sierra, F., Mondragón-Rodríguez, S. and Basurto-Islas, G. (2008) Truncation of tau protein and its pathological significance in Alzheimer's disease. *Journal of Alzheimer's disease: JAD*. **14**, 401–409.

Garg, S., Timm, T., Mandelkow, E.-M., Mandelkow, E. and Wang, Y. (2011a) Cleavage of Tau by calpain in Alzheimer's disease: the quest for the toxic 17 kD fragment. *Neurobiology of aging*. **32**, 1–14.

Garg, S., Timm, T., Mandelkow, E.-M., Mandelkow, E. and Wang, Y. (2011b) Cleavage of Tau by calpain in Alzheimer's disease: the quest for the toxic 17 kD fragment. *Neurobiology of aging*. **32**, 1–14.

Garwood, C. J., Pooler, a M., Atherton, J., Hanger, D. P. and Noble, W. (2011) Astrocytes are important mediators of Aβ-induced neurotoxicity and tau phosphorylation in primary culture. *Cell death and disease*. **2**, 167.

Gendreau, K. L. and Hall, G. F. (2013) Tangles, Toxicity, and Tau Secretion in AD - New Approaches to a Vexing Problem. *Frontiers in neurology*. **4**, 160.

Getz, G. S. (2012) Calpain Inhibition as a Potential Treatment of Alzheimer's Disease. *The American Journal of Pathology.* **181**, 388–391.

Ghiso, J. and Frangione, B. (2002) Amyloidosis and Alzheimer's disease. *Advanced Drug Delivery Reviews.* **54**, 1539–1551.

Giese, K. P. (2014) Generation of the Cdk5 activator p25 is a memory mechanism that is affected in early Alzheimer's disease. *Frontiers in molecular neuroscience*. **7**, 36.

Gleichmann, M. and Mattson, M. P. (2011) Neuronal Calcium Homeostasis and Dysregulation. *Antioxidants and Redox Signaling*. **14**, 1261–1273.

Glöckner, F., Meske, V., Lütjohann, D. and Ohm, T. G. (2011) Dietary cholesterol and its effect on tau protein: a study in apolipoprotein E-deficient and P301L human tau mice. *Journal of neuropathology and experimental neurology*. **70**, 292–301.

Goate, A., Chartier-Harlin, M. C., Mullan, M., Brown, J., Crawford, F., Fidani, L., Giuffra, L., Haynes, A., Irving, N. and James, L. (1991) Segregation of a missense mutation in the amyloid precursor protein gene with familial Alzheimer's disease. *Nature*. **349**, 704–706.

Gobbi, P., Castaldo, P., Minelli, A., Salucci, S., Magi, S., Corcione, E. and Amoroso, S. (2007) Mitochondrial localization of Na+/Ca2+ exchangers NCX1-3 in neurons and astrocytes of adult rat brain in situ. *Pharmacological research : the official journal of the Italian Pharmacological Society*. **56**, 556–565.

Goedert, M. and Jakes, R. (1990) Expression of separate isoforms of human tau protein: correlation with the tau pattern in brain and effects on tubulin polymerization. *The EMBO journal*. **9**, 4225–4230.

Goedert, M., Spillantini, M. G., Jakes, R., Rutherford, D. and Crowther, R. A. (1989) Multiple isoforms of human microtubule-associated protein tau: sequences and localization in neurofibrillary tangles of Alzheimer's disease. *Neuron*. **3**, 519–526.

Goldgaber, D., Lerman, M. I., McBride, O. W., Saffiotti, U. and Gajdusek, D. C. (1987) Characterization and chromosomal localization of a cDNA encoding brain amyloid of Alzheimer's disease. *Science (New York, N.Y.)*. **235**, 877–880.

Goll, D. E., Thompson, V. F., Li, H., Wei, W. and Cong, J. (2003) The calpain system. *Physiological reviews*. **83**, 731–801.

Golstein, P. and Kroemer, G. (2007) Cell death by necrosis: towards a molecular definition. *Trends in Biochemical Sciences.* 32, 37–43.

Gómez-Isla, T., Hollister, R., West, H., Mui, S., Growdon, J. H., Petersen, R. C., Parisi, J. E. and Hyman, B. T. (1997) Neuronal loss correlates with but exceeds neurofibrillary tangles in Alzheimer's disease. *Annals of Neurology*. **41**, 17–24.

Gómez-Sintes, R., Hernández, F., Bortolozzi, A., Artigas, F., Avila, J., Zaratin, P., Gotteland, J. P. and Lucas, J. J. (2007) Neuronal apoptosis and reversible motor deficit in dominant-negative GSK-3 conditional transgenic mice. *The EMBO journal*. **26**, 2743–2754.

Gomez-Villafuertes, R., Torres, B., Barrio, J., Savignac, M., Gabellini, N., Rizzato, F., Pintado, B., Gutierrez-Adan, A., Mellström, B., Carafoli, E. and Naranjo, J. R. (2005) Downstream regulatory element antagonist modulator regulates Ca2+ homeostasis and viability in cerebellar neurons. *The Journal of neuroscience : the official journal of the Society for Neuroscience*. **25**, 10822–10830.

Gong, Q. H., Wang, Q., Shi, J. S., Huang, X. N., Liu, Q. and Ma, H. (2007) Inhibition of caspases and intracellular free Ca2+ concentrations are involved in resveratrol protection against apoptosis in rat primary neuron cultures. *Acta Pharmacologica Sinica*. **28**, 1724–1730.

Goñi-Oliver, P., Lucas, J. J., Avila, J. and Hernández, F. (2007) N-terminal cleavage of GSK-3 by calpain: A new form of GSK-3 regulation. *Journal of Biological Chemistry*. **282**, 22406–22413.

Goode, B. L., Chau, M., Denis, P. E. and Feinstein, S. C. (2000) Structural and functional differences between 3-repeat and 4-repeat tau isoforms: Implications for normal tau function and the onset of neurodegenerative disease. *Journal of Biological Chemistry*. **275**, 38182–38189.

Götz, J., Chen, F., van Dorpe, J. and Nitsch, R. M. (2001) Formation of neurofibrillary tangles in P301l tau transgenic mice induced by Abeta 42 fibrils. *Science (New York, N.Y.)*. **293**, 1491–1495.

Götz, J., Probst, A., Spillantini, M. G., Schäfer, T., Jakes, R., Bürki, K. and Goedert, M. (1995) Somatodendritic localization and hyperphosphorylation of tau protein in transgenic mice expressing the longest human brain tau isoform. *The EMBO journal*. **14**, 1304–1313.

Gouras, G. K., Tsai, J., Naslund, J., Vincent, B., Edgar, M., Checler, F., Greenfield, J. P., Haroutunian, V., Buxbaum, J. D., Xu, H., Greengard, P. and Relkin, N. R. (2000) Intraneuronal Aβ42 Accumulation in Human Brain. *The American journal of pathology*. **156**, 15–20.

Gralle, M. and Ferreira, S. T. (2007) Structure and functions of the human amyloid precursor protein: the whole is more than the sum of its parts. *Progress in neurobiology*. **82**, 11–32.

Granic, I., Nyakas, C., Luiten, P. G. M., Eisel, U. L. M., Halmy, L. G., Gross, G., Schoemaker, H., Möller, A. and Nimmrich, V. (2010) Calpain inhibition prevents amyloid-β-induced neurodegeneration and associated behavioral dysfunction in rats. *Neuropharmacology*. **59**, 334–342.

Green, K. N., Demuro, A., Akbari, Y., Hitt, B. D., Smith, I. F., Parker, I. and LaFerla, F. M. (2008) SERCA pump activity is physiologically regulated by presenilin and regulates amyloid beta production. *Journal of Cell Biology*. **181**, 1107–1116.

Grienberger, C. and Konnerth, A. (2012) Imaging Calcium in Neurons. *Neuron.* **73**, 862–885.

Grolla, a a, Sim, J. a, Lim, D., Rodriguez, J. J., Genazzani, a a and Verkhratsky, a (2013) Amyloid-β and Alzheimer's disease type pathology differentially affects the calcium signalling toolkit in astrocytes from different brain regions. *Cell death and disease*. **4**, 623

Grundke-Iqbal, I., Iqbal, K., Tung, Y. C., Quinlan, M., Wisniewski, H. M. and Binder, L. I. (1986) Abnormal phosphorylation of the microtubule-associated protein tau (tau) in Alzheimer cytoskeletal pathology. *Proceedings of the National Academy of Sciences of the United States of America*. **83**, 4913–4917.

Grynspan, F., Griffin, W. R., Cataldo, A., Katayama, S. and Nixon, R. A. (1997) Active site-directed antibodies identify calpain II as an early- appearing and pervasive component of neurofibrillary pathology in Alzheimer's disease. *Brain Research*. **763**, 145–158.

Guerreiro, R., Wojtas, A., Bras, J., Carrasquillo, M., Rogaeva, E., Majounie, E., Cruchaga, C., Sassi, C., Kauwe, J. S. K., Younkin, S., Hazrati, L., Collinge, J., Pocock, J., Lashley, T., Williams, J., Lambert, J.-C., Amouyel, P., Goate, A., Rademakers, R., Morgan, K., Powell, J., St George-Hyslop, P., Singleton, A. and Hardy, J. (2013) TREM2 variants in Alzheimer's disease. *The New England journal of medicine*. **368**, 117–127.

Ha, H. C. and Snyder, S. H. (1999) Poly(ADP-ribose) polymerase is a mediator of necrotic cell death by ATP depletion. *Proceedings of the National Academy of Sciences of the United States of America*. **96**, 13978–13982.

Haass, C., Kaether, C., Thinakaran, G. and Sisodia, S. (2012) Trafficking and proteolytic processing of APP. *Cold Spring Harbor Perspectives in Medicine*. **2**, a006270.

Haass, C. and Selkoe, D. J. (2007) Soluble protein oligomers in neurodegeneration: lessons from the Alzheimer's amyloid beta-peptide. *Nature reviews. Molecular cell biology*. **8**, 101–112.

Halliwell, B. (2006) Oxidative stress and neurodegeneration: Where are we now? *Journal of Neurochemistry.* **97**, 1634–1658.

Hanger, D. P., Anderton, B. H. and Noble, W. (2009) Tau phosphorylation: the therapeutic challenge for neurodegenerative disease. *Trends in Molecular Medicine.* **15**, 112–119.

Hanger, D. P. and Noble, W. (2011) Functional implications of glycogen synthase kinase-3-mediated tau phosphorylation. *International journal of Alzheimer's disease*. **2011**, 352805.

Haraguchi, K., Kawamoto, a., Isami, K., Maeda, S., Kusano, a., Asakura, K., Shirakawa, H., Mori, Y., Nakagawa, T. and Kaneko, S. (2012) TRPM2 Contributes to Inflammatory and Neuropathic Pain through the Aggravation

of Pronociceptive Inflammatory Responses in Mice. *Journal of Neuroscience*. **32**, 3931–3941.

Hardy, J. A. and Higgins, G. A. (1992) Alzheimer's disease: the amyloid cascade hypothesis. *Science (New York, N.Y.)*. **256**, 184–185.

Hardy, J., Cowburn, R., Barton, A., Reynolds, G., Lofdahl, E., O'Carroll, A. M., Wester, P. and Winblad, B. (1987) Region-specific loss of glutamate innervation in Alzheimer's disease. *Neuroscience letters*. **73**, 77–80.

Harkany, T., Ábrahám, I., Timmerman, W., Laskay, G., Tóth, B., Sasvári, M., Kónya, C., Sebens, J. B., Korf, J., Nyakas, C., Zarándi, M., Soós, K., Penke, B. and Luiten, P. G. M. (2000a) β-Amyloid neurotoxicity is mediated by a glutamate-triggered excitotoxic cascade in rat nucleus basalis. *European Journal of Neuroscience*. **12**, 2735–2745.

Harkany, T., Ábrahám, I., Timmerman, W., Laskay, G., Tóth, B., Sasvári, M., Kónya, C., Sebens, J. B., Korf, J., Nyakas, C., Zarándi, M., Soós, K., Penke, B. and Luiten, P. G. M. (2000b) β-Amyloid neurotoxicity is mediated by a glutamate-triggered excitotoxic cascade in rat nucleus basalis. *European Journal of Neuroscience*. **12**, 2735–2745.

Harold, D., Abraham, R., Hollingworth, P., Sims, R., Gerrish, A., Hamshere, M. L., Pahwa, J. S., Moskvina, V., Dowzell, K., Williams, A., Jones, N., Thomas, C., Stretton, A., Morgan, A. R., Lovestone, S., Powell, J., Proitsi, P., Lupton, M. K., Brayne, C., Rubinsztein, D. C., Gill, M., Lawlor, B., Lynch, A., Morgan, K., Brown, K. S., Passmore, P. A., Craig, D., McGuinness, B., Todd, S., Holmes, C., Mann, D., Smith, A. D., Love, S., Kehoe, P. G., Hardy, J., Mead, S., Fox, N., Rossor, M., Collinge, J., Maier, W., Jessen, F., Schürmann, B., van den Bussche, H., Heuser, I., Kornhuber, J., Wiltfang, J., Dichgans, M., Frölich, L., Hampel, H., Hüll, M., Rujescu, D., Goate, A. M., Kauwe, J. S. K., Cruchaga, C., Nowotny, P., Morris, J. C., Mayo, K., Sleegers, K., Bettens, K., Engelborghs, S., De Deyn, P. P., Van Broeckhoven, C., Livingston, G., Bass, N. J., Gurling, H., McQuillin, A., Gwilliam, R., Deloukas, P., Al-Chalabi, A., Shaw, C. E., Tsolaki, M., Singleton, A. B., Guerreiro, R., Mühleisen, T. W., Nöthen, M. M., Moebus, S., Jöckel, K.-H., Klopp, N., Wichmann, H.-E., Carrasquillo, M. M., Pankratz, V. S., Younkin, S. G., Holmans, P. A., O'Donovan, M., Owen, M. J. and Williams, J. (2009) Genome-wide association study identifies variants at CLU and PICALM associated with Alzheimer's disease. *Nature genetics*. **41**, 1088–1093.

Hartley, D. M., Walsh, D. M., Ye, C. P., Diehl, T., Vasquez, S., Vassilev, P. M., Teplow, D. B. and Selkoe, D. J. (1999) Protofibrillar intermediates of amyloid beta-protein induce acute electrophysiological changes and progressive

neurotoxicity in cortical neurons. *The Journal of neuroscience : the official journal of the Society for Neuroscience*. **19**, 8876–8884.

Herrmann, N., Gauthier, S. and Lysy, P. G. (2007) Clinical practice guidelines for severe Alzheimer's disease. *Alzheimer's and dementia : the journal of the Alzheimer's Association*. **3**, 385–397.

Higgins, G. C., Beart, P. M. and Nagley, P. (2009) Oxidative stress triggers neuronal caspase-independent death: Endonuclease G involvement in programmed cell death-type III. *Cellular and Molecular Life Sciences*. **66**, 2773–2787.

Higuchi, M., Iwata, N., Matsuba, Y., Takano, J., Suemoto, T., Maeda, J., Ji, B., Ono, M., Staufenbiel, M., Suhara, T. and Saido, T. C. (2012) Mechanistic involvement of the calpain-calpastatin system in Alzheimer neuropathology. *The FASEB Journal.* **26**, 1204–1217.

Hinners, I., Hill, A., Otto, U., Michalsky, A., Mack, T. G. A. and Striggow, F. (2008) Tau kinase inhibitors protect hippocampal synapses despite of insoluble tau accumulation. *Molecular and Cellular Neuroscience*. **37**, 559–567.

Hoey, S. E., Williams, R. J. and Perkinton, M. S. (2009) Synaptic NMDA receptor activation stimulates alpha-secretase amyloid precursor protein processing and inhibits amyloid-beta production. *The Journal of neuroscience : the official journal of the Society for Neuroscience*. **29**, 4442–4460.

Hollenbeck, P. J. and Saxton, W. M. (2005) The axonal transport of mitochondria. *Journal of cell science*. **118**, 5411–5419.

Hollingworth, P., Harold, D., Sims, R., Gerrish, A., Lambert, J.-C., Carrasquillo, M. M., Abraham, R., Hamshere, M. L., Pahwa, J. S., Moskvina, V., Dowzell, K., Jones, N., Stretton, A., Thomas, C., Richards, A., Ivanov, D., Widdowson, C., Chapman, J., Lovestone, S., Powell, J., Proitsi, P., Lupton, M. K., Brayne, C., Rubinsztein, D. C., Gill, M., Lawlor, B., Lynch, A., Brown, K. S., Passmore, P. A., Craig, D., McGuinness, B., Todd, S., Holmes, C., Mann, D., Smith, A. D., Beaumont, H., Warden, D., Wilcock, G., Love, S., Kehoe, P. G., Hooper, N. M., Vardy, E. R. L. C., Hardy, J., Mead, S., Fox, N. C., Rossor, M., Collinge, J., Maier, W., Jessen, F., Rüther, E., Schürmann, B., Heun, R., Kölsch, H., van den Bussche, H., Heuser, I., Kornhuber, J., Wiltfang, J., Dichgans, M., Frölich, L., Hampel, H., Gallacher, J., Hüll, M., Rujescu, D., Giegling, I., Goate, A. M., Kauwe, J. S. K., Cruchaga, C., Nowotny, P., Morris, J. C., Mayo, K., Sleegers, K., Bettens, K., Engelborghs, S., De Deyn, P. P., Van Broeckhoven, C., Livingston, G., Bass, N. J., Gurling, H., McQuillin, A., Gwilliam, R., Deloukas, P., Al-Chalabi, A., Shaw, C. E., Tsolaki, M., Singleton, A. B., Guerreiro, R., Mühleisen, T. W.,

Nöthen, M. M., Moebus, S., Jöckel, K.-H., Klopp, N., Wichmann, H.-E., Pankratz, V. S., Sando, S. B., Aasly, J. O., Barcikowska, M., Wszolek, Z. K., Dickson, D. W., Graff-Radford, N. R., Petersen, R. C., van Duijn, C. M., Breteler, M. M. B., Ikram, M. A., DeStefano, A. L., Fitzpatrick, A. L., Lopez, O., Launer, L. J., Seshadri, S., Berr, C., Campion, D., Epelbaum, J., Dartigues, J.-F., Tzourio, C., Alpérovitch, A., Lathrop, M., Feulner, T. M., Friedrich, P., Riehle, C., Krawczak, M., Schreiber, S., Mayhaus, M., Nicolhaus, S., Wagenpfeil, S., Steinberg, S., Stefansson, H., Stefansson, K., Snaedal, J., Björnsson, S., Jonsson, P. V, Chouraki, V., Genier-Boley, B., Hiltunen, M., Soininen, H., Combarros, O., Zelenika, D., Delepine, M., Bullido, M. J., Pasquier, F., Mateo, I., Frank-Garcia, A., Porcellini, E., Hanon, O., Coto, E., Alvarez, V., Bosco, P., Siciliano, G., Mancuso, M., Panza, F., Solfrizzi, V., Nacmias, B., Sorbi, S., Bossù, P., Piccardi, P., Arosio, B., Annoni, G., Seripa, D., Pilotto, A., Scarpini, E., Galimberti, D., Brice, A., Hannequin, D., Licastro, F., Jones, L., Holmans, P. A., Jonsson, T., Riemenschneider, M., Morgan, K., Younkin, S. G., Owen, M. J., O'Donovan, M., Amouyel, P. and Williams, J. (2011) Common variants at ABCA7, MS4A6A/MS4A4E, EPHA1, CD33 and CD2AP are associated with Alzheimer's disease. *Nature genetics*. **43**, 429–435.

Honarnejad, K. and Herms, J. (2012) Presenilins: role in calcium homeostasis. *Int J Biochem Cell Biol*. **44**, 1983–1986.

Hong, M., Chen, D. C. R., Klein, P. S. and Lee, V. M. Y. (1997) Lithium reduces tau phosphorylation by inhibition of glycogen synthase kinase-3. *Journal of Biological Chemistry*. **272**, 25326–25332.

Hooper, C., Killick, R. and Lovestone, S. (2008) The GSK3 hypothesis of Alzheimer's disease. *Journal of Neurochemistry*. **104**, 1433–1439.

Hoover, B. R., Reed, M. N., Su, J., Penrod, R. D., Kotilinek, L. A., Grant, M. K., Pitstick, R., Carlson, G. A., Lanier, L. M., Yuan, L. L., Ashe, K. H. and Liao, D. (2010) Tau Mislocalization to Dendritic Spines Mediates Synaptic Dysfunction Independently of Neurodegeneration. *Neuron*. **68**, 1067–1081.

Hoshino, M., Dohmae, N., Takio, K., Kanazawa, I. and Nukina, N. (2003) Identification of a novel amino-terminal fragment of amyloid precursor protein in mouse neuroblastoma Neuro2a cell. *Neuroscience Letters*. **353**, 135–138.

Huang, H. C. and Jiang, Z. F. (2009) Accumulated amyloid-beta peptide and hyperphosphorylated tau protein: Relationship and links in Alzheimer's disease. *Journal of Alzheimer's Disease.* **16**, 15–27.

Huh, G. Y., Glantz, S. B., Je, S., Morrow, J. S. and Kim, J. H. (2001) Calpain proteolysis of alpha II-spectrin in the normal adult human brain. *Neuroscience letters*. **316**, 41–44.

Hung, K.-S., Hwang, S.-L., Liang, C.-L., Chen, Y.-J., Lee, T.-H., Liu, J.-K., Howng, S.-L. and Wang, C.-H. (2005) Calpain inhibitor inhibits p35-p25-Cdk5 activation, decreases tau hyperphosphorylation, and improves neurological function after spinal cord hemisection in rats. *Journal of neuropathology and experimental neurology*. **64**, 15–26.

Hutton, M., Lendon, C. L., Rizzu, P., Baker, M., Froelich, S., Houlden, H., Pickering-Brown, S., Chakraverty, S., Isaacs, A., Grover, A., Hackett, J., Adamson, J., Lincoln, S., Dickson, D., Davies, P., Petersen, R. C., Stevens, M., de Graaff, E., Wauters, E., van Baren, J., Hillebrand, M., Joosse, M., Kwon, J. M., Nowotny, P., Che, L. K., Norton, J., Morris, J. C., Reed, L. A., Trojanowski, J., Basun, H., Lannfelt, L., Neystat, M., Fahn, S., Dark, F., Tannenberg, T., Dodd, P. R., Hayward, N., Kwok, J. B., Schofield, P. R., Andreadis, A., Snowden, J., Craufurd, D., Neary, D., Owen, F., Oostra, B. A., Hardy, J., Goate, A., van Swieten, J., Mann, D., Lynch, T. and Heutink, P. (1998) Association of missense and 5'-splice-site mutations in tau with the inherited dementia FTDP-17. *Nature*. **393**, 702–705.

Hyman, B. T., Augustinack, J. C. and Ingelsson, M. (2005) Transcriptional and conformational changes of the tau molecule in Alzheimer's disease. *Biochimica et Biophysica Acta - Molecular Basis of Disease*. **1739**, 150–157.

Ikeda, K., Akiyama, H., Haga, C. and Haga, S. (1992) Evidence that neurofibrillary tangles undergo glial modification. *Acta Neuropathologica*. **85**, 101–104.

Ikeda, K., Haga, C., Oyanagi, S., Iritani, S. and Kosaka, K. (1992) Ultrastructural and immunohistochemical study of degenerate neurite-bearing ghost tangles. *Journal of Neurology*. **239**, 191–194.

Ikonomidou, C. and Turski, L. (2002) Why did NMDA receptor antagonists fail clinical trials for stroke and traumatic brain injury? Lancet Neurology. **1**, 383–386.

Iovino, M., Pfisterer, U., Holton, J. L., Lashley, T., Swingler, R. J., Calo, L., Treacy, R., Revesz, T., Parmar, M., Goedert, M., Muqit, M. M. K. and Spillantini, M. G. (2014) The novel MAPT mutation K298E: Mechanisms of mutant tau toxicity, brain pathology and tau expression in induced fibroblast-derived neurons. *Acta Neuropathologica*. **127**, 283–295.

Iqbal, K., Wisniewski, H. M., Grundke-Iqbal, I., Korthals, J. K. and Terry, R. D. (1975) Chemical pathology of neurofibrils. Neurofibrillary tangles of Alzheimer's presenile-senile dementia. *The journal of histochemistry and cytochemistry : official journal of the Histochemistry Society*. **23**, 563–569.

Irvine, G. B., El-Agnaf, O. M., Shankar, G. M. and Walsh, D. M. (2008) Protein Aggregation in the Brain: The Molecular Basis for Alzheimer's and Parkinson's Diseases. *Molecular Medicine*. **14**, 451–464.

Ito, H. and Hamerman, J. A. (2012) TREM-2, triggering receptor expressed on myeloid cell-2, negatively regulates TLR responses in dendritic cells. *European Journal of Immunology*. **42**, 176–185.

Ittner, L. M., Ke, Y. D., Delerue, F., Bi, M., Gladbach, A., van Eersel, J., Wölfing, H., Chieng, B. C., Christie, M. J., Napier, I. A., Eckert, A., Staufenbiel, M., Hardeman, E. and Götz, J. (2010) Dendritic function of tau mediates amyloid-beta toxicity in Alzheimer's disease mouse models. *Cell*. **142**, 387–397.

Iversen, L. L., Mortishire-Smith, R. J., Pollack, S. J. and Shearman, M. S. (1995) The toxicity in vitro of beta-amyloid protein. *Biochemical Journal*. **311**, 1–16.

Iwamoto, T. and Kita, S. (2006) YM-244769, a novel Na+/Ca2+ exchange inhibitor that preferentially inhibits NCX3, efficiently protects against hypoxia/reoxygenation-induced SH-SY5Y neuronal cell damage. *Molecular pharmacology*. **70**, 2075–2083.

Janssen, J. C., Beck, J. A., Campbell, T. A., Dickinson, A., Fox, N. C., Harvey, R. J., Houlden, H., Rossor, M. N. and Collinge, J. (2003) Early onset familial Alzheimer's disease: Mutation frequency in 31 families. *Neurology*. **60**, 235–239.

Jellinger, K. A. and Stadelmann, C. (2000) Mechanisms of cell death in neurodegenerative disorders. *Journal of neural transmission. Supplementum*. **59**, 95–114.

Jellinger, K. A. and Stadelmann, C. H. (2000) The enigma of cell death in neurodegenerative disorders. *Journal of neural transmission. Supplementum*. **2000**, 21–36.

Jervis, G. A. (1948) Early senile dementia in mongoloid idiocy. *The American journal of psychiatry*. **105**, 102–106.

Jho, Y. S., Zhulina, E. B., Kim, M. W. and Pincus, P. A. (2010) Monte Carlo simulations of tau proteins: Effect of phosphorylation. *Biophysical Journal*. **99**, 2387–2397.

Jin, N., Yin, X., Gu, J., Zhang, X., Shi, J., Qian, W., Ji, Y., Cao, M., Gu, X., Ding, F., Iqbal, K., Gong, C.-X. and Liu, F. (2015) Truncation and Activation of Dual Specificity Tyrosine-phosphorylation-regulated Kinase 1A by Calpain I: a Molecular Mechanism Linked to Tau Pathology in Alzheimer's Disease. *Journal of Biological Chemistry*. **10**, 1074

Jin, N., Yin, X., Yu, D., Cao, M., Gong, C.-X., Iqbal, K., Ding, F., Gu, X. and Liu, F. (2015) Truncation and activation of GSK-3beta by calpain I: a molecular mechanism links to tau hyperphosphorylation in Alzheimer's disease. *Scientific reports*. **5**, 8187.

Jo, D. G., Lee, J. Y., Hong, Y. M., Song, S., Inhee, M. J., Koh, J. Y. and Jung, Y. K. (2004) Induction of pro-apoptotic calsenilin/DREAM/KChIP3 in Alzheimer's disease and cultured neurons after amyloid-beta exposure. *Journal of Neurochemistry*. **88**, 604–611.

Johnson, G. V. W. and Stoothoff, W. H. (2004) Tau phosphorylation in neuronal cell function and dysfunction. *Journal of cell science*. **117**, 5721–5729.

Jucker, M. and Walker, L. C. (2013) Self-propagation of pathogenic protein aggregates in neurodegenerative diseases. *Nature*. **501**, 45–51.

Juin, P., Pelletier, M., Oliver, L., Tremblais, K., Grégoire, M., Meflah, K. and Vallette, F. M. (1998) Induction of a caspase-3-like activity by calcium in normal cytosolic extracts triggers nuclear apoptosis in a cell-free system. *Journal of Biological Chemistry*. **273**, 17559–17564.

Kaneko, S., Kawakami, S., Hara, Y., Wakamori, M., Itoh, E., Minami, T., Takada, Y., Kume, T., Katsuki, H., Mori, Y. and Akaike, A. (2006) A critical role of TRPM2 in neuronal cell death by hydrogen peroxide. *Journal of pharmacological sciences*. **101**, 66–76.

Kar, S., Slowikowski, S. P. M., Westaway, D. and Mount, H. T. J. (2004) Interactions between beta-amyloid and central cholinergic neurons: implications for Alzheimer's disease. *Journal of psychiatry and neuroscience : JPN*. **29**, 427–441.

Kasparová, J., Lisá, V., Tucek, S. and Dolezal, V. (2001) Chronic exposure of NG108-15 cells to amyloid beta peptide (A beta(1-42)) abolishes calcium influx via N-type calcium channels. *Neurochemical research*. **26**, 1079–1084.

Kaufmann, S. H., Desnoyers, S., Ottaviano, Y., Davidson, N. E. and Poirier, G. G. (1993) Specific proteolytic cleavage of poly(ADP-ribose) polymerase: An early marker of chemotherapy-induced apoptosis. *Cancer Research*. **53**, 3976–3985.

Kauppinen, T. M., Suh, S., Higashi, Y., Berman, A. E., Escartin, C., Won, S., Wang, C., Cho, S.-H., Gan, L. and Swanson, R. A. (2011) Poly(ADP-ribose)polymerase-1 modulates microglial responses to amyloid β. *Journal of Neuroinflammation.* **8**, 152.

Kelly, B. L. and Ferreira, A. (2006) β-amyloid-induced dynamin 1 degradation is mediated by N-methyl-D-aspartate receptors in hippocampal neurons. *Journal of Biological Chemistry*. **281**, 28079–28089.

Kelly, B. L., Vassar, R. and Ferreira, A. (2005) β-amyloid-induced dynamin 1 depletion in hippocampal neurons: A potential mechanism for early cognitive decline in Alzheimer disease. *Journal of Biological Chemistry*. **280**, 31746–31753.

Kerokoski, P., Suuronen, T., Salminen, A., Soininen, H. and Pirttilä, T. (2002) Cleavage of the cyclin-dependent kinase 5 activator p35 to p25 does not induce tau hyperphosphorylation. *Biochemical and Biophysical Research Communications*. **298**, 693–698.

Keverne, J. and Ray, M. (2008) Neurochemistry of Alzheimer's disease. *Psychiatry.* **7**, 6–8.

Khachaturian, Z. S. (1989) Calcium, membranes, aging and Alzheimer's disease: Introduction and overview. *Annals of the New York Academy of Sciences.* **568**, 1–4.

Khatoon, S., Grundke-Iqbal, I. and Iqbal, K. (1994) Levels of normal and abnormally phosphorylated tau in different cellular and regional compartments of Alzheimer disease and control brains. *FEBS letters*. **351**, 80–84.

Khoutorsky, A. and Spira, M. E. (2009) Activity-dependent calpain activation plays a critical role in synaptic facilitation and post-tetanic potentiation. *Learning and memory (Cold Spring Harbor, N.Y.)*. **16**, 129–141.

Kim, S. H., Henkel, J. S., Beers, D. R., Sengun, I. S., Simpson, E. P., Goodman, J. C., Engelhardt, J. I., Siklós, L. and Appel, S. H. (2003) PARP expression is increased in astrocytes but decreased in motor neurons in the spinal cord of

sporadic ALS patients. *Journal of neuropathology and experimental neurology*. **62**, 88–103.

Kim, Y.-H. and Koh, J.-Y. (2002) The role of NADPH oxidase and neuronal nitric oxide synthase in zinc-induced poly(ADP-ribose) polymerase activation and cell death in cortical culture. *Experimental neurology*. **177**, 407–418.

Kiselyov, K., Chen, J., Rbaibi, Y., Oberdick, D., Tjon-Kon-Sang, S., Shcheynikov, N., Muallem, S. and Soyombo, A. (2005) TRP-ML1 is a lysosomal monovalent cation channel that undergoes proteolytic cleavage. *Journal of Biological Chemistry*. **280**, 43218–43223.

Kiss, R., Kovács, D., Tompa, P. and Perczel, A. (2008) Local structural preferences of calpastatin, the intrinsically unstructured protein inhibitor of calpain. *Biochemistry*. **47**, 6936–6945.

Koffie, R. M., Meyer-Luehmann, M., Hashimoto, T., Adams, K. W., Mielke, M. L., Garcia-Alloza, M., Micheva, K. D., Smith, S. J., Kim, M. L., Lee, V. M., Hyman, B. T. and Spires-Jones, T. L. (2009) Oligomeric amyloid beta associates with postsynaptic densities and correlates with excitatory synapse loss near senile plaques. *Proceedings of the National Academy of Sciences of the United States of America*. **106**, 4012–4017.

Kojro, E., Gimpl, G., Lammich, S., Marz, W. and Fahrenholz, F. (2001) Low cholesterol stimulates the nonamyloidogenic pathway by its effect on the alpha -secretase ADAM 10. *Proceedings of the National Academy of Sciences of the United States of America*. **98**, 5815–5820.

Kontush, A. (2001) Amyloid-beta: An antioxidant that becomes a pro-oxidant and critically contributes to Alzheimer's disease. *Free Radical Biology and Medicine*. **31**, 1120–1131.

Koppel, J., Campagne, F., Vingtdeux, V., Dreses-Werringloer, U., Ewers, M., Rujescu, D., Hampel, H., Gordon, M. L., Christen, E., Chapuis, J., Greenwald, B. S., Davies, P. and Marambaud, P. (2011) CALHM1 P86L polymorphism modulates CSF Aβ levels in cognitively healthy individuals at risk for Alzheimer's disease. *Molecular medicine (Cambridge, Mass.)*. **17**, 974–979.

Kovalevich, J. and Langford, D. (2013) 'Considerations for the Use of SH - SY5Y Neuroblastoma Cells in Neurobiology', in *Neuronal Cell Culture: Methods and Protocols*. **2013**, 9–21.

Kuchibhotla, K. V., Goldman, S. T., Lattarulo, C. R., Wu, H. Y., Hyman, B. T. and Bacskai, B. J. (2008) Abeta Plaques Lead to Aberrant Regulation of Calcium

Homeostasis In Vivo Resulting in Structural and Functional Disruption of Neuronal Networks. *Neuron*. **59**, 214–225.

Kuhn, P.-H., Wang, H., Dislich, B., Colombo, A., Zeitschel, U., Ellwart, J. W., Kremmer, E., Rossner, S. and Lichtenthaler, S. F. (2010) ADAM10 is the physiologically relevant, constitutive alpha-secretase of the amyloid precursor protein in primary neurons. *The EMBO journal*. **29**, 3020–3032.

Kulijewicz-Nawrot, M., Syková, E., Chvátal, A., Verkhratsky, A. and Rodríguez, J. J. (2013) Astrocytes and glutamate homoeostasis in Alzheimer's disease: a decrease in glutamine synthetase, but not in glutamate transporter-1, in the prefrontal cortex. *ASN neuro*. **5,** 273–282.

Kulikov, A. V, Rzhaninova, A. A., Goldshtein, D. V and Boldyrev, A. A. (2007) Expression of NMDA receptors in multipotent stromal cells of human adipose tissue under conditions of retinoic acid-induced differentiation. *Bulletin of experimental biology and medicine*. **144**, 626–629.

Kurnellas, M. P., Donahue, K. C. and Elkabes, S. (2007) Mechanisms of neuronal damage in multiple sclerosis and its animal models: role of calcium pumps and exchangers. *Biochemical Society transactions*. **35**, 923–926.

Kyratzi, E. and Efthimiopoulos, S. (2014) Calcium regulates the interaction of amyloid precursor protein with Homer3 protein. *Neurobiology of Aging*. **35**, 2053–2063.

Lacor, P. N., Buniel, M. C., Chang, L., Fernandez, S. J., Gong, Y., Viola, K. L., Lambert, M. P., Velasco, P. T., Bigio, E. H., Finch, C. E., Krafft, G. A. and Klein, W. L. (2004) Synaptic targeting by Alzheimer's-related amyloid beta oligomers. *The Journal of neuroscience : the official journal of the Society for Neuroscience*. **24**, 10191–10200.

LaFerla, F. M. (2002) Calcium dyshomeostasis and intracellular signalling in Alzheimer's disease. *Nature reviews. Neuroscience*. **3**, 862–872.

LaFerla, F. M., Green, K. N. and Oddo, S. (2007) Intracellular amyloid-beta in Alzheimer's disease. *Nature reviews. Neuroscience*. **8**, 499–509.

LaFerla, F. M. and Oddo, S. (2005) Alzheimer's disease: Abeta, tau and synaptic dysfunction. *Trends in molecular medicine*. **11**, 170–176.

Lai, M. K. P., Chen, C. P., Hope, T. and Esiri, M. M. (2010) Hippocampal neurofibrillary tangle changes and aggressive behaviour in dementia. *Neuroreport*. **21**, 1111–1115.

Lambert, J. C., Grenier-Boley, B., Chouraki, V., Heath, S., Zelenika, D., Fievet, N., Hannequin, D., Pasquier, F., Hanon, O., Brice, A., Epelbaum, J., Berr, C., Dartigues, J. F., Tzourio, C., Campion, D., Lathrop, M. and Amouyel, P. (2010) Implication of the immune system in Alzheimer's disease: evidence from genome-wide pathway analysis. *Journal of Alzheimer's Disease*. **20**, 1107–1118.

Lambert, J. C., Ibrahim-Verbaas, C. a, Harold, D., Naj, a C., Sims, R., Bellenguez, C., DeStafano, a L., Bis, J. C., Beecham, G. W., Grenier-Boley, B., Russo, G., Thorton-Wells, T. a, Jones, N., Smith, a V, Chouraki, V., Thomas, C., Ikram, M. a, Zelenika, D., Vardarajan, B. N., Kamatani, Y., Lin, C. F., Gerrish, a, Schmidt, H., Kunkle, B., Dunstan, M. L., Ruiz, a, Bihoreau, M. T., Choi, S. H., Reitz, C., Pasquier, F., Cruchaga, C., Craig, D., Amin, N., Berr, C., Lopez, O. L., De Jager, P. L., Deramecourt, V., Johnston, J. a, Evans, D., Lovestone, S., Letenneur, L., Morón, F. J., Rubinsztein, D. C., Eiriksdottir, G., Sleegers, K., Goate, a M., Fiévet, N., Huentelman, M. W., Gill, M., Brown, K., Kamboh, M. I., Keller, L., Barberger-Gateau, P., McGuiness, B., Larson, E. B., Green, R., Myers, a J., Dufouil, C., Todd, S., Wallon, D., Love, S., Rogaeva, E., Gallacher, J., St George-Hyslop, P., Clarimon, J., Lleo, a, Bayer, a, Tsuang, D. W., Yu, L., Tsolaki, M., Bossù, P., Spalletta, G., Proitsi, P., Collinge, J., Sorbi, S., Sanchez-Garcia, F., Fox, N. C., Hardy, J., Deniz Naranjo, M. C., Bosco, P., Clarke, R., Brayne, C., Galimberti, D., Mancuso, M., Matthews, F., Moebus, S., Mecocci, P., Del Zompo, M., Maier, W., Hampel, H., Pilotto, a, Bullido, M., Panza, F., Caffarra, P., Nacmias, B., Gilbert, J. R., Mayhaus, M., Lannefelt, L., Hakonarson, H., Pichler, S., Carrasquillo, M. M., Ingelsson, M., Beekly, D., Alvarez, V., Zou, F., Valladares, O., Younkin, S. G., Coto, E., Hamilton-Nelson, K. L., Gu, W., Razquin, C., Pastor, P., Mateo, I., Owen, M. J., Faber, K. M., Jonsson, P. V, Combarros, O., O'Donovan, M. C., Cantwell, L. B., Soininen, H., Blacker, D., Mead, S., Mosley, T. H., Bennett, D. a, Harris, T. B., Fratiglioni, L., Holmes, C., de Bruijn, R. F., Passmore, P., Montine, T. J., Bettens, K., Rotter, J. I., Brice, a, Morgan, K., Foroud, T. M., Kukull, W. a, Hannequin, D., Powell, J. F., Nalls, M. a, Ritchie, K., Lunetta, K. L., Kauwe, J. S., Boerwinkle, E., Riemenschneider, M., Boada, M., Hiltuenen, M., Martin, E. R., Schmidt, R., Rujescu, D., Wang, L. S., Dartigues, J. F., Mayeux, R., Tzourio, C., Hofman, a, Nöthen, M. M., Graff, C., Psaty, B. M., Jones, L., Haines, J. L., Holmans, P. a, Lathrop, M., Pericak-Vance, M. a, Launer, L. J., Farrer, L. a, van Duijn, C. M., Van Broeckhoven, C., Moskvina, V., Seshadri, S., Williams, J., Schellenberg, G. D. and Amouyel, P. (2013) Meta-analysis of 74,046 individuals identifies 11 new susceptibility loci for Alzheimer's disease. *Nature genetics*. **45**, 1452–1458.

Laske, C., Stellos, K., Kempter, I., Stransky, E., Maetzler, W., Fleming, I. and Randriamboavonjy, V. (2015) Increased cerebrospinal fluid calpain activity and microparticle levels in Alzheimer's disease. *Alzheimer's and dementia : the journal of the Alzheimer's Association*. **11**, 465–474.

Lee, C. R., Machold, R. P., Witkovsky, P. and Rice, M. E. (2013) TRPM2 channels are required for NMDA-induced burst firing and contribute to H(2)O(2)-dependent modulation in substantia nigra pars reticulata GABAergic neurons. *The Journal of neuroscience : the official journal of the Society for Neuroscience*. **33**, 1157–1168.

Lee, M. S., Kwon, Y. T., Li, M., Peng, J., Friedlander, R. M. and Tsai, L. H. (2000) Neurotoxicity induces cleavage of p35 to p25 by calpain. *Nature*. **405**, 360–364.

Lee, V. M., Goedert, M. and Trojanowski, J. Q. (2001) Neurodegenerative tauopathies. *Annual review of neuroscience*. **24**, 1121–1159.

Lewis, J., Dickson, D. W., Lin, W. L., Chisholm, L., Corral, A., Jones, G., Yen, S. H., Sahara, N., Skipper, L., Yager, D., Eckman, C., Hardy, J., Hutton, M. and McGowan, E. (2001) Enhanced neurofibrillary degeneration in transgenic mice expressing mutant tau and APP. *Science (New York, N.Y.)*. **293**, 1487–1491.

Liang, B., Duan, B. Y., Zhou, X. P., Gong, J. X. and Luo, Z. G. (2010) Calpain activation promotes BACE1 expression, amyloid precursor protein processing, and amyloid plaque formation in a transgenic mouse model of Alzheimer disease. *Journal of Biological Chemistry*. **285**, 27737–27744.

Liang, Z., Liu, F., Grundke-Iqbal, I., Iqbal, K. and Gong, C. X. (2007) Down-regulation of cAMP-dependent protein kinase by over-activated calpain in Alzheimer disease brain. *Journal of Neurochemistry*. **103**, 2462–2470.

Lim, D., Ronco, V., Grolla, A. A., Verkhratsky, A. and Genazzani, A. A. (2014) Glial Calcium Signalling in Alzheimer's Disease. *Reviews of physiology, biochemistry and pharmacology*. **167**, 45-65

Lindwall, G. and Cole, R. D. (1984) Phosphorylation affects the ability of tau protein to promote microtubule assembly. *Journal of Biological Chemistry*. **259**, 5301–5305.

Lippens, G., Sillen, A., Landrieu, I., Amniai, L., Sibille, N., Barbier, P., Leroy, A., Hanoulle, X. and Wieruszeski, J.-M. (2007) Tau aggregation in Alzheimer's disease: what role for phosphorylation? *Prion*. **1**, 21–25.

Lipton, S. A. (2004) Failures and successes of NMDA receptor antagonists: molecular basis for the use of open-channel blockers like memantine in the treatment of acute and chronic neurologic insults. *NeuroRx : the journal of the American Society for Experimental NeuroTherapeutics*. **1**, 101–110.

Lipton, S. A. (2006) Paradigm shift in neuroprotection by NMDA receptor blockade: memantine and beyond. *Nature reviews. Drug discovery*. **5**, 160–170.

Liu, C.-C., Liu, C.-C., Kanekiyo, T., Xu, H. and Bu, G. (2013) Apolipoprotein E and Alzheimer disease: risk, mechanisms and therapy. *Nature reviews. Neurology*. **9**, 106–118.

Liu, F., Iqbal-Grundke, I., Iqbal, K., Oda, Y., Tomizawa, K. and Gong, C. X. (2005) Truncation and activation of calcineurin A by calpain I in Alzheimer disease brain. *Journal of Biological Chemistry*. **280**, 37755–37762.

Liu, J., Chang, L., Roselli, F., Almeida, O. F. X., Gao, X., Wang, X., Yew, D. T. and Wu, Y. (2010) Amyloid-beta induces caspase-dependent loss of PSD-95 and synaptophysin through NMDA receptors. *Journal of Alzheimer's Disease*. **22**, 541–556.

Liu, J., Gao, X. and Wu, Y. (2008) N-Methyl-*D*-Aspartate Receptors Mediate Excitotoxicity in Amyloid Beta-Induced Synaptic Pathology of Alzheimer's Disease. *Neuroembryology and Aging*. **5**, 134–143.

Liu, L., Xing, D. and Chen, W. R. (2009) beta-Calpain regulates caspase-dependent and apoptosis inducing factor-mediated caspase-independent apoptotic pathways in cisplatin-induced apoptosis. *International Journal of Cancer*. **125**, 2757–2766.

Liu, M. C., Kobeissy, F., Zheng, W., Zhang, Z., Hayes, R. L. and Wang, K. K. W. (2011) Dual vulnerability of tau to calpains and caspase-3 proteolysis under neurotoxic and neurodegenerative conditions. *ASN neuro*. **3**, e00051.

Liu, X., Van Vleet, T. and Schnellmann, R. G. (2004) The role of calpain in oncotic cell death. *Annual review of pharmacology and toxicology*. **44**, 349–370.

Lloret, A., Badia, M. C., Giraldo, E., Ermak, G., Alonso, M. D., Pallardó, F. V., Davies, K. J. A. and Viña, J. (2011) Amyloid-β toxicity and tau hyperphosphorylation are linked via RCAN1 in Alzheimer's disease. *Journal of Alzheimer's Disease*. **27**, 701–709.

Lott, I. T. (1982) Down's syndrome, aging, and Alzheimer's disease: a clinical review. *Annals of the New York Academy of Sciences*. **396**, 15–27.

Love, S., Barber, R. and Wilcock, G. K. (1999) Increased poly(ADP-ribosyl)ation of nuclear proteins in Alzheimer's disease. *Brain*. **122**, 247–253.

Lu, X., Rong, Y. and Baudry, M. (2000) Calpain-mediated degradation of PSD-95 in developing and adult rat brain. *Neuroscience Letters*. **286**, 149–153.

Lue, L. F., Kuo, Y. M., Roher, A. E., Brachova, L., Shen, Y., Sue, L., Beach, T., Kurth, J. H., Rydel, R. E. and Rogers, J. (1999) Soluble amyloid beta peptide concentration as a predictor of synaptic change in Alzheimer's disease. *The American journal of pathology*. **155**, 853–862.

Luo, X. and Lee Kraus, W. (2012) On par with PARP: Cellular stress signaling through poly(ADP-ribose) and PARP-1. *Genes and Development*. **26**, 417–432.

Lyketsos, C. G., Carrillo, M. C., Ryan, J. M., Khachaturian, A. S., Trzepacz, P., Amatniek, J., Cedarbaum, J., Brashear, R. and Miller, D. S. (2011) Neuropsychiatric symptoms in Alzheimer's disease. *Alzheimer's and dementia : the journal of the Alzheimer's Association.* **7**, 532–539.

Lytton, J. (2007) Na+/Ca2+ exchangers: three mammalian gene families control Ca2+ transport. *The Biochemical journal*. **406**, 365–382.

Magi, S., Castaldo, P., Carrieri, G., Scorziello, A., Di Renzo, G. and Amoroso, S. (2005) Involvement of Na+-Ca2+ exchanger in intracellular Ca2+ increase and neuronal injury induced by polychlorinated biphenyls in human neuroblastoma SH-SY5Y cells. *J Pharmacol Exp Ther*. **315**, 291–296.

Mahley, R. W. (1988) Apolipoprotein E: cholesterol transport protein with expanding role in cell biology. *Science*. **240**, 622–630.

Mairet-Coello, G., Courchet, J., Pieraut, S., Courchet, V., Maximov, A. and Polleux, F. (2013) The CAMKK2-AMPK Kinase Pathway Mediates the Synaptotoxic Effects of Aβ Oligomers through Tau Phosphorylation. *Neuron*. **78**, 94–108.

Maltsev, A. V., Santockyte, R., Bystryak, S. and Galzitskaya, O. V. (2014) Activation of neuronal defense mechanisms in response to pathogenic factors triggering induction of amyloidosis in Alzheimer's disease. *Journal of Alzheimer's Disease*. **40**, 19–32.

Mandir, A. S., Poitras, M. F., Berliner, A. R., Herring, W. J., Guastella, D. B., Feldman, A., Poirier, G. G., Wang, Z. Q., Dawson, T. M. and Dawson, V. L. (2000) NMDA but not non-NMDA excitotoxicity is mediated by Poly(ADP-ribose) polymerase. *The Journal of neuroscience : the official journal of the Society for Neuroscience*. **20**, 8005–8011.

Mangialasche, F., Solomon, A., Winblad, B., Mecocci, P. and Kivipelto, M. (2010) Alzheimer's disease: clinical trials and drug development. *Lancet neurology*. **9**, 702–716.

Manolio, T. A., Collins, F. S., Cox, N. J., Goldstein, D. B., Hindorff, L. A., Hunter, D. J., McCarthy, M. I., Ramos, E. M., Cardon, L. R., Chakravarti, A., Cho, J. H., Guttmacher, A. E., Kong, A., Kruglyak, L., Mardis, E., Rotimi, C. N., Slatkin, M., Valle, D., Whittemore, A. S., Boehnke, M., Clark, A. G., Eichler, E. E., Gibson, G., Haines, J. L., Mackay, T. F. C., McCarroll, S. A. and Visscher, P. M. (2009) Finding the missing heritability of complex diseases. *Nature*. **461**, 747–753.

Mark, R. J., Hensley, K., Butterfield, D. A. and Mattson, M. P. (1995) Amyloid beta-peptide impairs ion-motive ATPase activities: evidence for a role in loss of neuronal Ca2+ homeostasis and cell death. *The Journal of neuroscience : the official journal of the Society for Neuroscience*. **15**, 6239–6249.

Marlow, L., Canet, R. M., Haugabook, S. J., Hardy, J. A., Lahiri, D. K. and Sambamurti, K. (2003) APH1, PEN2, and Nicastrin increase Aβ levels and γ-secretase activity. *Biochemical and Biophysical Research Communications*. **305**, 502–509.

Martin, L., Latypova, X. and Terro, F. (2011) Post-translational modifications of tau protein: Implications for Alzheimer's disease. *Neurochemistry International*. **58**, 458–471.

Mastrangelo, M. A. and Bowers, W. J. (2008) Detailed immunohistochemical characterization of temporal and spatial progression of Alzheimer's disease-related pathologies in male triple-transgenic mice. *BMC neuroscience*. **9**, 81.

Matarin, M., Salih, D. A., Yasvoina, M., Cummings, D. M., Guelfi, S., Liu, W., Nahaboo Solim, M. A., Moens, T. G., Paublete, R. M., Ali, S. S., Perona, M., Desai, R., Smith, K. J., Latcham, J., Fulleylove, M., Richardson, J. C., Hardy, J. and Edwards, F. A. (2015) A Genome-wide Gene-Expression Analysis and Database in Transgenic Mice during Development of Amyloid or Tau Pathology. *Cell Reports*. **10**, 633–644.

Mathews, P. M., Jiang, Y., Schmidt, S. D., Grbovic, O. M., Mercken, M. and Nixon, R. A. (2002) Calpain activity regulates the cell surface distribution of amyloid precursor protein. Inhibition of calpains enhances endosomal generation of beta-cleaved C-terminal APP fragments. *Journal of Biological Chemistry*. **277**, 36415–36424.

Mattson, M. P. (2002) Oxidative stress, perturbed calcium homeostasis, and immune dysfunction in Alzheimer's disease. *Journal of neurovirology*. **8**, 539–550.

Mattson, M. P., Cheng, B., Davis, D., Bryant, K., Lieberburg, I. and Rydel, R. E. (1992) beta-Amyloid peptides destabilize calcium homeostasis and render human cortical neurons vulnerable to excitotoxicity. *The Journal of neuroscience : the official journal of the Society for Neuroscience*. **12**, 376–389.

Mattson, M. P., LaFerla, F. M., Chan, S. L., Leissring, M. A., Shepel, P. N. and Geiger, J. D. (2000) Calcium signaling in the ER: its role in neuronal plasticity and neurodegenerative disorders. *Trends Neurosci*. **23**, 222–229.

Mayeux, R. and Hyslop, P. S. G. (2008) Alzheimer's disease: advances in trafficking. *The Lancet. Neurology*. **7**, 2–3.

McBrayer, M. and Nixon, R. a (2013) Lysosome and calcium dysregulation in Alzheimer's disease: partners in crime. *Biochemical Society transactions*. **41**, 1495–1502.

McCollum, A. T., Nasr, P. and Estus, S. (2002) Calpain activates caspase-3 during UV-induced neuronal death but only calpain is necessary for death. *Journal of Neurochemistry*. **82**, 1208–1220.

McLaurin, J., Kierstead, M. E., Brown, M. E., Hawkes, C. A., Lambermon, M. H. L., Phinney, A. L., Darabie, A. A., Cousins, J. E., French, J. E., Lan, M. F., Chen, F., Wong, S. S. N., Mount, H. T. J., Fraser, P. E., Westaway, D. and St George-Hyslop, P. (2006) Cyclohexanehexol inhibitors of Abeta aggregation prevent and reverse Alzheimer phenotype in a mouse model. *Nature medicine*. **12**, 801–808.

McLean, C. A., Cherny, R. A., Fraser, F. W., Fuller, S. J., Smith, M. J., Beyreuther, K., Bush, A. I. and Masters, C. L. (1999) Soluble pool of Aβ amyloid as a determinant of severity of neurodegeneration in Alzheimer's disease. *Annals of Neurology*. **46**, 860–866.

McNulty, S. and Fonfria, E. (2005) The role of TRPM channels in cell death. *Pflugers Archiv European Journal of Physiology*. **451**, 235–242.

Medeiros, R., Kitazawa, M., Chabrier, M.A., Cheng, D., Baglietto-Vargas, D., Kling, A., Moeller, A., Green, K.N. and LaFerla, F.M. (2012) Calpain inhibitor A-705253 mitigates Alzheimer's disease-like pathology and cognitive decline in aged 3xTgAD mice. *American Journal of Pathology*. **181**, 616-25.

Mégnin-Chanet, F., Bollet, M. A. and Hall, J. (2010) Targeting poly(ADP-ribose) polymerase activity for cancer therapy. *Cellular and molecular life sciences: CMLS*. **67**, 3649–3662.

Michaelis, M. L., Johe, K. and Kitos, T. E. (1984) Age-dependent alterations in synaptic membrane systems for Ca2+ regulation. *Mechanisms of ageing and development*. **25**, 215–225.

Miller, B. a (2004) Inhibition of TRPM2 function by PARP inhibitors protects cells from oxidative stress-induced death. *British journal of pharmacology*. **143**, 515–516.

Mohmmad Abdul, H., Baig, I., LeVine, H., Guttmann, R. P. and Norris, C. M. (2011) Proteolysis of calcineurin is increased in human hippocampus during mild cognitive impairment and is stimulated by oligomeric Abeta in primary cell culture. *Aging Cell*. **10**, 103–113.

Molinaro, P., Cataldi, M., Cuomo, O., Viggiano, D., Pignataro, G., Sirabella, R., Secondo, A., Boscia, F., Pannaccione, A., Scorziello, A., Sokolow, S., Herchuelz, A., Di Renzo, G. and Annunziato, L. (2013) Genetically modified mice as a strategy to unravel the role played by the Na(+)/Ca (2+) exchanger in brain ischemia and in spatial learning and memory deficits. *Advances in experimental medicine and biology*. **961**, 213–222.

Molinaro, P., Viggiano, D., Nisticò, R., Sirabella, R., Secondo, A., Boscia, F., Pannaccione, A., Scorziello, A., Mehdawy, B., Sokolow, S., Herchuelz, A., Di Renzo, G. F. and Annunziato, L. (2011) Na+ -Ca2+ exchanger (NCX3) knock-out mice display an impairment in hippocampal long-term potentiation and spatial learning and memory. *The Journal of neuroscience : the official journal of the Society for Neuroscience*. **31**, 7312–7321.

Molnár, Z., Soós, K., Lengyel, I., Penke, B., Szegedi, V. and Budai, D. (2004) Enhancement of NMDA responses by beta-amyloid peptides in the hippocampus in vivo. *Neuroreport*. **15**, 1649–1652.

Morales-Corraliza, J., Berger, J. D., Mazzella, M. J., Veeranna, Neubert, T. A., Ghiso, J., Rao, M. V., Staufenbiel, M., Nixon, R. A. and Mathews, P. M. (2012) Calpastatin modulates APP processing in the brains of beta-amyloid depositing but not wild-type mice. *Neurobiology of Aging*. **33**, 9-18

Morris, G. P., Clark, I. A. and Vissel, B. (2014) Inconsistencies and controversies surrounding the amyloid hypothesis of Alzheimer's disease. *Acta neuropathologica communications*. **2**, 135.

Morris, M., Knudsen, G. M., Maeda, S., Trinidad, J. C., Ioanoviciu, A., Burlingame, A. L. and Mucke, L. (2015) Tau post-translational modifications in wild-type and human amyloid precursor protein transgenic mice. *Nature neuroscience*. **18**, 1183–1189.

Morris, M., Maeda, S., Vossel, K. and Mucke, L. (2011) The Many Faces of Tau. *Neuron.* **70**, 410–426.

Morton, A. J., Hammond, C., Mason, W. T. and Henderson, G. (1992) Characterisation of the L- and N-type calcium channels in differentiated SH-SY5Y neuroblastoma cells: calcium imaging and single channel recording. *Brain research. Molecular brain research*. **13**, 53–61.

Mouton-Liger, F., Paquet, C., Dumurgier, J., Bouras, C., Pradier, L., Gray, F. and Hugon, J. (2012) Oxidative stress increases BACE1 protein levels through activation of the PKR-eIF2α pathway. *Biochimica et Biophysica Acta - Molecular Basis of Disease*. **1822**, 885–896.

Mrak, R. E., Sheng, J. G. and Griffin, W. S. (1996) Correlation of astrocytic S100 beta expression with dystrophic neurites in amyloid plaques of Alzheimer's disease. *Journal of neuropathology and experimental neurology*. **55**, 273–279.

Mufson, E. J., Ward, S. and Binder, L. (2014) Prefibrillar tau oligomers in mild cognitive impairment and Alzheimer's disease. *Neurodegenerative Diseases*. **13**, 151–153.

Mukrasch, M. D., Biernat, J., Von Bergen, M., Griesinger, C., Mandelkow, E. and Zweckstetter, M. (2005) Sites of tau important for aggregation populate β-structure and bind to microtubules and polyanions. *Journal of Biological Chemistry*. **280**, 24978–24986.

Mullan, M., Crawford, F., Axelman, K., Houlden, H., Lilius, L., Winblad, B. and Lannfelt, L. (1992) A pathogenic mutation for probable Alzheimer's disease in the APP gene at the N-terminus of beta-amyloid. *Nature genetics.* **1**, 345–347.

Muller, W., Meske, V., Berlin, K., Scharnagl, H., Marz, W. and Ohm, T. G. (1998) Apolipoprotein E isoforms increase intracellular Ca2+ differentially through a omega-agatoxin IVa-sensitive Ca2+-channel. *Brain pathology (Zurich, Switzerland)*. **8**, 641–653.

Murachi, T. (1990) Calpain and calpastatin. *Rinsho byori. The Japanese journal of clinical pathology*. **38**, 337–346.

Murrey, H. E., Gama, C. I., Kalovidouris, S. A., Luo, W.-I., Driggers, E. M., Porton, B. and Hsieh-Wilson, L. C. (2006a) Protein fucosylation regulates synapsin Ia/Ib expression and neuronal morphology in primary hippocampal neurons. *Proceedings of the National Academy of Sciences of the United States of America*. **103**, 21–26.

Murrey, H. E., Gama, C. I., Kalovidouris, S. A., Luo, W.-I., Driggers, E. M., Porton, B. and Hsieh-Wilson, L. C. (2006b) Protein fucosylation regulates synapsin Ia/Ib expression and neuronal morphology in primary hippocampal neurons. *Proceedings of the National Academy of Sciences of the United States of America* . **103**, 21–26.

Nadler, Y., Alexandrovich, A., Grigoriadis, N., Hartmann, T., Jagannatha Rao, K. S., Shohami, E. and Stein, R. (2008) Increased expression of the beta-secretase components presenilin-1 and nicastrin in activated astrocytes and microglia following traumatic brain injury. *GLIA*. **56**, 552–567.

Naj, A. C., Jun, G., Beecham, G. W., Wang, L.-S., Vardarajan, B. N., Buros, J., Gallins, P. J., Buxbaum, J. D., Jarvik, G. P., Crane, P. K., Larson, E. B., Bird, T. D., Boeve, B. F., Graff-Radford, N. R., De Jager, P. L., Evans, D., Schneider, J. A., Carrasquillo, M. M., Ertekin-Taner, N., Younkin, S. G., Cruchaga, C., Kauwe, J. S. K., Nowotny, P., Kramer, P., Hardy, J., Huentelman, M. J., Myers, A. J., Barmada, M. M., Demirci, F. Y., Baldwin, C. T., Green, R. C., Rogaeva, E., St George-Hyslop, P., Arnold, S. E., Barber, R., Beach, T., Bigio, E. H., Bowen, J. D., Boxer, A., Burke, J. R., Cairns, N. J., Carlson, C. S., Carney, R. M., Carroll, S. L., Chui, H. C., Clark, D. G., Corneveaux, J., Cotman, C. W., Cummings, J. L., DeCarli, C., DeKosky, S. T., Diaz-Arrastia, R., Dick, M., Dickson, D. W., Ellis, W. G., Faber, K. M., Fallon, K. B., Farlow, M. R., Ferris, S., Frosch, M. P., Galasko, D. R., Ganguli, M., Gearing, M., Geschwind, D. H., Ghetti, B., Gilbert, J. R., Gilman, S., Giordani, B., Glass, J. D., Growdon, J. H., Hamilton, R. L., Harrell, L. E., Head, E., Honig, L. S., Hulette, C. M., Hyman, B. T., Jicha, G. A., Jin, L.-W., Johnson, N., Karlawish, J., Karydas, A., Kaye, J. A., Kim, R., Koo, E. H., Kowall, N. W., Lah, J. J., Levey, A. I., Lieberman, A. P., Lopez, O. L., Mack, W. J., Marson, D. C., Martiniuk, F., Mash, D. C., Masliah, E., McCormick, W. C., McCurry, S. M., McDavid, A. N., McKee, A. C., Mesulam, M., Miller, B. L., Miller, C. A., Miller, J. W., Parisi, J. E., Perl, D. P., Peskind, E., Petersen, R. C., Poon, W. W., Quinn, J. F., Rajbhandary, R. A., Raskind, M., Reisberg, B., Ringman, J. M., Roberson, E. D., Rosenberg, R. N., Sano, M., Schneider, L. S., Seeley, W., Shelanski, M. L., Slifer, M. A., Smith, C. D., Sonnen, J. A., Spina, S., Stern, R. A., Tanzi, R. E., Trojanowski, J. Q., Troncoso, J. C., Van Deerlin, V. M., Vinters, H. V, Vonsattel, J. P., Weintraub, S., Welsh-Bohmer, K. A., Williamson, J., Woltjer, R. L., Cantwell, L. B., Dombroski, B. A., Beekly, D., Lunetta, K. L., Martin, E. R., Kamboh, M. I., Saykin, A. J., Reiman, E. M., Bennett, D. A., Morris, J. C., Montine, T. J., Goate, A. M., Blacker, D., Tsuang, D. W., Hakonarson, H., Kukull,

W. A., Foroud, T. M., Haines, J. L., Mayeux, R., Pericak-Vance, M. A., Farrer, L. A. and Schellenberg, G. D. (2011) Common variants at MS4A4/MS4A6E, CD2AP, CD33 and EPHA1 are associated with late-onset Alzheimer's disease. *Nature genetics*. **43**, 436–441.

Nakagawa, T. and Yuan, J. (2000) Cross-talk between two cysteine protease families: Activation of caspase-12 by calpain in apoptosis. *Journal of Cell Biology*. **150**, 887–894.

Naranjo, J. R. and Mellström, B. (2012) Ca2+-dependent transcriptional control of Ca2+ homeostasis. *Journal of Biological Chemistry.* **287**, 31674–31680.

Naziroğlu, M. (2011) TRPM2 cation channels, oxidative stress and neurological diseases: Where are we now? *Neurochemical Research*. **36**, 355–366.

Nedergaard, M. (1994) Direct signaling from astrocytes to neurons in cultures of mammalian brain cells. *Science (New York, N.Y.)*. **263**, 1768–1771.

Nelson, O., Supnet, C., Liu, H. and Bezprozvanny, I. (2010) Familial Alzheimer's disease mutations in presenilins: effects on endoplasmic reticulum calcium homeostasis and correlation with clinical phenotypes. *Journal of Alzheimer's disease : JAD*. **21**, 781–793.

Nicholls, D. G. and Budd, S. L. (1998) Mitochondria and neuronal glutamate excitotoxicity. Biochimica et Biophysica Acta – Bioenergetics. **1366**, 97–112.

Nicholson, A. M. and Ferreira, A. (2009) Increased membrane cholesterol might render mature hippocampal neurons more susceptible to beta-amyloid-induced calpain activation and tau toxicity. *The Journal of neuroscience : the official journal of the Society for Neuroscience*. **29**, 4640–4651.

Nikoletopoulou, V. and Tavernarakis, N. (2012) Calcium homeostasis in aging neurons. *Frontiers in Genetics.* **3**, 200.

Nilsson, E., Alafuzoff, I., Blennow, K., Blomgren, K., Hall, C. M., Janson, I., Karlsson, I., Wallin, A., Gottfries, C. G. and Karlsson, J. O. (1990) Calpain and calpastatin in normal and Alzheimer-degenerated human brain tissue. *Neurobiology of aging*. **11**, 425–431.

Nixon, R. A. (2003) The calpains in aging and aging-related diseases. Ageing Research Reviews. **2**, 407–418.

Nixon, R. A., Saito, K. I., Grynspan, F., Griffin, W. R., Katayama, S., Honda, T., Mohan, P. S., Shea, T. B. and Beermann, M. (1994) Calcium-activated neutral

proteinase (calpain) system in aging and Alzheimer's disease. *Annals of the New York Academy of Sciences*. **747**, 77–91.

Noble, D. and Herchuelz, A. (2007) Role of Na/Ca exchange and the plasma membrane Ca(2+)-ATPase in cell function. Conference on Na/Ca Exchange. *EMBO Reports*. **8**, 228–232.

Noble, W., Hanger, D. P., Miller, C. C. J. and Lovestone, S. (2013) The importance of tau phosphorylation for neurodegenerative diseases. *Frontiers in Neurology*. 4 JUL.

Noble, W., Olm, V., Takata, K., Casey, E., Mary, O., Meyerson, J., Gaynor, K., LaFrancois, J., Wang, L., Kondo, T., Davies, P., Burns, M., Veeranna, Nixon, R., Dickson, D., Matsuoka, Y., Ahlijanian, M., Lau, L. F. and Duff, K. (2003) Cdk5 is a key factor in tau aggregation and tangle formation in vivo. *Neuron*. **38**, 555–565.

Noble, W., Planel, E., Zehr, C., Olm, V., Meyerson, J., Suleman, F., Gaynor, K., Wang, L., LaFrancois, J., Feinstein, B., Burns, M., Krishnamurthy, P., Wen, Y., Bhat, R., Lewis, J., Dickson, D. and Duff, K. (2005) Inhibition of glycogen synthase kinase-3 by lithium correlates with reduced tauopathy and degeneration in vivo. *Proceedings of the National Academy of Sciences of the United States of America*. **102**, 6990–6995.

Noble, W., Pooler, A. M. and Hanger, D. P. (2011) Advances in tau-based drug discovery. *Expert Opinion on Drug Discovery.* **6**, 797–810.

Nordstedt, C., Gandy, S. E., Alafuzoff, I., Caporaso, G. L., Iverfeldt, K., Grebb, J. A., Winblad, B. and Greengard, P. (1991) Alzheimer beta/A4 amyloid precursor protein in human brain: aging-associated increases in holoprotein and in a proteolytic fragment. *Proceedings of the National Academy of Sciences of the United States of America*. **88**, 8910–8914.

O'Brien, M. a., Moravec, R. a. and Riss, L. (2001) Poly (ADP-ribose) polymerase cleavage monitored in situ in apoptotic cells. *BioTechniques*. **30**, 886–891.

O'Brien, R. J. and Wong, P. C. (2011) Amyloid precursor protein processing and Alzheimer's disease. *Annual review of neuroscience*. **34**, 185–204.

Oda, A., Tamaoka, A. and Araki, W. (2010) Oxidative stress up-regulates presenilin 1 in lipid rafts in neuronal cells. *Journal of Neuroscience Research*. **88**, 1137–1145.

Oddo, S., Caccamo, A., Shepherd, J. D., Murphy, M. P., Golde, T. E., Kayed, R., Metherate, R., Mattson, M. P., Akbari, Y. and LaFerla, F. M. (2003) Triple-transgenic model of Alzheimer's Disease with plaques and tangles: Intracellular Aβ and synaptic dysfunction. *Neuron*. **39**, 409–421.

Oh, M. M., Oliveira, F. A., Waters, J. and Disterhoft, J. F. (2013) Altered calcium metabolism in aging CA1 hippocampal pyramidal neurons. *The Journal of neuroscience : the official journal of the Society for Neuroscience*. **33**, 7905–7911.

Pacher, P., Mabley, J. G., Soriano, F. G., Liaudet, L., Komjáti, K. and Szabó, C. (2002) Endothelial dysfunction in aging animals: the role of poly(ADP-ribose) polymerase activation. *British journal of pharmacology*. **135**, 1347–1350.

Pannaccione, A., Secondo, A., Molinaro, P., D'Avanzo, C., Cantile, M., Esposito, A., Boscia, F., Scorziello, A., Sirabella, R., Di Renzo, G. and Annunziato, L. (2012) A New Concept: A 1-42 Generates a Hyperfunctional Proteolytic NCX3 Fragment That Delays Caspase-12 Activation and Neuronal Death. *Journal of Neuroscience*. **32**, 10609–10617.

Paola, D., Domenicotti, C., Nitti, M., Vitali, A., Borghi, R., Cottalasso, D., Zaccheo, D., Odetti, P., Strocchi, P., UM, M., Tabaton, M. and MA, P. (2000) Oxidative stress induces increase in intracellular amyloid b-protein production and selective activation of bI and bII PKCs in NT2 cells. *Biochemical and Biophysical Research Communications*. **268**, 642–646.

Parent, A., Linden, D. J., Sisodia, S. S. and Borchelt, D. R. (1999) Synaptic transmission and hippocampal long-term potentiation in transgenic mice expressing FAD-linked presenilin 1. *Neurobiology of disease*. **6**, 56–62.

Park, L., Wang, G., Moore, J., Girouard, H., Zhou, P., Anrather, J. and Iadecola, C. (2014) The key role of transient receptor potential melastatin-2 channels in amyloid-β-induced neurovascular dysfunction. *Nature Communications*. **5**, 5318

Park, S.-Y. and Ferreira, A. (2005) The generation of a 17 kDa neurotoxic fragment: an alternative mechanism by which tau mediates beta-amyloid-induced neurodegeneration. *The Journal of neuroscience : the official journal of the Society for Neuroscience*. **25**, 5365–5375.

Parpura, V., Grubišic, V. and Verkhratsky, A. (2011) Ca2+ sources for the exocytotic release of glutamate from astrocytes. Biochimica et Biophysica Acta - Molecular Cell Research. **1813**, 984–991.

Parpura, V. and Verkhratsky, A. (2012) Homeostatic function of astrocytes: Ca(2+) and Na(+) signalling. *Translational neuroscience*. **3**, 334–344.

Parra, M. A., Abrahams, S., Logie, R. H., Méndez, L. G., Lopera, F. and Della Sala, S. (2010) Visual short-term memory binding deficits in familial Alzheimer's disease. *Brain : a journal of neurology*. **133**, 2702–2713.

Parsons, C. G., Stöffler, A. and Danysz, W. (2007) Memantine: a NMDA receptor antagonist that improves memory by restoration of homeostasis in the glutamatergic system - too little activation is bad, too much is even worse. *Neuropharmacology*. **53**, 699–723.

Pascale, a and Etcheberrigaray, R. (1999) Calcium alterations in Alzheimer's disease: pathophysiology, models and therapeutic opportunities. *Pharmacological research : the official journal of the Italian Pharmacological Society*. **39**, 81–88.

Patrick, G. N., Zukerberg, L., Nikolic, M., de la Monte, S., Dikkes, P. and Tsai, L. H. (1999) Conversion of p35 to p25 deregulates Cdk5 activity and promotes neurodegeneration. *Nature*. **402**, 615–622.

Patterson, K. R., Remmers, C., Fu, Y., Brooker, S., Kanaan, N. M., Vana, L., Ward, S., Reyes, J. F., Philibert, K., Glucksman, M. J. and Binder, L. I. (2011) Characterization of prefibrillar Tau oligomers in vitro and in Alzheimer disease. *The Journal of biological chemistry*. **286**, 23063–23076.

Pearson, J. M., Heilbronner, S. R., Barack, D. L., Hayden, B. Y. and Platt, M. L. (2011) Posterior cingulate cortex: Adapting behavior to a changing world. *Trends in Cognitive Sciences.* **15**, 143–151.

Peck, A., Sargin, M. E., LaPointe, N. E., Rose, K., Manjunath, B. S., Feinstein, S. C. and Wilson, L. (2011) Tau isoform-specific modulation of kinesin-driven microtubule gliding rates and trajectories as determined with tau-stabilized microtubules. *Cytoskeleton*. **68**, 44–55.

Pei, J. J., Tanaka, T., Tung, Y. C., Braak, E., Iqbal, K. and Grundke-Iqbal, I. (1997) Distribution, levels, and activity of glycogen synthase kinase-3 in the Alzheimer disease brain. *Journal of neuropathology and experimental neurology*. **56**, 70–78.

Perez, M., Hernandez, F., Lim, F., Nido, J. D. and Avila, J. (2003) Chronic lithium treatment decreases mutant tau protein aggregation in a transgenic mouse model. *Journal of Alzheimer's Disease*. **5**, 301–308.

Perraud, A. L., Schmitz, C. and Scharenberg, A. M. (2003) TRPM2 Ca2+ permeable cation channels: From gene to biological function. *Cell Calcium.* **33**, 519–531.

Perry, E., Walker, M., Grace, J. and Perry, R. (1999) Acetylcholine in mind: A neurotransmitter correlate of consciousness? *Trends in Neurosciences.* **22**, 273–280.

Pickering-Brown, S. M., Baker, M., Nonaka, T., Ikeda, K., Sharma, S., Mackenzie, J., Simpson, S. A., Moore, J. W., Snowden, J. S., De Silva, R., Revesz, T., Hasegawa, M., Hutton, M. and Mann, D. M. A. (2004) Frontotemporal dementia with Pick-type histology associated with Q336R mutation in the tau gene. *Brain*. **127**, 1415–1426.

Pierrot, N., Santos, S. F., Feyt, C., Morel, M., Brion, J. P. and Octave, J. N. (2006) Calcium-mediated transient phosphorylation of tau and amyloid precursor protein followed by intraneuronal amyloid-β accumulation. *Journal of Biological Chemistry*. **281**, 39907–39914.

Pike, B. R., Flint, J., Dave, J. R., Lu, X.-C. M., Wang, K. K. K., Tortella, F. C. and Hayes, R. L. (2004) Accumulation of calpain and caspase-3 proteolytic fragments of brain-derived alphaII-spectrin in cerebral spinal fluid after middle cerebral artery occlusion in rats. *Journal of cerebral blood flow and metabolism : official journal of the International Society of Cerebral Blood Flow and Metabolism*. **24**, 98–106.

Piskunova, T. S., Yurova, M. N., Ovsyannikov, A. I., Semenchenko, A. V, Zabezhinski, M. A., Popovich, I. G., Wang, Z.-Q. and Anisimov, V. N. (2008) Deficiency in Poly(ADP-ribose) Polymerase-1 (PARP-1) Accelerates Aging and Spontaneous Carcinogenesis in Mice. *Current gerontology and geriatrics research*. **2008**, 754190.

Plane, J. M., Shen, Y., Pleasure, D. E. and Deng, W. (2010) Prospects for minocycline neuroprotection. *Archives of neurology*. **67**, 1442–1448.

Plattner, F., Angelo, M. and Giese, K. P. (2006) The roles of cyclin-dependent kinase 5 and glycogen synthase kinase 3 in tau hyperphosphorylation. *The Journal of biological chemistry*. **281**, 25457–25465.

Pooler, A. M. and Hanger, D. P. (2010) Functional implications of the association of tau with the plasma membrane. *Biochemical Society transactions*. **38**, 1012–1015.

Poorkaj, P., Bird, T. D., Wijsman, E., Nemens, E., Garruto, R. M., Anderson, L., Andreadis, A., Wiederholt, W. C., Raskind, M. and Schellenberg, G. D. (1998) Tau is a candidate gene for chromosome 17 frontotemporal dementia. *Annals of neurology*. **43**, 815–825.

Portelius, E., Andreasson, U., Ringman, J. M., Buerger, K., Daborg, J., Buchhave, P., Hansson, O., Harmsen, A., Gustavsson, M. K., Hanse, E., Galasko, D., Hampel, H., Blennow, K. and Zetterberg, H. (2010) Distinct cerebrospinal fluid amyloid beta peptide signatures in sporadic and PSEN1 A431E-associated familial Alzheimer's disease. *Molecular neurodegeneration*. **5**, 2.

Portelius, E., Brinkmalm, G., Tran, A., Andreasson, U., Zetterberg, H., Westman-Brinkmalm, A., Blennow, K. and Öhrfelt, A. (2010) Identification of novel N-terminal fragments of amyloid precursor protein in cerebrospinal fluid. *Experimental Neurology*. **223**, 351–358.

Porter, A. G. and Jänicke, R. U. (1999) Emerging roles of caspase-3 in apoptosis. *Cell death and differentiation*. **6**, 99–104.

Pozueta, J., Lefort, R., Ribe, E. M., Troy, C. M., Arancio, O. and Shelanski, M. (2013) Caspase-2 is required for dendritic spine and behavioural alterations in J20 APP transgenic mice. *Nature communications*. **4**, 1939.

Price, K. A., Varghese, M., Sowa, A., Yuk, F., Brautigam, H., Ehrlich, M. E. and Dickstein, D. L. (2014) Altered synaptic structure in the hippocampus in a mouse model of Alzheimer's disease with soluble amyloid-β oligomers and no plaque pathology. *Molecular neurodegeneration*. **9**, 41.

Price, S. A., Held, B. and Pearson, H. A. (1998) Amyloid beta protein increases Ca2+ currents in rat cerebellar granule neurones. *Neuroreport*. **9**, 539–545.

Qian, W., Jin, N., Shi, J., Yin, X., Jin, X., Wang, S., Cao, M., Iqbal, K., Gong, C. X. and Liu, F. (2013) Dual-specificity tyrosine phosphorylation-regulated kinase 1A (Dyrk1A) enhances tau expression. *Journal of Alzheimer's Disease*. **37**, 529–538.

Ramsden, M., Henderson, Z. and Pearson, H. A. (2002) Modulation of Ca2+ channel currents in primary cultures of rat cortical neurones by amyloid beta protein (1-40) is dependent on solubility status. *Brain Research*. **956**, 254–261.

Ranciat-McComb, N. S., Bland, K. S., Huschenbett, J., Ramonda, L., Bechtel, M., Zaidi, A. and Michaelis, M. L. (2000) Antisense oligonucleotide suppression

of Na+/Ca2+ exchanger activity in primary neurons from rat brain. *Neuroscience Letters*. **294**, 13–16.

Rao, M. V, Mohan, P. S., Peterhoff, C. M., Yang, D.-S., Schmidt, S. D., Stavrides, P. H., Campbell, J., Chen, Y., Jiang, Y., Paskevich, P. A., Cataldo, A. M., Haroutunian, V. and Nixon, R. A. (2008) Marked calpastatin (CAST) depletion in Alzheimer's disease accelerates cytoskeleton disruption and neurodegeneration: neuroprotection by CAST overexpression. *The Journal of neuroscience : the official journal of the Society for Neuroscience*. **28**, 12241–12254.

Rao, M. V., McBrayer, M. K., Campbell, J., Kumar, a., Hashim, a., Sershen, H., Stavrides, P. H., Ohno, M., Hutton, M. and Nixon, R. a. (2014) Specific Calpain Inhibition by Calpastatin Prevents Tauopathy and Neurodegeneration and Restores Normal Lifespan in Tau P301L Mice. *Journal of Neuroscience*. **34**, 9222–9234.

Rapoport, M., Dawson, H. N., Binder, L. I., Vitek, M. P. and Ferreira, A. (2002) Tau is essential to beta -amyloid-induced neurotoxicity. *Proceedings of the National Academy of Sciences of the United States of America*. **99**, 6364–6369.

Ravulapalli, R., Campbell, R. L., Gauthier, S. Y., Dhe-Paganon, S. and Davies, P. L. (2009) Distinguishing between calpain heterodimerization and homodimerization. *FEBS Journal*. **276**, 973–982.

Raz, Y. and Miller, Y. (2013) Interactions between Abeta and Mutated Tau Lead to Polymorphism and Induce Aggregation of Abeta-Mutated Tau Oligomeric Complexes. *PLoS ONE*. **8**, e73303.

Reinhard, C., Hébert, S. S. and De Strooper, B. (2005) The amyloid-beta precursor protein: integrating structure with biological function. *The EMBO journal*. **24**, 3996–4006.

Reitz, C. (2012) Alzheimer's disease and the amyloid cascade hypothesis: A critical review. *International Journal of Alzheimer's Disease.* **2012**, 369808

Reyes, R. C., Verkhratsky, A. and Parpura, V. (2012) Plasmalemmal Na + /Ca 2+ exchanger modulates Ca 2+ -dependent exocytotic release of glutamate from rat cortical astrocytes. *ASN NEURO*. **4**, 33–45.

Rivest, S. (2015) TREM2 enables amyloid [beta] clearance by microglia. *Cell Research*. **25**, 535–536.

Robakis, N. K., Ramakrishna, N., Wolfe, G. and Wisniewski, H. M. (1987) Molecular cloning and characterization of a cDNA encoding the cerebrovascular and the neuritic plaque amyloid peptides. *Proceedings of the National Academy of Sciences of the United States of America*. **84**, 4190–4194.

Rodríguez, J. J., Olabarria, M., Chvatal, A. and Verkhratsky, A. (2009) Astroglia in dementia and Alzheimer's disease. *Cell death and differentiation*. **16**, 378–385.

Rodriguez-Arellano, J. J., Parpura, V., Zorec, R. and Verkhratsky, A. (2015) Astrocytes in physiological aging and Alzheimer's disease. *Neuroscience.* **S0306–4522**, 31-37

Rose, C. R. and Konnerth, A. (2001) Stores not just for storage. intracellular calcium release and synaptic plasticity. *Neuron*. **31**, 519–522.

Rozemuller, J. M., Eikelenboom, P. and Stam, F. C. (1986) Role of microglia in plaque formation in senile dementia of the Alzheimer type. An immunohistochemical study. *Virchows Archiv. B, Cell pathology including molecular pathology*. **51**, 247–254.

Rubio-Moscardo, F., Setó-Salvia, N., Pera, M., Bosch-Morató, M., Plata, C., Belbin, O., Gené, G., Dols-Icardo, O., Ingelsson, M., Helisalmi, S., Soininen, H., Hiltunen, M., Giedraitis, V., Lannfelt, L., Frank, A., Bullido, Mj., Combarros, O., Sánchez-Juan, P., Boada, M., Tárraga, L., Pastor, P., Pérez-Tur, J., Baquero, M., Molinuevo, J. L., Sánchez-Valle, R., Fuentes-Prior, P., Fortea, J., Blesa, R., Muñoz, F. J., Lleó, A., Valverde, M. A. and Clarimón, J. (2013) Rare Variants in Calcium Homeostasis Modulator 1 (CALHM1) Found in Early Onset Alzheimer's Disease Patients Alter Calcium Homeostasis. *PLoS ONE*. **8**, e74203.

Saavedra, L., Mohamed, A., Ma, V., Kar, S. and de Chaves, E. P. (2007) Internalization of beta-amyloid peptide by primary neurons in the absence of apolipoprotein E. *The Journal of biological chemistry*. **282**, 35722–35732.

Saez, M. E., Ramirez-Lorca, R., Moron, F. J. and Ruiz, A. (2006) The therapeutic potential of the calpain family: new aspects. *Drug Discovery Today.* **11**, 917–923.

Saito, K., Elce, J. S., Hamos, J. E. and Nixon, R. A. (1993) Widespread activation of calcium-activated neutral proteinase (calpain) in the brain in Alzheimer disease: a potential molecular basis for neuronal degeneration. *Proceedings*

of the National Academy of Sciences of the United States of America. **90**, 2628–2632.

Scheff, S. W., Price, D. A., Ansari, M. A., Roberts, K. N., Schmitt, F. A., Ikonomovic, M. D. and Mufson, E. J. (2015) Synaptic change in the posterior cingulate gyrus in the progression of Alzheimer's disease. *Journal of Alzheimer's disease : JAD*. **43**, 1073–1090.

Schilling, T. and Eder, C. (2011) Amyloid-β-induced reactive oxygen species production and priming are differentially regulated by ion channels in microglia. *Journal of Cellular Physiology*. **226**, 3295–3302.

Schneider, L. S., Mangialasche, F., Andreasen, N., Feldman, H., Giacobini, E., Jones, R., Mantua, V., Mecocci, P., Pani, L., Winblad, B. and Kivipelto, M. (2014) Clinical trials and late-stage drug development for Alzheimer's disease: An appraisal from 1984 to 2014. *Journal of Internal Medicine*. **275**, 251–283.

Schreiber, V., Dantzer, F., Ame, J.-C. and de Murcia, G. (2006) Poly(ADP-ribose): novel functions for an old molecule. *Nature reviews. Molecular cell biology*. **7**, 517–528.

Scovassi, A. and Poirier, G. G. (1999) Poly(ADP-ribosylation) and apoptosis. *Molecular and Cellular Biochemistry*. **199**, 125–137.

Selenica, M.-L., Jensen, H. S., Larsen, A. K., Pedersen, M. L., Helboe, L., Leist, M. and Lotharius, J. (2007) Efficacy of small-molecule glycogen synthase kinase-3 inhibitors in the postnatal rat model of tau hyperphosphorylation. *British journal of pharmacology*. **152**, 959–979.

Selkoe, D. J. (2002) Alzheimer's disease is a synaptic failure. *Science (New York, N.Y.)*. **298**, 789–791.

Selkoe, D. J. (2001) Clearing the brain's amyloid cobwebs. *Neuron.* **32**, 177–180.

Sepulveda-Falla, D., Barrera-Ocampo, A., Hagel, C., Korwitz, A., Vinueza-Veloz, M. F., Zhou, K., Schonewille, M., Zhou, H., Velazquez-Perez, L., Rodriguez-Labrada, R., Villegas, A., Ferrer, I., Lopera, F., Langer, T., De Zeeuw, C. I. and Glatzel, M. (2014) Familial Alzheimer's disease-associated presenilin-1 alters cerebellar activity and calcium homeostasis. *Journal of Clinical Investigation*. **124**, 1552–1567.

Serrano-Pozo, A., Frosch, M. P., Masliah, E. and Hyman, B. T. (2011) Neuropathological alterations in Alzheimer disease. *Cold Spring Harbor perspectives in medicine.* **1**, a006189.

Seshadri, S., Fitzpatrick, A. L., Ikram, M. A., DeStefano, A. L., Gudnason, V., Boada, M., Bis, J. C., Smith, A. V, Carassquillo, M. M., Lambert, J. C., Harold, D., Schrijvers, E. M. C., Ramirez-Lorca, R., Debette, S., Longstreth, W. T., Janssens, A. C. J. W., Pankratz, V. S., Dartigues, J. F., Hollingworth, P., Aspelund, T., Hernandez, I., Beiser, A., Kuller, L. H., Koudstaal, P. J., Dickson, D. W., Tzourio, C., Abraham, R., Antunez, C., Du, Y., Rotter, J. I., Aulchenko, Y. S., Harris, T. B., Petersen, R. C., Berr, C., Owen, M. J., Lopez-Arrieta, J., Varadarajan, B. N., Becker, J. T., Rivadeneira, F., Nalls, M. A., Graff-Radford, N. R., Campion, D., Auerbach, S., Rice, K., Hofman, A., Jonsson, P. V, Schmidt, H., Lathrop, M., Mosley, T. H., Au, R., Psaty, B. M., Uitterlinden, A. G., Farrer, L. A., Lumley, T., Ruiz, A., Williams, J., Amouyel, P., Younkin, S. G., Wolf, P. A., Launer, L. J., Lopez, O. L., van Duijn, C. M. and Breteler, M. M. B. (2010) Genome-wide analysis of genetic loci associated with Alzheimer disease. *JAMA : the journal of the American Medical Association*. **303**, 1832–1840.

Shankar, G. M., Bloodgood, B. L., Townsend, M., Walsh, D. M., Selkoe, D. J. and Sabatini, B. L. (2007) Natural oligomers of the Alzheimer amyloid-beta protein induce reversible synapse loss by modulating an NMDA-type glutamate receptor-dependent signaling pathway. *The Journal of neuroscience : the official journal of the Society for Neuroscience*. **27**, 2866–2875.

Shankar, G. M. and Walsh, D. M. (2009) Alzheimer's disease: synaptic dysfunction and Abeta. *Molecular neurodegeneration*. **4**, 4 – 8.

Shea, T. B. and Ekinci, F. J. (1999) Biphasic Effect of Calcium Influx on Tau Phosphorylation: Phosphorylation: Biphasic Effect of Calcium Influx on Tau Phosphorylation: Involvement of Calcium-Dependent Phosphatase and Kinase Activities. *Journal of Alzheimer's disease : JAD*. **1**, 353–360.

Shinohara, M., Fujioka, S., Murray, M. E., Wojtas, A., Baker, M., Rovelet-Lecrux, A., Rademakers, R., Das, P., Parisi, J. E., Graff-Radford, N. R., Petersen, R. C., Dickson, D. W. and Bu, G. (2014) Regional distribution of synaptic markers and APP correlate with distinct clinicopathological features in sporadic and familial Alzheimer's disease. *Brain*. **137**, 1533–1549.

Siman, R., Card, J. P. and Davis, L. G. (1990) Proteolytic processing of beta-amyloid precursor by calpain I. *The Journal of neuroscience : the official journal of the Society for Neuroscience*. **10**, 2400–2411.

Simons, M., Keller, P., De Strooper, B., Beyreuther, K., Dotti, C. G. and Simons, K. (1998) Cholesterol depletion inhibits the generation of beta-amyloid in hippocampal neurons. *Proceedings of the National Academy of Sciences of the United States of America*. **95**, 6460–6464.

Simonyi, A., He, Y., Sheng, W., Sun, A. Y., Wood, W. G., Weisman, G. A. and Sun, G. Y. (2010) 'Targeting NADPH oxidase and phospholipases A2 in alzheimer's disease', in *Molecular Neurobiology*. **2010**, 73–86.

Simpkins, K. L., Guttmann, R. P., Dong, Y., Chen, Z., Sokol, S., Neumar, R. W. and Lynch, D. R. (2003) Selective activation induced cleavage of the NR2B subunit by calpain. *The Journal of neuroscience : the official journal of the Society for Neuroscience*. **23**, 11322–11331.

Sing, C. F. and Davignon, J. (1985) Role of the apolipoprotein E polymorphism in determining normal plasma lipid and lipoprotein variation. *American journal of human genetics*. **37**, 268–285.

Sisodia, S. S. (1992) Beta-amyloid precursor protein cleavage by a membrane-bound protease. *Proceedings of the National Academy of Sciences of the United States of America*. **89**, 6075–6079.

Sisodia, S. S. and St George-Hyslop, P. H. (2002) gamma-Secretase, Notch, Abeta and Alzheimer's disease: where do the presenilins fit in? *Nature reviews. Neuroscience*. **3**, 281–290.

Sivanesan, S., Tan, A. and Rajadas, J. (2013) Pathogenesis of Abeta oligomers in synaptic failure. *Current Alzheimer research*. **10**, 316–323.

Smith, I. F., Green, K. N. and LaFerla, F. M. (2005) Calcium dysregulation in Alzheimer's disease: Recent advances gained from genetically modified animals. *Cell Calcium.* **38**, 427–437.

Sokka, A.-L., Putkonen, N., Mudo, G., Pryazhnikov, E., Reijonen, S., Khiroug, L., Belluardo, N., Lindholm, D. and Korhonen, L. (2007) Endoplasmic reticulum stress inhibition protects against excitotoxic neuronal injury in the rat brain. *Journal of Neuroscience*. **27**, 901–908.

Sokolow, S., Luu, S. H., Headley, A. J., Hanson, A. Y., Kim, T., Miller, C. A., Vinters, H. V. and Gylys, K. H. (2011) High levels of synaptosomal Na+-Ca2+ exchangers (NCX1, NCX2, NCX3) co-localized with amyloid-beta in human cerebral cortex affected by Alzheimer's disease. *Cell Calcium*. **49**, 208–216.

Song, L., De Sarno, P. and Jope, R. S. (2002) Central role of glycogen synthase kinase-3beta in endoplasmic reticulum stress-induced caspase-3 activation. *The Journal of biological chemistry*. **277**, 44701–44708.

Sorimachi, H. and Ono, Y. (2012) Regulation and physiological roles of the calpain system in muscular disorders. *Cardiovascular Research.* **96**, 11–22.

Spillantini, M. G. and Goedert, M. (2013) Tau pathology and neurodegeneration. *The Lancet Neurology.* **12**, 609–622.

St George-Hyslop, P. H., Tanzi, R. E., Polinsky, R. J., Haines, J. L., Nee, L., Watkins, P. C., Myers, R. H., Feldman, R. G., Pollen, D., Drachman, D. and et al. (1987) The genetic defect causing familial Alzheimer's disease maps on chromosome 21. *Science*. **235**, 885–890.

Stancu, I.-C., Vasconcelos, B., Terwel, D. and Dewachter, I. (2014) Models of β-amyloid induced Tau-pathology: the long and 'folded' road to understand the mechanism. *Molecular neurodegeneration*. **9**, 51.

Stanford, P. M., Halliday, G. M., Brooks, W. S., Kwok, J. B., Storey, C. E., Creasey, H., Morris, J. G., Fulham, M. J. and Schofield, P. R. (2000) Progressive supranuclear palsy pathology caused by a novel silent mutation in exon 10 of the tau gene: expansion of the disease phenotype caused by tau gene mutations. *Brain : a journal of neurology.* **123**, 880–893.

Steiner, H. (2008) The catalytic core of gamma-secretase: presenilin revisited. *Current Alzheimer research*. **5**, 147–157.

Stelzmann, R. A., Schnitzlein, H. N. and Murtagh, F. R. (1995) An English translation of Alzheimer's 1907 paper, 'uber eine eigenartige erkankung der hirnrinde'. *Clinical Anatomy.* **8**, 429–431.

Stéphan, A., Laroche, S. and Davis, S. (2001) Generation of aggregated beta-amyloid in the rat hippocampus impairs synaptic transmission and plasticity and causes memory deficits. *The Journal of neuroscience : the official journal of the Society for Neuroscience*. **21**, 5703–5714.

Stoothoff, W., Jones, P. B., Spires-Jones, T. L., Joyner, D., Chhabra, E., Bercury, K., Fan, Z., Xie, H., Bacskai, B., Edd, J., Irimia, D. and Hyman, B. T. (2009) Differential effect of three-repeat and four-repeat tau on mitochondrial axonal transport. *Journal of Neurochemistry*. **111**, 417–427.

Storandt, M., Mintun, M. A., Head, D. and Morris, J. C. (2009) Cognitive decline and brain volume loss as signatures of cerebral amyloid-beta peptide deposition identified with Pittsburgh compound B: cognitive decline associated with Abeta deposition. *Archives of neurology*. **66**, 1476–1481.

Streit, W. J. and Xue, Q. S. (2012) Alzheimer's disease, neuroprotection, and CNS immunosenescence. *Frontiers in Pharmacology*. **3**, 138.

Strittmatter, W. J., Saunders, A. M., Schmechel, D., Pericak-Vance, M., Enghild, J., Salvesen, G. S. and Roses, A. D. (1993) Apolipoprotein E: high-avidity binding to beta-amyloid and increased frequency of type 4 allele in late-onset familial Alzheimer disease. *Proceedings of the National Academy of Sciences of the United States of America*. **90**, 1977–1981.

Strosznajder, J. B., Jeśko, H. and Strosznajder, R. P. (2000) Effect of amyloid beta peptide on poly(ADP-ribose) polymerase activity in adult and aged rat hippocampus. *Acta biochimica Polonica*. **47**, 847–854.

Struble, R. G., Ala, T., Patrylo, P. R., Brewer, G. J. and Yan, X. X. (2010) Is brain amyloid production a cause or a result of dementia of the Alzheimer's type? *Journal of Alzheimer's Disease.* **22**, 393–399.

Stutzmann, G. E., Caccamo, A., LaFerla, F. M. and Parker, I. (2004) Dysregulated IP3 signaling in cortical neurons of knock-in mice expressing an Alzheimer's-linked mutation in presenilin1 results in exaggerated Ca2+ signals and altered membrane excitability. *The Journal of neuroscience : the official journal of the Society for Neuroscience*. **24**, 508–513.

Stutzmann, G. E. and Mattson, M. P. (2011) Endoplasmic reticulum Ca(2+) handling in excitable cells in health and disease. *Pharmacological reviews*. **63**, 700–727.

Stutzmann, G. E., Smith, I., Caccamo, A., Oddo, S., Parker, I. and Laferla, F. (2007) Enhanced ryanodine-mediated calcium release in mutant PS1-expressing Alzheimer's mouse models. *Annals of the New York Academy of Sciences*. **1097**, 265–277.

Su, B., Wang, X., Nunomura, A., Moreira, P. I., Lee, H., Perry, G., Smith, M. A. and Zhu, X. (2008) Oxidative stress signaling in Alzheimer's disease. *Current Alzheimer research*. **5**, 525–532.

Suen, K.-C., Lin, K.-F., Elyaman, W., So, K.-F., Chang, R. C.-C. and Hugon, J. (2003) Reduction of calcium release from the endoplasmic reticulum could only provide partial neuroprotection against beta-amyloid peptide toxicity. *Journal of neurochemistry*. **87**, 1413–1426.

Sumoza-Toledo, A. and Penner, R. (2011) TRPM2: a multifunctional ion channel for calcium signalling. *The Journal of physiology*. **589**, 1515–1525.

Sun, L., Yau, H. Y., Wong, W. Y., Li, R. a., Huang, Y. and Yao, X. (2012) Role of trpm2 in H2O2-induced cell apoptosis in endothelial cells. *PLoS ONE*. **7**, 1–10.

Sun, S., Zhang, H., Liu, J., Popugaeva, E., Xu, N. J., Feske, S., White, C. L. and Bezprozvanny, I. (2014) Reduced synaptic STIM2 expression and impaired store-operated calcium entry cause destabilization of mature spines in mutant presenilin mice. *Neuron*. **82**, 79–93.

Supnet, C. and Bezprozvanny, I. (2010) The dysregulation of intracellular calcium in Alzheimer disease. *Cell Calcium.* **47**, 183–189.

Suzuki, A. (1997) Amyloid beta-protein induces necrotic cell death mediated by ICE cascade in PC12 cells. *Experimental cell research*. **234**, 507–511.

Swatton, J. E., Sellers, L. A., Faull, R. L. M., Holland, A., Iritani, S. and Bahn, S. (2004) Increased MAP kinase activity in Alzheimer's and Down syndrome but not in schizophrenia human brain. *The European journal of neuroscience*. **19**, 2711–2719.

Swindall, A. F., Stanley, J. A. and Yang, E. S. (2013) PARP-1: Friend or foe of DNA damage and repair in tumorigenesis? *Cancers*. **5**, 943–958.

Szenczi, O., Kemecsei, P., Holthuijsen, M. F. J., Van Riel, N. A. W., Van Der Vusse, G. J., Pacher, P., Szabó, C., Kollai, M., Ligeti, L. and Ivanics, T. (2005) Poly(ADP-ribose) polymerase regulates myocardial calcium handling in doxorubicin-induced heart failure. *Biochemical Pharmacology*. **69**, 725–732.

Takahashi, N., Kozai, D., Kobayashi, R., Ebert, M. and Mori, Y. (2011) Roles of TRPM2 in oxidative stress. *Cell Calcium*. **50**, 279–287.

Takashima, A., Noguchi, K., Sato, K., Hoshino, T. and Imahori, K. (1993) Tau protein kinase I is essential for amyloid beta-protein-induced neurotoxicity. *Proceedings of the National Academy of Sciences of the United States of America*. **90**, 7789–7793.

Tang, K. S., Suh, S. W., Alano, C. C., Shao, Z., Hunt, W. T., Swanson, R. A. and Anderson, C. M. (2010) Astrocytic poly(ADP-ribose) polymerase-1 activation leads to bioenergetic depletion and inhibition of glutamate uptake capacity. *GLIA*. **58**, 446–457.

Taniguchi, S., Fujita, Y., Hayashi, S., Kakita, A., Takahashi, H., Murayama, S., Saido, T. C., Hisanaga, S., Iwatsubo, T. and Hasegawa, M. (2001) Calpain-mediated degradation of p35 to p25 in postmortem human and rat brains. *FEBS Letters*. **489**, 46–50.

Tanzi, R. E., Gusella, J. F., Watkins, P. C., Bruns, G. A., St George-Hyslop, P., Van Keuren, M. L., Patterson, D., Pagan, S., Kurnit, D. M. and Neve, R. L. (1987)

Amyloid beta protein gene: cDNA, mRNA distribution, and genetic linkage near the Alzheimer locus. *Science (New York, N.Y.)*. **235**, 880–884.

Teipel, S., Heinsen, H., Amaro, E., Grinberg, L. T., Krause, B. and Grothe, M. (2014) Cholinergic basal forebrain atrophy predicts amyloid burden in Alzheimer's disease. *Neurobiology of Aging*. **35**, 482–491.

Terry, R. D., Masliah, E., Salmon, D. P., Butters, N., DeTeresa, R., Hill, R., Hansen, L. A. and Katzman, R. (1991) Physical basis of cognitive alterations in Alzheimer's disease: Synapse loss is the major correlate of cognitive impairment. *Annals of Neurology*. **30**, 572–580.

Texidó, L., Martín-Satué, M., Alberdi, E., Solsona, C. and Matute, C. (2011) Amyloid β peptide oligomers directly activate NMDA receptors. *Cell Calcium*. **49**, 184–190.

Thibault, O., Gant, J. C. and Landfield, P. W. (2007) Expansion of the calcium hypothesis of brain aging and Alzheimer's disease: Minding the store. *Aging Cell*. **6**, 307–317.

Thomas, S. J. and Grossberg, G. T. (2009) Memantine: a review of studies into its safety and efficacy in treating Alzheimer's disease and other dementias. *Clinical interventions in aging.* **4**, 367–377.

Tomita, S., Kirino, Y. and Suzuki, T. (1998) Cleavage of Alzheimer's amyloid precursor protein (APP) by secretases occurs after O-glycosylation of APP in the protein secretory pathway. Identification of intracellular compartments in which APP cleavage occurs without using toxic agents that interfere. *The Journal of biological chemistry*. **273**, 6277–6284.

Town, T., Zolton, J., Shaffner, R., Schnell, B., Crescentini, R., Wu, Y., Zeng, J., DelleDonne, A., Obregon, D., Tan, J. and Mullan, M. (2002) p35/Cdk5 pathway mediates soluble amyloid-beta peptide-induced tau phosphorylation in vitro. Journal of Neuroscience Research. **69**, 362–372.

Trinchese, F., Fa', M., Liu, S., Zhang, H., Hidalgo, A., Schmidt, S. D., Yamaguchi, H., Yoshii, N., Mathews, P. M., Nixon, R. A. and Arancio, O. (2008) Inhibition of calpains improves memory and synaptic transmission in a mouse model of Alzheimer disease. *The Journal of clinical investigation*. **118**, 2796–2807.

Trinchese, F., Liu, S. and Zhang, H. (2008) Inhibition of calpains improves memory and synaptic transmission in a mouse model of Alzheimer disease. *The Journal of clinical investigation*. **118**, 2796–2807.

Tsuji, T., Shimohama, S., Kimura, J. and Shimizu, K. (1998) m-calpain (calcium-activated neutral proteinase) in alzheimer's disease brains. *Neuroscience Letters*. **248**, 109–112.

Tsujinaka, T., Kajiwara, Y., Kambayashi, J., Sakon, M., Higuchi, N., Tanaka, T. and Mori, T. (1988) Synthesis of a new cell penetrating calpain inhibitor (calpeptin). *Biochemical and biophysical research communications*. **153**, 1201–1208.

Tu, H., Nelson, O., Bezprozvanny, A., Wang, Z., Lee, S. F., Hao, Y. H., Serneels, L., De Strooper, B., Yu, G. and Bezprozvanny, I. (2006) Presenilins Form ER Ca2+ Leak Channels, a Function Disrupted by Familial Alzheimer's Disease-Linked Mutations. *Cell*. **126**, 981–993.

Ueda, K., Shinohara, S., Yagami, T., Asakura, K. and Kawasaki, K. (1997) Amyloid beta protein potentiates Ca2+ influx through L-type voltage-sensitive Ca2+ channels: a possible involvement of free radicals. *Journal of neurochemistry*. **68**, 265–271.

Uttara, B., Singh, A. V, Zamboni, P. and Mahajan, R. T. (2009) Oxidative stress and neurodegenerative diseases: a review of upstream and downstream antioxidant therapeutic options. *Current neuropharmacology*. **7**, 65–74.

Vagnoni, A., Perkinton, M. S., Gray, E. H., Francis, P. T., Noble, W. and Miller, C. C. J. (2012) Calsyntenin-1 mediates axonal transport of the amyloid precursor protein and regulates aβ production. *Human Molecular Genetics*. **21**, 2845–2854.

Vagnoni, A., Rodriguez, L., Manser, C., De Vos, K. J. and Miller, C. C. J. (2011) Phosphorylation of kinesin light chain 1 at serine 460 modulates binding and trafficking of calsyntenin-1. *Journal of cell science*. **124**, 1032–1042.

Vaisid, T., Kosower, N. S., Katzav, A., Chapman, J. and Barnoy, S. (2007a) Calpastatin levels affect calpain activation and calpain proteolytic activity in APP transgenic mouse model of Alzheimer's disease. *Neurochemistry International*. **51**, 391–397.

Vaisid, T., Kosower, N. S., Katzav, A., Chapman, J. and Barnoy, S. (2007b) Calpastatin levels affect calpain activation and calpain proteolytic activity in APP transgenic mouse model of Alzheimer's disease. *Neurochemistry International*. **51**, 391–397.

Vardarajan, B. N., Ghani, M., Kahn, A., Sheikh, S., Sato, C., Barral, S., Lee, J. H., Cheng, R., Reitz, C., Lantigua, R., Reyes-Dumeyer, D., Medrano, M., Jimenez-

Velazquez, I. Z., Rogaeva, E., St George-Hyslop, P. and Mayeux, R. (2015) Rare coding mutations identified by sequencing of Alzheimer disease genome-wide association studies loci. *Annals of Neurology*. **78**, 487–498.

Veeranna, Kaji, T., Boland, B., Odrljin, T., Mohan, P., Basavarajappa, B. S., Peterhoff, C., Cataldo, A., Rudnicki, A., Amin, N., Li, B. S., Pant, H. C., Hungund, B. L., Arancio, O. and Nixon, R. A. (2004) Calpain mediates calcium-induced activation of the erk1,2 MAPK pathway and cytoskeletal phosphorylation in neurons: relevance to Alzheimer's disease. *The American journal of pathology*. **165**, 795–805.

Velez-Pardo, C., Arroyave, S. T., Lopera, F., Castano, A. D. and Jimenez Del Rio, M. (2001) Ultrastructure evidence of necrotic neural cell death in familial Alzheimer's disease brains bearing presenilin-1 E280A mutation. *Journal of Alzheimer's Disease*. **3**, 409–415.

Vella, L. J. and Cappai, R. (2012) Identification of a novel amyloid precursor protein processing pathway that generates secreted N-terminal fragments. *The FASEB Journal*. **26**, 2930–2940.

Verkhratsky, A. and Kettenmann, H. (1996) Calcium signalling in glial cells. *Trends in neurosciences*. 19 (8), 346–352.

Verkhratsky, A., Marutle, A., Rodríguez-Arellano, J. J. and Nordberg, A. (2014) Glial Asthenia and Functional Paralysis: A New Perspective on Neurodegeneration and Alzheimer's Disease. *The Neuroscientist : a review journal bringing neurobiology, neurology and psychiatry*. **10**, 1 – 17.

Verkhratsky, A., Noda, M. and Parpura, V. (2013) Sodium Calcium Exchange: A Growing Spectrum of Pathophysiological Implications. *Adv Exp Med Biol*. **961**, 295–305.

Verkhratsky, A., Olabarria, M., Noristani, H. N., Yeh, C. Y. and Rodriguez, J. J. (2010) Astrocytes in Alzheimer's Disease. *Neurotherapeutics*. **7**, 399–412.

Verkhratsky, A. and Shmigol, A. (1996) Calcium-induced calcium release in neurones. *Cell calcium*. **19**, 1–14.

Verkhratsky, A. and Toescu, E. C. (2003) Endoplasmic reticulum Ca(2+) homeostasis and neuronal death. *Journal of cellular and molecular medicine*. **7**, 351–361.

Verwer, R. W. H., Hermens, W. T. J. M. C., Dijkhuizen, P., ter Brake, O., Baker, R. E., Salehi, A., Sluiter, A. A., Kok, M. J. M., Muller, L. J., Verhaagen, J. and Swaab, D.

F. (2002) Cells in human postmortem brain tissue slices remain alive for several weeks in culture. *The FASEB journal : official publication of the Federation of American Societies for Experimental Biology*. **16**, 54–60.

Vetrivel, K. S. and Thinakaran, G. (2006) Amyloidogenic processing of beta-amyloid precursor protein in intracellular compartments. *Neurology*. **66**, 69–S73.

Vetrivel, K. S., Zhang, Y., Xu, H. and Thinakaran, G. (2006) Pathological and physiological functions of presenilins. *Molecular neurodegeneration*. **1**, 4.

Virág, L., Scott, G. S., Antal-Szalmás, P., O'Connor, M., Ohshima, H. and Szabó, C. (1999) Requirement of intracellular calcium mobilization for peroxynitrite-induced poly(ADP-ribose) synthetase activation and cytotoxicity. *Molecular pharmacology*. **56**, 824–833.

Vitvitsky, V. M., Garg, S. K., Keep, R. F., Albin, R. L. and Banerjee, R. (2012) Na + and K + ion imbalances in Alzheimer's disease. *Biochimica et Biophysica Acta - Molecular Basis of Disease*. **1822**, 1671–1681.

Volicer, L., Harper, D. G., Manning, B. C., Goldstein, R. and Satlin, A. (2001) Sundowning and circadian rhythms in Alzheimer's disease. *American Journal of Psychiatry*. **158**, 704–711.

Vosler, P. S., Brennan, C. S. and Chen, J. (2008) Calpain-mediated signaling mechanisms in neuronal injury and neurodegeneration. *Molecular Neurobiology.* **38**, 78–100.

Vosler, P. S., Sun, D., Wang, S., Gao, Y., Kintner, D. B., Signore, A. P., Cao, G. and Chen, J. (2009) Calcium dysregulation induces apoptosis-inducing factor release: Cross-talk between PARP-1- and calpain- signaling pathways. *Experimental Neurology*. **218**, 213–220.

Wadia, P. M. and Lang, A. E. (2007) The many faces of corticobasal degeneration. *Parkinsonism and Related Disorders*. **13**, 336 – 340.

Walsh, D. M., Klyubin, I., Fadeeva, J. V, Cullen, W. K., Anwyl, R., Wolfe, M. S., Rowan, M. J. and Selkoe, D. J. (2002a) Naturally secreted oligomers of amyloid beta protein potently inhibit hippocampal long-term potentiation in vivo. *Nature*. **416**, 535–539.

Walsh, D. M. and Selkoe, D. J. (2007) Abeta oligomers - A decade of discovery. Journal of Neurochemistry 101 p.1172–1184.

Wang, J., Dickson, D. W., Trojanowski, J. Q. and Lee, V. M. (1999) The levels of soluble versus insoluble brain Abeta distinguish Alzheimer's disease from normal and pathologic aging. *Experimental neurology*. **158**, 328–337.

Wang, L.-B., Zhang, L.-Y. and Shan, C.-H. (2010) [A new form of cell death: Parthanatos]. *Yi chuan = Hereditas / Zhongguo yi chuan xue hui bian ji*. **32**, 881–885.

Wang, S. H., Liao, X. M., Liu, D., Hu, J., Yin, Y. Y., Wang, J. Z. and Zhu, L. Q. (2012) NGF promotes long-term memory formation by activating poly(ADP-ribose) polymerase-1. *Neuropharmacology*. **63**, 1085–1092.

Wang, Y., Dawson, V. L. and Dawson, T. M. (2009) Poly(ADP-ribose) signals to mitochondrial AIF: A key event in parthanatos. *Experimental Neurology.* **218**, 193–202.

Wang, Y. and Mattson, M. P. (2014) L-type Ca2+ currents at CA1 synapses, but not CA3 or dentate granule neuron synapses, are increased in 3xTgAD mice in an age-dependent manner. *Neurobiology of Aging*. **35**, 88–95.

Warren, M. W., Zheng, W., Kobeissy, F. H., Cheng Liu, M., Hayes, R. L., Gold, M. S., Larner, S. F. and Wang, K. K. W. (2007) Calpain- and caspase-mediated alphaII-spectrin and tau proteolysis in rat cerebrocortical neuronal cultures after ecstasy or methamphetamine exposure. *The international journal of neuropsychopharmacology / official scientific journal of the Collegium Internationale Neuropsychopharmacologicum (CINP)*. **10**, 479–489.

Waxman, E. A., Baconguis, I., Lynch, D. R. and Robinson, M. B. (2007) N-methyl-D-aspartate receptor-dependent regulation of the glutamate transporter excitatory amino acid carrier 1. *Journal of Biological Chemistry*. **282**, 17594–17607.

Webster, S. J., Bachstetter, A. D., Nelson, P. T., Schmitt, F. A. and Van Eldik, L. J. (2014) Using mice to model Alzheimer's dementia: an overview of the clinical disease and the preclinical behavioral changes in 10 mouse models. *Frontiers in Genetics*. **5**, 88.

Weggen, S. and Beher, D. (2012) Molecular consequences of amyloid precursor protein and presenilin mutations causing autosomal-dominant Alzheimer's disease. *Alzheimer's Research and Therapy.* **4**, 9.

Wei, W., Nguyen, L. N., Kessels, H. W., Hagiwara, H., Sisodia, S. and Malinow, R. (2010) Amyloid beta from axons and dendrites reduces local spine number and plasticity. *Nature neuroscience*. **13**, 190–196.

Wen, Y., Planel, E., Herman, M., Figueroa, H. Y., Wang, L., Liu, L., Lau, L.-F., Yu, W. H. and Duff, K. E. (2008) Interplay between cyclin-dependent kinase 5 and glycogen synthase kinase 3 beta mediated by neuregulin signaling leads to differential effects on tau phosphorylation and amyloid precursor protein processing. *The Journal of neuroscience : the official journal of the Society for Neuroscience*. **28**, 2624–2632.

Whittemore, E. R., Loo, D. T., Watt, J. A. and Cotmans, C. W. (1995) A detailed analysis of hydrogen peroxide-induced cell death in primary neuronal culture. *Neuroscience*. **67**, 921–932.

Wilcock, G., Howe, I., Coles, H., Lilienfeld, S., Truyen, L., Zhu, Y., Bullock, R. and Kershaw, P. (2003) A long-term comparison of galantamine and donepezil in the treatment of Alzheimer's disease. *Drugs and Aging*. **20**, 777–789.

Wong, C. W., Quaranta, V. and Glenner, G. G. (1985) Neuritic plaques and cerebrovascular amyloid in Alzheimer disease are antigenically related. *Proceedings of the National Academy of Sciences of the United States of America*. **82**, 8729–8732.

Wood, J. G., Mirra, S. S., Pollock, N. J. and Binder, L. I. (1986) Neurofibrillary tangles of Alzheimer disease share antigenic determinants with the axonal microtubule-associated protein tau (tau). *Proceedings of the National Academy of Sciences of the United States of America*. **83**, 4040–4043.

Wood-Kaczmar, A., Deas, E., Wood, N. W. and Abramov, A. Y. (2013) 'The role of the mitochondrial NCX in the mechanism of neurodegeneration in Parkinson's disease', in *Advances in Experimental Medicine and Biology*. **2013**, 241–249.

Wray, S. and Noble, W. (2009) Linking amyloid and tau pathology in Alzheimer's disease: the role of membrane cholesterol in Abeta-mediated tau toxicity. *The Journal of neuroscience : the official journal of the Society for Neuroscience*. **29**, 9665–9667.

Wu, A. and Colvin, R. A. (1994) Characterization of exchange inhibitory peptide effects on Na+/Ca2+ exchange in rat and human brain plasma membrane vesicles. *Journal of neurochemistry*. **63**, 2136–2143.

Wu, H., Hudry, E., Hashimoto, T., Kuchibhotla, K., Fan, Z., Spires-jones, T., Xie, H., Arbel-ornath, M., Cynthia, L., Bacskai, B. J. and Hyman, B. T. (2010) Amyloid Beta (A-beta) induces the morphological neurodegenerative tried of spine loss, dendritic simplification, and neuritic dystrophies through calcineurin (CaN) activation. *Journal of Neuroscience*. **30**, 2636–2649.

Wu, H.-Y. and Lynch, D. R. (2006) Calpain and synaptic function. *Molecular neurobiology*. **33**, 215–236.

Wu, Y., Liang, S., Oda, Y., Ohmori, I., Nishiki, T., Takei, K., Matsui, H. and Tomizawa, K. (2007) Truncations of amphiphysin I by calpain inhibit vesicle endocytosis during neural hyperexcitation. *The EMBO journal*. **26**, 2981–2990.

Wyss-Coray, T. (2006) Inflammation in Alzheimer disease: driving force, bystander or beneficial response? *Nature medicine*. **12**, 1005–1015.

Xie, Y. F., MacDonald, J. F. and Jackson, M. F. (2010) TRPM2, calcium and neurodegenerative diseases. *International Journal of Physiology, Pathophysiology and Pharmacology*. **2**, 95–103.

Yagishita, S., Itoh, Y., Nan, W. and Amano, N. (1981) Reappraisal of the fine structure of Alzheimer's neurofibrillary tangles. *Acta neuropathologica*. **54**, 239–246.

Yamamoto, S., Shimizu, S., Kiyonaka, S., Takahashi, N., Wajima, T., Hara, Y., Negoro, T., Hiroi, T., Kiuchi, Y., Okada, T., Kaneko, S., Lange, I., Fleig, A., Penner, R., Nishi, M., Takeshima, H. and Mori, Y. (2008) TRPM2-mediated Ca2+influx induces chemokine production in monocytes that aggravates inflammatory neutrophil infiltration. *Nature medicine*. **14**, 738–747.

Yamamoto, S., Wajima, T., Hara, Y., Nishida, M. and Mori, Y. (2007) Transient receptor potential channels in Alzheimer's disease. *Biochimica et biophysica acta*. **1772**, 958–967.

Yamashima, T. (2013) Reconsider Alzheimer's disease by the 'calpain-cathepsin hypothesis'-A perspective review. *Progress in Neurobiology.* **105**, 1–23.

Yano, Y., Shiba, E., Kambayashi, J., Sakon, M., Kawasaki, T., Fujitani, K., Kang, J. and Mori, T. (1993) The effects of calpeptin (a calpain specific inhibitor) on agonist induced microparticle formation from the platelet plasma membrane. *Thrombosis research*. **71**, 385–396.

Yeh, T. Y. J., Sbodio, J. I. and Chi, N. W. (2006) Mitotic phosphorylation of tankyrase, a PARP that promotes spindle assembly, by GSK3. *Biochemical and Biophysical Research Communications*. **350**, 574–579.

Yildiz-Unal, A., Korulu, S. and Karabay, A. (2015) Neuroprotective strategies against calpain-mediated neurodegeneration. *Neuropsychiatric Disease and Treatment*. **11**, 297–310.

Yuan, J. (2009) Neuroprotective strategies targeting apoptotic and necrotic cell death for stroke. *Apoptosis.* **14**, 469–477.

Yuen, E. Y., Ren, Y. and Yan, Z. (2008) Postsynaptic density-95 (PSD-95) and calcineurin control the sensitivity of N-methyl-D-aspartate receptors to calpain cleavage in cortical neurons. *Molecular pharmacology*. **74**, 360–370.

Zempel, H., Thies, E., Mandelkow, E. and Mandelkow, E.-M. (2010) Abeta oligomers cause localized Ca(2+) elevation, missorting of endogenous Tau into dendrites, Tau phosphorylation, and destruction of microtubules and spines. *The Journal of neuroscience : the official journal of the Society for Neuroscience*. **30**, 11938–11950.

Zhang, S., Lin, Y., Kim, Y.-S., Hande, M. P., Liu, Z.-G. and Shen, H.-M. (2007) c-Jun N-terminal kinase mediates hydrogen peroxide-induced cell death via sustained poly(ADP-ribose) polymerase-1 activation. *Cell death and differentiation*. **14**, 1001–1010.

Zhang, W., Chu, X., Tong, Q., Cheung, J. Y., Conrad, K., Masker, K. and Miller, B. a. (2003) A novel TRPM2 isoform inhibits calcium influx and susceptibility to cell death. *Journal of Biological Chemistry*. **278**, 16222–16229.

Zhang, W., Hirschler-Laszkiewicz, I., Tong, Q., Conrad, K., Sun, S.-C., Penn, L., Barber, D. L., Stahl, R., Carey, D. J., Cheung, J. Y. and Miller, B. a (2006) TRPM2 is an ion channel that modulates hematopoietic cell death through activation of caspases and PARP cleavage. *American journal of physiology. Cell physiology*. **290**, 1146–1159.

Zhang, Y., Thompson, R., Zhang, H. and Xu, H. (2011) APP processing in Alzheimer's disease. *Molecular brain*. **4**, 3.

Zheng, W. H., Bastianetto, S., Mennicken, F., Ma, W. and Kar, S. (2002) Amyloid beta peptide induces tau phosphorylation and loss of cholinergic neurons in rat primary septal cultures. *Neuroscience*. **115**, 201–211.

Zigman, W. B., Devenny, D. A., Krinsky-McHale, S. J., Jenkins, E. C., Urv, T. K., Wegiel, J., Schupf, N. and Silverman, W. (2008) Alzheimer's Disease in Adults with Down Syndrome. *International review of research in mental retardation*. **36**, 103–145.

Zou, Z., Liu, C., Che, C. and Huang, H. (2014) Clinical genetics of Alzheimer's disease. *BioMed Research International.* **2014**, 291862